



# Development of models for integrating renewables and energy storage components in smart grid applications

Mahmoud Barakat

## ► To cite this version:

Mahmoud Barakat. Development of models for integrating renewables and energy storage components in smart grid applications. Electric power. Normandie Université, 2018. English. NNT : 2018NORMC217 . tel-01981668

**HAL Id: tel-01981668**

**<https://theses.hal.science/tel-01981668>**

Submitted on 15 Jan 2019

**HAL** is a multi-disciplinary open access archive for the deposit and dissemination of scientific research documents, whether they are published or not. The documents may come from teaching and research institutions in France or abroad, or from public or private research centers.

L'archive ouverte pluridisciplinaire **HAL**, est destinée au dépôt et à la diffusion de documents scientifiques de niveau recherche, publiés ou non, émanant des établissements d'enseignement et de recherche français ou étrangers, des laboratoires publics ou privés.

## THÈSE

**Pour obtenir le diplôme de doctorat**

**Spécialité GENIE ELECTRIQUE**

**Préparé au sein de l'Université de Caen Normandie**

### **Development of Models for Inegrating Renewables and Energy Storage Components in Smart Grid Applications**

**Présentée et soutenue par  
Mahmoud BARAKAT**

**Thèse soutenue publiquement le 26/06/2018  
devant le jury composé de**

M. MOHAMED MACHMOUM	Professeur des universités, UNIVERSITE NANTES	Rapporteur du jury
M. AHMED RACHID	Professeur des universités, UNIVERSITE AMIENS PICARDIE JULES VERNE	Rapporteur du jury
M. DIDIER CHAMAGNE	Professeur des universités, UNIVERSITE BESANCON FRANCHE COMTE	Président du jury
M. JEAN-PAUL GAUBERT	Professeur des universités, UNIVERSITE POITIERS	Membre du jury
M. BOUBEKEUR TALA-IGHIL	Maître de conférences, UNIVERSITE CAEN NORMANDIE	Membre du jury
M. HAMID GUALOUS	Professeur des universités, UNIVERSITE CAEN NORMANDIE	Directeur de thèse
M. DANIEL HISSEL	Professeur des universités, UNIVERSITE BESANCON FRANCHE COMTE	Co-directeur de thèse

**Thèse dirigée par DANIEL HISSEL et HAMID GUALOUS, Laboratoire universitaire des sciences appliquées de cherbourg (Caen)**



# Acknowledge

I would like to declare my grateful, thanks to those who helped, supported, and guided me for following my dissertation.

To those who drove and pushed me from my childhood until now, my parents that did as possible as they can to have the best.

To my family, my dear wife and my two sons, the moon and the two sons of my life.

I would like to thank also my professors at the Electrical Power and Machines department, Faculty of Engineering, Helwan University of Egypt. They well educated me during the undergraduate studies and supervised my master thesis. Many thanks to Prof. Radwan Hassan Abdel Hamid who strongly supported and recommended me to have the full grant Ph.D. scholarship.

Many thanks to Prof. Hamid GUALOUS who accepted me as one of his students, supervised, and directed my thesis.

During the thesis, I really received some scientific comments and ideas that represent the main work of my thesis. These are the ideas and the help of Prof. Daniel HISSEL, the co-director of the thesis.

If I worked hard and tried to overcome all the difficulties and the hard times I faced during the study, it is thanked Dr. Boubekeur TALA-IGHIL who worked with me hand in hand. Really, he did not hesitate any time to support me and give me very good advice and ideas scientifically and personally.

The contact point between LUSAC laboratory and me is Dr. Moatez ELSIED who worked hard with me even before I arrived at the laboratory and supported me a lot.

Many thanks to the IT team work of Caen Normandy University, site of Cherbourg that supported the JADE platform installation and the Java programming. Many Thanks to the IUT electronic workshops technicians that helped me in designing and performing some experimental work.

Finally, I will stay all my life declare my honor and my gratitude to my country, the Arab Republic of Egypt that is the source of all issues that I had, have and will have. Even under the very difficult conditions, it financed not only my study but also the residence of my family to be beside me during these three years of the thesis.

At the beginning and at the end and all the times, Thanks to my God, **ALLAH**.

**Mahmoud BARAKAT, Cherbourg, France**  
**Friday, 4<sup>th</sup> May 2018.**



# Contents

General Introduction .....	7
Chapter 1, Literature Survey.....	11
1. Introduction.....	13
2. Smart Grid Activities Literature Survey.....	19
2.1. The Management and Optimization of Smart Grid with Renewables High Integration.....	20
2.1.1. Centralized Management System.....	21
2.1.2. Decentralized Management System.....	23
2.2. Renewable Energy Resources Intermittency with Energy Storage Systems Integration and Electric Vehicles.....	35
2.3. Smart Grid Advanced Control.....	41
2.3.1. Single Smart Micro Grid.....	41
2.3.2. Smart Multi-Micro grids Control.....	44
2.4. Smart Grid Stability Analysis and Power Quality.....	45
2.5. Smart Grid Modeling, Simulation, and Representation.....	47
2.6. Smart Grid Communication and Advanced Metering.....	49
3. Conclusion.....	51
Chapter 2, Component Layer (Hybrid Marine-Hydrogen System) Modeling and Energetic Macroscopic Representation.....	53
1. Introduction.....	55
2. System Energetic Macroscopic Representation and Modeling.....	59
2.1. Marine current turbine.....	59
2.1.1. Marine current turbine model.....	60
2.1.2. Permanent magnet synchronous generator model.....	61
2.2. MW Scale PEM Electrolyzer system.....	63
2.3. PEM fuel cell modeling.....	72
2.4. Storage tank modeling.....	75
2.5. Load demands modeling.....	76
2.6. LiFePO <sub>4</sub> battery modeling.....	78
2.7. Power electronic converters modeling.....	80
2.8. DC-link modeling with load filter and transformer.....	81

3. Hybrid Marine-Hydrogen Active Power Generation System Global Energetic Macroscopic Representation.....	82
4. Conclusion.....	84
Chapter 3, Centralized Energy Management and Low-Level Control Systems.....	87
1. Introduction.....	89
2. Tuning Chains definition.....	89
2.1. Machine Side Converter (MSC) Tuning chain.....	89
2.2. Load Side Converter (LSC) Tuning Chain.....	91
2.3. Electrolyzer Side Converter and Fuel Cell (ESC, FCSC-Buck, Boost) Tuning Chain...	91
2.4. Battery Side Converter (BSC, Bi-directional) Tuning Chain.....	92
3. Control Strategies.....	92
3.1. Marine Current Turbine (MCT) Control strategies.....	92
3.1.1. Power control strategy (PCS).....	93
3.1.2. Flux control Strategy (FCS).....	93
3.2. Load Side Converter Control Strategy.....	98
3.3. Electrolyzer and Fuel Cell Side Converter Control Strategy.....	98
3.4. Battery Side Converter Control Strategy.....	100
4. Simulation and Results.....	102
4.1. Loss Minimization Results.....	108
4.2. System Performance with Variable Marine Current Speed.....	111
5. Conclusion.....	116
Chapter 4, JADE Based Multi-Agent Decentralized Energy Management System.....	119
1. Introduction.....	121
2. Multi-Agent Platform Selection.....	122
3. JADE Platform.....	130
4. MATLAB/SIMULINK-JADE Interface.....	134
5. JADE based Multi-Agent Energy Management System of the Hybrid Marine-Hydrogen Power Generation System.....	136
5.1. Isolated Mode MAS Energy Management.....	136
5.2. Grid-Connected Mode MAS Energy Management System.....	144
6. SGAM Scope of the Proposed JADE Based MAS.....	148
7. Conclusion.....	151
Conclusion and Future Work.....	153

Extended French abstract.....	159
Appendix A, Active Marine-Hydrogen Hybrid Power Generation System Model Parameters.....	177
Appendix B, Source Codes of the Hybrid Marine-Hydrogen JADE Based MAS Management System.....	181
References.....	209





## ➤ General Introduction

The traditional power system network suffers from many problems concerning different points of view (power shortages, uneconomical operation, environmental impacts, etc.). The smart grid is a new topology of the power system network that depends on the renewables instead of the traditional fossil fuels power plants. The smart grid requires powerful management with two-way communication between the generation and the demand sides. It has many challenges and scientific problems that need to be studied and analyzed as follow:

- The traditional grid infrastructure must be adapted for the renewables high penetration rates.
- The selection (technically and economically) of the suitable energy storage system is essential in a smart grid to ensure stable, secure and healthy operation under the different operating conditions.
- The energy management and optimization of the smart grid component layer considering the generation and demand sides constraints and conditions.
- A powerful, redundant, and fully protected communication system is essential.
- The modeling and the representation of the smart grid (with the interaction between its different layers) are required for better understanding of the interaction between the layers (power domain, communication, management, etc.).

The smart grid modeling enables the study, the analysis, and the design of novel solutions for all these challenges. Based on all the above, this study presents the modeling and the management of the hybrid marine current- hydrogen active power generation system. The marine current energy is selected based on the high renewables integration objective of the smart grid. The marine current energy is a premature technology and has many economic and technological challenges that need to be studied. The electric machinery selection and the power transmission system are the main challenges facing the marine current system integration into the main grid. The tidal energy suffers from monthly and seasonal variations that require a storage system able to ensure the sustainable energy feeding (Intermittency enhancement). The Hydrogen system is selected based on the energy storage technologies state of the art. The hydrogen system has a long charging/discharging cycle (in the range of days or weeks) that is more suitable to the daily and weekly variations of the marine currents. Moreover, the hydrogen chain considers many forms of end-user utilization (e.g., electricity generation by the fuel cell, fuel cell based electric vehicles fueling or directly

transmitted in storage tanks or via the natural gas network). The MW scale proton exchange membrane (PEM) electrolyzers are new technology systems for the renewables intermittency improvement in the long-term timescale. The PEM electrolyzers and fuel cell have a specific dynamic response that must be respected to avoid systems aging and components degradation. The  $\text{LiFeO}_4$  Battery is selected to cover the fast dynamics of the electrical power. This technology of battery has the advantages of the battery high energy density and the supercapacitor high power density. The hybrid marine–hydrogen system configuration requires an efficient energy management system. This system must have the capability of monitoring and survey the different system components (mechanical, electromechanical, electrochemical, and electrical domains). One of the power optimization and management techniques is the MAS (Multi-Agent System) that is a type of the decentralized management system. This study presents the MAS to control and manage the whole system in the smart grid framework. The energetic macroscopic representation (EMR) is selected as a system representation technique for a better understanding of the interaction between the different system physical components. The thesis consists mainly of four chapters that are described in the following paragraphs.

Chapter 1 presents the smart grid definitions and state of the art concerning its different research directions. The main directions are the renewables integrations, the energy storage system for improving the renewables intermittency, the management systems topologies, the advanced control systems, the communication systems and the smart grid modeling and representation. Finally, the main outcomes of the literature survey are presented that depend on proposing a pilot case study of the SGAM (Smart Grid Architecture Model).

Chapter 2 discusses in details the EMR (Energetic Macroscopic Representation) of the active marine-hydrogen power generation system. The proposed system represents the component layer of the SGAM that integrates a fixed pitch direct drive tidal turbine that is coupled mechanically with a PMSG (Permanent Magnet Synchronous Generator). The standardized household load profile presents the demand side for modeling residential loads. The hydrogen system represents the main energy storage and balance system for improving the marine currents intermittency. The hydrogen system consists of an MW scale PEM (Proton Exchange Membrane) electrolyzer and fuel cell. The  $\text{LiFePO}_4$  battery is integrated into the system to cover the fast electrical dynamics. The EMR of each subsystem is formulated firstly while the global system EMR is synthesized by integrating all the components together based on the physical causality principal of the EMR.

Chapter 3 analyzes the low-level control system and the centralized energy management systems design. The low-level control systems are designed based on defining the tuning chains. The considered chains are the machine (PMSG) side converter, the load side converter, the electrolyzer side converter, the fuel cell side converter and the battery side converter. The PMSG has two main control strategies that are the power control and the flux control. The power control strategy represents the MPPT (Maximum Power Point Tracking) when the turbine runs below the base speed and the power limitation at the rated value when it runs above the base speed. The flux strategy is the flux weakening control that is activated above the rated speed to protect the PMSG from overvoltages and overcurrents. A new flux control topology has been proposed that is called the losses minimization (output maximization) for, as the name proposes, maximizing the PMSG efficiency when it runs below the base speed. The control strategy of the load side converter depends on feeding a fixed voltage and fixed frequency at the load terminals as the system runs in the stand-alone mode. The control strategies of the electrolyzer and the fuel cell sides represent the tracking of the current reference values provided by the energy management system. The battery side converter is controlled to cover the fast dynamics of the electrical power and stabilize the DC-link voltage. The centralized energy management systems consider all the constraints and recommendations of the different subsystems to balance the energy between the generation (marine current system) and the consumption (residential loads) by providing the operating point (in the form of the reference values) to the electrolyzer and the fuel cell control systems.

Chapter 4 considers the MAS (Multi-Agent System) as a paradigm of the decentralized energy management system. There are many platforms of the MAS, and consequently, it is required to discuss the platforms comparison and selection for developing the proposed system. Based on the evaluation, the JADE (Java Agent Development Environment) is selected. The design and the development procedure of the decentralized MAS for energy management of the marine-hydrogen power generation system are presented. Two modes of system operation evaluate the MAS management system performance compared with the centralized one. The first is the stand-alone mode to compare the effectiveness of the system with the centralized one. The second is the grid-connected mode to analyze the system scalability and flexibility. Finally, the whole system is scoped from the SGAM point of view as a pilot case study representing its model.



# **Chapter 1**

## **Literature Survey**



## 1. Introduction

The traditional power grid as shown in Fig. 1.1 consists of four main sectors: generation, transmission, distribution, and consumption. Considering a few examples of central power plants, the generation of electricity usually uses flowing water, fossil or nuclear fuels as energy sources to drive electromechanical generators. Depending on the location of the used energy sources and the availability of the cooling water sources, generation stations may be built in locations far away from the heavily populated and main consumption centers, which requires an energy transmission system. An economic long-distance energy transmission requires the voltage to be stepped up to a higher level via overhead transmission lines. Upon the arrival, the voltage is stepped down for distribution stations, which distribute the electrical energy for different types of loads (residential, commercial, industrial, etc.). This architecture of traditional power grid suffers from many problems that can be listed as follow:

- The generation-consumption shortage due to the continued population growth that requires more sources integration.
- The non-sustainable nature of traditional fossil fuels and its economic instability.
- The safety problems and the social acceptance of nuclear energy.
- The environmental problems; mainly the greenhouse effect (global warming) due to CO<sub>2</sub> emissions from fossil fuels burning and to the disposal of nuclear waste.
- The fact that the traditional power grid is a unidirectional power flow in nature [1]–[6].

Sustainable and renewable energy sources [wind, PV (Photovoltaic), solar thermal and marine current energy (Tidal), Ocean Wave ...] have become the most attractive and socially accepted ones worldwide, due to their free availability, sustainability, and environmentally friendly nature. All over the world, there are strong trends of renewables high integration. Based on IEA's new policies scenario, the amount of renewables-based generated electrical energy will be increased from 5105 TWh in 2013 to 13400 TWh in 2040. This expansion will represent more than one-third of global electricity generation (including hydro) and 44% of the growth in electricity generation from 2013 to 2040 as shown in Fig. 1.2. The Wind and hydro each represents a third of this growth while biomass accounts for 12% and PV for 17% while the rest comes from geothermal, concentrated solar power and the marine. In this scenario, the United States, European Union, China, and India represent 90% of the wind installation capacity growth and more than 80% of the growth in PV capacity [6], [7].



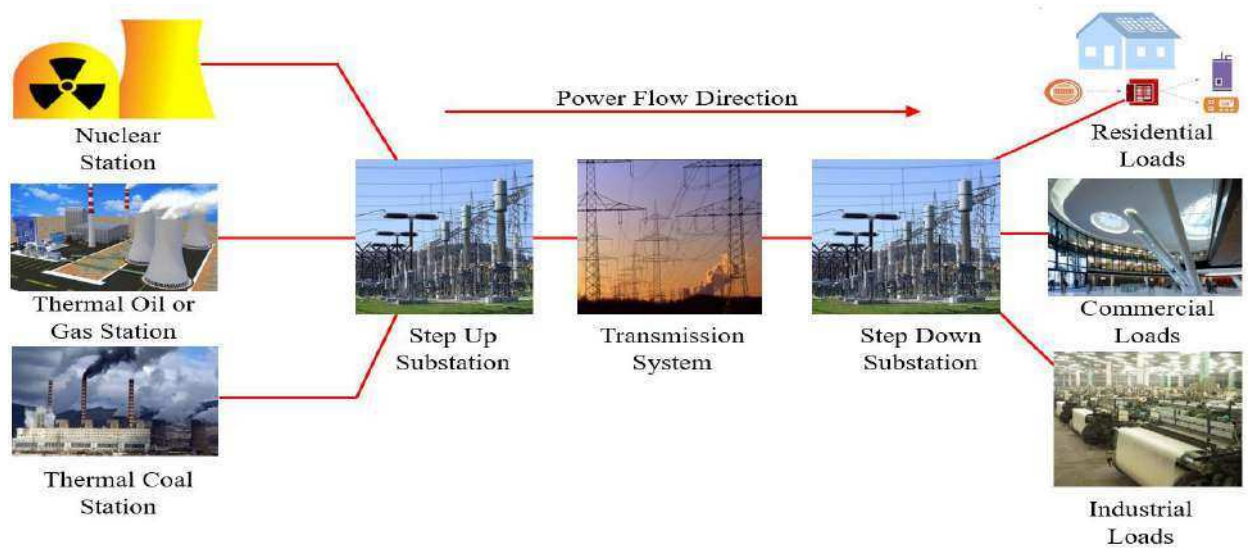


Fig. 1.1. Conventional Power System Architecture Model.

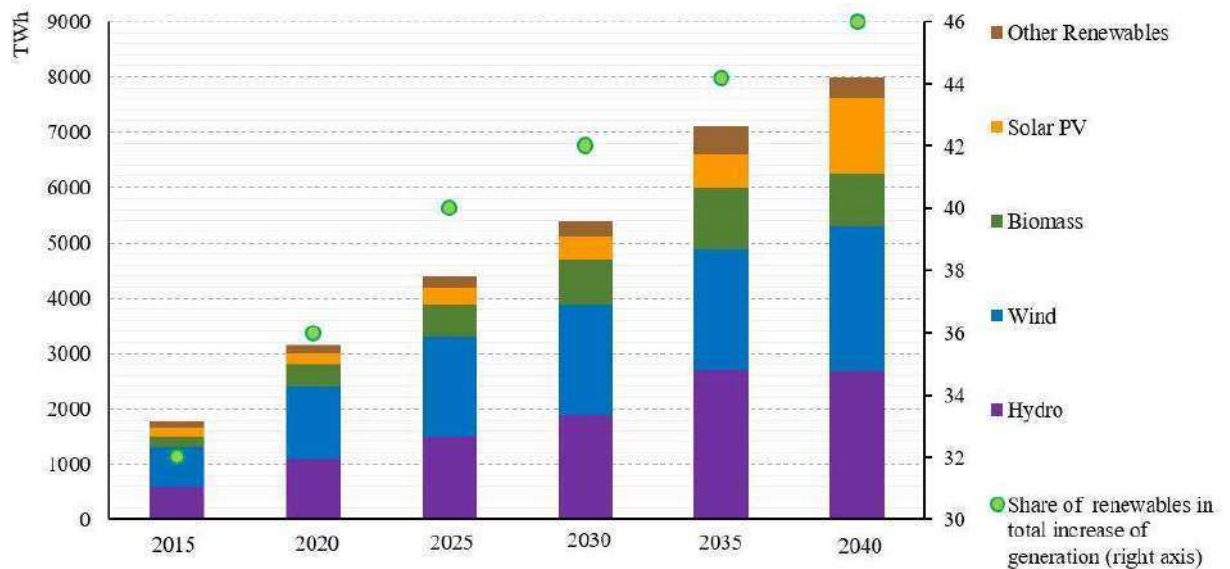


Fig. 1.2. Incremental Global Renewables-Based Electricity Generation Relative to 2009 by Technology in IEA's New Policies Scenario [6], [7].

Due to these scenarios, the CO<sub>2</sub> Emissions from the power sector will increase by 25% from 11.8 G tone in 2009 to 14.8 G tone in 2035. With taking into consideration the growth of electricity generation during this period, which will be three times larger, there will be a 30% reduction in CO<sub>2</sub> emissions as shown in Fig. 1.3. Each generation unit released 530 grams per kWh in 2009; this level of emission is prospected to be 375 grams in 2035. This reduction is due to the replacement of coal and oil-based generation units by the lower carbon nuclear and renewable based technologies, as well as the improvements of the coal and gas generation units' efficiency [7]. One of the approaches to reduce the CO<sub>2</sub> emissions also sustaining the use of traditional fossil fuels power plants is CO<sub>2</sub> sequestration.

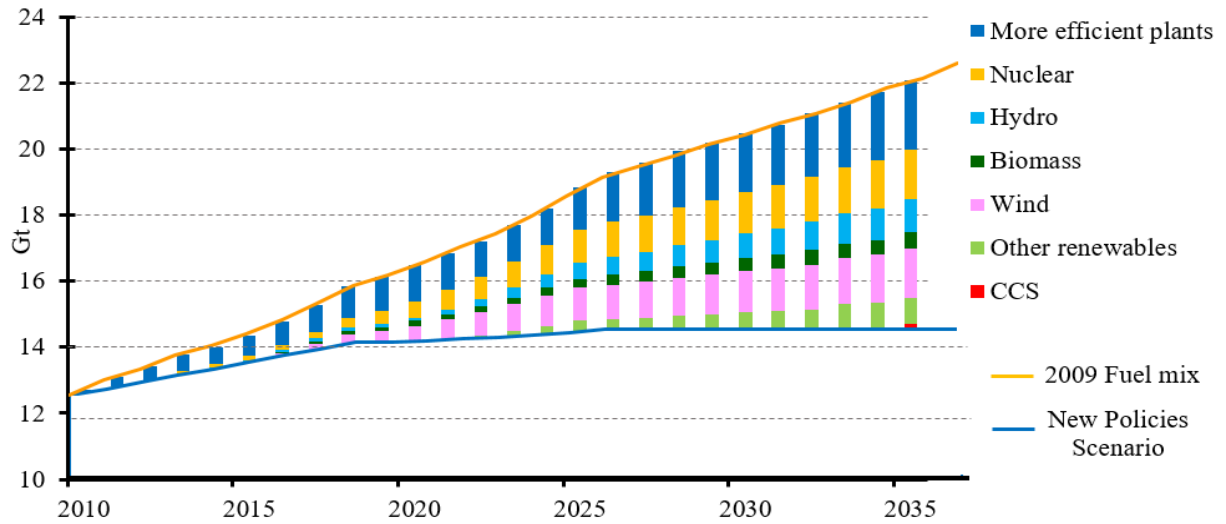


Fig. 1.3. Global CO<sub>2</sub> Emission Savings in Power Generation Relative to the 2009 Fuel Mix in the New Policies Scenario [6].

The CO<sub>2</sub> sequestration is the CCS (Capture and Secure Storage) of the anthropogenic carbon that would be emitted to the atmosphere. The carbon capture is the separation of CO<sub>2</sub> from its large sources (fossil fuels power plants, cement and iron industries, ammonia production, industrial boilers, and natural gas wells). The storage consists of CO<sub>2</sub> injection into huge geologic and oceanic reservoirs for long periods of time (hundreds or thousands of years) in a secure manner. The achievement of these scenarios makes each country has its scenario for renewable energy integration. In the following paragraphs, the scenarios of U.K (United Kingdom), Australia, European Union and Sweden are presented. Having 15% of total energy demand met by renewable energy sources by 2020 is the main goal of U.K. The target of Northern Ireland is to produce 40% renewable electricity while the Scotland 2020 target is 11% RHI (Renewable Heat Incentive). The Wales government has indicated that it has the potential to produce twice as much renewable electricity in 2025 compared to 2011 and to deliver 4 GW from the marine. The general trend of U.K is to have 30 – 40% of all energy consumed met by renewable sources by 2030 based on eight technologies as shown in Tab 1.1 [8]. For Australia, the main goal is to have 20% of the electricity demand supplied by renewable energy sources by 2020 with different estimations of each technology roadmap. The offshore and onshore wind energy will provide 20% of the renewable-generated energy by 2020. The climate and location of Australia are suitable for ensuring 5% of demand by 2030 and possibly up to 25% by 2060. Geothermal sources are also estimated to be providing 7% of Australia baseload power by 2030 while the biofuels share about 29% of electricity by 2040 [9].

<b>Technology</b>	<b>Central Range For 2020 (TWh)</b>
Onshore Wind	24 - 32
Offshore Wind	33 – 58
Biomass	32 – 50
Marine	1
Biomass Heat (non-domestic)	36 – 50
Air Source Ground Heat Pump (non-domestic)	16 – 22
Renewable Transport	Up to 48
Others (including hydro, geothermal, solar and domestic heat)	14
Estimated 15% target	234

Table 1.1 The UK Technology Break Down (TWh) for the Central View of Deployment in 2020 [8].

For the EU (European Union), the integration of renewable energy sources in electricity generation will be 35% by 2020 while it is aimed to be 43% by 2030 and 56% by 2050 with technologies sharing ratio indicated in Tab 1.2 [10]. In Sweden, the aim is to have almost 100% of energy provided by renewable energy sources (mainly wind and PV) as shown in Fig. 1.4. The wind power generation will increase up to 20 TWh by 2020 and 30 TWh in 2030 to reach 45 TWh in 2050. A similar increase is also a goal in the photovoltaic, which will reach 32 TWh by 2050. Due to this scenario, there will be a 30% reduction of the CO<sub>2</sub> Emissions by 2020 compared to 1990, it is prospected to reach 50% by 2030 [11]. The integration of marine energy (tidal and wave) is low as it remains under research and development, but there are strong trends in its integration in the European Union as shown in Fig. 1.5 [12]. Renewable energy sources cannot be considered as constant or sustainable, as they vary from a season to another, from a day to another and from an hour to another during each day. Systems using solar energy (photovoltaic and solar thermal) are only available during the day. The tidal varies from ebb to flood as a sine wave with a different period (two ebbs and two floods during 24 hours) while the wind is variable all day long and every day, consequently it is difficult to be forecasted. This feature of renewables is called the intermittency and can exhibit reliability, stability, and power quality problems for the power system, even else, it is an isolated or grid connected. One of the renewable intermittency proposed solution is energy storage systems integration. There are different types of energy storage systems, which are reviewed and compared based on their characteristics in the following sections. By the integration of these different systems (renewables, energy storage, and the demand side), the whole power system cannot be considered as a unidirectional conventional power system (shown in Fig.1.1). The power system architecture must be reformed into more flexible, scalable and powerful management topology that is called a smart grid.

Technology	2020 Ratio and Capacity	2030 Ration and Capacity	2050 Ratio and Capacity
Wind	14.5% (207 GW)	18% (255 GW)	25% (367 GW)
PV	4.8% (137.5 GW)	7% (183 GW)	11% (299 GW)
Biomass and Waste Combustion (as a source of Thermal Power Plants)	17.3% 51.6 GW	22% 53.2 GW	31.5% 57.3 GW
CHP	33%	35%	41%
Hydro	10-11%		
Geothermal	0.2%	----->	0.6%
Tidal and Wave	0.2%	----->	0.6%

Table 1.2 The EU Technologies Integration Ratio from 2020 to 2050 [10].

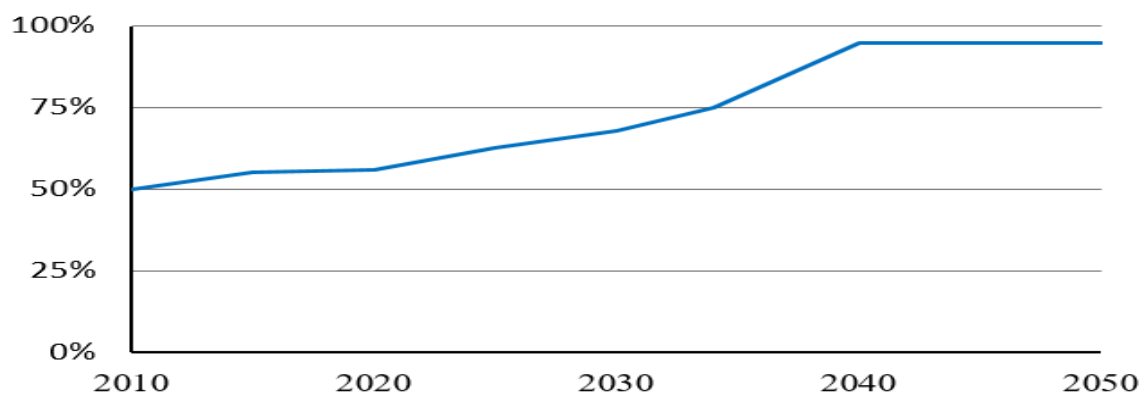


Fig. 1.4. The Share of Renewables in the Sweden Electricity Production Mix [11].

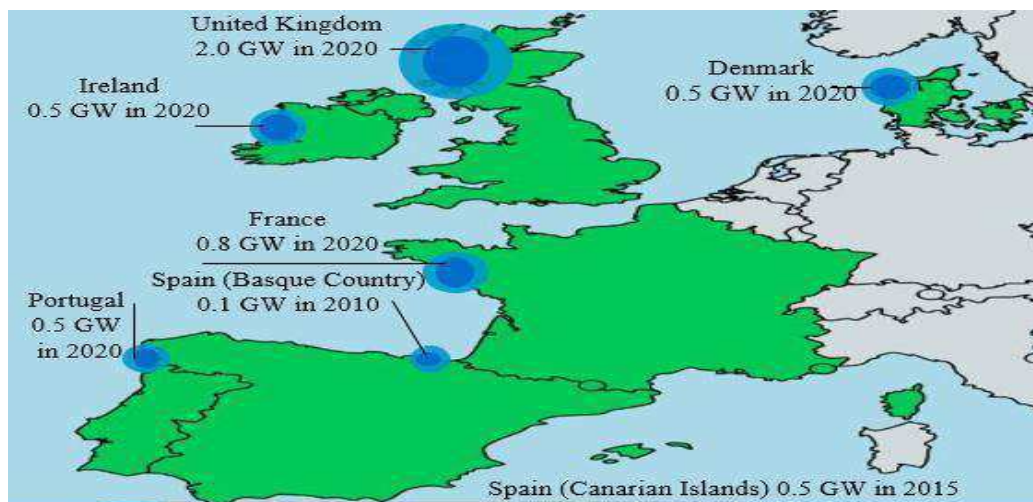


Fig. 1.5. The National European Marine Energy Target [12].

The smart grid has different definitions and objectives all over the world due to each state's power grid conditions and characteristics. For instance, the United States addresses retrofitting existent grid infrastructures, promoting clean energy and wide use of plug-in hybrid electric vehicles [13]. The EU attaches much importance to such issues as optimizing

grid facilities operation and management and enhancing the competence of grid to accommodate the integration of renewables [13]. In Japan, smart grid focuses on addressing the problems incurred by the introduction of large-scale dispersed PV power system [13]. While the state grid corporation of China has proposed the "Strong Smart Grid" with UHV (Ultrahigh High Voltage) transmission networks as the major power transmission grids to improve the energy efficiency, the power safety, and the reliability [13]. Table 3 shows the main differences between the traditional power grid and the smart grid [1]–[5]. Concerning the clear and coherent architecture of the smart grid, Fig. 1.6 shows the SGAM (Smart Grid Architecture Model), which describes the new topology of the power grid with its different layers. The SGAM is a three-dimensional model that merges the dimension of the five interoperability layers (Business, Function, Information, Communication, and Component) with the two dimensions of the smart grid plane.

Conventional Power System	Smart Grid
Electromechanically Controlled	Digitally Controlled
Unidirectional Communication	Bidirectional Communication
Centralized Generation	Distributed Generation
Few Sensors	Sensors Throughout
Manual Monitoring	Self-Monitoring
Manual Restoration	Self-Healing
Failures and Blackouts	Adaptive Islanding
Limited Control	Pervasive Control
Few Customer Choices	Demand Side Management

Table 1.3 Conventional and Smart Grids Comparison [1]–[5].

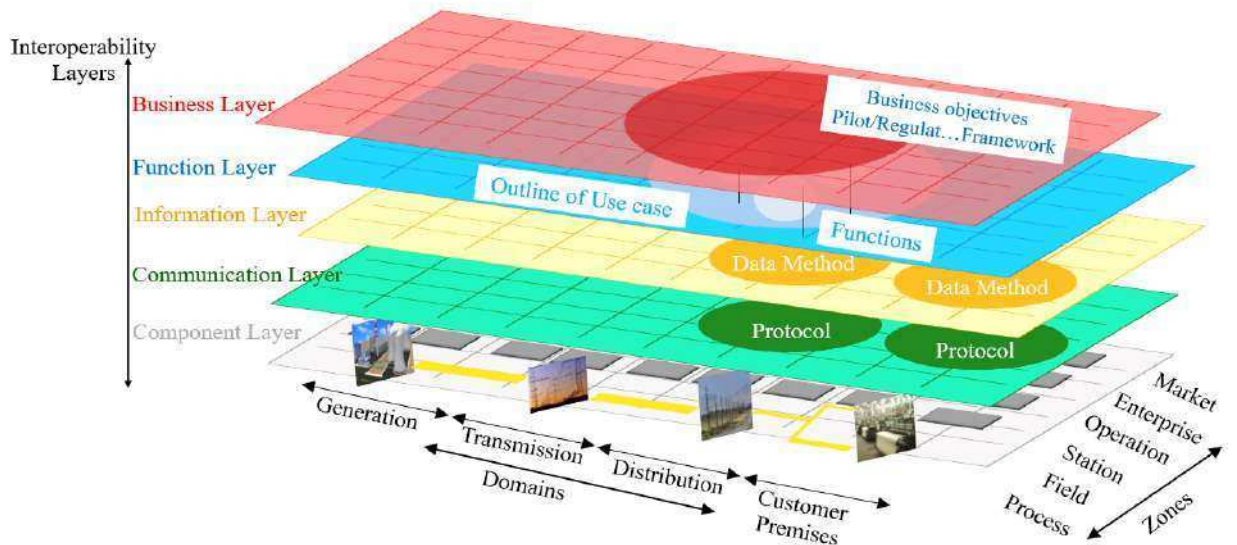


Fig. 1.6. Smart Grid Architecture Model [14]–[16].



The first dimension of the SGAM is the zone that represents the hierarchical levels of the management (Process, Field, Station, Operation, Enterprise, and Market). The second dimension of the SGAM is the domains, which represents the components of the complete electrical power network (bulk generation, transmission, distribution, DER (Distributed Energy Resources), and customers premises) [14]–[16]. The technology roadmap of the smart grid defines the different technologies for more smartness, based on the domains of the grid (generation, transmission, distribution, and customers) as shown in Fig. 1.7. Tables 1.4 and 1.5 summarize the development trends and briefly describe each technology [17]. Due to these definitions, the following points represent the different literature smart grid activities:

- The management and optimization of power network with the high integration of renewable energy sources
- The intermittency of renewable energy sources, energy storage systems and electric vehicles.
- Advanced control of the smart grid.
- Stability and Power Quality.
- Smart Grid Modeling, Simulation, and Representation.
- Communication and Advanced Metering Systems.

## 2. Smart Grid Activities Literature Survey

The smart grid activities, as described above, are the main six technologies like R&D (Research and Development) directions defined by the smart grid technology roadmap. The following subsections present the literature survey of these activities and research points.

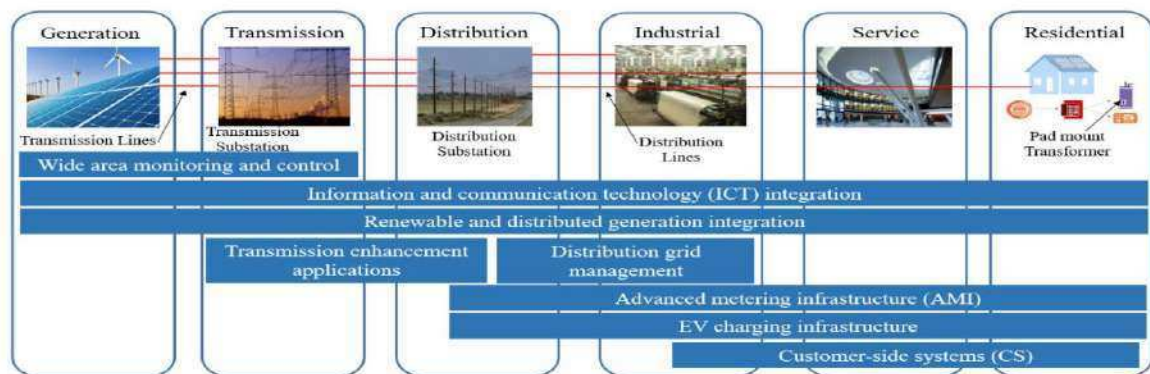


Fig. 1.7. Smart Grid Technology Areas [17].

Technology	Maturity Level	Development
Wide area monitoring and control	Developing	Fast
Information and communication	Mature	Fast
Renewable and distributed generation integration	Developing	Fast
Transmission applications	Mature	Moderate
Distribution networks management	Developing	Moderate
Advanced metering infrastructure	Mature	Moderate
Electric vehicle infrastructure	Developing	Fast
Demand-side systems	Developing	Fast

Table 1.4 Maturity Levels and Developments Trends of Smart Grid [17].

Technology	Hardware	Software
Wide Area Monitoring AND Control (WAMC)	Phase measurement units (PMU) and other sensor equipment's	Supervisory Control and Data Acquisition (SCADA), Wide Area Monitoring systems (WAMS), Wide Area Adaptive Protection, Control and Automation (WAAPCA), Wide Area Situational Awareness (WASA)
Information and Communication Technology Integration	Communication equipment (Power Line Carrier, WIMAX, LTE, RF mesh network, Cellular), Routers, Relays, Switches, Gateway, Computers (Servers)	Enterprise Resource Planning software (ERP), Customer Information System (CIS)
Renewable and Distributed Generation Integration	Power conditioning equipment for bulk power and grid support, Communication and control hardware for generation and enabling storage technology	Energy Management System (EMS), Distribution Management System (DMS), SCADA, Geographic Information System (GIS)
Transmission Applications	Superconductors, FACTS, HVDC	Network stability analysis, automatic recovery systems
Distribution Network Management (DNM)	Automated re-closers, Switches and Capacitors, Remote controlled distributed generation and storage, Transformer sensor, Wire and cable sensor	GIS, Distribution Management System (DMS), Outage Management System (OMS), Workforce Management System (WMS)
Advanced Metering Infrastructure (AMI)	Smart meter, In-home Displays, Servers, Relays	Meter Data Management System (MDMS)
Electric Vehicle Infrastructure	Charging infrastructure, batteries, Inverters	Energy billing, Smart grid-to-Vehicle Charging (G2V) and discharging Vehicle-to-Grid (V2G) methodologies
Demand Side Systems (DSS)	Smart appliances, Routers, In-home display, Building automation systems, Thermal accumulators, Smart Thermostat	Energy dashboards, Energy Management Systems (EMS), Energy applications for smartphones and tablets

Table 1.5 Smart Grid Technologies [17].

### 2.1. The Management and Optimization of Smart Grid with Renewables High Integration

The high integration of renewable energy sources, considering their intermittent nature, requires more powerful management system. The main goal of the management is the optimization of the power balance between generation and demand sides with giving a higher priority for renewables taking into consideration the two side's constraints. This

goal is mathematically reformed as an objective function of economic profit and environmental impact maximization. The environmental impact considers the reduction of the greenhouse gas (GHG) Emissions. There are different classifications of the energy management systems. Based on the topology of the management, there are centralized and decentralized (e.g., Multi-Agent) management systems. The physical domain point of view exhibits the generation and demand sides management (GSM), (DSM) systems. In this subsection, the latest studies of the power system management are reviewed due to its topology classification.

#### 2.1.1. Centralized Management System

M.Macedo et al. [18] have presented the DSM technique using an ANN (Artificial Neural Network) to classify the different load curves that define the best demand-side management technique. The DSM prospected success is to provide the consumers with a better energy service (faults, defects and blackouts duration reduction) at a lower cost. The most frequently used DSM techniques, shown in Fig 1.8, are peak reduction techniques, filling valleys, moving tips, conservation strategy, strategic growth, and flexible modeling techniques. S.Plathottam et al. [19] have discussed the ED (Economic Dispatch) problem on a power system consisting of the wind, hydro, pumped hydro, thermal power plants, and energy storage, considering photovoltaic as a negative load. The ED has been converted into an optimization problem that has the objectives of minimizing the cost of the energy purchase based on the fuel prices and the LOCE (Levelized Cost of Energy). The objective function of the optimization problem takes into consideration the availability of sources and their constraints. The SA (Simulated Annealing) and PSO (Particle Swarm Optimization) techniques have been used and compared with other techniques (genetic algorithm) to compare and confirm the results. Y.Zheng et al. [13] have studied the IRSP (Integrated Resource Strategic Planning) for interconnected smart grids with the objective of renewables and DSM integration. They have proposed a smart grid topology to interconnect six regional power grids of China by a UHV transmission network and promote the cross region use of renewable energy.



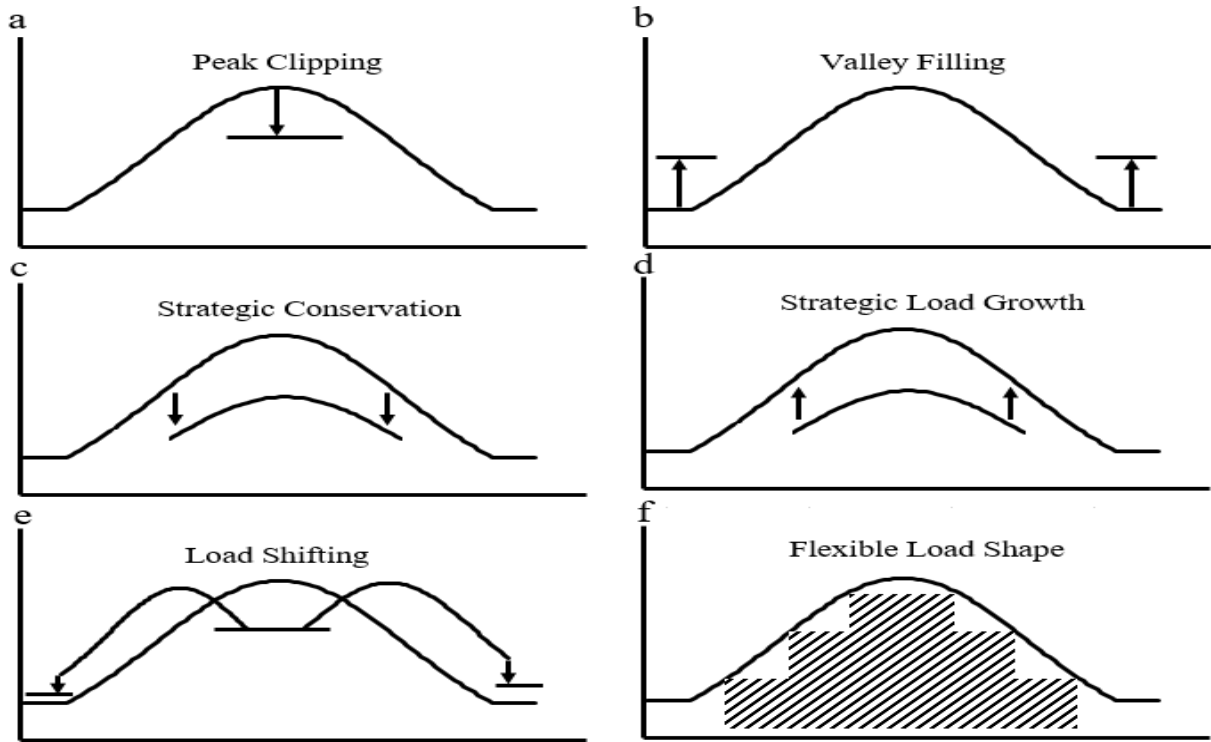


Fig. 1.8. Demand Side Management Techniques [18].

They concluded that thanks to the integrated resource planning with the cross – region transmission and peak regulation by EPPs (Efficiency Power Plants), China could save 784 TWh of electricity generated, reduce 999 M tone of CO<sub>2</sub> emissions, and utilize more than 243 TWh of renewable energy. M.Silvestre et al. [20] have presented a new variables representation to meet the integral constraints in a considered timeframe. The representation, called F- coding, is based on Fourier analyses and takes advantage of the property of sinusoidal functions to have zero-valued integral. The proposed representation provides the ability to add new constraints to the optimization problem, such as setting the maximum power flow through the converter interfacing the storage system to the grid. The used optimization technique is an NSGAI (Non-dominated Sorting Genetic Algorithm), which is applied to a smart grid involving renewable energy sources and an energy storage system. K. Zhou et al. [21] have proposed a new model of a microgrid optimal load distribution to achieve the prospected smart grid economic and intelligent power generation and distribution. A review of the existing optimal load distribution models and their shortcomings has also been presented. G. Boukettaya et al. [22] have proposed a dynamic power management strategy of a grid-connected hybrid generation system with a flywheel energy storage for residential applications. The hybrid generation system consists of wind and photovoltaic power generation systems. The proposed management system depends on the peak load limitation and the load shedding. The management takes into

consideration the maximum and the minimum limits of both the main grid and the flywheel as well as the penalty of consuming power from the grid at peak intervals. It is concluded that this strategy enables the system operator and supervisor to switch from the maximum power to the power regulation operating modes. Wei-Deng et al. [23] have addressed the optimal battery management and the rightsizing problem in the presence of renewable energy sources. They have also presented the different pricing schemes for the power purchasing from the main grid (constant pricing, real-time pricing, and two-time scale pricing). This study has proposed a stochastic optimization solution that aims to minimize the long-term average operational cost of a data center as a case study. Three optimal control policies under the three different pricing schemes have been analyzed to decide the financial viability of the investments in battery energy storage. M.Elsied et al. [24] have presented the analysis, the modeling and the control of an AC microgrid. In this study, the majority of the MGEMC (Micro-Grid Energy Management Center) have been used to optimize and control the power flow from the different renewables to feed the load. The microgrid integrated different distributed energy resources such as wind, tidal, fuel cell and microturbine in main utility grid connection mode. The management is based on purchasing power from the main utility in case of renewables power shortage and vice versa. The same authors have presented two other studies. The first one [25] has introduced an energy management system of the MG (MicroGrid) based on GA (Genetic Algorithm) optimization. The main objectives of the optimization are the energy cost minimization and the reduction of pollutant emissions while taking into consideration the MG system constraints and the higher priority of renewables for load feeding. The second study [26] has proposed another optimization technique for the same micro-grid topology, called an AIMMS (Advanced Integrated Multidimensional Modeling Software). This study has compared the performance of the GA to the AIMMS and concluded that the AIMMS is faster and more precise than the GA especially for a high number of constraints and many objectives.

### 2.1.2. Decentralized Management System

Before reviewing the decentralized management system, its definition and the comparison with the centralized system shall be presented. There are three types of management and control systems (Central – Hierarchical, Distributed – Hierarchical and Decentralized) as shown in Fig. 1.9. The central – hierarchical management system consists of one master control entity and other slave low-level control entities as shown in Fig. 1.9 (a). The management and control orders (set points) are the outputs of the master entity which are performed by

the slave entities. In the hierarchically-distributed management system, the high-level control entity is only responsible for global optimization verification by surveying and monitoring the whole system. Each control entity performs the management and optimization of each physical unit and provides feedback to the high-level one as shown in Fig. 1.9 (b). The decentralized management system consists of many control entities; each one performs full optimization and management of its physical unit, and they can communicate to each other, peer to peer, to deliver or receive information as shown in Fig. 1.9 (c). The decentralized system can be considered to be a hierarchically-distributed one when removing the master entity and if the surveying duties are replaced in between the control entities due to the operating conditions and the availability of each one. The hierarchically-distributed management system, which is more similar to the decentralized one, can be considered as a multi-agent system, as it takes advantage of avoiding the single point of failure over than the centralized system [27]. A multi-agent system became one of the most attractive and powerful tools in developing and controlling a complex system. A multi-agent system consists of several agents working together in harmony and synchronization to achieve the main system task [28]. There are different definitions of an agent but following Wooldridge's definition [29], it is an entity that can react autonomously in response to environmental changes, and it must have the following characteristics:

- Reactivity: the agent can react promptly to the variation in its environment and based on its main function.
- Proactiveness: the agent can be goal-directed.
- Social ability: the agent can communicate with other agents to deliver or receive information [30], [31].

After the definition of the multi-agent system and the main characteristics of each unit agent, the following paragraphs present a brief review of the latest projects and studies, which include the application of multi-agent control in the smart grid. There are two main groups of projects as follow:

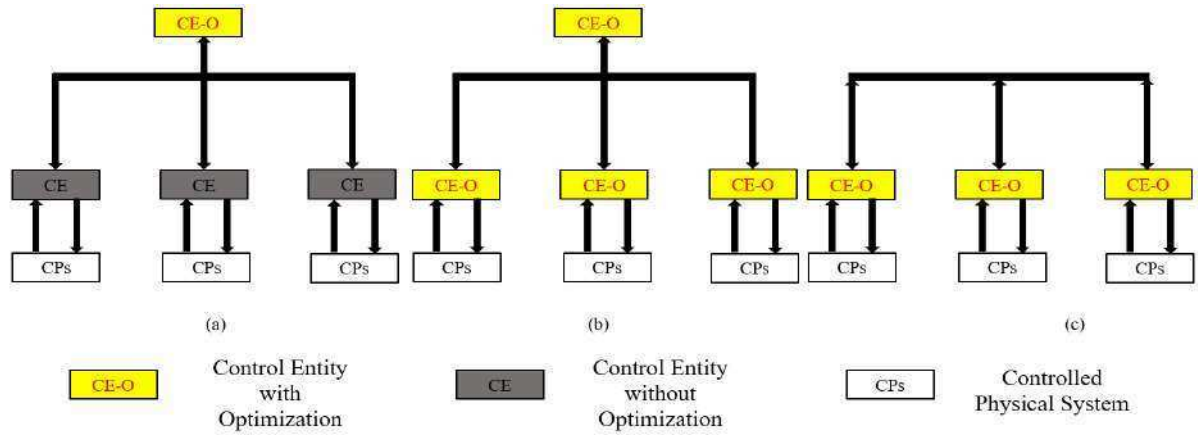


Fig. 1.9. Management and Control Systems Topologies [27].

- Economically oriented control systems: this system is called MOS (Market-Oriented System). The multi-agent system is used to minimize the cost of feeding the power from the generation units. The considered units can be in the same power plant (microgrid) or shared between different power plants (microgrids). Each power plant consists of different sources (conventional or renewable), and each source has its agent (Control Entity, CE). The cost optimization (minimization) is a periodical process (every 500 ms or several minutes). This study can be expanded by combining the ability to forecast the load and source with the optimization process for each period that is called an auction. At the end of each auction, the initialization order is provided to the unit or the grid with the minimum cost to get in the work to supply the required power [31].
- Grid-oriented system: the multi-agent control system is responsible for the safe and reliable operation of the smart grid especially under variation of grid topology (grid reconfiguration) and transient conditions. The grid reconfiguration represents the isolation, the reconnection, and the faulty part separation activities with the main grid. The voltage (reactive power) and frequency (active power) control mainly ensure the safe and the reliable mode. One of the most attractive applications of multi-agent is the multi microgrids control. Each microgrid is responsible for feeding its loads in the safe and reliable mode of operation while keeping its stability. In case of surplus power, the microgrid will negotiate for selling its surplus energy to the neighbors and vice-versa. In both cases of purchasing or

selling, each microgrid control system maintains the stability of its voltage and frequency [31].

In the following section, the latest studies about the multi-agent management in smart grid are reviewed.

H. Feroze et al. [28] have presented a study of the multi-agent control system for the smart grid. The main objective of this study is to design, develop, and implement a multi-agent control with a 100% safe operation. The safe operation represents the secure feeding of the critical loads at different operating conditions while feeding the non-critical loads with taking into consideration the limited renewables capacity during the main grid outage. The main components of the studied system are the physical microgrid and the cyber (multi-agent) systems. The physical system is a very simple distribution network and consists of the main grid, the renewable energy sources, and two types of loads (critical – non-critical). The physical system is modeled by using the MATLAB/SIMULINK software. Different types of a multi-agent open source software are compared to select the most applicable and suitable one. ). R. Gupta et al. [32] have presented a MAS (Multi-Agent System) framework to operate and control a smart grid. The proposed multi-agent system consists of seven agents as follows:

SGC (Smart Grid Controller), LAGs (Load Agents), a WTAG (Wind Turbine Agent), PVAG (Photovoltaic Agents), an MHTAG (Micro-Hydro Turbine Agent), DAGs (Diesel Agents), and a BAG (Battery Agent). The load agents represent a consumer or energy buyer while WTAG, PVAGs, MHTAG, and DAGs represent producers or energy sellers and the BAG can be either a seller or buyer depending on the state of charge. The proposed MAS is used to study the system performance during different time slots (day and night) and different operating conditions (power surplus and shortage). In this study, the roles and functions of each agent are defined while building the model. The main conclusion of this study is the effectiveness of the proposed multi-agent control system for smart grid applications due to the negotiations and coordination skills between the smart grid control agent (SGC) and the other agents. Y. Eddy et al. [33] have presented a MAS for a distributed management of microgrids. The proposed MAS based on the IEEE FIPA (IEEE Foundation of Intelligent Physical Agent) standards to coordinate the market operations between the different the microgrids. The model results have emphasized the effectiveness

of the multi-agent system and its applicability to support the autonomous microgrid operation. The proposed MAS consists of a DG (Distributed Generation) agent, Load (Demand) agent, MCE (Market Clearing Engine) agent, CO (Coordination) agent, UG (Utility Grid) agent and other ancillary agents as shown in Fig. 1.10. The main role of each agent is defined in the study while all of the physical power components have been modeled using the MATLAB/SIMULINK software. The CO agent, which is called a MACSIMJX (Multi-Agent Control for Simulink Java Extension). The MACSIMJX performs the coordination between the MATLAB/SIMULINK software and JADE platform and manages the agent task force. T. Logenthiran et al. [34] have proposed a multi-agent system for the energy resource scheduling of an isolated power system with distributed resources, which consists of microgrids and lumped loads. The energy resource scheduling consists of three main stages; the first stage is the modification of each microgrid to satisfy its internal loads. The second stage consists of finding the optimal economic bids to export the power to the whole network while taking into consideration the competition of energy sales prices. The last one is the rescheduling of each microgrid to satisfy the total demand. The simulated system consists of three microgrids with distributed resources and five lumped loads. The proposed multi-agent allowed obtaining an efficient energy management system with the minimal possible cost. The studied system is implemented via a FIPA compliant JADE open source platform. The same multi-agent control system has been extended by the same authors and applied for the real-time operation of a microgrid in the RTDS (Real-Time Digital Simulator) [35].

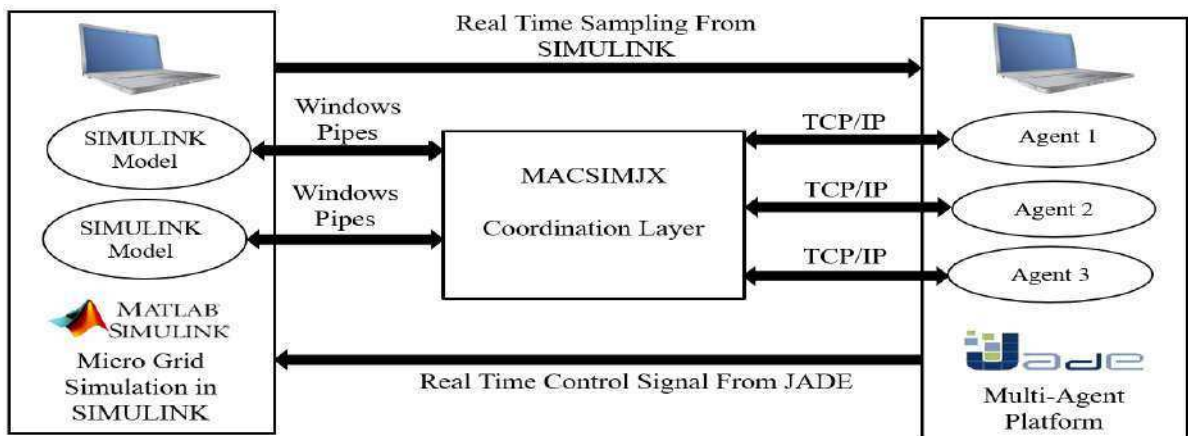


Fig. 1.10. Schematic diagram of Multi-Agent System with MACSIMJX interface [33].

The simulated power network consists of PV modules, fuel cells, DC-DC Converters, Inverters, critical loads, energy storage, and the main grid as shown in Fig. 1.11. The multi-agent control system has been designed to forecast the sources availability and the load level to manage the power feeding in between microgrids economically and reliably as shown in Fig. 1.12. H. Shirzeh et al. [36] have presented a MAS for the management of the renewable energy resources and power storage systems connected to the distribution network. The MAS managed the connection and disconnection of the resources using the plug-play algorithm to achieve the balance between supply and demand.

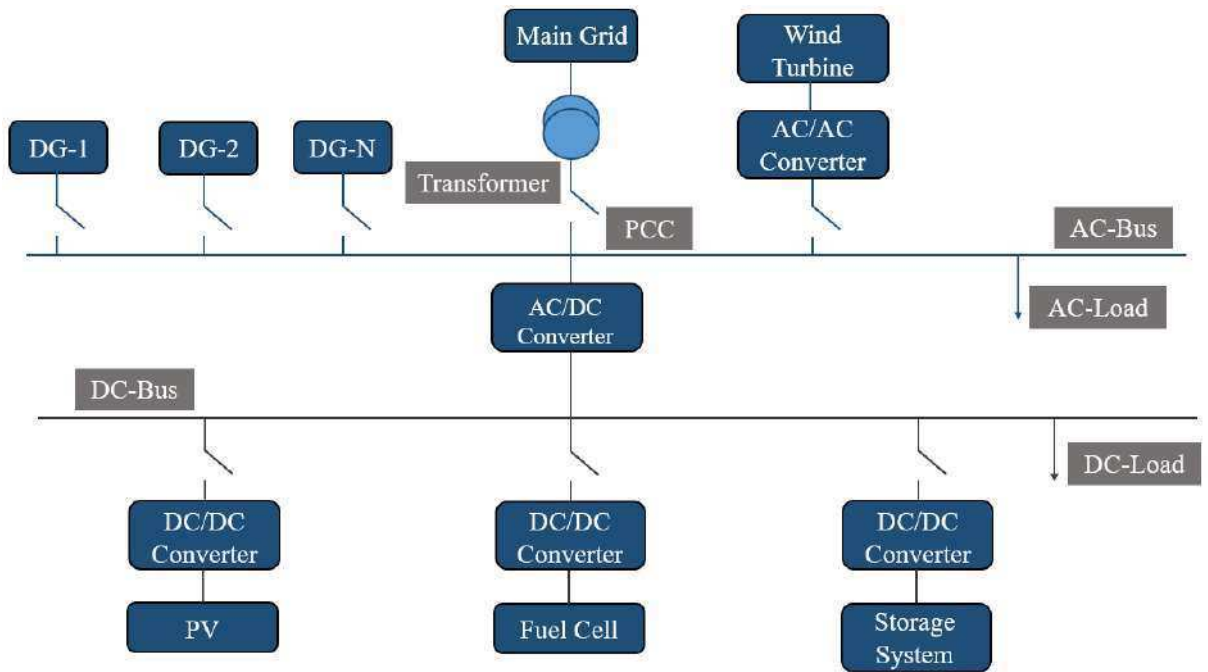


Fig. 1.11. Schematic Diagram of the Hybrid Micro-Grid Simulated using RTDS [34].

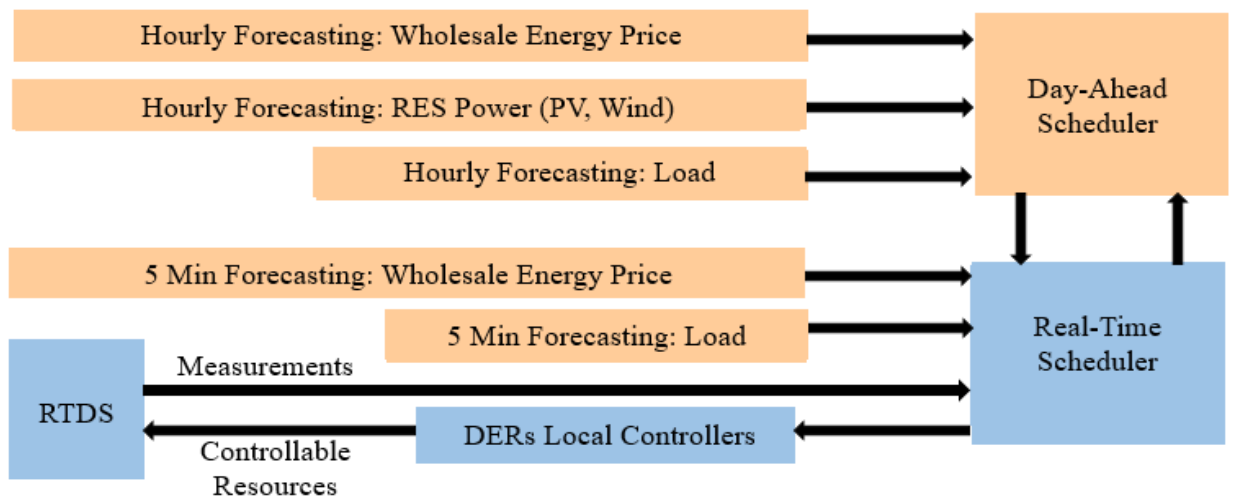


Fig. 1.12. The Real-Time Operational Architecture of the MAS Micro-Grid Management [34].

The proposed MAS has been validated by using an IEEE 34 test feeder network that has been modeled by using a PSCAD platform. The MATLAB/SIMULINK has been used for the modeling of the integrated renewable sources that also provide the interface between the PSCAD and the JADE platform of MAS. The simulation results have shown the effectiveness of the proposed MAS management for the balancing of the power.

K.Wu et al. [37] have presented a multi-agent based energy coordination control system for grid-connected large-scale wind – photovoltaic power generation units. The system has been designed to address the challenges of low operation efficiency, poor stability, and complex decision making. The adopted system based on negotiation model for contract net protocol with the non-fixed client-server cooperative mechanism among agents. The energy coordination process solved the global optimal energy distribution plan of the system by considering the self-constraint and the control objective of each agent. The proposed improved particle swarm algorithm has enabled the system optimization to achieve the maximum economic benefits thanks to the stable operation.

T. Dethlefs et al. [38] have addressed the construction of an efficient distributed optimization algorithm in conjunction with generic software architecture. A distributed multi-agent architecture has been presented with a generic consumer model and an energy exchange market as well as further roles and components. Ant colony algorithm has been used as a tool to optimize the energy consumption in a nature-inspired self-organizing way. This approach has been used to enable the energy consumption of a group of heterogeneous loads to be balanced with the available wind power plant generation. The definition of (DSM) has been presented by P.Palensky et al. [39] as a portfolio of measures to improve the energy system on the side of consumption. It ranges from improving energy efficiency by using better materials, to settling smart energy tariffs with incentives consumption patterns, and even a sophisticated real-time control of distributed energy resources. This study has also overviewed all the techniques of DSM, the latest studies, and the projects. B. Menon et al. [40] have presented a sophisticated fuzzy MAS approach for the representation of distributed energy sources. A co-operation algorithm has been devised to understand how efficiently the agents work for each other. Based on preset rules and definitions, the agents of the MAS have decided how much power each source had to



contribute to the varying load conditions and co-operation between agents by using the JADE platform. A five-layered FLC (Fuzzy Logic Controller) has been designed to implement this decision-making ability of the agents. J. Lagorse et al. [41] have presented an EMS (Distributed Energy Management System) to control the energy flow of a HES (Hybrid Energy Storage System). The HES consisted of photovoltaic modules, fuel cells, batteries, supercapacitors and the load. The distributed controller based on a MAS technology, which has been used to manage the collaboration between all the HES elements to reach the global coordination. The detailed description of the agents has been presented in the study. The battery agent has been designed based on a fuzzy logic controller to manage the charge, discharge and to protect the battery considering its SOC (State of Charge) and the DC bus state. C. Nguyen et al. [42] have proposed a distributed algorithm for service restoration, with distributed energy storage support, following fault detection, location, and isolation. The distributed algorithm based on the principle of the intelligent agent while the proposed system consisted of two main agents. The first was the switch agent who has the main function of fault detection, location, and isolation then restoration of the load. The second was the distributed energy storage agent, which supported the system in both grid-connection and isolation operation modes. Two case studies on the modified IEEE 34 node test feeder have been presented to validate the efficiency of the proposed system. H. Kim et al. [43] have proposed a multi-agent system for autonomous microgrid operations. They have designed the functionalities of the agents, interactions among agents and an effective agent protocol. The proposed system has been implemented by using an ADIPS/DASH framework as an agent platform. The proposed multi-agent system for the microgrid operation, based on the proposed scheme, has been tested through the internet to show the functionality and feasibility of a distributed environment. J. Lagorse et al. [44] have proposed a distributed management system based on the paradigm of the multi-agent system. After reviewing the previous studies, the application of the MAS to power management in a hybrid power source has been presented. The MATLAB – Simulink State-Flow toolbox has been utilized as a MAS platform. The selection of the state-flow basis, in contrast to object-oriented languages (including Java) as the second choice, has preferred in the case of very large systems where the

communications are very advanced. Figure. 1.13. shows the state-flow representation of the proposed MAS. The main conclusion of this study is the ability of the state-flow diagrams to be rapidly used on a real system through, for example, the rapid prototyping solution proposed by the dSPACE company. S. Jin et al. [45] have developed a thread group mechanism to implement highly granular multithreaded computation in an open source smart grid simulator, based on a next-generation agent. The performance of the multi-threading code showed very favorable scalability properties, resource utilization and much shorter execution time for large-scale simulation of the complex power grid. M. Narkhede et al. [46] have reviewed the latest applications of the multi-agent system in operation and control of a smart grid, presenting its future scope in the smart grid's applications. I. Chung et al. [47] have presented the development of a microgrid control system using MAS, as well as the demonstration of the demand response programs during a power shortage. In the proposed MAS, the agents have been implemented using microcontrollers. The Zigbee wireless communication technology has been applied for efficient data communication in the MAS. The study concluded that the power system models of the distributed generators and loads could be implemented in the real-time simulator using the Opal-RT system. The whole test system, which includes real-time system simulation and agent hardware, has been implemented in a hardware-in-the-loop simulation framework. A. Zidan et al. [48] have applied the smart grid concept and technologies to construct a self-healing framework for the smart distribution network. The proposed multi-agent system was designed to locate and isolate the faults, then decide and implement the Switching operations to restore the out-of-service loads. The proposed MAS based on two main layers: the zone agents and the feeder agents; the functions of each one has been defined. The simulation results have shown the effectiveness of the proposed control framework. A. Álvarez et al. [49] have presented a management system for an utility-connected low-voltage microgrid composed of three nodes: a wind turbine, battery, and a variable load. The microgrid has been managed by a three-layered hierarchical automation system: the RMU (Remote Monitoring Unit) layer, the iNode layer, and the iSocket layer. The automation system has permitted two possible control modes: a centralized mode and a distributed mode. The study has presented the description of each layer and their communication protocol.

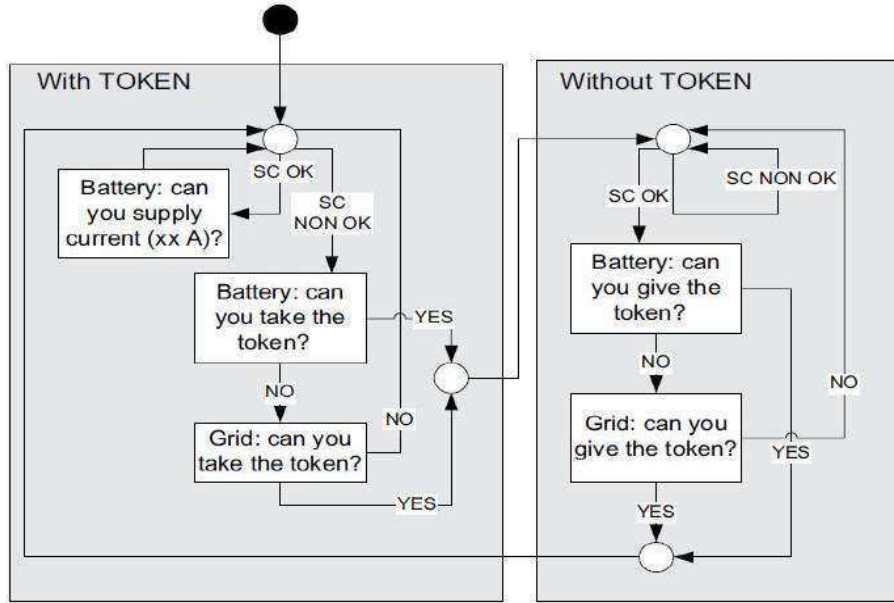


Fig. 1.13. The Proposed Simplified State-Flow Agent Representation [44].

Y. Xu et al. [50] have proposed a fully distributed multi-agent based load restoration algorithm. In obedience to the algorithm, each agent makes a synchronized load restoration decision according to the discovered information. During the information discovery process, agents only communicate with their direct neighbors, and the global information is discovered based on the Average-Consensus Theorem. This way, total net power, indexes, and demands of loads that are ready for restoration can be obtained. Then the load restoration problem can be modeled and solved using existing algorithms for the 0–1 Knapsack problem. The knapsack problem is a problem in combinatorial optimization; given a set of items, each with a mass and value, determine the number of each item included in a collection so that the total weight is inferior or equal to a given limit and the total value is as large as possible. The 0–1 Knapsack problem is a type of optimization technique, which allows two possibilities, based on the role of each item: accepted as one and rejected as zero. Z. Zhou et al. [51] have simulated an electricity market with DR (Demand Response) for different types of commercial buildings by using ABMS (Agent-Based Modeling and Simulation) techniques. The study has focused on the consumption behavior of commercial buildings with different levels of DR penetration in different market structures. The results indicated that there is a noticeable impact on commercial buildings with price-responsive demand on the electricity market. This impact

differs with different scales of DR participation under different levels of market competition. Z. Xiao et al. [52] have presented the challenge of the distributed control of a modern electric grid incorporating clusters of residential microgrids; a hierarchical MAS has been proposed as a solution. The issues of how to realize the hierarchical MAS and how to improve coordination and control strategies have been discussed. The British Telecom Labs developed Zeus MAS framework, which consists of an API (Application Programming Interface), code generator, agent and social monitoring tools, programming documentation, and three case studies (including a sample fruit market). The platform has been written in Java and is an open-source [53]. Based on MATLAB and ZEUS platforms, bilateral switching between the grid-connected mode and the island mode has performed under control of the proposed MAS.

J. Kodama et al. [54] have proposed a multi-agent system based on the CNP (Contract Net Protocol), intended to achieve a distributed approach for the restoration of the power distribution networks. In the proposed system, agents have been assigned to areas sectioned by switches and constantly exchanged environmental information between themselves. The information has been used to construct a CNP overlay network to guard against network accidents. A genetic algorithm optimized the parameters of the CNP required for robustness and effectiveness of the operation phase. When a network accident occurs, the agents restore the power distribution service autonomously through the constructed CNP overlay network. The simulation results have indicated that the CNP exhibits the effective restoration of the distribution network thanks to the cooperation among agents. Z. Jiang [55] has presented an agent-based power-sharing scheme for active hybrid power sources. The simulation studies have investigated the effectiveness of the proposed agent-based scheme. The studied system is a hybrid power source that can be used in a solar car as the main propulsion power module. The results have indicated that an agent-based control framework is an effective tool for the coordination of the various energy sources and the management of the power/voltage profiles. The same author has presented an agent-based control framework for the distributed-energy-resource microgrids [56]. The features of the agent technology have been discussed with its application on the agent-based control framework for the distributed energy resources (DER) microgrid. The effectiveness of the proposed framework has

been analyzed by the simulation studies on a dc-distributed energy system. The simulation results have indicated that the agent-based control framework is effective for the coordination of the various distributed energy resources, the management of the power and the voltage profiles. R. Lum et al. [57] have demonstrated an agent-based approach using the contract-net protocol to control a distributed energy resources system. The software simulation has been performed with the necessary communication and coordination structure to create scalable and robust management. The negotiations between agents have implemented the distributed coordination to satisfy power demand. S.Abras et al. [58] have presented the principles of the home automation system (HAS). The main objective of home automation is the power management that adapts the power consumption to the available power resources according to the user comfort and the cost criteria. The proposed system based on a multi-agent paradigm. Each agent has embedded into a powerful resource or equipment, which may be an environment (thermal-air, thermal-water, ventilation, luminous) or a service (washing, cooking). The cooperation and the coordination between the different actions of the agents enabled to achieve an acceptable and near-optimal solution. The control algorithm has been decomposed into two complementary mechanisms. The first is the emergency mechanism, which protected from constraint violations. The second mechanism is the anticipation mechanism, which computed the best set points according to the predicted consumptions and productions following the user criteria. The study has detailed a negotiation protocol used by the two mechanisms and has presented some preliminary simulation results. L. Tolbert et al. [59] have presented a scalable multi-agent paradigm for controlling a distributed energy resources. The proposed MAS main goals are higher system reliability, a better power quality, and more efficient power generation and consumption. This study has designed a dynamic hybrid multi-agent system as a tool to achieve the control scalability of a large power network (generation, transmission, load, and compensation sources). Ancillary agents have been developed for system stability, harmonic and reactive current compensation. F. Brazier et al. [60] have discussed the compositional development method DESIRE to analyze, design, implement and verify a multi-agent system capable of negotiation for load management. F. Ygge et al. [61] have proposed a decentralized approach to the problem of power load

management by modeling it as a computational market. The proposed approach is very efficient and scalable, has a superlinear rate of convergence to the equilibrium, and requires few iterations even when the number of agents is in the order of one thousand.

## *2.2. Renewable Energy Resources Intermittency with Energy Storage Systems Integration and Electric Vehicles*

T.R. Ayodele et al. [62] have discussed the problem of wind power intermittency and the mitigation techniques using different energy storage technologies. This study has presented the growth rate of the integration of wind energy into the power grid and the future trends. In 2014, a joint venture between Mitsubishi and Vestas announced a single wind turbine generator of 8 MW. It had envisaged that a single wind farm in the capacity of over 1000 MW might be possible in the future. The effect of the integration of this amount of variable wind power on the main grid must be considered especially on the grid stability and power balancing techniques. Due to the study, the integration of energy storage systems can be a solution to the energy balancing and the grid stabilization problems. There are different energy storage techniques with different features and characteristics. J.O. Petinrin et al. [63] have reviewed the energy storage systems used with smart grids and their effects on the system performance from different points of view as Shown in Table 1.6. The following points represent the conclusion of this review:

- Wind power intermittency is not a concern when the penetration level is inferior to 10% of the total load. However, in the case of high penetration level ( $>20\%$ ), the regulation capacity of a control area will reduce. Hence, additional control may be required to maintain the integrity of the grid.
- A suitable energy storage device combined with the wind turbines can firm and shape the wind power output, transforming the wind generation into a firm and predictable energy source. It has concluded that no single storage technology can meet up with all criteria. Thus, the hybrid energy storage system is being explored as a potential solution. This point of research can be generalized not only for wind power generation systems but also for all types of renewables.

System	Principle	Advantages	Disadvantages	Applications
Flywheel	Utilizes the kinetic energy stored in a high inertial mass	Little environmental impact, long life, insensitive to a depth of discharge, high peak power capacity, high efficiency, and rapid response	Low energy density, high rate of discharge, and high cost	Active and reactive stability control
Pumped Hydroelectric Storage (PHS)	Uses up water level reservoir to store energy	Moderate efficiency, long storage duration, large capacity, long life, and low cycle cost	A site with a specific topology, large land use, high capital cost, and adverse effect on the environment	Energy management, Frequency control, and reserve provision
Compressed Air Energy Storage (CAES)	Use pre-compressed air to store energy, 40% less gas fuel for gas turbine generator	High energy and power capacities, moderate long storage duration, moderate capital cost, quick startup, moderate efficiency, and long life	Adverse environmental impact requires burning fossil fuels, difficult to site, and slow response	Energy management, frequency control, and reserve provision
Superconducting magnet (SCMES)	Stores energy in a direct current (DC) magnetic field	High energy and power capacity, short response time, long lifetime, very high efficiency	Requires to be kept at a low temperature, low energy density, high capital cost	Power quality improvement, angular stability control, and voltage support
Supercapacitor	Kind of energy storage device with high capacitance, thousands of times larger than the conventional	High power density, fast response, moderate efficiency, and long life	Expensive, low energy density, limited power system applications, and high discharge rate	Power quality, stability control, and voltage support
Batteries	Customer-side electrochemical energy storage devices with different types Sodium-sulfur (Na-S), Nickel Cadmium (Ni-Cd), Lithium-ion (Li-ion), Zinc bromide (Zn-Br)	High energy density, high efficiency, fast response speed with large storage facility	Expensive, short lifetime, definite operating conditions for charging and discharging, safety and environmental issues	Voltage support, stability control, and load leveling
Vehicle to Grid (V2G)	Utilizes the energy storage system in electric vehicles (Batteries, Supercapacitors or hybrid)	User-friendly, plug and play technology	Still an immature technology, high cost, complex control system	Distributed generation microgrids, and smart grid systems

Hydrogen	Electrochemical process for hydrogen production which is stored to be used as a fuel cell source or gasification	Duality with electricity, storable, few environment impacts, transportable, moderate efficiency	Cost and safety issues	Microgrids, electric vehicles, and electric ships
----------	--	---	------------------------	---

Table 1.6 Different Energy Storage System Technologies Characteristics [62], [63].

A literature review dealing with the excess energy storage methods and the analysis of their effective utilization has been carried out by M. Ismail et al. [64] The review has shown that considerable amounts of excess energy can be left unutilized because of running hybrid renewable energy systems. Some studies have suggested dumping the excess energy through dumped loads while others have proposed utilizing this excess energy. Various methods have been proposed for this purpose. For grid-connected hybrid systems, any excess energy can be injected into the grid. In a standalone operation, one of the proposals is to use the excess energy to produce hydrogen, using electrolyzers, to be stored in hydrogen storage tanks and utilized by the fuel cells when there is a shortage in the power supply. Water heating, water pumping, and space heating-cooling systems are other alternatives to utilize the excess energy. For some special cases, it has proposed that the excess energy could be used for water desalination. Studies also have revealed that the COE (Cost of Energy) can be reduced if this excess energy is utilized. In this study, scenario-based case studies have been carried out to relate the cost of energy production to the utilization of the excess energy for various hybrid system configurations. Analyses of specific systems in both the Palestinian and the Malaysian case studies have shown that there is a considerable reduction in the COE production when the excess energy is utilized. Robert L. Fares et al. [65] have used two lithium-ion battery modeling circuits (Fig. 1.14) to assess the withstand ability and lifespan of the studied grid islanding by using the experimental data collected from an Austin, Texas smart grid test-bed. A comparison between three battery capacities of 25 kWh, 50 kWh, and 75 kWh with photovoltaic integration has been performed based on the model. The battery banks have been used near the distribution transformers that are called CES (Community Energy Storage). The smart grid under study consisted of 21 homes in Austin, Texas with rooftop PV modules and its load consumption. The data of this smart grid have been collected with a one-minute resolution. The following points can summarize the main conclusion of this study:



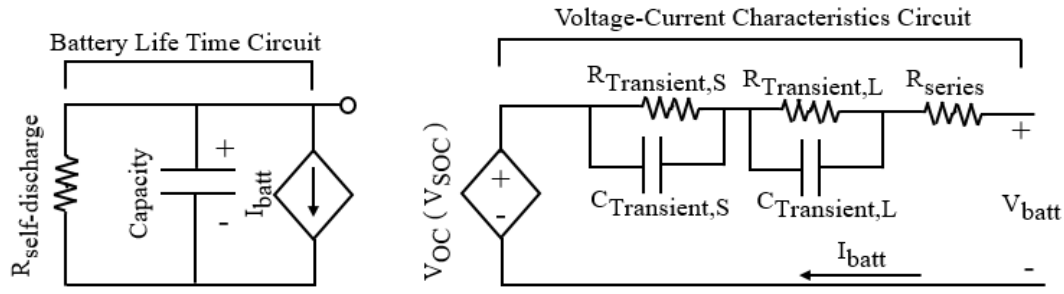


Fig. 1.14. Lithium-Ion Battery Proposed Modeling Circuits [65].

- Increasing photovoltaic integration does not affect the withstanding time in the case of evening peak load.
- Adding CES with photovoltaic lengthens the withstand lifetime.

Tao Ma et al. [66] have proposed a HES, which combines a battery for long-term energy management and a supercapacitor for fast dynamic power regulation applied to the renewable energy power supply systems of a remote area. The performance of the proposed system has been theoretically investigated using the MATLAB/Simulink software. The practical verification has been analyzed by using an experimental test bench. The results have shown that the battery is the primary source of energy for long periods and the supercapacitor worked as the auxiliary power source to smooth the peak power. This system combined the high power and energy densities of the battery and supercapacitor as shown in Fig. 1.15 with the extension of the battery life as well. The hybrid battery-supercapacitor energy storage system can be integrated with the remote, isolated power systems integrating renewables as power sources. M.Suberu et al. [67] have presented an extensive review of the three different state-of-the-art kinds of ESS (Energy Storage Systems); Pumped hydroelectricity storage, batteries, and hydrogen. The main function of these systems was the mitigation of intermittency in RE (Renewable Energy) sources. Within the context of the review, advantages, and disadvantages of the various technologies have also been presented. Additionally, it has also pinpointed the different areas of applications of ESS for RE integration and has offered a summary of factors to be considered in the selection of the appropriate energy storage technology for either commercial or domestic application. This study has concluded that ESSs selection depends on the performance characteristics and the used fuel source, as well as that no single ESS can meet all the possible requirements to be called a supreme ESS.

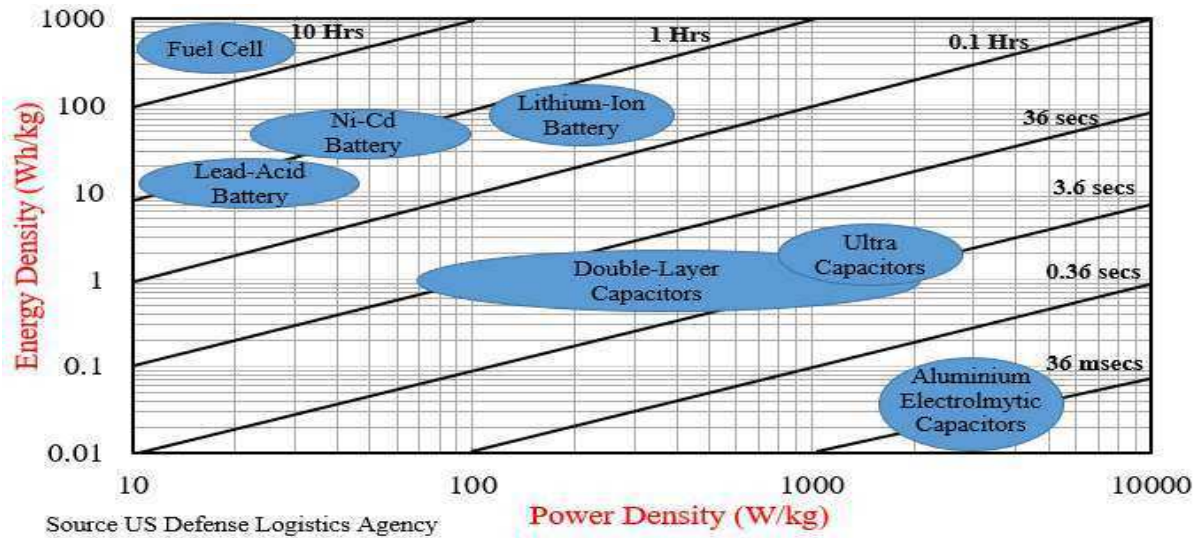


Fig. 1.15. Power-Energy Density Curves of The Different Energy Storage Systems [66].

S. Hasan et al. [68] have presented a comparison between four different kinds of energy storage technology: compressed air, flywheel, hydrogen, and superconducting magnetic to solve the problem of wind renewable energy system intermittency. The compressed air system can be used as bulk energy storage to provide constant active power even at a low wind speed compared with flywheel, hydrogen and superconducting magnetic systems. It requires a suitable control and thus needs to be only switched on at low wind speed and high demand. The flywheel and the superconducting magnetic systems can enhance the quality of the active power by absorbing the surplus power at high wind speed to be used at low wind speed with the suitable charging and discharging control of the DC link. The hydrogen system can be coupled with a stochastic power generation to improve the performance of a weak grid system. B. Ge et al. [69] have proposed an energy-storage-system-based power control of grid-connected wind farm to improve the intermittency. The proposed energy storage system has been designed to improve the power quality and the stability of the power system. The energy storage system used the VRFB (Vanadium Redox Flow Battery) that is suitable for large-scale power energy storage due to its advantage of maintaining stable terminal voltage under a wide state SOC range (within 20–80%). The results (theoretically and experimentally) have shown the effectiveness of the VRB energy storage system on smoothing and stabilizing the power even under severe wind power variations. S.Kamali et al. [70] have discussed the different applications of electrical energy storage technologies in the smart power systems emphasizing on the collaboration of such entities with the renewables. The role of ESS in intelligent

microgrids has also been discussed especially the effect of renewables stochastic nature on the power quality. The concerned technologies are the flywheel, the electrochemical systems, the pumped hydroelectric, and the compressed air, with presenting their operating principles. The application of each type in the power system area has been investigated and compared. A. Foley et al. [71] have presented a review of the latest research activities in the smart grids involving renewable energy sources and electric vehicles. This study has concluded that there are weak points regarding the delivery of sustainable renewable energy sources, the future using of energy storage systems, and the smart grid technology due to the lack of:

- International standards
- Real competitive market environments
- Government and regulatory policy
- Limited product realization and commercialization, particularly at the distributed level.

O. Onar et al. [72] have designed and modeled a wind/FC (Fuel Cell)/UC (Ultra-Capacitor) hybrid power system for a grid-independent user with an appropriate power flow controller. The intermittency of the wind power has been enhanced by the integration of the FC/UC system. When the wind-generated power is higher than the load demand, the surplus power has been used to feed the electrolyzer to generate hydrogen. In case of energy shortage, the stored hydrogen has been fed to the fuel cell for electricity generation. The ultra-capacitor has only been used to compensate the peak load.

A. Aktas et al. [73] have proposed a hybrid energy storage system composed of a battery and an ultra-capacitor supplied from a photovoltaic power source. The proposed energy storage system has been used to enhance the intermittency of photovoltaic generated power. The studied system has been modeled under two operating conditions as follow:

- When the generated PV power was higher than the load demand, the surplus power was used to charge batteries.
- When the generated power was lower than the load demand, the shortage of power has been met by the battery. Due to the slow response of the battery concerning the transfer from charging to discharging mode, the ultra-capacitor has been used to cover the sudden increase in the load until the battery gets in the mode.

The hybridization of the battery and the ultra-capacitor enhances the system performance while reducing the energy storage system cost and ratings. F. Mwasilu et al. [74] have presented an intensive review of the EVs (Electric Vehicles) interaction in the smart grid infrastructure. The integration of the renewables with the EVs has been discussed, and it has noted that the electric vehicles can provide ancillary services to the grid. These services are the voltage and the frequency regulation, leveraging of the real power, the reactive power support to enhance the operational efficiency, the electric grid security, and the reduction of the power system operating cost. The review has discussed the infrastructure of the smart grid, involving electric vehicles, especially the advanced communication, the control, and the metering technologies. The effective V2G (Vehicle to Grid) operation mode must take into consideration the challenge of battery wearing under frequent charge-discharge cycles. The latest studies have announced the promising results of lithium-ion batteries in this application. L. Drude et al. [75] have analyzed the peak demand energy market for a V2G in the urban region of Florianopolis, Brazil. The study has described the known V2G-concepts and has introduced two different dispatch strategies developed for the Brazilian energy market in the light of new 2014 tariff regulations. It has turned out that the electric-vehicles can be used as a grid-stabilization strategy, but the announced tariff regulations may lead to a destabilization if there are too many cars offering their internal storage for V2G grid support. Adequate energy policy strategies must be introduced to avoid the conflicts of interest that might stem from the different perspectives of grid operators and EV owners. In contrast to the previous analysis, this research has assumed the battery degradation has a function of the DOD (Depth of Discharge), which is known for a specific battery.

### *2.3. Smart Grid Advanced Control*

The reviewed advanced control techniques have been applied to two types of smart grid topologies: the single smart microgrid and the smart multi-micro grids.

#### *2.3.1. Single Smart Micro Grid*

R. Arulmurugan et al. [76] have modeled and designed a fuzzy logic controller based on Hopfield NN (Neural Network) for PV maximum power tracking under partial shading of PV modules. The partial shading of PV modules changes the system parameters which requires the adaptation of the fuzzy logic controller

membership functions. The Hopfield neural network has been used to adapt the controller. The effectiveness of the proposed controller has been verified theoretically by the MATLAB/SIMULINK model and practically by a prototype of the system with the possibility of using the adaptive fuzzy in the future. M.Farhadi et al. [77] have proposed an adaptive energy management method for a redundant hybrid DC microgrid to reduce the pulse load mitigation. This study has analyzed and compared between three energy management methods study as follow:

- DVC (Direct Voltage Control): in this method, one converter has been used to fix the grid voltage while operating at maximum power under load pulse. It is a simple method, but it is disruptive to the system.
- CCA (Continuous Current Averaging): this method passes on the rule of the equality between the power consumed from the grid to the average required load power under pulse load. The bus voltage variations have been kept within certain limits to solve the DVC method disruptively. The CCA method cannot track the pulse load variations, and it suffers from an accumulation error in the control of the grid with high redundancy that can cause severe under or overvoltages.
- AEC (Adaptive Energy Calculator): this method calculates the total required current that must be injected by the converters based on the consumption and the supercapacitor bus voltage. The average current of the pulse load ( $i_{pav}$ ) per pulse duration  $T$  is calculated to improve the CCA method error accumulation while the average voltage is modified within a certain limit.

The main objective of the real-time EMS (Energy Management System) proposed in this study is to define the best control mode and set the current or the voltage set points of each converter. The set points definition based on the required power from the grid, the availability of the sources and the state of charge of the battery. The control mode has been defined based on the supercapacitor state (if it is connected, the mode would be current control mode. Otherwise, it would be voltage control mode, giving the priority of voltage control to the converter with the maximum power rating or the grid-connected one). The proposed energy management method has been experimentally tested under different load schemes and grid conditions. The results have shown that

the EMS with AEC technique has caused 0.84% more bus voltage variation than the DVC method. However, it effectively eliminates the high current pulsations of the converter as well as prevents the power and frequency fluctuations of the generator. The proposed method has been tested under the sudden variations of the load pulse duty ratio and compared with the CCA method. The results have shown the effectiveness of the method to adjust the total reference current during the transient time. The bus voltage has been maintained within the limit even if the measurement has a considerable error percent of up to 10%. The proposed method has been tested while disconnecting the supercapacitor, and the results have shown the effectiveness of the method for grid self-reconfiguring by stabilizing the DC grid voltage and power sharing. A. Mohamed et al. [78] have proposed an effective algorithm to optimize the distribution system operation in a smart grid, from cost and system stability points of view. The studied energy commitment problem has been considered as a day-ahead energy management system. The objective was to have the loads feeding at the least possible cost while giving a higher priority to renewable energy sources and keep the battery SOC around a definite value (60% in this case). In this study, the Non-linear regression technique has been used to obtain forecasting models for the wind and the load power by using historical data (last four years data of wind and load power). The MAPE (Mean Absolute Percent Error) has been used to evaluate the accuracy of the forecasting model. It is the difference between the real and the predicted value vectors. The utilized forecasting technique provided MAPE of 2.12% and 2.45% for wind and load power respectively. An adaptive linear time series model has been developed to simulate the last 14 years data of the PV with a MAPE of 0.97%. A fuzzy logic controller has also been proposed, to control the power-sharing between the grid and the battery, and to ensure its healthy operation. The proposed algorithm has a saving economic impact on the consumers with providing the ability of the utility grid demand shifting which is also beneficial to the grid. M. Elshaer et al. [79] have studied some aspects related to the design and the implementation of grid-connected DC microgrids by designing a prototype system. A fully controlled rectifier has been designed to tie the main AC grid to the DC microgrid. The vector decoupling controlled SPWM (Sinusoidal Pulse Width Modulation) technique has been used to maintain a constant output DC voltage for the DC microgrid. The main outcome

of this study is the design of a smart controller that allows a quite stable wide range of loading of the DC microgrid that is important to its operation. A modified DC-DC converter has also been used to allow the simultaneous control of the current and the voltage for power sharing. This smart controller has been adapted for the high-quality integration of the FC (Fuel Cells) energy into a DC-ZEDS (Zonal Electric Distribution System) by A. Mohamed et al. [80]. A comparison between the conventional boost converter and a modified topology boost converter has been presented, to investigate its compatibility with the nature of variable voltage and pulsating current of the fuel cell. Another modified topology of the DC-DC boost converter was compared with the conventional boost converter to integrate the sustainable energy sources into the DC zonal electric distribution systems [81]. The modified topology can provide constant DC link voltage from the different sources with the variable voltage and pulsate current. This topology enhances the performance and the lifetime of the renewable energy system components. A. Mohamed et al. [82] have studied the aspects related to the connectivity of DC microgrids to the main AC grid by utilizing the bi-directional AC-DC/ DC-DC converters. The modified fully controlled rectifier has been used to feed power in both directions from AC to the DC side and vice versa. A vector decoupling controlled SPWM with the proposed smart controller of the wide operating range has been used to control the active and the reactive power. These facilities can control the power flow in both directions at a unity power factor.

### 2.3.2. Smart Multi-Micro grids Control

N. Eghtedarpour et al. [83] have proposed a decentralized control strategy based on a two-stage modified drop method for the control of the IC (Interlinking Converter) interfacing DC and AC microgrids. By measuring the AC microgrid frequency and the DC microgrid voltage and using the proposed drop characteristics, the power management strategy has been provided. This strategy defines the power reference for the IC controller to share between the existing power sources in both AC and DC microgrids depending on the power demand. By using the proposed drop method, the IC can perform the power-sharing between the two microgrids and the transition from grid-connected to island mode. The performance of the proposed method has been demonstrated through

a time domain simulation of a hybrid AC/DC microgrid in the PSCAD/EMTDC software. J. Vasiljevska et al. [84] have presented a control system that has been housed at the HV (High Voltage)/MV (Medium Voltage) substations. The proposed system can also be used for the management of the micro-generation, active loads and energy storage that are subjected to different constraints. Some of these constraints involve inter-temporal relations, such as the ones related to energy storage levels in consecutive time moments. The system functionality has especially been oriented to deal with the stressed MV network operation involving overload and excessive voltage drops situations.

#### *2.4. Smart Grid Stability Analysis and Power Quality*

M. Saqib et al. [85] have addressed the technical issues that arise whenever the wind power is to be integrated into the main grid. These issues, in general, are the power quality and the need for reactive power compensation. Moreover, these issues, in particular, have been explored in the context of a realistic case study for a proposed 50 MW wind farm integration to Pakistan's national grid. The studied systems have been modeled in MATLAB/ Simulink. The study has also highlighted the role of the STATCOM (Static Synchronous Compensator) as a smooth reactive power source for the improvement of the power quality of this wind integrated power system. R. Kamel [86] has presented a comprehensive survey of the FRT (Fault Ride Through) techniques and controllers which already have been implemented and proposed for different types of wind generation systems. The study has proposed, designed and tested three economic attractive FRT controllers to enable FSWG (Fixed Speed Wind Generation) system to overcome and ride through a fault in the isolated microgrid. The proposed controllers are an SFCL (Superconductor Fault Current Limiter), a VRG (Variable Ratio Gearbox), and a modified PAC (Pitch Angle Controller). The results have proved that SFCL only needs 1.5 s to restore system stability, and the maximum speed is 120% of the rated value. The PAC has taken 13 s to restore system stability with 145% maximum speed while VRG has taken 4.5 s to restore stability with 133% maximum speed. The author has also studied the effects of the fault type using the hybridization of the three techniques. M. El Moursi et al. [87] have proposed a novel CVC (Coordinated Voltage Control) scheme that relies on dynamically changing the control topology (Master-Slave) for the distributed generation sources and the OLTC (Online Tap Changer) of the smart grid. The coordination based on the voltage and the reactive



power constraints. The proposed CVC has been tested in steady state and transient response conditions. The tested transient response conditions are the load excursion/reduction and the three phases to ground faults. The results have shown the effectiveness of the proposed scheme in enhancing the voltage profile, maximizing the reactive power reserve up to 62% and improving the FRT ability. The proposed method has also enhanced the transient stability margin by increasing the MCCT (Maximum Critical Clearing Time). M. Sarkhanloo et al. [88] have proposed a new control strategy for a small wind farm to study the transient stability improvement. The considered farm consists of a 2.5 MVA SCIG (Squirrel Cage Induction Generator) based fixed speed wind turbine and a 5 MVA DFIG (Doubly Fed Induction Generator) based variable speed wind turbine. The wind farm has been modeled by using PSCAD/EMTDC software while the DSVM (Discrete Space Vector Modulation) of the DPC (Direct Power Control) has been used to control the DFIG. The proposed control strategy has been tested under grid transients of (Three lines-ground and two lines-ground faults). The simulation results have shown the effectiveness of the proposed technique by putting forward a reduction of the speed acceleration of the SCIG and reducing the DC-link voltage of both the DFIG and the rotor currents during the transient conditions. M.Kyaw et al. [89] have studied the fault ride through and voltage regulation of grid-connected wind farms. The grid codes for the integration of a wind farm focuses on the following points:

- Continuous voltage operating range must be from 0.9 p.u. to 1.1 p.u.
- Voltage fluctuation range of  $\pm 5\%$ .
- Reactive power capability from 0.09 (Lag) to 0.9 (Lead).
- Fault ride through. (The time when the wind turbine must be connected even under voltage sag due to grid transients such as faults varies from country grid code or standard to another)

An aggregated model of grid-connected (2 MW\*250) DFIGs driven by wind turbines has been used to study the effectiveness of the proposed control method to enhance the FTR (Fault Ride Through) ability during grid faults and voltage regulation under wind variations. The control based on the DFIG converter and the pitch angle controllers. The results of the study have exhibited the enhancement in voltage regulation and fault ride through and tracked the maximum power.

## 2.5. *Smart Grid Modeling, Simulation, and Representation*

As aforementioned, the smart grid can simply be considered as a power system infrastructure with advanced ICT (Information and Communication Technology) to facilitate monitoring and controlling the network from the generation to the customer's sides. The main purpose of the advanced smart grid is to have the ability of the intermittent renewables integration while guarding the power system stability and the continuity of load feeding. The electric vehicles with their V2G and G2V operation modes are very useful techniques as a flexible energy storage system for the smart grid. The smart grid model must have the ability to describe the conventional sources, the renewable energy sources, the energy storage systems, the information and the communication system, and the smart metering. There are many difficulties and challenges of smart grid modeling which can be summarized in the following points:

- The grid stability and reliability analysis require a simulation period of hours or days. One of the challenges is the ability to model very high switching frequency power electronic converters, which are the main power handling tools in the smart grid with acceptable computational costs.
- The smart grid (with its different layers) must have the ability to investigate the effect of the communication time delay on its performance.

One of the proposed smart grid modeling methods is the real-time simulation. In the following paragraphs, a brief review of the latest real-time simulation studies is presented. F. Guo et al. [90] have presented the latest state-of-the-art technology concerning the smart grid real-time simulation. The real-time simulation platform presented in this study has utilized a switch event interpolation solver, and parallel computation technologies, combined with advanced hardware to simulate hundreds of switches at switching frequencies up to 10 kHz. By combining the advanced power system simulator with the state-of-the-art network simulator, the system can simulate the communication networks in the smart grids. The case study of the modeled smart grid contains LES (Local Energy Storage) batteries, PV modules, a wind energy conversion system, power conditioning converters, and solid-state switches. The results have been divided into two schemes as follow:

- Without communication latency, which has shown the effectiveness of the proposed model in simulating the system with a high number of switches and

high switching frequencies of 10 kHz for a long period to study the slow response phenomena.

- With communication latency, which utilizes a SITL (System-In-The-Loop) OPNET software to simulate the communication networks with the power network at the real time. The results have shown the effects of the communication delay on the power system performance. This real-time simulation can be used to study the new control strategies and the dynamic reconfiguration of both communication and power networks within the smart grid.

W. Li et al. [91] have studied the real-time simulation of a wind turbine generator coupled to a battery-supercapacitor hybrid ESS. The advantages of the RT (Real-Time) simulation over offline simulation programs (according to the study) are as follow:

- High computational power with the high-speed I/O modules of the RT simulator.
- The real-time simulation provides the ability to simulate the slow response phenomena besides the capability of modeling the high switching frequencies power converters with time step ranges of nanoseconds and microseconds.
- The HIL (Hardware In Loop) simulation can accelerate the control prototyping cycle with a lower cost compared with the physical setup or field tests.

The real-time simulation has been used in this study to model a hybrid vanadium-redox flow battery with a supercapacitor energy storage system. The permanent magnet synchronous generator has been mechanically coupled with the wind turbine to investigate the variable power smoothing. The hybrid ESS and wind systems have been tied to the main grid via IGBT power electronics converters. The HIL simulator has simulated the total plant while another real-time simulator platform has been used for the system controller modeling.

There are a lot of interactions and relationships between all of the physical domain components in the smart grid. The simple representation of these reactions enables the better system operation understanding and the effective control schemes design. The EMR (Energetic Macroscopic Representation) is a graphical representation of the system based on the action-reaction principle (their product represents the instantaneous power). EMR has been developed to describe the complex electromechanical systems at the University of Lille in France since 2000. It is a very simple technique of system representation and has a group of principles and elements

[92], [93]. The following paragraphs present a brief review of the different system topologies EMR representation. A. Tabanjat et al. [94] have presented the EMR of a hybrid PV-PEM EL (Photovoltaic-Proton Exchange Membrane Electrolyzer) system as a part of a system efficiency enhancement study. The EMR has been used to build the model of the whole system, which consists of electrical, electrochemical, thermal, and hydraulic submodels. J. Solano et al. [95] have proposed a PCS (Practical Control Structure) and energy management strategy of HEV (Hybrid Electric Vehicle) test bed. The electrical system of this vehicle consists of supercapacitors, batteries, and a fuel cell. The PCS has been designed based as a part of the whole hybrid electric vehicles system EMR. The PCS has been used to evaluate the different energy management strategies. In this study, each component in the system (battery, supercapacitors, fuel cell with its all accessories, and power electronic converters) has been represented using EMR. K. Agbli et al. [96] have studied multi-physics modeling of a hydrogen-based electrical energy storage system. The studied system consisted of a PV power generation system and hybrid energy storage (battery-supercapacitor) as the electrical parts. The accessories of the PEM fuel cell are the PEM electrolyzer, the hydrogen storage tank, the buffer tank, the pressure regulator, and the heat exchanger. Each of these components has been represented using EMR individually, and then the EMR of the whole system has been built. The main conclusion of this study is the ability of EMR to represent large systems with different components and multiphysics with the simple entity-by-entity representation and the adaptation of EMR to represent the photovoltaic (PV) modules. W. Lhomme et al. [97] have presented an EMR of a PV power generation system that consists of PV modules, DC filter, two DC-DC converters, a battery energy storage system, and a DC motor driving pump. The MPPT (Maximum Power Point Tracking) control has been used to extract the maximal available power. The EMR has been firstly created by building the EMR of each part and combining all the representations in one form to have the EMR of the whole system. The classical perturbation and observation algorithm has been used as an MPPT While the EMR inversion mode has been used for system control design.

## 2.6. *Smart Grid Communication and Advanced Metering*

K.Reddy et al. [98] have reviewed the integration, control, ICCM (Information Communication, Control, and Metering) technologies in the smart grid. The definition of the high integration of distributed renewable energy sources with their suitable power

converters AC or DC has been presented. The smart control, following the author's definitions, is the maximization of the output energy from each source with the variable climatic conditions. The communication is the adaptation of the suitable communication technology between the different domains in the smart grid. Protocols usually set the communication standards for smart grids, and most of them involve the interconnection of SCL (Secure Communication Line) to the main control unit. The adapted technologies are the LAN (Local Area Network), the HAN (Home Area Network), and the WAN (Wide Area Network). The interconnection should be accompanied by a firewall at various levels for the cybersecurity of the smart grid. The smart metering employed in smart grids provides the additional information about the electrical energy consumed compared to conventional energy meters. The smart metering can measure the energy parameters of the load remotely and transfer the data to the communication network. Y. Yan et al. [99] have studied the background and motivation of communication infrastructures in the smart grid and have summarized the major requirements that smart grid communications must meet. This study has discussed the challenges of the communication system in the smart grid like the Security. The Security is a challenging issue since the on-going smart grid systems are facing increasing vulnerabilities as there is more and more automation, remote monitoring/controlling and supervision entities are interconnected. E. Ancillotti et al. [100] have critically reviewed the smart grid concepts, with a special focus on the role that communication, networking, and middleware technologies could have in the transformation of existing electric power systems into smart grids. This study has presented a conceptual model of the communication systems for smart grids, adopting a data-centric perspective. The functional components, technologies, network topologies and communication services that required supporting smart grid communications have been identified. The fundamental research challenges in this field, including the communication reliability, the timeliness, the data management services, and the autonomic behaviors have been presented. Finally, the main solutions proposed in the literature for each of them have been discussed with identifying the future research directions.

### 3. Conclusion

This chapter presents the literature survey and state of the art concerning the smart grid research and development (R&D) directions that depend mainly on the renewables high integration in the future new policies scenarios. The marine current energy system is a premature technology and still in the research phase. As a result, the tidal turbine is selected to be studied and modeled as the main source of the proposed system energy. The renewables intermittency (mainly, the marine current variations) exhibits many challenges considering the power system stability and the energy continuity especially the stand-alone mode of operation. The energy storage systems and technologies are one of the proposed solutions to the renewables intermittency. The literature survey indicates that there is no one source or technology can meet all the system requirements and the hybridization is the more efficient solution. The hydrogen system is selected as the main energy storage technology due to its characteristics of long charging/discharging cycle (in the range of days and weeks) that are more suitable for the marine current variations. The power system dynamics are faster than the electrochemical hydrogen system dynamics. Thus, it is required to integrate an auxiliary energy storage system to cover the fast electrical dynamics for providing the safe and the secure operation of the hydrogen system components. Based on the surveyed energy storage systems state of the art, the LiFeO<sub>4</sub> Battery system is selected due to its compromise between the supercapacitor high power density and the battery high energy density. The demand side management system is one of the smart grid research direction to provide the efficient utilization of energy. The integration of the marine current energy with hybrid hydrogen-battery energy storage systems is the main objective of the study based on the smart grid architecture model (SGAM). Due to the SGAM, the management system is a vital layer that optimizes the system operation considering the different components constraints and operating conditions. The centralized and the decentralized control and management systems are compared to select the suitable paradigm for the proposed system. The centralized system suffers from the single point of common failure that weakens the system redundancy and reliability. The decentralized multi-agent system (MAS) is selected as the energy management technology to enhance the system scalability and redundancy based its agent paradigm. There are different surveyed MAS platforms while the JADE is the most applied one. The management system (JADE based MAS) represents the function and the business layers of the SGAM. The interface between the physical layer (MATLAB/Simulink model of the proposed marine-hydrogen system) and the function and the business layers

(JADE based MAS) represents the data and the communication layers of the SGAM. The communication topologies and protocols play an important role in the performance of the smart grid as the literature indicates. Hence, the MACSimJX tool is selected to interface the JADE and the MATLAB/Simulink platforms. The physical layer (marine current-hydrogen systems) can be considered as a heterogeneous domain (electromechanical, electrochemical, thermodynamics and electrical). Thus, it is required to select a powerful representation technique for better understanding the interaction in between the different systems. The energetic macroscopic representation, due to the literature, is a simple graphical representation method based on the integral and physical causality principles. Consequently, it is selected to represent the system to be more readable and facilitate the powerful control strategies design.

**Chapter 2**

**Component Layer (Hybrid Marine-Hydrogen System)**

**Modeling and Energetic Macroscopic Representation**





## 1. Introduction

Renewables, as discussed in Ch.1, suffer from severe seasonal, daily and hourly variations that can limit their integration or exhibit more requirements and conditions to have a normal and safe operation of isolated or grid-connected systems. The energy storage system can be considered as an energy buffer for balancing the generation-consumption power difference of the isolated power systems. As mentioned in the previous chapter, there are different energy storage systems, each of which has specified characteristics make it the best choice for a particular function or application (Refer to Table 1.6 of Ch.1). The marine current power generation systems convert the kinetic energy of the water flow mass into electrical energy. Thus, the system has a daily variation due to the change of the marine current speed from ebb to flood. As long as, it suffers from variation during the month from the spring tides (during the full and new moons) to the neap tides (during the quarter moons) as shown in Fig. 2.1. There are different load types (household, agriculture, commercial, industrial) that define the load profiles during the day. The load profiles also change from summer to winter, for example, the household load profile changes from summer to winter by adding the space and water heating. Due to these characteristics and variations of generation and consumption, the selected energy storage system must sustain for long periods of charging and discharging (daily periods). The literature survey and the comparison of the different energy storage system indicate that the hydrogen system can meet these requirements and operating conditions as shown in Fig. 2.2 [101]. The hydrogen energy and fuel cells can be considered as renewable sources and gains more attention all over the world. The hydrogen is a clean and efficient energy carrier with an environmentally friendly nature as the only byproduct is the water [102], [103].

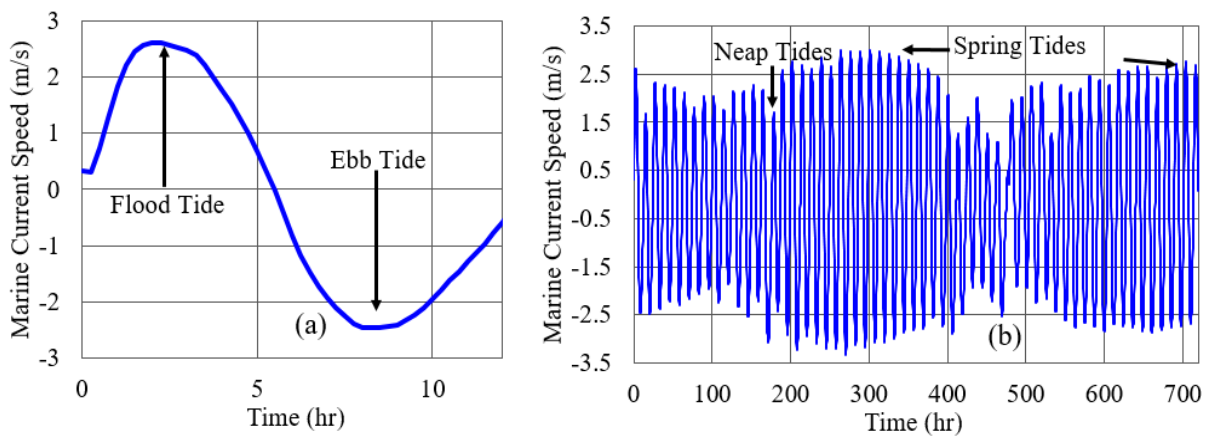


Fig. 2.1. Marine Current Speed General Wave Form during Half a Day (a) and One Month (b).

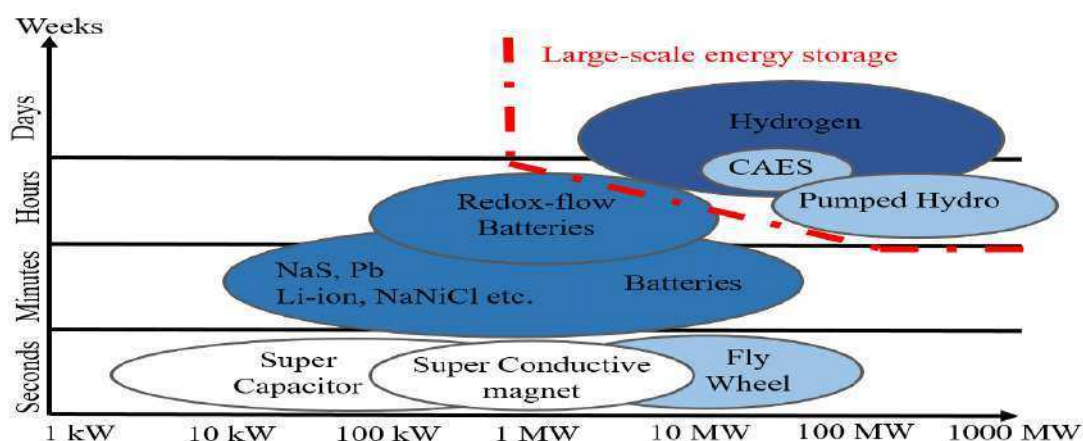


Fig. 2.2. Energy Storage Systems Power and Time Ranges [101].

The hydrogen has the highest energy per unit mass and the minimum greenhouse gas emission compared to the other fuels as shown in Table 2.1 [103]. The hydrogen economy is an expression that is used to indicate the role of the hydrogen system in the future of energy scenario, especially smart grid [102]. The hydrogen system consists of four main subsystems: generation, storage, transmission, and final conversion (or reuse) [101]. The hydrogen generation system is a chemical (or electrochemical) transformation of the input energy into hydrogen. There are different hydrogen generation systems:

- Steam Methane Reforming (SMR),
- Oil/Naphtha Reforming,
- Coal Gasification,
- Water Electrolysis,
- Biological System,

Fuel Type	Chemical Structure	Carbon Content %	Fuel Material (Feedstock)	Energy per Unit Mass (J/kg)	Specific Carbon Emissions (kg C / kg Fuel)
Hydrogen	H <sub>2</sub>	0	Natural gas, methanol, and water electrolysis, biomass	141.9	0.00
Ethanol	C <sub>2</sub> H <sub>5</sub> OH	52	Corn, grains, or agriculture waste (cellulose)	29.9	0.5
Biodiesel	Methyl esters of C <sub>12</sub> to C <sub>22</sub> fatty acids	77	Fats and oils from sources such as Soybeans, waste cooking oil, animal fats, and rapeseed	37	0.5
Methanol	CH <sub>3</sub> OH	37.5	Natural gas, woody biomass	22.3	0.5
Natural gas	CH <sub>4</sub>	75	Underground reserves	50.00	0.46
Gasoline	C <sub>4</sub> to C <sub>12</sub>	74	Crude oil	47.4	0.86

Table 2.1 Fuel Types Energy per Unit Mass and Specific Carbon Emission [103].

The first three are the traditional methods that depend on the fossil fuels and has the disadvantages of greenhouse gas emissions. However, they represent the most utilized methods for hydrogen production (96% of total hydrogen production worldwide) while the last two approaches are environmental friendly nature with a low share in global hydrogen production (4%) as shown in Fig. 2.3 [103]. This chapter presents the smart grid component layer (Domains) modeling based on a case study of an active power generation system considering a hybrid marine current-hydrogen isolated power system configuration. The expression of active power generation system has been used in the literature to describe a hybrid wind, electrolyzer, Fuel Cell and supercapacitor power system [104]. The active power generation system means converting the renewables static intermittent nature into a dynamic system that can survive in all operating conditions by integrating energy storage systems to balance the generation-consumption difference. The considered case study consists of an FFDD-MCT (Fixed Pitch Direct Drive Marine Current Turbine) power generation system, an MW scale PEM (Proton Exchange Membrane) electrolyzer, an MW scale PEM Fuel Cell and the residential loads as shown in Fig. 2.4. The standard household load profile is selected to model an island residential loads variation that provides an isolated power system configuration. This system architecture exhibits the advantage of the generation (MCT) citation near to the load (Island) for avoiding of the main tidal system technical and economic challenge, which is the power transmission system. The MCT system utilizes a PMSG (Permanent Magnet Synchronous Generator) to convert the MCT mechanical energy into electricity and feed it to a DC link via a fully controlled rectifier. The PEM electrolyzer and fuel cell are interfaced to the DC link via DC-DC converters for balancing the power flow between the load and the MCT system as controlled current sources. Three-phase inverter connects the load to the DC-link. The inverter is controlled to feed a constant AC voltage on the load terminals. The PEM electrolyzer and fuel cell time response must be respected for avoiding systems aging and providing the secure operation.

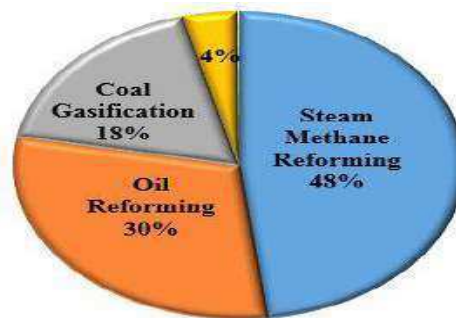


Fig. 2.3. Hydrogen Production Methods Global Share [103].

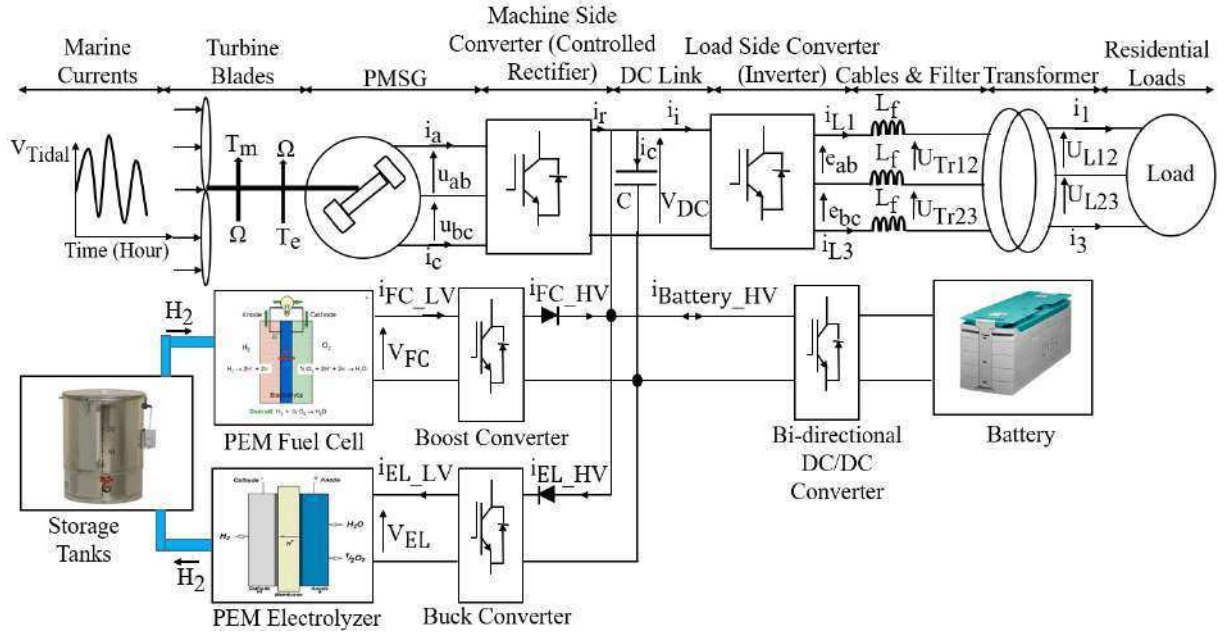


Fig. 2.4. Hybrid Marine Current-Hydrogen Active Power Generation System.

Thus, an auxiliary energy storage system must be integrated to smooth the fast dynamics. The Lithium-Ion  $\text{LiFePO}_4$  battery is connected to the DC-link via a bi-directional DC-DC converter as a voltage controlled source for stabilizing the DC link voltage that is indirectly considered as a power smoothing technique. This technology of Lithium-Ion battery has the advantages of the battery high energy density as long as the supercapacitor high power density. The system consists of many heterogeneous domains components (mechanical, electromechanical, electrical, and electrochemical). The design of the control system requires a well and clear understanding of the relations between all the subsystems. The energetic macroscopic representation (EMR) is used to represent each subsystem and to design the suitable control strategies of the whole system. As aforementioned in Ch1, the EMR was developed in 2000 at the University of Lille in France to describe complex electromechanical systems. It is a very simple representation technique with a group of principles and elements [92], [93]. Since then, EMR has evolved into a more generic tool for representation of Multi-physics systems. It has already been used in many studies [94]–[97], [105]–[109] for representation, modeling, and management of various systems (e.g., Wind and the Photovoltaic (PV) energy conversion systems, Electric Vehicles (EV), hydrogen energy storage system and PEM electrolyzer). The EMR makes the system more readable and well understood based on the integral and physical causality principals between the different subsystems. The system consists of basic subsystems (pictograms) related together based on the physical causality (action-reaction) as shown in Table 2.2. The product of the

action and the reaction of any subsystem represents the instantaneous power transferred from or to it. These pictograms describe each element in the system by functions as follow: energy sources (green ovals), accumulation elements (orange rectangles), conversion elements without energy accumulation (various pictograms) and coupling elements for energy distribution (orange overlapped pictograms) [97]. EMR follows a specific procedure for system modeling as follow:

- The development of each subsystem EMR individually,
- Developing the general EMR of the whole system by integrating the subsystems EMR based on the integral and physical causality principals,
- System tune chains definition based on the reverse representation principal,
- Designing the suitable control strategies based on the defined tune chains,
- The development of the system model by using the suitable modeling platform.

The following sections discuss the EMR of the proposed hybrid marine-hydrogen active power generation system.

## 2. System Energetic Macroscopic Representation and Modeling

The following subsections describe the system EMR, of the MCT, PEM MW scale electrolyzer, the PEM fuel cell and the LiFePO<sub>4</sub> Battery systems. Each subsystem EMR is presented first to felicitate the physical behavior understanding and makes the equations more readable.

### 2.1. Marine current turbine modeling

The marine current system (Fig. 2.4) consists of mainly of the tidal turbine and the direct drive PMSG. Each component has the equations that describe its performance. Many studies [110]–[119] have discussed the model of the marine current power generation system.

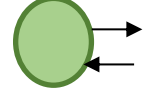
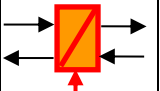
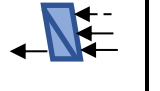
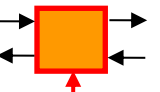
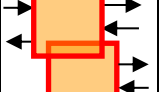
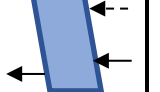
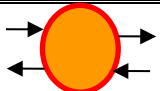
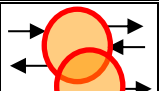

	Source element (Source of energy)		Accumulation element (energy storage)		Indirect inversion (Closed-Loop control)
	Mono-physical conversion element(no energy storage)		Mono-physical coupling element (energy distribution)		Direct inversion (Open-Loop control)
	Multi-physical conversion element (no energy storage)		Multi-physical coupling element (energy distribution)		Coupling inversion (energy criteria)

Table 2.2 Elements of EMR and Control Structure [97].

### 2.1.1. Marine current turbine model

The marine current turbine is the system, which converts the kinetic energy of water tides into mechanical power. There are different types of the tidal turbines, but the fixed pitch turbine is the scope of this study as it is the most applicable to the marine current applications based on the literature survey. The EMR of the turbine has two pictograms. The source of energy, which is the marine currents with the marine current speed as an action while the mechanical force is the reaction. The mono-physical conversion system, which is the turbine that converts the kinetic energy of the marine currents into mechanical energy (rotational motion) as shown in Fig. 2.5.

The available power from marine currents  $P_t$  is estimated based on (2.1) (source of energy pictogram-Fig. 2.5).

$$P_t = 0.5 \rho A V^3 \quad (2.1)$$

[Where:  $A$  is the swept area of the turbine ( $\pi R^2$ ).  $R$  is the turbine radius.  $\rho$  is the seawater density ( $1027 \text{ kg/m}^3$ ).  $V$  is the marine current speed in m/s].

The extracted power from the turbine ( $P_m$ ) is a function of the turbine power coefficient ( $C_p$ ). The power coefficient depends mainly on the turbine parameters (the tip speed ratio ( $\lambda$ ) and the pitch angle) due to (2.2). The power coefficient of the studied fixed pitch turbine is a function of the tip speed ratio that depends on its aerodynamic design. A lookup table is used to represent the relationship that has a maximum  $C_p$  value of 0.45 at 6.3 tip speed ratio as shown in Fig 2.6. The tidal turbine MPPT (Maximum Power Point Tracking) based mainly on these values. The turbine developed torque  $T_m$  is estimated based on (2.4) by considering the turbine mechanical rotational speed  $\Omega$  (mono-physical pictogram-Fig. 2.5).

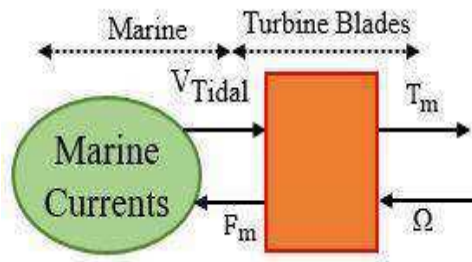


Fig. 2.5. Tidal Turbine EMR.

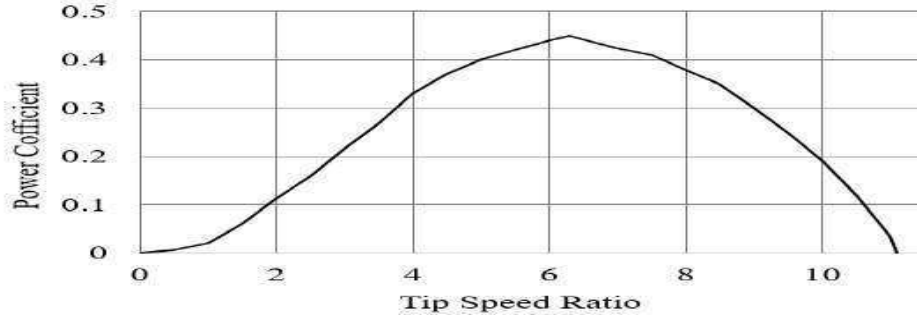


Fig. 2.6. The Power Coefficient Characteristic of the Studied Turbine.

$$P_m = 0.5 \rho A V^3 C_p \quad (2.2)$$

$$\lambda = \frac{R\Omega}{V} \quad (2.3)$$

$$T_m = \frac{P_m}{\Omega} = 0.5 \pi \rho R^5 \Omega^2 \frac{C_p}{\lambda^3} = 0.5 \pi \rho R^5 \Omega^2 C_T \quad (2.4)$$

#### 2.1.2. Permanent magnet synchronous generator model

The generator is the system, which converts the mechanical energy extracted from the turbine into electrical energy. Figure 2.7 illustrates the EMR of the PMSG. The two accumulation elements describe the mechanical coupling between the turbine and the generator and the electrical generator windings. The multi-physical conversion element represents the electromagnetic conversion of the mechanical energy into electrical energy while the park transformation element is represented by the mono-physical conversion [105]. There are many studies [116], [119] that have discussed the PMSG modeling. The detailed d-q model of PMSG in the synchronous reference frame, which used in this study and the model, has been presented in [120]. Figure 2.8 shows the d-q axis equivalent circuits of the generator in the rotor field synchronous reference frame.

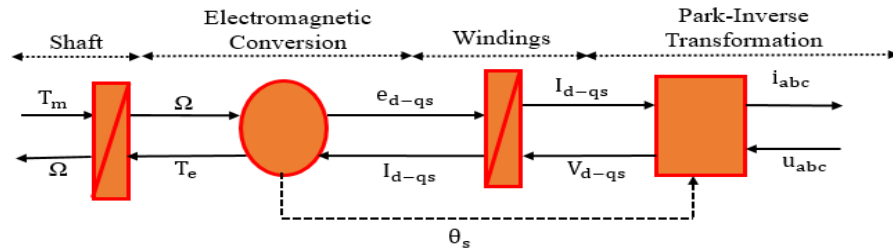


Fig. 2.7. EMR of the PMSG [105].



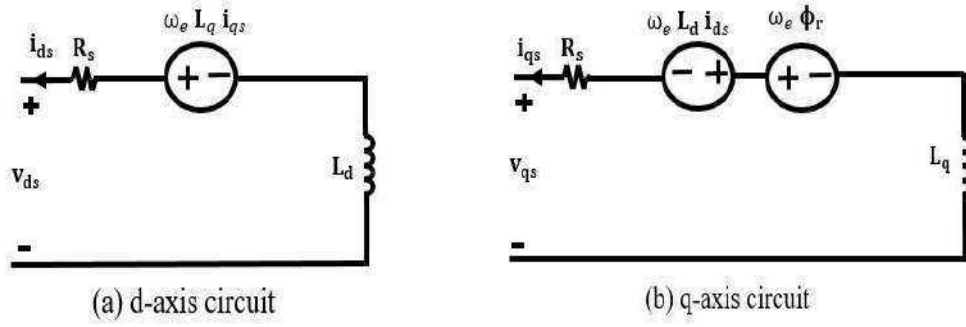


Fig. 2.8. The PMSG d-q axis Equivalent Circuits in The Synchronous Reference Frame [120].

Equations (2.5-2.8) describe the PMSG windings dynamics (Electromagnetic conversion and winding pictograms-Fig. 2.7).

$$V_{ds} = -R_s i_{ds} - \omega_e \phi_{qs} + \frac{d\phi_{ds}}{dt} \quad (2.5)$$

$$V_{qs} = -R_s i_{qs} + \omega_e \phi_{ds} + \frac{d\phi_{qs}}{dt} \quad (2.6)$$

$$\Phi_{ds} = -L_d i_{ds} + \phi_r \quad (2.7)$$

$$\Phi_{qs} = -L_q i_{qs} \quad (2.8)$$

[Where:  $V_{ds}$ ,  $V_{qs}$ ,  $i_{ds}$ ,  $i_{qs}$  are the d-q axis voltages and currents respectively.  $R_s$  the resistance of the machine stator.  $L_d$ ,  $L_q$  are the d-q axis inductances of the machine.  $\Phi_{ds}$ ,  $\phi_{qs}$  are the d-q axis flux linkages respectively.  $\Phi_r$  is the flux of the permanent magnet.  $\omega_e$  is the electrical rotational speed of the generator ( $\omega_e = P\Omega$ ) and  $P$  is the number of pole pairs].

Equation (2.9) presents the developed electromagnetic torque of the machine (Electromagnetic conversion pictogram-Fig. 2.7). Equation (2.10) shows the motion equation of the tidal turbine mechanical shaft and the generator (shaft pictogram).

$$T_e = \frac{3P}{2} (i_{qs} \phi_{qs} - i_{ds} \phi_{ds}) \quad (2.9)$$

$$T_m - T_e = J \frac{d\Omega}{dt} + F\Omega \quad (2.10)$$

[Where:  $J$  is the turbine and generator inertia, and  $F$  is the friction].

The electrical losses of the machine are the copper losses and the core losses which are estimated based on (2.11) and (2.12) (Park-Inverse Transformation Pictogram-Fig. 2.7) [110], [113], [119]. The core losses of the machine at the base voltage and frequency is 2.5 Watt/kg while the estimated core mass is 4000kg of the iron [119].

$$P_{cu} = \frac{3}{2} (i_{ds}^2 + i_{qs}^2) R_s \quad (2.11)$$

$$P_{core} = P_{Fe0} \left( \frac{u_s}{u_0} \right)^2 \left( \frac{f}{f_0} \right)^{-0.7} \quad (2.12)$$

[Where:  $P_{cu}$ ,  $P_{core}$  are the copper and core losses respectively.  $P_{Fe0}$  are the core losses of the machine core material at the base voltage  $U_0$  and the base frequency  $f_0$  in Watt/kg.  $U_s$  and  $f$  are the operating voltage and frequency respectively].

## 2.2. MW Scale PEM electrolyzer modeling

There are different types of electrolyzers based on the kind of the considered electrolyte as follow:

- Alkaline Electrolyte
- Acid Electrolyte
- Acid Polymer Electrolyte
- Alkaline Polymer Electrolyte
- Solid Oxide

Each of them has its characteristics, advantages, and disadvantages [121]. The most applicable and commercially utilized types are the alkaline and the acid polymer electrolyte that is called the polymer electrolyte membrane (or proton exchange membrane). Thus, more details are available in the literature for these two types as shown in Table 2.3 [102], [121]. The alkaline type is a mature technology and can be considered as most applicable for large-scale hydrogen production. Moreover, it is cheap materials technology, highly durable, high corrosion resistance. However, it suffers from many problems such as the handling of potassium hydroxide, the inability to produce high-pressure hydrogen, the need to maintain the temperature about 80°C to support the high current density [102].

Type	Alkaline	Acid	Acid Polymer Electrolyte	Alkaline Polymer Electrolyte	Solid Oxide
Charge Carrier	$\text{OH}^{-1}$	$\text{H}^{+1}$	$\text{H}^{+1}$	$\text{OH}^{+1}$	$\text{O}^{2-}$
Reactant	Water	Water	Water	Water	Steam
Electrolyte	$\text{Na}^+$ or KOH	$\text{H}_2\text{SO}_4$ or $\text{H}_2\text{PO}_4$	Polymer	Polymer	Ceramic
Electrodes	Nickel	Ir and Pt	Ir and Pt	Ni and Ag	Nickel cermet
Temperature ( $^{\circ}\text{C}$ )	60-80	150	50-80	60	>500
Commercial Alkaline and PEM Electrolyzer Stacks Technical Specifications					
Rated production ( $\text{Nm}^3/\text{h}$ )	1-760		0.265-30		
Rated power (kW)	2.8-3534		1.8-174		
Specific energy consumption ( $\text{kWh}/\text{Nm}^3$ )	4.5-7.5		5.8-7.3		
Efficiency (%) HHV	50-70.8		48.5-65.5		
Maximum pressure (bar)	Up to 30		7.9-85		
Hydrogen purity (vol. %)	99.3-99.999		99.999		
System cost ( $\text{€}/\text{kg}$ )	1000-1200		1900-2300		
System lifetime (year)	20-30		10-20		

Table 2.3 Comparison of Electrolyzers Technologies and Technical Specifications [102], [121].

The PEM electrolyzer has more advantages especially for renewables application such as high-energy efficiency, high production rates (high current density), small footprint, operation with high load variations and the ability of generation high-pressure hydrogen up to 350 bar. The PEM electrolyzer has a production operation range from 5% (some new products from 0%) to 100% without any safety problems while the alkaline suffers from hazards in case of operation lower than 25% [102]. The PEM electrolyzer has the disadvantages for a short lifetime and the high cost due to utilizing expensive fabricating materials besides their sensitivity to the temperature and pressure. Based on the comparison, it is evident that the PEM electrolyzer is the most practically and economically choice for the renewables applications. Before discussing the model of the PEM electrolyzer, the following paragraph discusses its architecture with defining the main function of each component as shown in Fig. 2.9. The PEM electrolyzer consists mainly of an acidic polymer thin layer that represents a solid electrolyte instead of the liquid electrolyte like in the alkaline electrolyzer. This thin layer of the membrane is the key point of the PEM electrolyzer main advantage of compact and small footprint design. The membrane allows only the hydrogen positive proton to pass with low resistance and force the electrons to pass through the external circuits. The electrodes are the electrocatalyst materials, which are fabricated from the PMG (Platinum Metal Group) to enhance the efficiency and the reaction kinetics. The two electrodes are coated or deposited directly on the membrane to support the compact design. The

combination of the two electrodes and the membrane represents the heart of the cell and is called the membrane electrode assembly (MEA). The current collectors are thin porous layers and can be considered as a flow channel. They enable the current flow to the electrodes as long as feed the reactant water to the MEA with removing the produced gasses bubbles from the electrodes. The bipolar plates enable the electrical connection to the external circuit beside enhancing the flow of the reactant water inside the cell and the produced gasses outside it. The bipolar plates play a major role in the configuration of the connection of the cells in the stack (series or parallel) and represent the most expensive component in the cell as shown in Fig. 2.10. The frame with sealings is the external enclosure of the cells that prevents the water and gas leakage to the surrounding environment [122]. There are many studies [123]–[130] that have discussed the alkaline electrolyzer modeling and control in different applications as it is a mature technology. Up to our best information, PEM electrolyzer modeling studies are scarce. Moreover, there are no studies about the MW scale electrolyzer modeling.

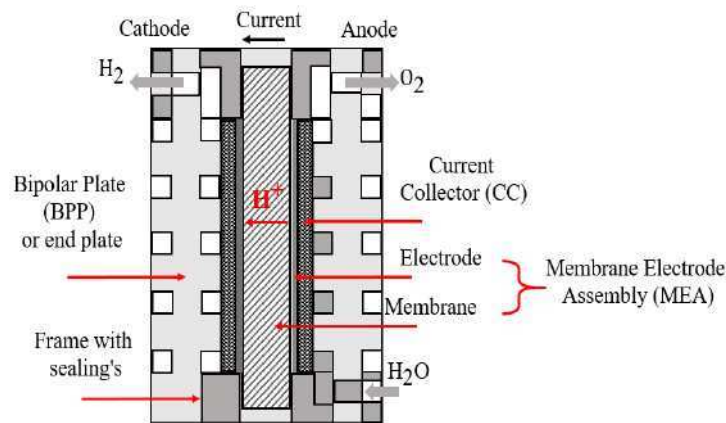


Fig. 2.9. Single PEM Electrolyzer Cell Architecture [122].

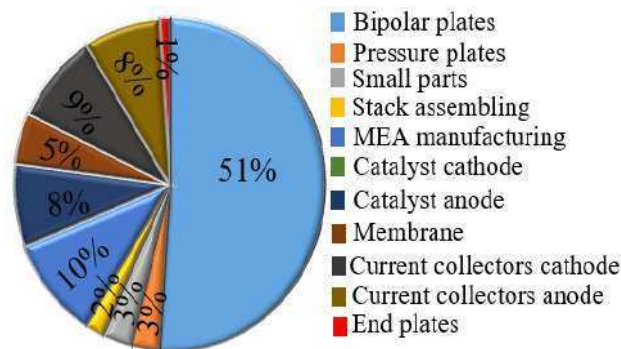


Fig. 2.10. PEM Stack Cost Breakdown [102].

There are two types of PEM electrolyzer models. The first type uses the lumped electrical components (resistance, inductance, and capacitance) to formulate an equivalent circuit representing the various electrolyzer layers as an analytical solution. This type is validated by fitting the model to a real electrolyzer experimental data. The second model is a distributed model with the help of numerical analysis by using the computational fluid dynamics [131]. The dynamic model of the PEM electrolyzer with considering four main ancillaries: anode, cathode, membrane, and voltage has been suggested in [132] to illustrate the renewables integration ability and the interactions in between. This model has ignored critical phenomena's and parameters of the electrolyzer such as the kinetics of the chemical reactions and the effect of the temperature and the pressure on the performance. The graphical EMR model of the PEM electrolyzer has been presented in [133] to visualize the interconnection between the different multi-physics phenomena's (thermal, electrochemical, thermodynamics, fluidic and electrical). This model has taken into consideration the temperature effect on the electrolyzer parameters and consequently on the overall performance. The model validation has been tested by comparing the static characteristics of the model and a small-scale laboratory electrolyzer. The utilization of the EMR makes the proposed model more readable and easy to understand while it is on a small-scale PEM electrolyzer module of 50 W. This model is used and adapted (as discussed in chapter 3) to represent an MW scale electrolyzer that can be integrated with the MCT system. It is important to consider that the electrolyzer system EMR requires the inherent gas flows representation. The gas flow presents the thermal-pneumatic and the thermal-fluidic energies simultaneously while their separation is not possible. Thus, the representation of these phenomena's considering the EMR physical causality probably provides blocks with many inputs and outputs (not two of action-reaction variables as usual). This type of representation is called a pseudo-EMR as an analogy to pseudo-Bond Graph. This representation provides the flexibility of representing the system parameters and consequently have blocks with many input and output ports (four in the considered PEM electrolyzer model [93]). Otherwise, this approach is not compatible with the action-reaction physical causality and the power flow phenomena of the conventional EMR. A new approach has been proposed in [134] to represent the multiport EMR pictograms into a new EMR model with considering the two domains (thermal-fluidic or thermal-pneumatic) as a carrier and carried domains. Figure 2.11 shows the proposed EMR of the PEM electrolyzer that is divided into three sections.

The yellow area considers the electrical model; the green area represents the electrochemical and the thermodynamic model while the white area represents the thermo-fluidic and the thermos-pneumatic models. The suggested EMR in this study depends mainly on the physical causality principle between the different variables as shown in Table 2.4 considering a fixed water tank temperature [133], [134]. The electrolyzer is an electrochemical device, which utilizes the electrical energy for water molecules separation into hydrogen and oxygen due to (2.13).



This reaction happens in two steps of the oxygen and the hydrogen evolution reactions at the anode and the cathode due to (2.14) and (2.15) respectively.

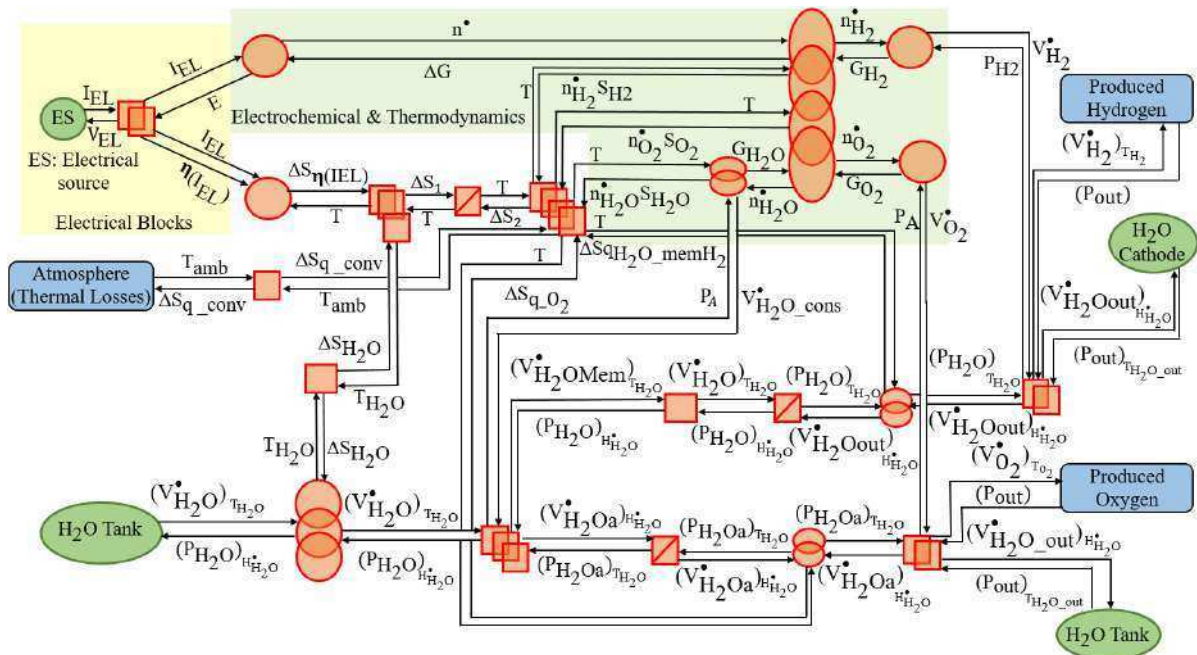


Fig. 2.11. The EMR of the PEM Electrolyzer [133], [134].

Physical domain	Action	Reaction
Electrical	Voltage $V_{EL}$ (volt)	Current $I_{EL}$ (amp)
Thermodynamic	Gibbs free energy $\Delta G$ (J/mol)	Molar flow $n^*$ (mol/s)
Thermal	Temperature $T$ (K)	Entropy flow $n^*S$ (W/K)
Fluidic	Pressure (Pa)	Volume flow $V^*$ (m <sup>3</sup> /s)

Table 2.4 Physical Causality Parameters of PEM Electrolyzer [133].

The reaction represents electrochemical, thermal and fluidic phenomena's happen simultaneously. At the STC (Standard Testing Conditions), the reaction is an endothermic reaction requires thermal energy for processing. This energy is called the Gibbs free energy ( $\Delta G$ ) of the reaction and is supplied by the electrical source connected to the electrolyzer terminals. The required voltage to supply this amount of energy is called the thermodynamic voltage, or the Nernst voltage, that is estimated based on (2.16).

$$E_{\text{ref}} = \frac{\Delta G}{nF} = 1.229 \text{ V}_{(\text{Standard conditions; } T=298 \text{ K, } p=1 \text{ atm})} \quad (2.16)$$

[Where:  $E_{\text{ref}}$  is the thermodynamic voltage at standard conditions,  $n$  is the number of electrons produced from the reaction (2 for one water molecule),  $F$  is Faraday constant (96485 C/mol),  $T$  is the temperature and  $p$  is the pressure in the atmosphere (atm)].

The concentrations of the reactant and the temperature effects of this voltage can be estimated due to (2.17), (2.18).

$$E = E_{\text{Nernst}} = E_{\text{ref}} + \frac{RT}{2F} \ln\left(\frac{P_{\text{H}_2} P_{\text{O}_2}^{0.5}}{P_{\text{H}_2\text{O}}}\right) \quad (2.17)$$

$$E_{\text{ref}} = 1.5184 - 1.5421 \times 10^{-3} T - 9.523 \times 10^{-5} T \ln(T) + 9.84 \times 10^{-8} T^2 \quad (2.18)$$

[Where:  $E$  is the thermodynamic voltage,  $E_{\text{Nernst}}$  is the Nernst voltage,  $R$  is the gas constant (8.3144 J/ (K mol)), ( $P_{\text{H}_2}, P_{\text{O}_2}, P_{\text{H}_2\text{O}}$ ) are the concentrations of hydrogen, oxygen, and water respectively].

When the voltage of 1.229 Volt is applied to the electrolyzer cell, one water molecule splits into half-molecule of oxygen and one molecule of hydrogen, but they recombine to form again the water molecule, which is called the reversible reaction. There is another amount of energy that is required to react in one direction is called the entropy ( $S$ ). Both of the entropy and the Gibbs free energy of the reaction represent its enthalpy ( $\Delta H$ ). The enthalpy determines the applied voltage to have one direction reaction, which is called the thermo-neutral voltage ( $V_{\text{tn}}$ ) due to (2.19). The reaction enthalpy at the standard conditions is 285.83 kJ/mol, which provides a thermo-neutral voltage of 1.482V.

$$V_{\text{tn}} = \frac{\Delta H}{nF} = \frac{\Delta G + T \Delta S}{nF} = E + \frac{T \Delta S}{nF} \quad (2.19)$$

The molar flow ( $\dot{n}$ , mol/s) of the different species (i: hydrogen, oxygen and the water) depends mainly on the electrolyzer current ( $I_{EL}$ ), and it is estimated due to (2.20).

$$\dot{n}_i = \dot{n}_{H_2O} = \dot{n}_{H_2} = 2\dot{n}_{O_2} = \frac{I_{EL}}{2F} \eta_F \quad (2.20)$$

[Where:  $\eta_F$  is the faradic efficiency].

The output gas volume flow ( $\dot{V}_{gas}^\bullet$ , m<sup>3</sup>/s) can be estimated based on the molar flow with considering the pressure and the temperature due to (2.21).

$$\dot{V}_{gas}^\bullet = \dot{n}_{(H_2 \text{ or } O_2)} \left( \frac{RT}{p} \right) \quad (2.21)$$

The thermoneutral voltage represents the required voltage for one water molecule electrolysis in the ideal case while in the real; there are other potentials necessary for the reaction. These overpotentials ( $\eta(I_{EL})$ ) represent the activation voltages of the evolution reactions and the voltage drop on all the components, and they are mainly functions of the electrolyzer current. The electrolyzer actual cell voltage ( $V_{EL}$ ) represents all these overpotentials with the thermo-neutral voltage due to (2.22).

$$V_{EL} = V_{tn} + \eta(I_{EL}) \quad (2.22)$$

There are three main overpotentials of the PEM electrolyzer as follow: the activation ( $\eta_{act}$ ), the diffusion ( $\eta_{diff}$ ) and the Ohmic ( $\eta_{Ohmic}$ ).

The activation over potential represents the required potential for the chemical reactions ignition to convert the reactant water into hydrogen and oxygen. It represents the biggest over potential, especially at low current densities operation. Equation (2.23) shows that there are two activations overpotentials: the first is the anode ( $\eta_{act-anode}$ ) while the second is the cathode ( $\eta_{act-cathode}$ ). The main parameters affecting these overpotentials are the anode and the cathode exchange current densities ( $j_{oA}$ ,  $j_{oC}$  respectively, A/cm<sup>2</sup>) as long as their charge transfer coefficients ( $\alpha_A$ ,  $\alpha_C$  respectively). These parameters depend mainly on the materials and the compositions of the electrodes, which represent the catalyst for the chemical reactions.

$$\eta_{act} = \eta_{act-anode} + \eta_{act-cathode} = \frac{RT}{2\alpha_A F} \sinh^{-1} \left( \frac{I_{EL}}{2A * j_{oA}} \right) + \frac{RT}{2\alpha_C F} \sinh^{-1} \left( \frac{I_{EL}}{2A * j_{oC}} \right) \quad (2.23)$$

[Where: A is the active area of the cell (cm<sup>2</sup>)].



The diffusion over potential represents the barrier of electrical current transfer due to the concentration of the produced gasses at the MEA that can be estimated due to (2.24).

$$\eta_{\text{diff}} = \frac{RT}{4F} \ln\left(\frac{C_{\text{O}_2\text{me}}}{C_{\text{O}_20}}\right) + \frac{RT}{2F} \ln\left(\frac{C_{\text{H}_2\text{me}}}{C_{\text{H}_20}}\right) \quad (2.24)$$

[Where:  $C_{\text{O}_2\text{me}}, C_{\text{H}_2\text{me}}$  are the oxygen and hydrogen concentrations at the membrane and  $C_{\text{O}_20}, C_{\text{H}_20}$  are the oxygen and hydrogen concentration at the reference conditions respectively].

The Ohmic overpotential depends mainly on the proton conductivity of the membrane, the electrical conductivity of the electrodes and the bipolar plates. The electrodes and bipolar plate's effect on the Ohmic overpotential can be neglected compared to the membrane effect. Thus, the Ohmic overpotential is estimated by considering only the membrane due to (2.25).

$$\eta_{\text{Ohmic}} = \frac{\phi}{\sigma_m} j \quad (2.25)$$

[Where:  $\phi$  is the membrane thickness ( $\mu\text{m}$ ).  $\sigma_m$  is the membrane conductivity (S/cm), and  $j$  is the operating-current density ( $\text{A}/\text{cm}^2$ )].

By considering the equations (2.17-2.19) and (2.22-2.25), the current-voltage characteristic can be obtained and analyzed. The main parameters affecting this curve and consequently the electrolyzer design and performance are the exchanged current densities and the charge transfer coefficients of the anode and cathode besides the conductivity of the membrane. The proposed model in [133] has used Matlab/Simulink curves fitting tools to determine the values of the parameters to be fitted with the experimental data of the small-scale laboratory electrolyzer utilized during the study. The effect of the temperature on these parameters has also been investigated by the same methodology to analyze its effect on the electrolyzer performance. The overpotentials and the change of entropy are converted into heat dissipation inside the electrolyzer environment (MEA especially), which is expressed by equation (2.26).

$$T \Delta S = 2 F \eta(I_{\text{EL}}) = 2F(\eta_{\text{act}} + \eta_{\text{diff}} + R_e j) \quad (2.26)$$

Based on (2.26) the entropy flow ( $n \Delta S$ ), which represents the heat flow inside the electrolyzer to the outside environment, can be expressed due to (2.27).

$$\dot{n} \Delta S = I_{EL} \frac{(\eta_{act} + \eta_{diff} + \eta_{Ohmic})}{T} \quad (2.27)$$

Due to the heat and the water flows inside the electrolyzer, the hydration and the temperature of the membrane change which affects its performance. The analysis of these characteristics represents the electrolyzer thermo-fluidic and thermo-pneumatic models, which have been discussed in details in [133]. The PEM electrolyzer stack is a group of cells connected in series and (or) parallel to extend the hydrogen production rate. The stack modeling depends mainly on the number of cell in the stack  $N_{cell}$ , connected in series in most cases. The cell current is the same stack current ( $I_{ST}$ ) in series configuration due to (2.28) while the number of the cell multiplies the stack voltage ( $V_{ST}$ ) and the flow rates of input water ( $\dot{n}_{H_2O\_ST}$ ) and output gasses ( $\dot{n}_{H_2\_ST}, \dot{n}_{O_2\_ST}$ ) due to (2.29, 2.30).

$$I_{ST} = I_{EL} = j * A \quad (2.28)$$

$$V_{ST} = N_{cell} * V_{EL} \quad (2.29)$$

$$\dot{n}_{H_2O\_ST} = \dot{n}_{H_2\_ST} = 2 * \dot{n}_{O_2\_ST} = \frac{I_{ST}}{2F} * \eta_F * N_{cell} = \dot{n}_i * N_{cell} \quad (2.30)$$

The electrolyzer efficiency  $\epsilon_{EL}$  is estimated by considering the system input (electrical energy) and the output (hydrogen gas). There are two values of the hydrogen energy; the higher heating value (HHV: 286 kJ/mol) and the lower heating value (LHV: 241.95 kJ/mol) that are used in the efficiency estimation. The difference between the two values is the water vaporization energy (LHV is the dry hydrogen energy while HHV is the hydrated hydrogen energy). The literature indicates that the HHV is more applicable for the electrolyzer efficiency estimation due to (2.31).

$$\epsilon_{EL} = \frac{HHV * \dot{n}_{H_2}}{I_{EL} * V_{EL}} = \frac{HHV * I_E}{2 * F * I_{EL} * V_{EL}} = \frac{\frac{HHV}{2F}}{V_{EL}} = \frac{1.482}{V_{EL}} \quad (2.31)$$

The main factor of the stack design is the cell design. The cell design depends mainly on the current density parameter that represents the hydrogen production rate and the operating voltage due to the polarization curve. Generally, the high current density operation provides high production rate and small MEA active area, which participates in reducing the capital cost (CAPEX). Otherwise, the high current density increases the

operating voltage and reduces the efficiency consequently increases the energy consumption that means high operating cost (OPEX). Thus, the cell design is the selection of the optimal operating point to balance between the CAPEX and the OPEX [102]. The electrolyzer EMR (Fig. 2.11) yellow area considers the equations (2.22, 2.25, 2.28, 2.29, 2.31); the green area represents the equations (2.16-2.20, 2.21, 2.30) and the white area represents the rest of the model.

### 2.3. PEM fuel cell modeling

The fuel cell is an electrochemical device that converts the chemical energy of the hydrogen into electrical energy (DC-current) [135]. Thus, it can be considered the reversible process of electrolyzer system with the reversed terminal polarity. There are different types of fuel cells characterized by various parameters that provide each with definite advantages for specific applications as shown in Table 2.5. The main advantages of the PEM fuel cell in contrast to the other types are a low-temperature operation that provides a fast dynamic response, the safe operation and the high efficiency even with partial loading. The PEM has a compact design due to the solid polymer electrolyte with a small thickness, which provides a small footprint system. The main disadvantages of the PEM fuel cell are the high cost and the limited lifetime (about five years or 40000 hours as a stationary application) [136], [137]. The PEM fuel cell has the same structure and components of the PEM electrolyzer (shown in Fig. 2.9) as follow: bipolar plates (flow channels), a current collector (gas diffusion layers), the membrane and the electrodes (membrane electrode assembly MEA) that represent the main section of the cell. There are many studies [138]–[144] that have presented the mathematical and the dynamic model of the PEM fuel cell. The objectives of these studies varied from the interrelation with the equivalent electrical circuits to the description of the behavior under different operating conditions: transient, steady state, load commutation and mass transportation limitations due to the different electrochemical phenomena. Other studies [145]–[150] have reported the various methods of optimum model parameters extraction by using different techniques (SA (Simulated Annealing) or empirically) and the polarization static characteristics analysis under different operating conditions specifically for transportation applications. All the proposed models have been validated by using the experimental data of PEM fuel cell stacks with power ratings varied from 1.2W up to 250 kW.

Parameter	Polymer Electrolyte (PEFC)	Phosphoric acid (PAFC)	Alkaline (AFC)	Solid Oxide (SOFC)	Molten carbonate (MCFC)
Electrolyte	Polymer (Perfluorosulfonated acid polymer)	Phosphoric acid	Alkali (KOH) with concentrations (A-85%, B-50%)	Ceramic ( $Y_2O_3$ , $ZrO_2$ )	Molten carbonate salt (Li, Na, K)
Operating temperature ( $^{\circ}C$ )	80	150-220	A-250 B-150	800-1000	600-700
Fuel	$H_2$	$H_2$	$H_2$	$H_2$ , CO, and $CH_4$	$H_2$ , CO, $CO_2$ , and $CH_4$
Oxidant	$O_2$ or air	$O_2$ or air	$O_2$ or air	$O_2$ or air	$O_2$ or air
Efficiency (%)	35-45	35-45	50-70	50-55	40-50

Table 2.5 Different Types of Fuel Cells and Characteristics [135], [151].

The MW scale PEM fuel cell integration in the studied system requires understanding its interactions, dynamics and considering all the phenomena by using a simpler model. Figure 2.12 shows the global EMR of the fuel cell proposed in [152] that is divided into five sections. The fluidic model of the anode is the area (A); the fluidic model of the cathode is the area (B); the cooling water fluidic model is the area (C); the electrochemical and thermodynamic model is the area (D), and the electrical model is the area (E). The proposed model in [152] can be considered identical to the PEM electrolyzer one with reviewing the activation, ohmic, diffusion and concentration voltages as under potentials despite overpotentials due to (2.32).

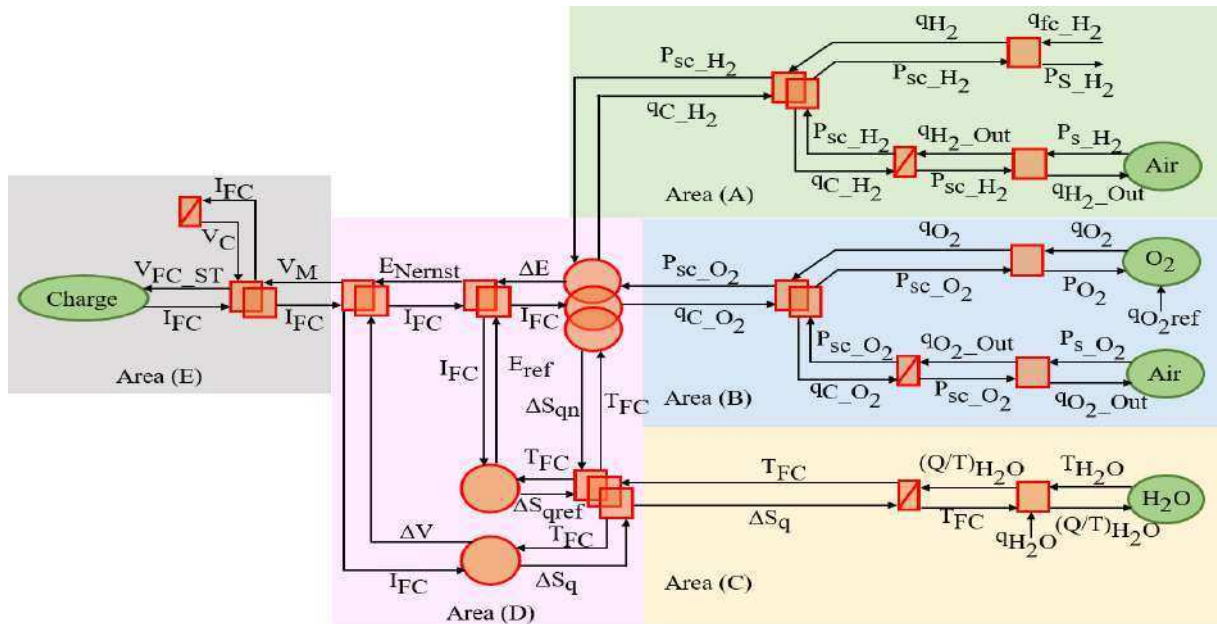


Fig. 2.12. The PEM Fuel Cell EMR [152].

$$V_{FC\_ST} = N_{FC}(V_M + V_C) \quad (2.32)$$

[Where:  $V_{FC\_ST}$  is the fuel cell stack voltage,  $N_{FC}$  is the number of series fuel cells in the stack,  $V_M$  is the cell voltage without the electrode impedance voltage,  $V_C$  is the electrode impedance voltage].

The cell voltage is estimated based on the Nernst voltage with considering the voltage drops due to (2.33) and (2.34).

$$V_M = E_{Nernst} - \Delta V - R_m * I_{FC} \quad (2.33)$$

$$\Delta V = A * T_{FC} * \ln\left(\frac{I_{FC} + I_n}{I_0}\right) + B * T_{FC} * \ln\left(1 - \frac{I_{FC}}{I_l}\right) \quad (2.34)$$

[Where:  $\Delta V$  is the concentration and activation voltage drops.  $R_m$  is the ohmic cell resistance ( $m\Omega$ ).  $I_{FC}$  is the cell current.  $A$  and  $B$  are the activation and concentration voltages coefficients.  $T_{FC}$  is the fuel cell temperature (K).  $I_n$  is the internal current (mA).  $I_0$  is the exchange current (mA), and  $I_l$  is the current limit (A)].

The effects of the temperature and the pressure on the Nernst voltage are due to (2.35-2.37).

$$E_{Nernst} = E_{ref} + \Delta E \quad (2.35)$$

$$\Delta E = A_{cd} \ln\left(\frac{P_{SCH_2}}{P_0}\right) + B_{cd} \ln\left(\frac{P_{SCO_2}}{P_0}\right) \quad (2.36)$$

$$E_{ref} = \alpha + \beta * T_{FC} + \gamma * T_{FC}^2 + \delta * T_{FC}^3 + v * T_{FC} * \ln(T_{FC}) \quad (2.37)$$

[Where:  $\Delta E$  is the voltage variation due to pressure.  $A_{cd}$ ,  $B_{cd}$  are the Nernst voltage coefficients (V/K).  $P_{SCH_2}$ ,  $P_{SCO_2}$  are the hydrogen and oxygen partial pressures on sites catalytic (Pa).  $P_0$  is the reference pressure (Pa).  $\alpha$ ,  $\beta$ ,  $\gamma$ ,  $\delta$ , and  $v$  are the reversible voltage coefficients (V, V/K, V/K<sup>2</sup>, V/K<sup>3</sup>, V/K respectively)].

The cell voltage across the impedance electrode is estimated by (2.38) with considering the ions and electrons charges transfer between the diffusion layers and the electrode/electrolyte as a double layer capacitor.

$$\frac{V_C}{I_{FC}} = \frac{R_t}{1 + C_p * R_t} \quad (2.38)$$

[Where:  $R_t$  and  $C_P$  are the electrode impedance resistance in  $m\Omega$  and the double layer capacitance in  $mF$ , respectively].

The volume flow rates of the consumed hydrogen and oxygen ( $q_{C\_H_2}$ ,  $q_{C\_O_2}$  in  $m^3/s$ ) are estimated with considering their pressures at the stack entry ( $P_{H_2}$ ,  $P_{O_2}$ ) and the number of series connected fuel cells in the stack ( $N_{FC}$ ) due to (2.39) and (2.40) respectively.

$$q_{C\_H_2} = \frac{I_{FC}}{2 * F} * \frac{R * T_{FC}}{P_{H_2}} * N_{FC} \quad (2.39)$$

$$q_{C\_O_2} = \frac{I_{FC}}{4 * F} * \frac{R * T_{FC}}{P_{O_2}} * N_{FC} \quad (2.40)$$

The fuel cell efficiency  $\varepsilon_{FC}$  is estimated due to (2.41) by the same procedure of electrolyzer but with considering hydrogen LHV as the system input and the electrical energy as the system output.

$$\varepsilon_{FC} = \frac{I_{FC} * V_{FC}}{LHV * n_{H_2}} = \frac{2 * F * I_{FC} * V_{FC}}{LHV * I_{FC}} = \frac{V_{FC}}{\frac{LHV}{2F}} = \frac{V_{FC}}{1.229} \quad (2.41)$$

The fuel cell EMR (Fig 2.12) represents (2.39) by the area A; (2.40) by area B; (2.34)-(2.37) by area D; (2.32), (2.33), (2.38) by area E and the rest of the model by area C.

#### 2.4. Storage tank modeling

The amount of the hydrogen stored in the tank ( $Q_{H_2}$ , in  $m^3$ ) depends on the hydrogen volume production and consumption flow rates by the electrolyzer and fuel cell ( $q_{EL\_H_2}$ ,  $q_{FC\_H_2}$ ) respectively. Due to the efficiency, the electrolyzer and the fuel cell do not work simultaneously to avoid the electricity-to-electricity round utilizing an electrical storage system while it is a hydrogen generation system. The pressure of the produced hydrogen from the electrolyzer ( $P_{-H_2}$ ) is 30 bar while the fuel cell input pressure ( $P_{S\_H_2}$ ) is a little bit more than one bar. Consequently, a pressure regulator is used to step down the hydrogen pressure from the tank to the fuel cell level. Figure 2.13 exhibits the pressure regulator physical causality that has been presented in [96] and depends on the regulator stability study discussed in [153]. Thus, the EMR of the

pressure regulator is a mono-physical conversion element as shown in Fig 2.13. The storage tank EMR consists of an accumulation element as shown in Fig. 2.14 [96].

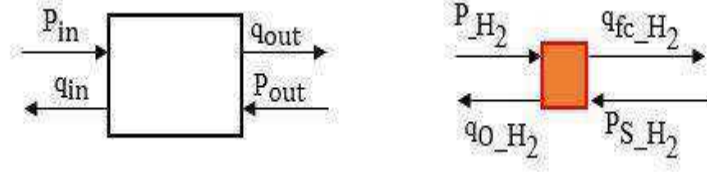


Fig. 2.13. Pressure Regulator Physical Causality and EMR [96].

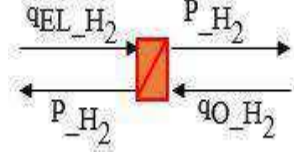


Fig. 2.14. Storage Tank EMR [96].

The storage tank hydrogen volume, in  $m^3$ , during a time interval  $[t_0 - (t_0 + \Delta t)]$  with considering the initial volume  $Q_{H_2}(t_0)$  is estimated due to (2.42) [129].

$$Q_{H_2}(t_0 + \Delta t) = \int_{t_0}^{t_0 + \Delta t} (q_{EL\_H_2} - q_{O\_H_2}) dt + Q_{H_2}(t_0) \quad (2.42)$$

The hydrogen volume production and consumption flow rates of the MW scale PEM electrolyzer and fuel cell ( $q_{EL\_H_2}$ ,  $q_{O\_H_2}$  respectively) are determined due to (2.43-2.45) with considering the hydrogen molar mass  $m_{H_2} \approx 2g/mol$ , the number of electrolyzer and fuel cell stacks ( $N_{EL\_ST}$ ,  $N_{FC\_ST}$  respectively) and the pressure regulator.

$$q_{EL\_H_2} = m_{H_2} * n_{H_2\_ST} * N_{EL\_ST} \quad (2.43)$$

$$q_{FC\_H_2} = q_{C\_H_2} * N_{FC\_ST} \quad (2.44)$$

$$q_{O\_H_2} = \frac{q_{FC\_H_2} * P_{S\_H_2}}{P_{H_2}} \quad (2.45)$$

## 2.5. Load demands modeling

The full inverter connected to the load terminals is controlled as will be discussed later to feed a fixed three-phase AC voltage that can be represented by a source of energy element pictogram. The d-q transformation of the balanced three-phase AC source with a reference frame rotating synchronously with the voltage provides zero q-axis component of the voltage. Thus, the active and the reactive powers are represented due

to (2.46) and (2.47) respectively [154]. The load profile is modeled to have a unity power factor, which means zero q-axis component of the load current. By defining the demand profile, the load current can be determined with the help of equation (2.46). Thus, the load is modeled as a controlled current source with an active power profile representing the household standardized load profile (SLP).

$$P_L = \frac{3}{2} * (U_d * I_{Ld}) \quad (2.46)$$

$$Q_L = \frac{3}{2} * (U_{Ld} * I_{Lq}) \quad (2.47)$$

[Where:  $U_{Ld}$ ,  $U_{Lq}$  are d-q axis components of the load terminal voltage respectively.  $I_{Ld}$ ,  $I_{Lq}$  are the d-q axis components of the load current].

The load characteristics depend on the mix of consumers' types (household, offices and public buildings, commercial or industrial and agricultural plants) beside the population density. Standardized load profile represents the small consumers in general. Table 2.6 exhibits the twenty-seven different standardized load profiles have been developed in Europe for the different types of loads. All the profiles are estimated in quarter-hour time steps over the whole year in per unit based on 1000 kWh unit consumption [155], [156]. The World Energy Council determines the average household energy consumption be about 4000 kWh per year [157]. As a result, the household load profile represents four times the  $H_0$  standard load profile as shown in Fig. 2.15.

Type Number	Type Name	Description
1	$H_0$	Household
2	$G_0$	General business
3	$G_1$	Business on weekdays 8 am-6 pm
4	$G_2$	Business
5	$G_3$	Business passing through
6	$G_4$	Retail store/coiffeur
7	$G_5$	Bakery with Bakehouse
8	$G_6$	End-of-week business
9	$L_0$	Agricultural
10	$L_1$	Dairy farming/ sideline farmer
11	$L_2$	Rest of farmers
12	$U_0$	Interruptible water heating
13	$U_1$	Interruptible heating
14	$E_0$	Hydropower, wind power, biogas (fermentation gas)
15	$E_1$	Photovoltaics



16	ULA	Hot water tank without a recharge in the daytime
17	ULB	Hot water tank with recharge in the daytime
18	ULC	Night storage heater without a recharge in the daytime
19	ULD	Night storage heater with recharge in the daytime
20	ULE	A mix of heating and water heating without a recharge in the daytime
21	ELF	A mix of heating and water heating with recharge in the daytime
22	EAGU <sub>1</sub>	A special form of night storage heater without a recharge in the daytime
23	EAGU <sub>2</sub>	A special form of night storage heater with recharge in the daytime
24	HA	Household and water heating with one electricity meter (point of counting)
25	HF	Household and storage heating with one electricity meter (point of counting)
26	G <sub>7</sub>	Mobile telephone transmitting station
27	B <sub>1</sub>	Public lighting

Table 2.6 Different Standard Load Profiles for Small Consumers  
in the Low Voltage Grid [155], [156].

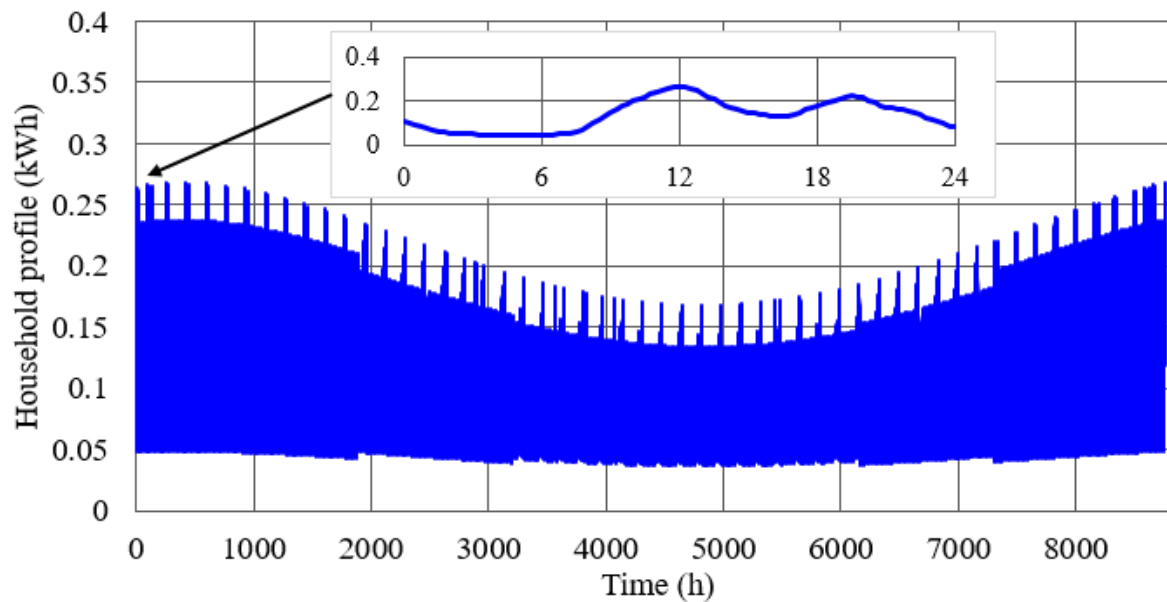


Fig. 2.15. Standardized Household Annually and Daily Load Profile.

## 2.6. *LiFePO<sub>4</sub> battery modeling*

The PEM fuel cell and electrolyzer systems have a definite time response that must be respected for avoiding the components aging and providing the healthy and secure system operation. The LiFePO<sub>4</sub> battery is selected to cover the fast power variations due to its dynamic response as shown in Fig. 2.16. This type of battery has the best advantages compared to the other types of power density, energy density, dynamic response and the efficiency points of view [158]. The battery EMR is a source and accumulation elements with action-reaction as shown in Fig. 2.17. The dynamic model of the LiFePO<sub>4</sub> battery cell has been presented in [159] that is based on a proposed cell

equivalent circuit shown in Fig. 2.18. The Shepherd model describes the relationship between the battery open circuit voltage ( $V_{OC} = E$ ) and the current due to (2.48), (2.49).

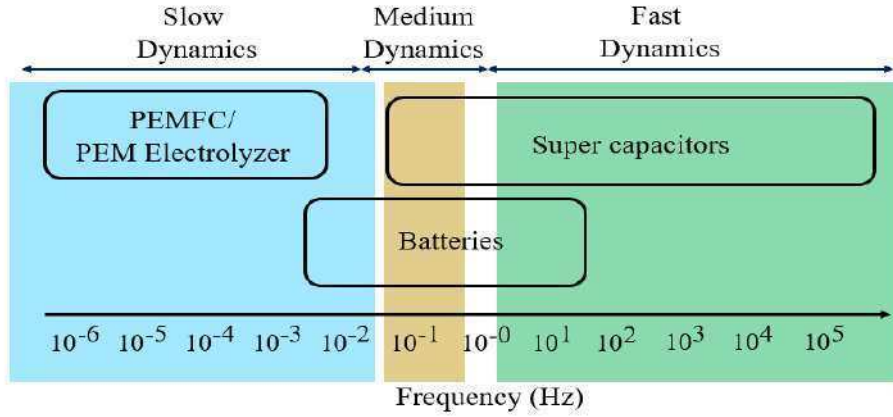


Fig. 2.16. Energy Storage Systems Dynamic Response [158].

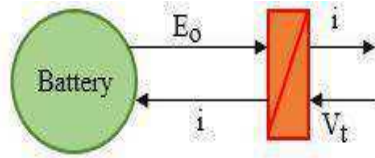


Fig. 2.17. LiFePO<sub>4</sub> Battery EMR.

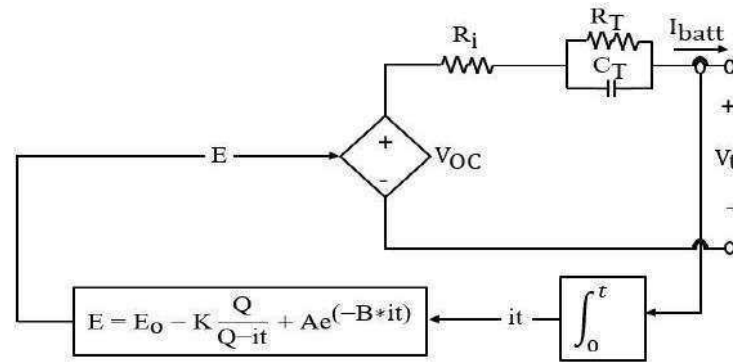


Fig. 2.18. LiFePO<sub>4</sub> Battery Cell Model [159].

$$E = E_0 - K \frac{Q}{Q - \int i dt} + A e^{(-B \int i dt)} \quad (2.48)$$

$$V_t = E - R_i * i \quad (2.49)$$

[Where:  $E$  is the open circuit voltage in Volt.  $i$  is the battery current in Amp.  $Q$  is the battery cell capacity in Ah.  $E_0$  is the electromotive force in Volt.  $V_t$  is the cell terminal voltage in Volt.  $R_i$  is the internal cell resistance in Ohm.  $A$  is the first Shepherd model constant (Exponential zone amplitude, in Volt).  $B$  is the second Shepherd model

constant (Exponential zone time constant inverse, in  $\text{Ah}^{-1}$ ) and  $K$  is the third Shepherd model constant (Polarization voltage in Volt).].

The Shepherd model constants ( $A$ ,  $B$ ,  $K$ ) are estimated by the help of the cell discharge curve as analyzed in [159]. The main problem of Shepherd model is the disability of describing the transient performance characteristics. The Thevenin model has added parallel-connected RC elements ( $R_T$ ,  $C_T$ ) to describe the charge and discharge transient characteristics. The proposed model integrates Shepherd and Thevenin models to have the dynamic cell model. The battery stack model depends mainly on the number of series-connected cells in the string and the number of parallel strings in the module. The source element pictogram (Fig. 2.17) represents the open circuit voltage, and the accumulation element considers the equations RC elements dynamics and the equations (2.48, 2.49).

## 2.7. Power electronic converters modeling

There are five converters in the system; the controlled rectifier interfaced with the PMSG, the inverter-interfaced with the load, the boost converter interfaced with the fuel cell, the buck converter interfaced with the electrolyzer and the DC-DC bidirectional converter interfaced with the battery. All the converters have common connections with the DC link as an input or an output. There are different power electronic converters modeling procedures based on the objective of the study. The main purpose of the system modeling is the power flow study. The representation of the different power electronic converters is a mono-physical conversion element due to their functions, which are the transformation of the AC power into DC power and vice-versa or the DC-DC power conversion. The tuning parameters of these items are the modulation indexes and the duty cycles of the converters as shown in Fig. 2.19. Thus, the GA (Generalized Average) model is used to represent the converters. Figure 2. 20 shows the circuit of the GA model of the controlled rectifier and the inverter that has been presented in [160], [161]. By the same modeling procedure, the generalized average model of the buck, the boost, and the bidirectional converters are proposed with considering their duty cycles.

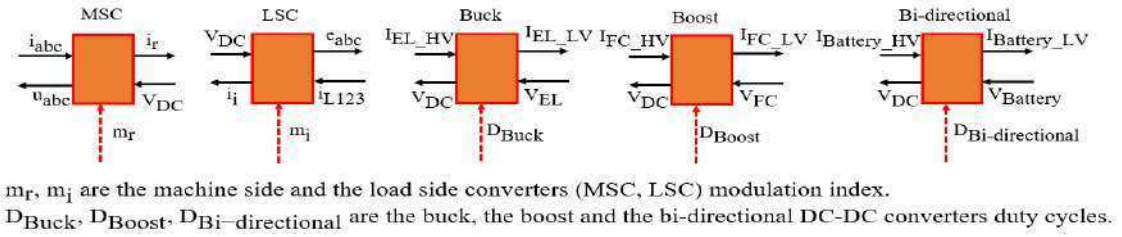


Fig. 2.19. The EMR of the System Power Electronic Converters.

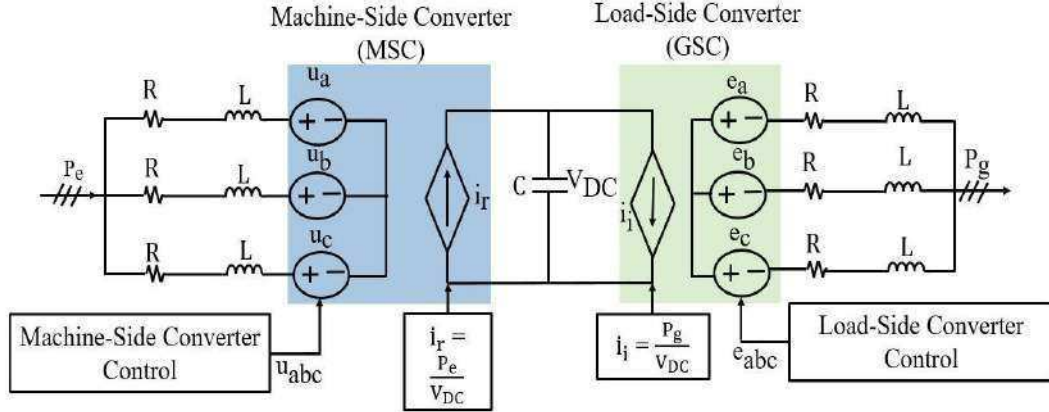


Fig. 2.20. The Generalized Average Model of the Machine and Load Side Converters [161].

## 2.8. DC-link modeling with load filter and transformer

The representation of DC link dynamics is an accumulation element connected to a mono-physical coupling element. The load, the transformer, and the connection cables (with the filter) dynamics are represented by source element, mono-physical conversion, and accumulation element respectively as shown in Fig. 2.21.

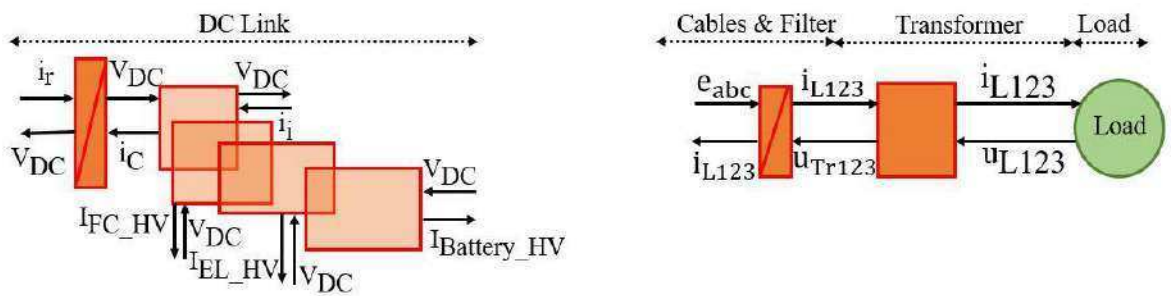


Fig. 2.21. The EMR of the DC-Link and the Demand Side Dynamics [96], [162].

The dynamics of the DC-link depend on the current flow in and outside the capacitance  $C$  (Fig. 2.4) due to (2.50) [154].

$$C \frac{dV_{DC}}{dt} = i_c = i_r + i_{FC\_HV} - i_i - i_{EL\_HV} + i_{B\_HV} \quad (2.50)$$

[Where:  $V_{DC}$  is the DC-link voltage in Volt.  $C$  is the DC-link capacitance in Farad.  $i_C$  is the DC-link current in Amp.  $i_r$  is the MSC output DC-current in Amp.  $i_{FC\_HV}$  is the fuel-cell current from the DC-link side in Amp.  $i_i$  is the LSC DC input current in Amp.  $i_{EL\_HV}$  is the electrolyzer current from the DC-link side in Amp and  $i_{B\_HV}$  is the battery current from the DC-link side in Amp (negative for charging)].

The DC-link voltage indicates the power balance between the generation and the demand due to (2.51) that is a reformulation of (2.50) with neglecting the power electronic converters losses [154].

$$C \frac{dV_{DC}}{dt} = \frac{P_g}{V_{DC}} + \frac{P_{FC}}{V_{DC}} - \frac{P_L}{V_{DC}} - \frac{P_{EL}}{V_{DC}} + \frac{P_B}{V_{DC}} \quad (2.51)$$

[Where:  $P_g$ ,  $P_{FC}$ ,  $P_{EL}$ ,  $P_L$ ,  $P_B$  are the MCT, the fuel cell, the electrolyzer, the load and the battery power respectively].

Based on the load model represented in (2.46), (2.47), the filter and the transformer dynamics can be represented due to (2.52), (2.53) [154], [163].

$$U_{Ld} = E_d - R * I_{Ld} - L \frac{dI_{Ld}}{dt} \quad (2.52)$$

$$0 = E_q - L * \omega * I_{Ld} \quad (2.53)$$

[Where:  $R$ ,  $L$  are the load filter, cable and transformer resistance and inductance, in Ohm and Henry respectively.  $U_{Ld}$  is the d-axis component of the fixed load voltage on the converter side of the transformer in Volt.  $E_d$ ,  $E_q$  are the d-q axis components of the inverter voltage in Volt and  $\omega$  is the required angular frequency of the load terminal voltage in rad/s.].

### 3. Hybrid Marine-Hydrogen Active Power Generation System Global Energetic Macroscopic Representation

The previous sections discuss the formalism of the hybrid marine-hydrogen active power generation subsystems EMR. The global system EMR is synthesized by integrating all the subsystems together considering the physical causality principle as shown in Fig. 2. 22. The global EMR makes the whole system more readable and analyzes the interaction between the different subsystems that are multidisciplinary domains from mechanical, electromechanical, electrical, electrochemical, and thermodynamics. Moreover, it helps in designing the power control and management strategies as discussed in the next chapter.

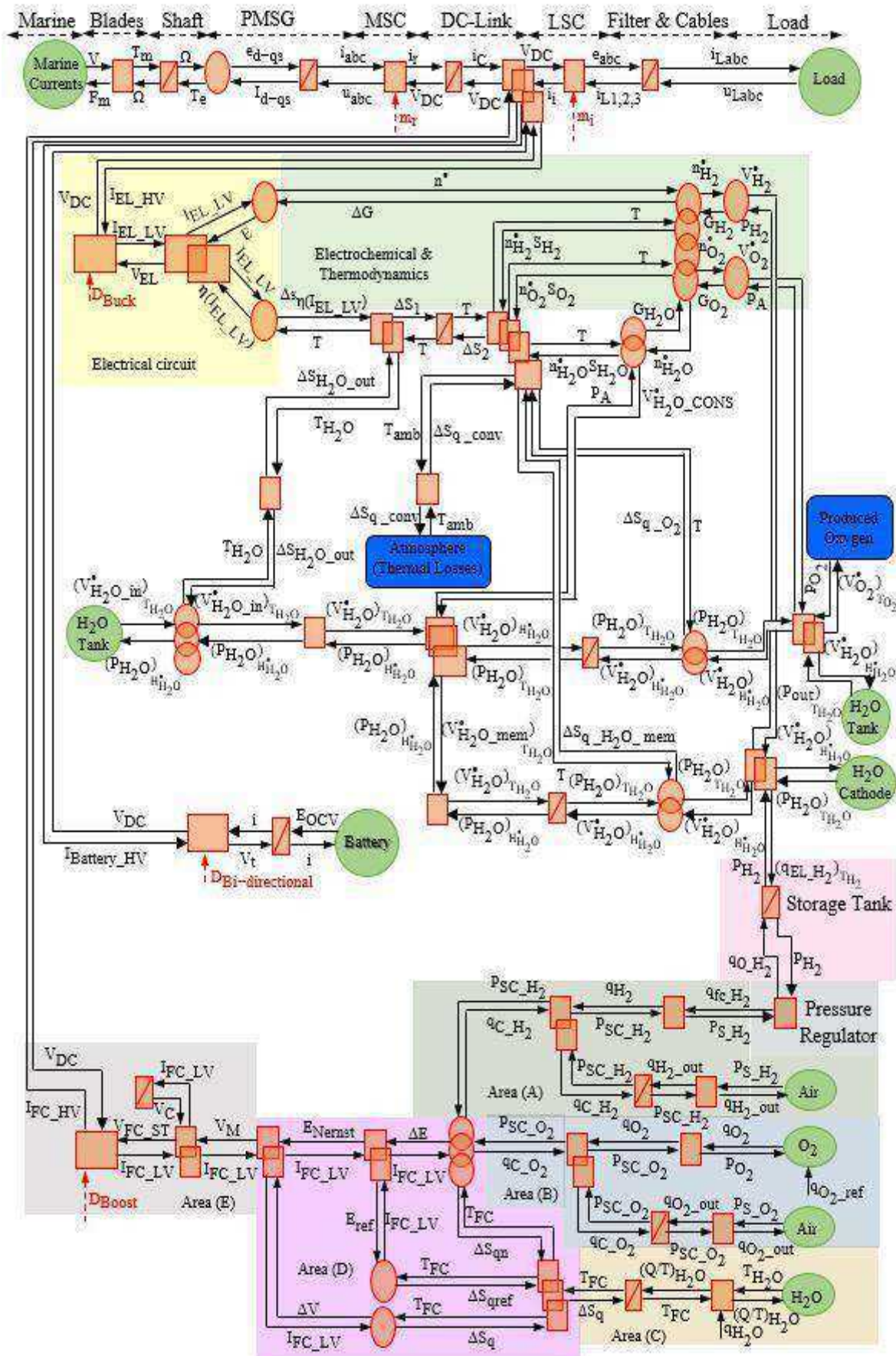


Fig. 2.22. Hybrid Marine-Hydrogen Active Power Generation System Global EMR.



#### 4. Conclusion

This chapter discusses the energetic macroscopic representation and modeling of the hybrid marine-hydrogen active power generation system. The active power generation is the system that converts the intermittent nature of the renewables (marine current energy) into a more dynamic performance by integrating the energy storage systems. There are many types of marine current energy system considering the mechanical turbine and the electric machine technologies. The tidal system state of the art indicates that the fixed pitch direct drive marine current system is the most applicable economically and technically. The direct drive technology eliminates the gearbox system that is the most frequently subjected to failure, and as a result, it requires more maintenance. Thus, the tidal turbine is directly mechanically coupled with the PMSG. The EMR of the PMSG based direct drive marine current power generation system has been formulated to clarify the interactions between the mechanical, electromechanical, and electrical components. The marine current energy suffers from daily and monthly variations. The hydrogen energy storage system has the advantage of long period charging/discharging cycles in the range of days and weeks. The PEM electrolyzer is selected to generate hydrogen in the case of surplus energy due to its wide operating range, small footprint and the ability to produce high-pressure hydrogen by using the electrical compressing characteristic. The PEM electrolyzer modeling studies are a scarce while, up to our best information, there are no studies about the MW scale PEM electrolyzer system. The EMR of a small scale PEM electrolyzer has been studied to be adapted for modeling the MW scale system. The PEM fuel cell has the same electrolyzer advantages that make it the best candidate for generating electricity in case of power shortage. The dynamics of the PEM electrolyzer and fuel cell are in the range of minutes while the electrical system dynamics are in the range of seconds and milliseconds. Thus, it is required to have an auxiliary energy storage system to cover these fast dynamics and avoiding the components aging of the PEM fuel cell and electrolyzer. The  $\text{LiFePO}_4$  battery has been selected due to its high energy and power densities. The standardized household load profile has been selected to represent the demand side variations. The household profile is selected to represent a residential island load for avoiding one of the most important economic and technical challenges of the renewables offshore technologies that is the transmission system. Thus, the system works in a standalone operation mode by feeding the generated energy (marine current energy) directly to the demand side (island residential loads). The energetic macroscopic representation provides the ability to describe each subsystem behavior based on the physical

causality principle. Thus, the EMR of each subsystem has been formalized to describe its model. The whole system EMR has been synthesized by integrating all the components together considering the interaction in between. The global EMR makes the system model more readable and facilitates the understanding of the interactions between the different subsystems. Thus, it is easier to design the power control and management systems based on the tuning chains definition as discussed in the next chapter.





# **Chapter 3**

## **Centralized Energy Management and Low-Level Control Systems**



## 1. Introduction

The design of the effective control strategies with the help of the EMR requires the detailed system analysis, which is called the tuning chain definition. Due to the physical causality principal of the EMR, the tuning parameter of each system is defined to visualize its effect on the system parameters. The control system design depends on defining the MCS (Maximum Control Structure) that considers all the system parameters measured and controllable. Hence, the MCS is filtered to the PCS (Practical Control Structure), which defines only the parameters that can be measured and control practically. This chapter discusses the tuning chains definition of the different subsystems and consequently the low-level control system designs. The low-level control system consists of the control entities attached to the physical components and receive their reference values from the management system. Then, a paradigm of a centralized energy management system is presented to evaluate the overall system performance in the standalone operation mode. A MATLAB/Simulink model of the system analyzes the system performance with the help of the detailed results based on the studied system parameters.

## 2. Tuning Chains Definition

The hybrid marine-hydrogen active power generation system (discussed in Ch2) integrates five tuning chains: one for the machine side converter (PMSG Converter) and the second for the load side converter while each DC-DC power electronic converters have a tuning chain based on its function and operation mode.

### 2.1. Machine Side Converter (MSC) Tuning chain

The MSC tuning chain definition requires studying the characteristics of the PMSG and the MCT (with its MPPT) to define the operating point. The PMSG characteristics are analyzed in [164] and show that the generator performance is affected mainly by its d-q axis terminal voltages while the rotational speed has a minor effect. Studies in [116], [119] present the MCT characteristics at different marine current speeds with its maximum power point tracking under the nominal speed and the power limitation above the base speed. The operating point of the MSC represents the intersection point between the generator characteristics and the MCT characteristics as shown in Fig. 3.1. The presented PMSG characteristics are the power versus the rotational speed at different d-axis voltages with the q-axis being constant (based on the reference frame alignment).

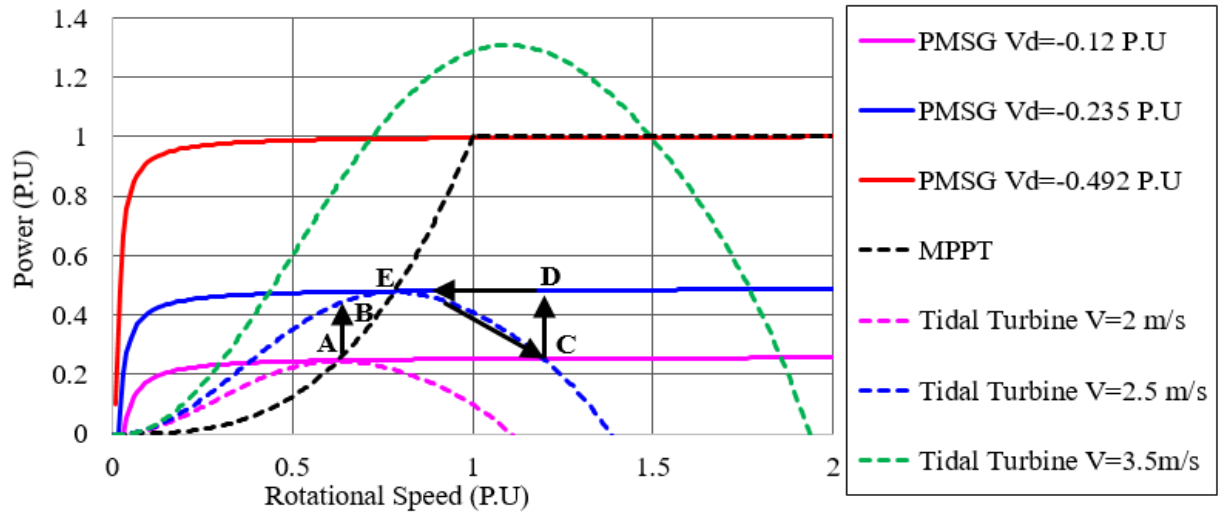


Fig. 3.1. Operating Point Definition based on MPPT, MCT, and PMSG Characteristics.

To define the operating point, suppose that the turbine operates at a marine current speed is 2 m/s (Pink Dotted Line). Then, the generator d-axis voltage is controlled to have the intersection with the MCT at its maximum power point (A). The marine current speed increases to 2.5 m/s (Blue Dotted Line) and consequently the operating point becomes (B) at the first instance due to the high inertia of the system so the speed will be constant at this instant. At (B), the applied turbine torque is greater than the generator electromagnetic developed torque. Thus, the generator starts to accelerate and the speed increase to the point (C). The controller begins to change the d-axis voltage of the generator to another characteristic (Blue Solid Line). The operating point changes from point (D) to the point of the maximum power at the new speed (E). As a result, the MSC tuning chain is defined as shown in Fig. 3.2.

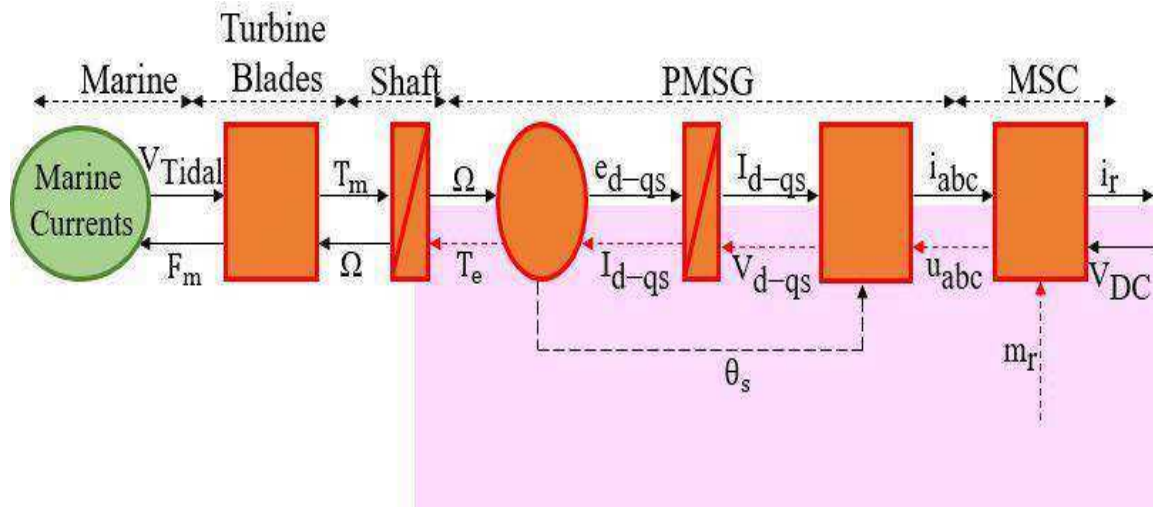


Fig. 3.2. MSC Tuning Chain.

## 2.2. Load Side Converter (LSC) Tuning Chain

The LSC is used to feed a fixed voltage, fixed frequency AC voltage on the load terminals. Equations (2.52) and (2.53) demonstrate that feeding a fixed AC voltage ( $U_{Ld}$ ) at a definite load level ( $I_{Ld}$ ) requires controlling the inverter d-q axis components of the inverter voltage ( $e_d, e_q$ ). From this analysis, the LSC tuning chain is presented as shown in Fig. 3.3.

### 2.3. Electrolyzer Side Converter and Fuel Cell (ESC, FCSC-Buck, Boost) Tuning Chain

The buck and the boost converters are used to control the electrolyzer and the fuel cell operating points at the reference values that are estimated by the system energy management system. The tuning parameter is the converter duty cycle that is used to control the electrolyzer or the fuel cell current as a controlled current source. Controlling the current determines the operating voltage and the produced or the consumed gases flow rates as shown in Fig. 3.4, Fig. 3.5.

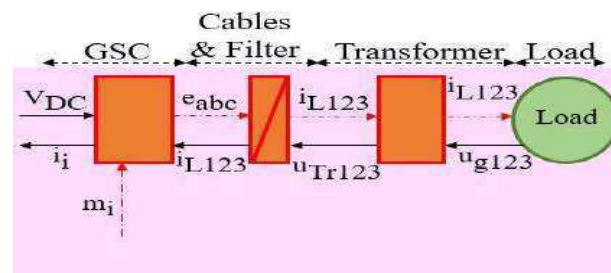


Fig. 3.3. LSC Tuning Chain.

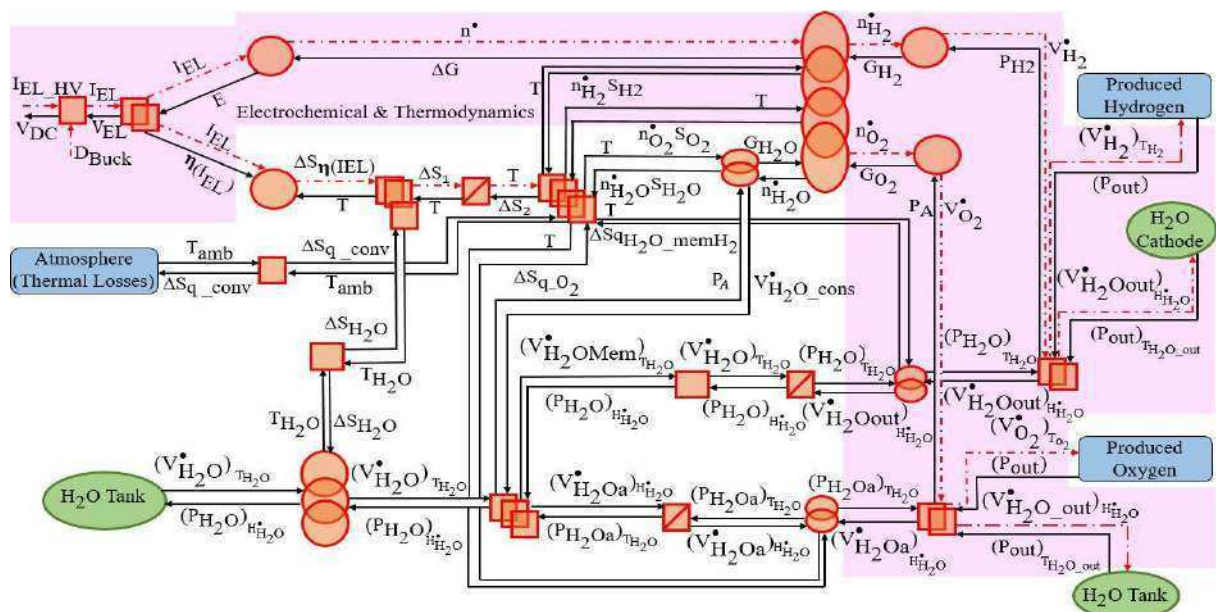


Fig. 3.4. ESC Tuning Chain.

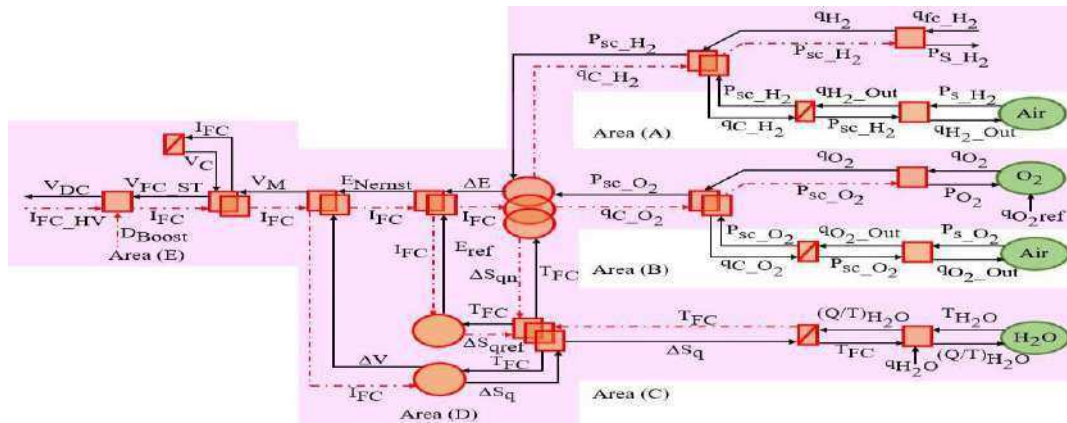


Fig. 3.5. FCSC Tuning Chain.

#### 2.4. Battery Side Converter (BSC, Bi-directional) Tuning Chain

There are many studies [165]–[168] that have considered the battery in a hybrid renewable-hydrogen storage system (electrolyzer and fuel cell) as a short-term energy buffer in the grid-connected mode. Moreover, the battery converter has been controlled for stabilizing the voltage and the frequency (Considering an AC power system) during the isolated mode. Consequently, the battery is used as a small energy buffer system (concerning the sizing) for stabilizing the DC-link voltage. Figure 3.6 exhibits the battery tuning chain.

### 3. Control Strategies

Based on the defined tuning chains, each system has its control strategies that are discussed in the following subsections.

### 3.1. Marine Current Turbine (MCT) Control strategies

The control strategies of the machine side converter are the Flux Control Strategy (FCS) and the active Power Control Strategy (PCS).

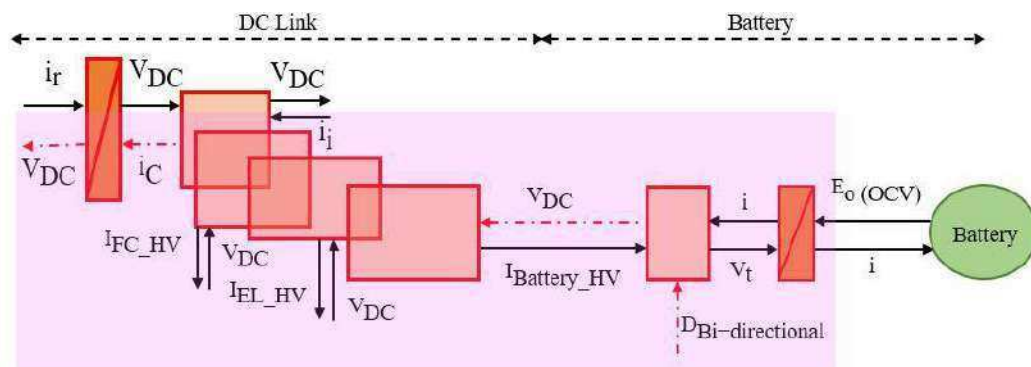


Fig. 3.6. BSC Tuning Chain.

### 3.1.1. Power control strategy (PCS)

The main goal is to control the active output power of the permanent magnet synchronous generator. There are two modes of this strategy: the maximum power point tracking mode when the machine is running below the base speed and the limitation power mode when the machine speed is above the base speed. The developed electromagnetic torque of the PMS represented in d-q axis frame rotating synchronously with the rotor flux ( $i_{ds}=0$ ) is due to (3.1) which is a reformation of (2.7) and (2.9) (refer to Ch2).

$$T_e = \frac{3}{2} P \Phi_r i_{qs} \quad (3.1)$$

The turbine torque in maximum power point tracking mode ( $T_{mopt}$ ) estimation (under the base speed) is based on (2.3) and (2.4) (refer to Ch2) by substituting the optimal values of  $C_p$  and  $\lambda$  (0.45 and 6.3 respectively) as shown in (3.2) [119].

$$T_{mopt} = \frac{P_m}{\Omega} = 0.5 \pi \rho R^5 \left(6.3 * \frac{R}{V}\right)^2 \frac{0.45}{6.3^3} = 4.45 \frac{R^7}{V^2} \quad (3.2)$$

At a steady-state operation, the electromagnetic torque of the machine equals the applied torque by the turbine, which provides the reference value of the q-axis current for the machine ( $i_{qs\_ref}$ ). When the machine runs at speed higher than the rated speed, the active power control changes the strategy from the MPPT to the power limitation. This strategy controls the machine to limit the generated power at its rated value for avoiding the generator overloading. The applied torque by the turbine in this mode is due to (3.3) [119].

$$T_{mopt} = \frac{P_{mrated}}{\Omega} = \frac{3}{2} P \Phi_r i_{qs} \quad (3.3)$$

### 3.1.2. Flux control Strategy (FCS)

This strategy also has two modes of operation. The first mode is the maximum torque/ampere mode that keeps ( $i_{dsref}=0$ ) when the machine runs below the rated speed. The second mode is the flux weakening control strategy that keeps the voltage and current of the machine under their rated values when it runs above the base speed. Studies about flux weakening strategies can be found in [119], [169] where detailed analyses are presented for the estimation of the speed limit



of the constant power mode ( $\Omega_{\text{con}}$ ) and the maximum operating speed ( $\Omega_{\text{max}}$ ) of the PMSG. At the maximum operating speed, it is possible to run the generator with regarding its voltage and current under their rated values. Equations (3.4) and (3.5) estimate the two - speed operating ranges for the modeled system [values of  $(2.4 \Omega_b)$  and  $(3.3 \Omega_b)$  respectively] [119].

$$\Omega_{\text{max}} = \frac{V_{\text{max}}}{\Phi_r - L_s I_{\text{max}}} \quad (3.4)$$

$$\Omega_{\text{con}} = \frac{\omega_b}{1 - 2\left(\frac{\omega_b L_s I_{\text{max}}}{V_{\text{max}}}\right)} \quad (3.5)$$

[Where:  $V_{\text{max}}$ ,  $I_{\text{max}}$  are the maximum voltage and current limits of the machine which are the peak phase voltage and current of the machine,  $L_s$  is the machine's stator inductance as ( $L_q = L_d$ ), and  $\omega_b$  is the electrical nominal base speed of the machine].

The voltage and current limits of the machine estimation rely on the d-q components using (3.6) and (3.7) [119], [169].

$$i_{\text{ds}}^2 + i_{\text{qs}}^2 \leq I_{\text{max}}^2 \quad (3.6)$$

$$v_{\text{ds}}^2 + v_{\text{qs}}^2 \leq V_{\text{max}}^2 \quad (3.7)$$

The equation (3.8) is the reformulation of the limit voltage equation (3.7) in steady state by neglecting the stator resistance and considering of ( $L_d = L_q = L_s$ ).

$$i_{\text{qs}}^2 + \left(i_{\text{ds}} + \frac{\Phi_r}{L_s}\right)^2 \leq \left(\frac{V_{\text{max}}}{\omega_e L_s}\right)^2 \quad (3.8)$$

The voltage and current limits equations (3.6 and 3.8) are represented graphically by two circles as shown in Fig. 3.7. This figure indicates that the current limit circle is independent of the operating speed while the limit voltage circle changes with it. The operating point of the machine is the intersection point between the two circles [119], [169]. The operating point at the rated speed is the intersection point between the green circle and the black one, which is point A.

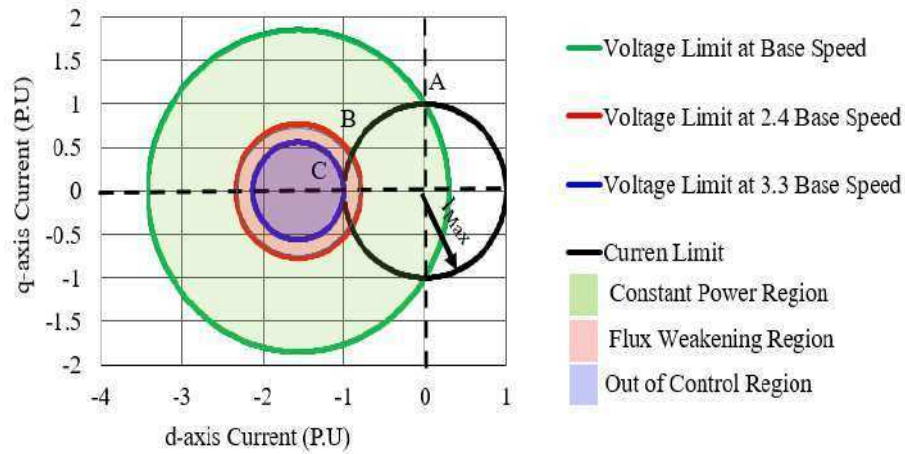


Fig. 3.7. PMSG Voltage and Current Limit Circles.

The figure shows the constant power range, which is the area between the green and red circles. The red circle is the graphical representation of the voltage limit at the maximum speed in the constant power range ( $2.4 \omega_b$ ) while the operating point at this speed is the point B. The area between the red and blue circles in the figure indicates the flux weakening control range by sustaining the machine voltage and current below their rated values. The maximum operating speed of the machine is the tangent point between the blue and black circles, which is point C. The blue region is the range of very high speed in which the flux weakening control is not effective to sustain the machine voltage and current under their rated values for that it is called out of control. Based on (3.6)-(3.8), the d-q axis currents for flux weakening control above the base speed is estimated using (3.9)-(3.11) [119]. By using (3.9) with the studied system parameters (refer to Appendix A [115]–[117], [119]), the d-axis current value at different operating speeds can be estimated using (3.12).

$$i_{dsref} = \frac{L_s}{2\Phi_r} \left[ \left( \frac{V_{max}}{\omega_e L_s} \right)^2 - \left( \frac{\Phi_r}{L_s} \right)^2 - I_{max}^2 \right] \quad (3.9)$$

$$i_{qsmax} = \left( \frac{\omega_b}{\omega_e} \right) I_{max} \leq i_{qsmax} \quad (3.10)$$

$$i_{qsmax} = \sqrt{I_{max}^2 - i_{dsref}^2} \quad (3.11)$$

$$i_{dsref} = \frac{141921786}{\omega_e^2} - 1443.07 \quad (3.12)$$

In the previous studies for the MCT system [115]–[117], [119],  $i_{dsref}$  is kept at zero below the base speed to have maximum (torque/ampere or T/A). Other studies [170]–[172] that have proposed the control of this current (due to (3.13)) for minimizing the electrical losses of the PMSM driven as a motor or by the wind turbine with defining its core resistance ( $R_c$ ). One of this work novelty is the adaptation of the output maximization (losses minimization) method for the MCT system. The reference value of this current is estimated using (3.14) which is a reformulation of (3.13) by using the modeled system parameters (refer to Appendix A).

$$i_{dsrefLM} = \frac{\omega_e^2 L_s (R_s + R_c) \lambda_r}{R_s R_c^2 + \omega_e^2 L_s^2 (R_s + R_c)} \quad (3.13)$$

$$i_{dsref} = \frac{0.3727 \omega_e^2}{129.33 + 1.82 * 10^{-4} * \omega_e^2} \quad (3.14)$$

The equation (3.14) is not a complex relation. For that, the MATLAB curve-fitting tool is used to linearize it due to (3.15). A third-order polynomial equation approximates the d-axis reference current in per-unit ( $i_{dsrefLMP,U}$ ) value relation based on the per-unit machine rotational speed ( $\omega_{eP,U}$ ) [172].

$$i_{dsrefLMP,U} = 0.049 \omega_{eP,U}^3 - 0.25 \omega_{eP,U}^2 + 0.0063 \omega_{eP,U} - 0.00035 \quad (3.15)$$

To evaluate the effect of the loss minimization on the maximum (torque/ampere), Figure 3.8 presents the q-axis, d-axis and the total currents in per unit based on the peak value of the rated generator phase current ( $I_{max}$ ). In this figure, it is clear that the difference between the q-axis current and the total current with loss minimization is small. The maximum (torque/ampere) mode controls the q-axis current with sustaining the d-axis at zero which means that the total current is the same q-axis current. Thus, the difference between the loss minimization and maximum torque per ampere modes of operation is not significant. Figure 3.9 shows the different MCT operation modes, which is drawn based on the studied system parameters (refer to Appendix A). Based on all the above control strategies, the MSC control system is designed as shown in Fig. 3.10.

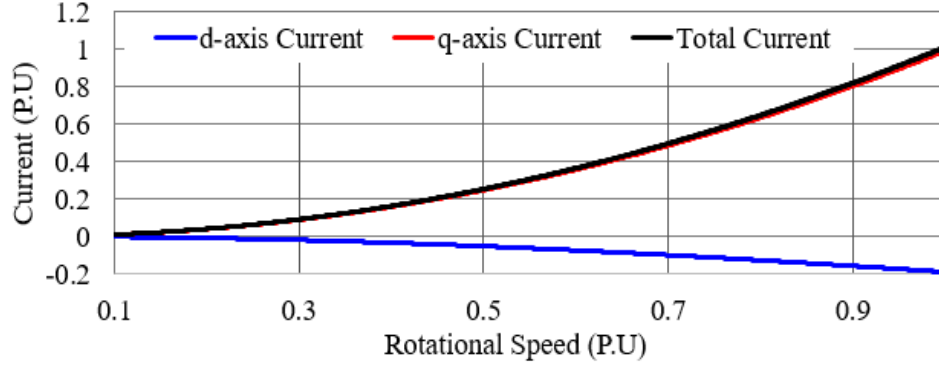


Fig. 3.8. PMSG d-q Axis Components and the Total Currents at Different Speeds.

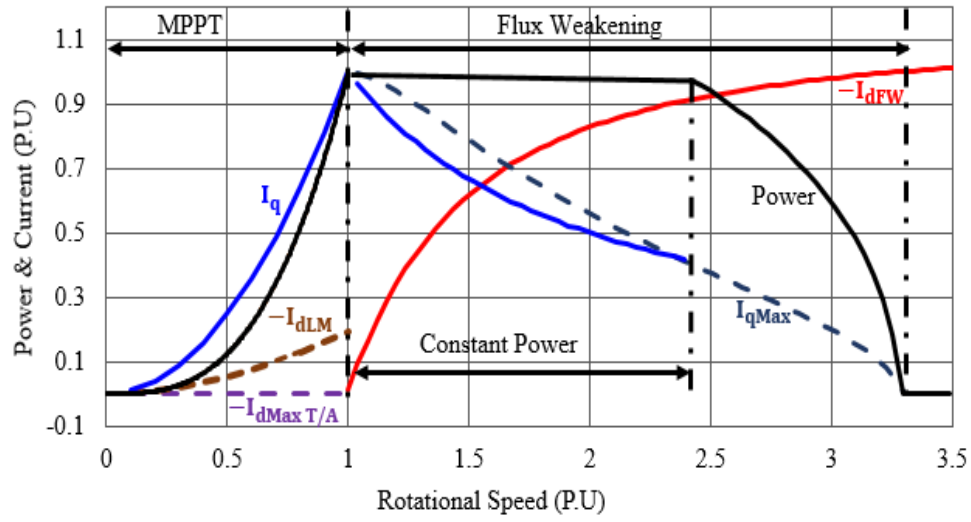


Fig. 3.9. Operation Modes of the Studied MCT.

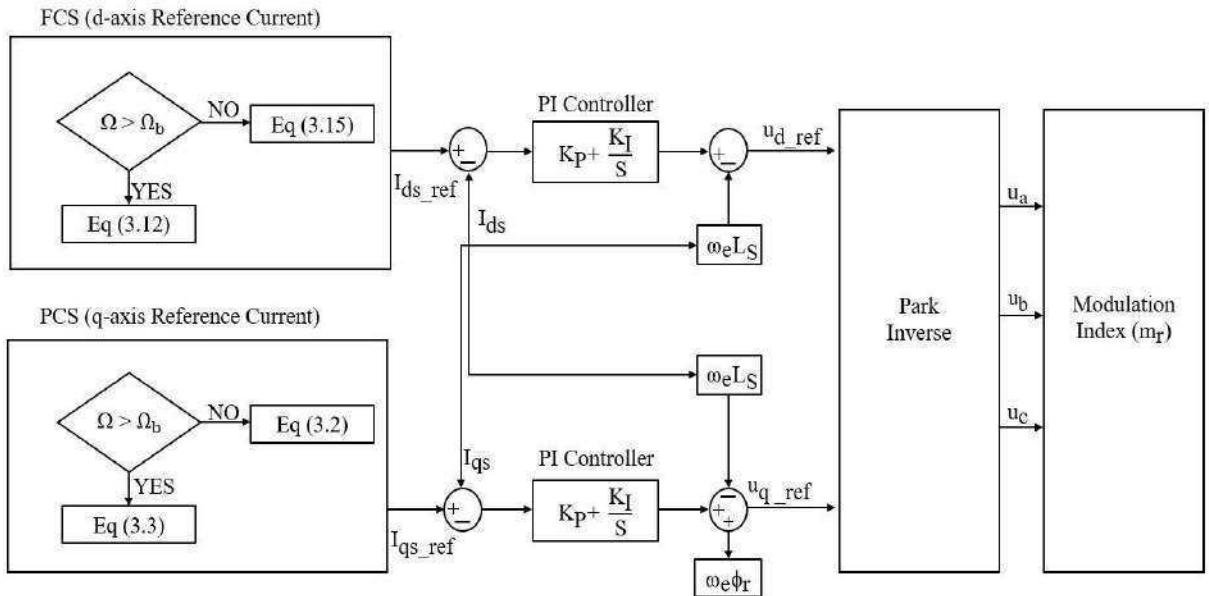


Fig. 3.10. MSC Control System based on the PCS and FCS.



The energy management system must also consider the battery safe operation that represents the current and the state of charge (SOC) limits. The current limit is the operation within the battery rated current for avoiding overloading. Based on the battery type, the manufacturer defines the SOC limits to ensure the healthy operation without overcharging or under discharging. The design of the energy management system determines the battery rating by the sizing procedure that has been discussed in [158]. The proposed energy management system estimates the electrolyzer operating point by filtering the power into slow and fast dynamic components. The filter time constant depends on the safe and the recommended electrolyzer dynamic response. The considered PEM electrolyzer system (as discussed in the following section) has a starting up a dynamic response in the range of five minutes that is compatible with the PEM energy storage systems dynamics (refer to Fig. 2.16) [158], [175]. Thus, the energy management system provides the fuel cell and the electrolyzer operating points as an output of a low pass filter with a time constant of 5 minutes with respecting the battery minimum and maximum SOC limits as shown in Fig. 3.12. The electrolyzer and the fuel cell converters are controlled current sources following the power operating points reformed as reference current values (assuming a fixed DC-link voltage).

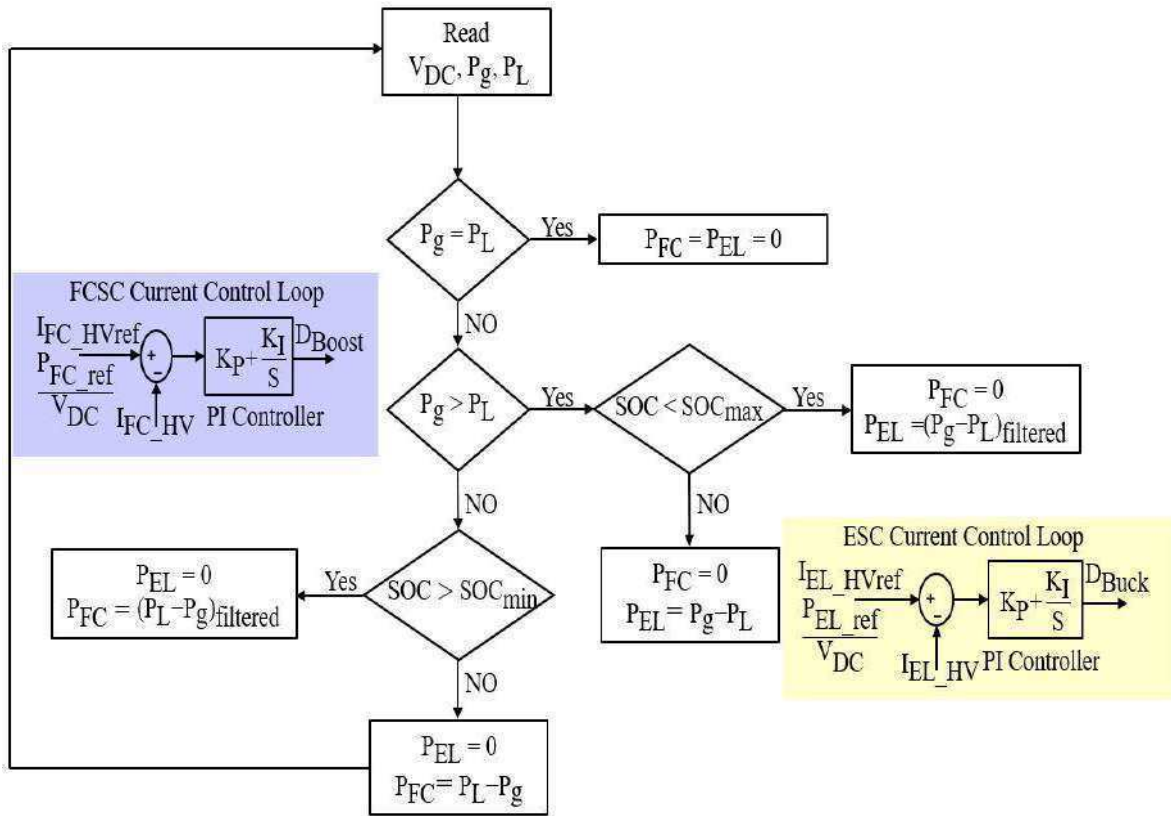


Fig. 3.12. Electrolyzer and Fuel Cell Side Converters Control Strategies.

### 3.4. Battery Side Converter Control Strategy

The battery side converter (BSC) is controlled based on definite control duties that stabilize the DC-link voltage and covering the fast dynamics power variations. By controlling the electrolyzer and the fuel cell operating point, the battery can cover the fast dynamics if its SOC allows charging or discharging. Otherwise, it stabilizes the DC-link voltage by considering the battery as a voltage source. The BSC controller consists of the dual loop as shown in Fig. 3.13. The external loop is a voltage control for stabilizing the DC-link voltage around a reference value ( $V_{DC-ref}$ ) with a battery reference current as an output. The inner loop follows the outer loop output to control the battery operating current.

Based on the whole system EMR and the control chains definition, the practical control structure of the active hybrid MCT/hydrogen power generation system is designed as shown in Fig. 3.14.

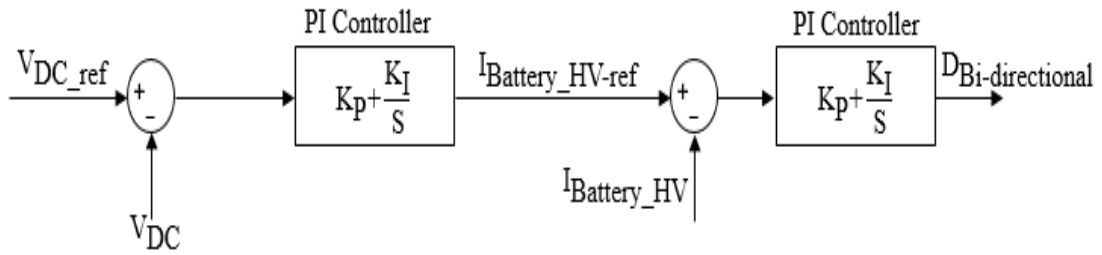


Fig. 3.13. BSC Control Strategy.



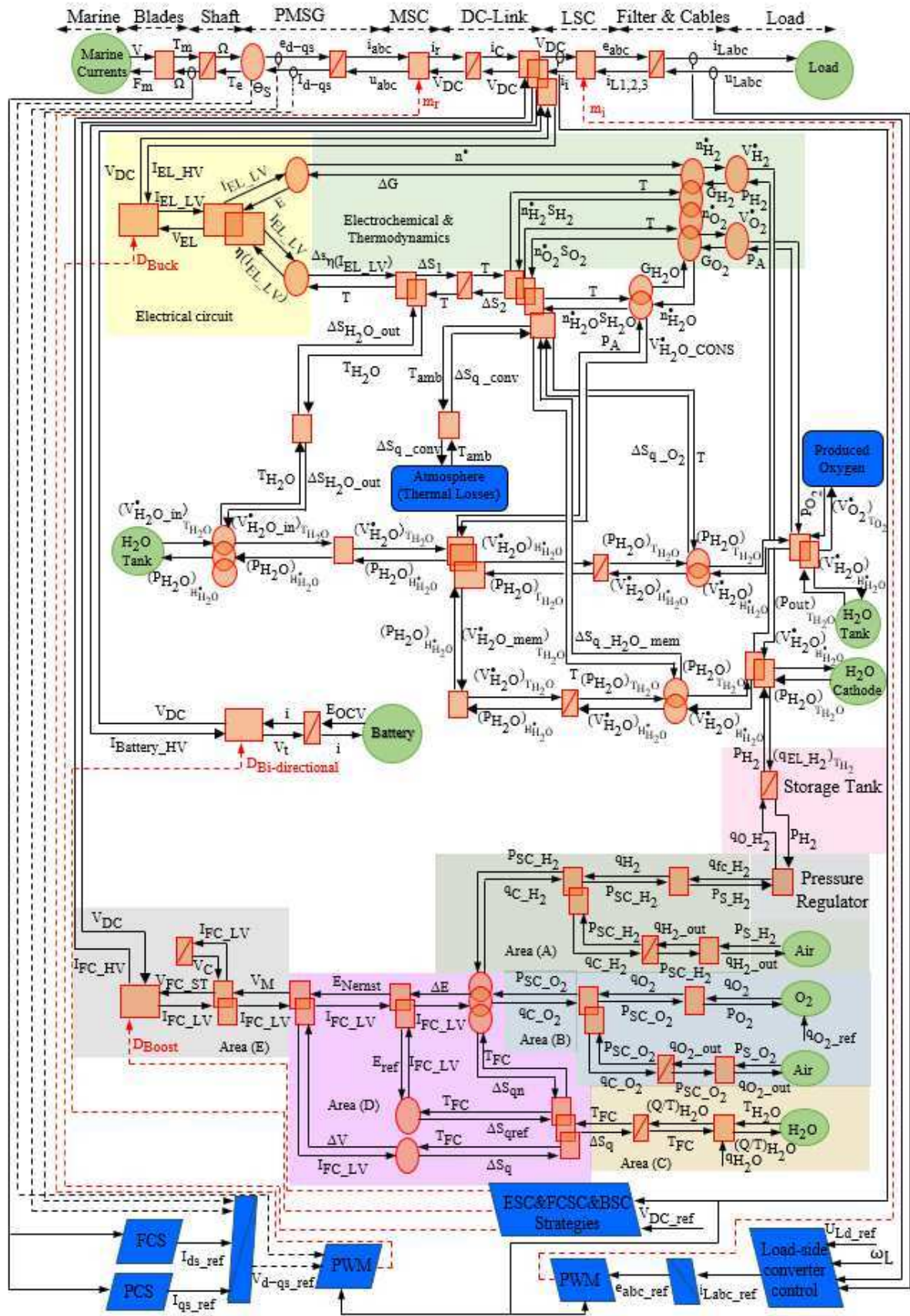


Fig. 3.14. The Hybrid MCT-Hydrogen Global EMR Considering the Practical Control Structure.



#### 4. Simulation and Results

A Matlab/Simulink model is built by considering all the system equations and control to analyze and study the hydrogen production process under marine current speed and load profile variations. The model parameters are categorized into groups for each system as follow:

- MCT system parameters
- MW scale PEM electrolyzer parameters
- MW scale PEM fuel cell parameters
- Battery parameters

The MCT current turbine system parameters represent the turbine, the PMSG, the DC-link, and the load side (including the cables, the filter, and the transformer) parameters (refer to Appendix A). The following subsections discuss the MW scale PEM electrolyzer, the PEM fuel cell and the battery parameters in details while their values also are indicated Appendix A.

The PEM electrolyzer model presented in [133] has a very high-level of accuracy due to its performance convergence with the original small-scale laboratory PEM electrolyzer (50 W- Fig. 3.15). This convergence has been validated based on the comparison between the static voltage-current polarization characteristics of the model (with the proposed parameters) and the experimental as shown in Fig. 3.16. The convergence estimation used the MATLAB “fit” tool with the sum of square error (sse), the coefficient of determination (rsquare), the degree-of-freedom (dfe), the adjusted coefficient of determination (adjsquare) and the root mean square error (rmse).

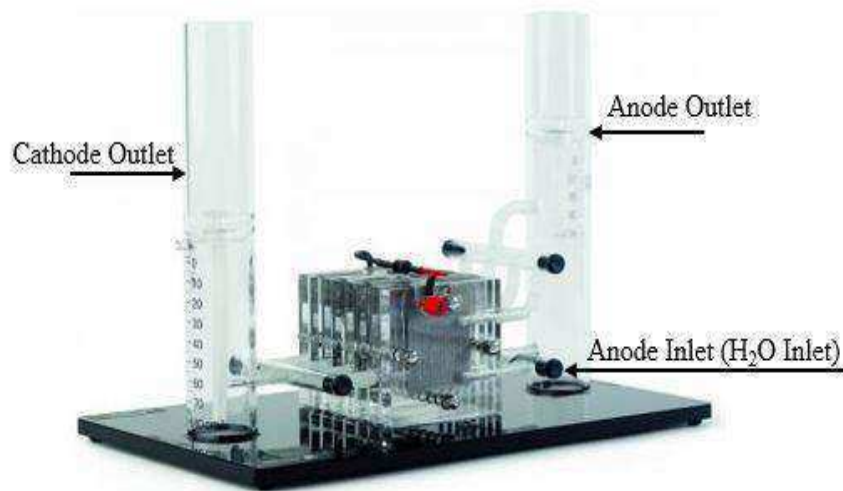


Fig. 3.15. Staxx7-HTECH PEM Electrolyzer Stack [133].

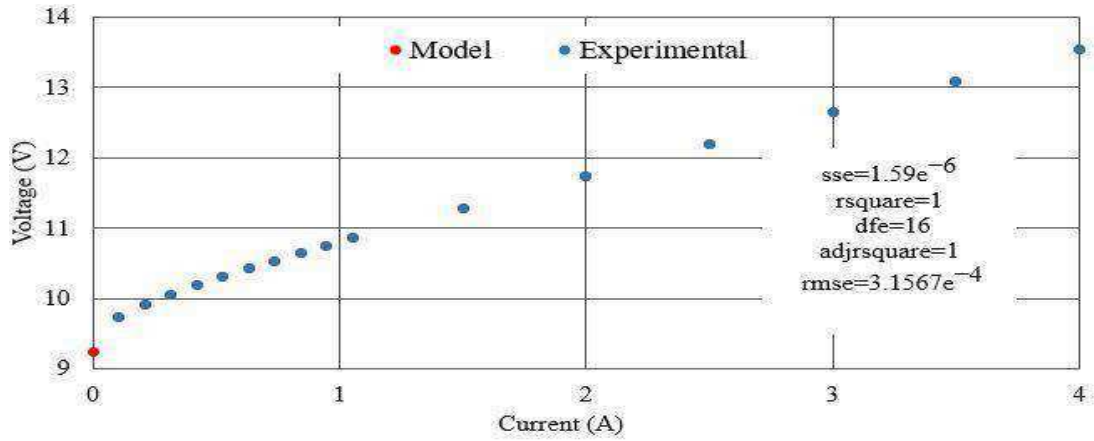


Fig. 3.16. PEM Electrolyzer Polarization Curve: Model-Experimental [133].

When the sse and rmse are closer to zero, the rsquare and adjsquare are closer to 1 which means an absolute convergence and fitting between the two characteristics. The effect of the different overpotentials on the polarization curve changes due to the operating current density as shown in Fig. 3.17. When the electrolyzer runs at lower current density, the activation voltage (especially the anode one) represents the bulk section of the overpotential while the others are minors. With increasing the current density, the effect of the activation stabilizes while the Ohmic one (especially the ionic) elevates with a slight electric voltage drop due to the high electrons conductivity of the electrodes, current collectors, and the bipolar plate's materials. At the rated current density ( $0.25 \text{ A/cm}^2$ ), the anode activation and the ionic voltages represent 40 and 55% of the total over potential consequently. The MW scale PEM electrolyzer module consists of some kW stacks connected in parallel to extend the hydrogen production ability for the different applications, e.g., the power-to-gas or fuel cell based vehicle refueling.

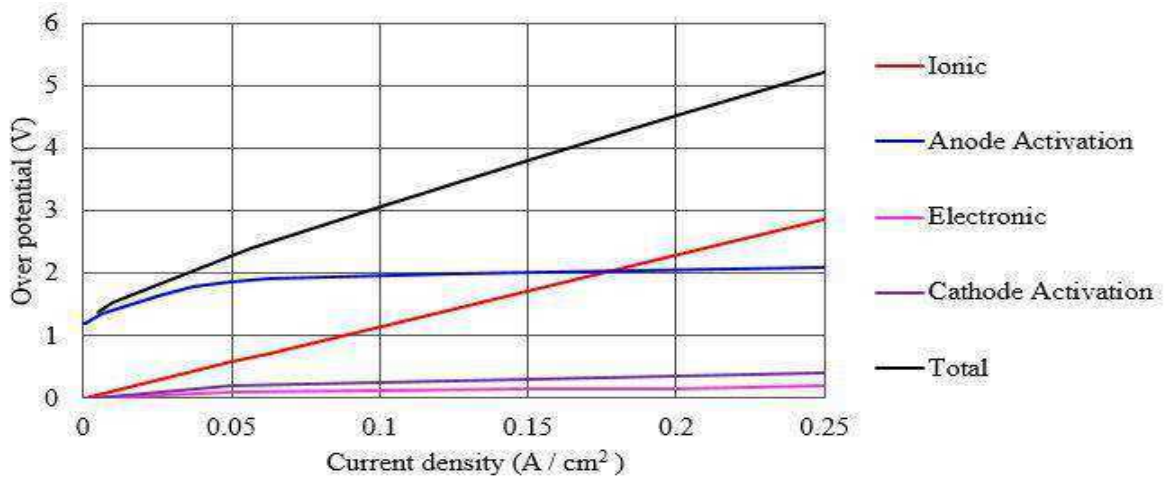


Fig. 3.17. Studied PEM Electrolyzer Module Overpotentials Contribution

The commercially available MW PEM electrolyzer products change in their hydrogen production rates from 30 Nm<sup>3</sup>/h (65 kg/day) with 30-bar output pressure up to 200 kg/day with 200-bar pressure in the future trends. The common feature of these modules is the high current density operation up to (3 A/cm<sup>2</sup>) [176]. Due to the literature survey (up to our best information), there is no static or dynamic models of the MW scale electrolyzer while there is a scarcity in the system parameters and characteristics to be used for modeling as shown in Table 3.1 [177]. Many manuals and publications [175], [178]–[181] have presented the first details of the 250 kW Proton Onsite PEM electrolyzer stack that is selected to be used and modeled. The studied small-scale (50 W) PEM electrolyzer model is modified based on the available parameters to represent the 250 kW stack. The rated power of the modeled MCT system is 1.5 MW. When the marine current speed is the rated, and there is no load demand, almost all the generated power must be converted into hydrogen. Thus, the MW scale PEM electrolyzer is designed to have six parallel stacks (NEL\_ST). The model is adapted by changing the main parameters (exchange current densities, the membrane conductivity and the charge transfer coefficients of the anode and the cathode).

Manufacturer	Series/Operating Pressure	H <sub>2</sub> rate (Nm <sup>3</sup> /h)	Energy Consumption (kWh/Nm <sup>3</sup> )	Partial Load Range (%)	Development Year (Commercially available)
Giner Electrochemical Systems	High pressure/85 bar 30 Kw Generator/25 bar	3.7 5.6	5.4 5.4	No details	2011
Hydrogenics	HyLYZER/25 bar 1 MW electrolyzer (development stage)	1 0-260	4.9 (stack) 7.2 System (not yet published)	0-100	2015 (Start of operation)
Proton Onsite	HOGEN S/14 bar	0.25-1	6.7	0-100	2000
	HOGEN H/15-30 bar	2-6	6.8-7.3	0-100	2006-2009
	HOGEN C/30bar	10-30	5.8-6.2	0-100	2010
	Electrolyzer with 250 kW stacks (at development stage)	>400	No details	No details	No details
H-TEC Systems	EL30/30bar	0.3-3.6	5.0-5.5	0-100	2011
ITM Power	HGAS, HPac, HFuel	≤260	No details	No details	2011
SIEMENS	SLYZER 100 100 kW (300 kW peak) 50bar	~20-22.5 At nominal load	No details	0-300	1998 (start of PEM Technology Development)
	SLYZER 200 stack 1.2 MW , 2.1 MW peak (at development stage)		No details	No details	2013-2015

Table 3.1 Overview of Leading Developers/Manufacturers of MW scale PEM Electrolyzers [177], [181]–[185].

The parameters estimation depends on the reverse engineering. The reverse engineering requirements are the polarization curve which is deduced from the Proton Onsite publications (Fig. 3.18) [181], the current density, the number of cells and the cell area (available from the stack manuals) [175], [178]–[180]. The reverse engineering procedure has been used already to build a model of SLYZER 200 Siemens PEM electrolyzer stack [186]. Figures 3.19 and 3.20 show the adopted model characteristics while the estimated parameters for the model compared to the small-scale one are listed in Table 3.2. The Key Performance Indicators (KPIs) of the PEM electrolyzer are the hydrogen production rate, the electrical power, the hydrogen pressure, the efficiency, the hydrogen purity, the lifetime, the degradation and the hydrogen production cost [102]. The first four KPIs are the most suitable to be also used for verifying the model accuracy. The model provides a hydrogen production and water consumption rates of 51 (Nm<sup>3</sup>/h) and 46 L/h respectively that are approximately the same real rates of the stack (Table 3.2) with taking into consideration that the model does not consider the Faraday efficiency. The voltage, current and power characteristics show the convergence of the model to the real stack performance while the operating voltage of the model is almost the same of the stack, which provides the same level of efficiency due to (2.31).

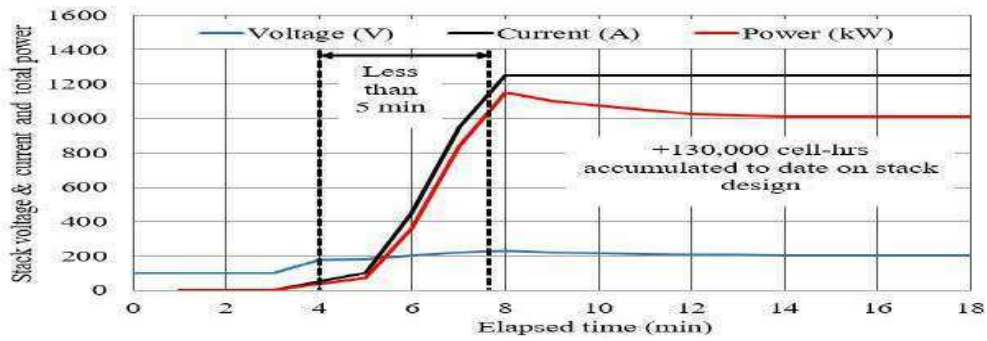


Fig. 3.18. Proton Onsite 250 kW Characteristics [181].

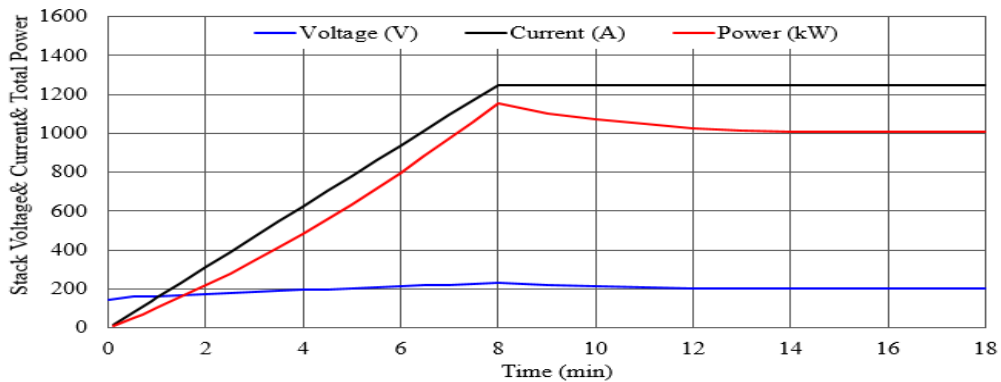


Fig. 3.19. Characteristics of the 250 kW Stack Adopted Model.

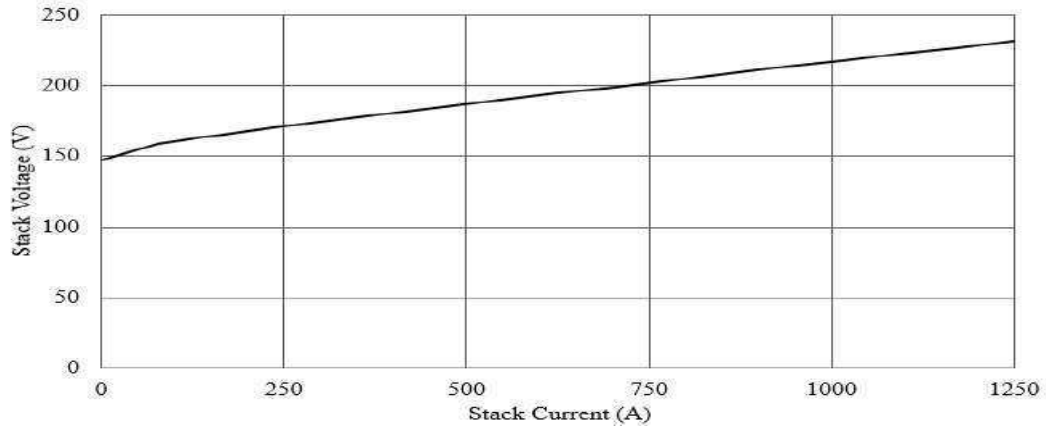


Fig. 3.20. Polarization Curve of the 250 kW Adopted Model.

Parameter	Small-scale studied model	Proton Onsite model
Power (kW)	0.05	250
MEA active area (cm <sup>2</sup> )	16	650
Number of cells	7	100
Output pressure (bar)	1	30
Current density (A/cm <sup>2</sup> )	0.25	1.9231
Anode exchange current density (A/cm <sup>2</sup> )	$0.1548 \cdot 10^{-2}$	$8 \cdot 0.1548 \cdot 10^{-2}$
Cathode exchange current density (A/cm <sup>2</sup> )	$0.3539 \cdot 10^{-1}$	$8 \cdot 0.3539 \cdot 10^{-1}$
Membrane conductivity (S/cm)	$0.9322 \cdot 10^{-2}$	$8 \cdot 0.9322 \cdot 10^{-2}$
Anode charge transfer coefficient	0.7178	0.7178
Cathode charge transfer coefficient	0.6395	0.6395
Hydrogen production rate (Nm <sup>3</sup> /h)	No details	50
Reactant water consumption rate (L/h)	No details	45

Table 3.2 Parameters of the Studied Small-Scale and Proton Onsite Stack Models [133], [175], [178]–[181].

The PEM fuel cell model presented in [152] has been modified and adapted to be in the range of MW scale by integrating six PEM fuel cell stacks (250 kW rating/stack) with the help of the parameters and the data illustrated in Table 3.3. The small-scale model has been validated by comparing their results with the experimental data under step load variations. Figures 3.21 and 3.22 show the power and the polarization curves of the small-scale and the 250 kW PEM fuel cell models that exhibit the convergence between the two models performance with different ratings. As aforementioned, the procedure of LiFePO<sub>4</sub> battery sizing is the same proposed in [158] by filtering the power variation based on the PEM electrolyzer and fuel cell dynamic response and considering the maximum of the fast dynamic power component as the stack rating. Thus, the battery stack rated power based on the studied system power profiles is 100 kW that is modeled based on the proposed cell model in [159].

Parameter	Small-scale model	250 kW STACK MODEL
Rated power	440 W	250 kW
Number of cells	20	1050
Number of stacks ( $N_{FC\_ST}$ )	1	6
Active area ( $\text{cm}^2$ )	340	1200
Current density ( $\text{A}/\text{cm}^2$ )	0.8	
Concentration and Activation voltages coefficients (A,B in V/K)	$6 \cdot 10^{-5}$ , $-1.5 \cdot 10^{-4}$ respectively	
Nernst voltage coefficients ( $A_{cd}$ , $B_{cd}$ , in V/K)	$300 \cdot 10^{-4}$ , $57 \cdot 10^{-5}$ respectively	
Reversible voltage coefficients ( $\alpha$ , $\beta$ , $\gamma$ , $\delta$ , $\nu$ )	1.4629, $-4.5 \cdot 10^{-4}$ , $1.0285 \cdot 10^{-8}$ , $9.519 \cdot 10^{-13}$ , $-5.989 \cdot 10^{-5}$ respectively	
Cell ohmic resistance ( $\text{m}\Omega$ )	150	
Cell impedance electrode resistance ( $\text{m}\Omega$ )	150	
Double layer capacitance (mF)	20	
Exchange current (mA)	0.03	
Current limit (A)	1	
Internal current (mA)	3	
Standard pressure (Pa)	$0.1 \cdot 10^6$	
Hydrogen pressure (Pa)	$0.1 \cdot 10^6$	
Oxygen pressure (Pa)	$0.21 \cdot 10^6$	
Fuel cell temperature ( $^{\circ}\text{C}$ )	50	

Table 3.3 Fuel Cell Model Parameters [149], [150], [152].

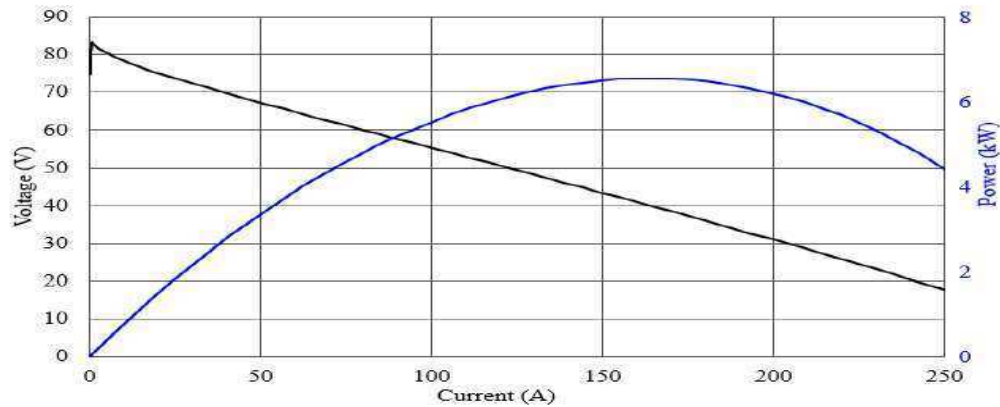


Fig. 3.20. Small-Scale PEM Fuel Cell Model Characteristics [152].

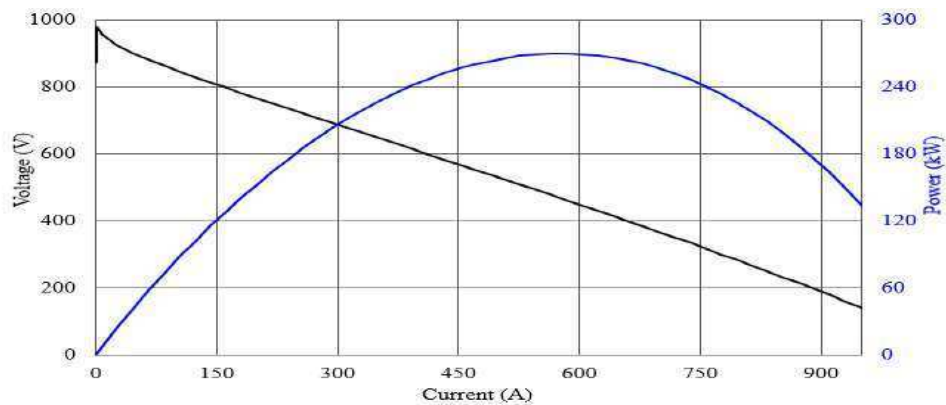


Fig. 3.21. Characteristics of the 250 kW PEM Fuel Cell Stack Model.

Studies [187], [188] have proposed the model of 250 kW battery stack that consists of some parallel-connected strings. Each string consists of some series-connected cells to have the stack power rating. The same procedure is used to estimate the parameters of the 100 kW battery stack. The proposed model in [159] considers a 3.2 V, 20 Ah battery cell (with estimating the cell model parameters) while the considered cell in [187], [188] is 3.2 V, 195 Ah. The later is used in the 100 kW battery stack model with estimating its parameters as shown in Table 3.4. The MATLAB/SIMULINK Control Toolbox (Auto-Tune ) is used to tune the system PI controller's gains. The results are divided into two parts: the first presents the loss minimization while the second discusses the system performance with a marine current speed daily profile to evaluate the effectiveness of the different control strategies. The second part depends on the real data of the Alderney Race (Raz Blanchard in French). This site is situated between the Alderney Island and La Hague Cape (France) and capitalizes about half of the national resource [173].

#### 4.1. Loss Minimization Results

There are two tested control strategies for the FCS (below the rated value): one with maximum (torque /ampere,  $i_{dsref} = 0$ ) and the other with the d-axis reference current estimated based on the loss minimization calculations. As discussed in section 3.1, the control mode of the turbine below the rated marine current speed (3.2 m/s) is the maximum power point tracking. The relation between the marine current and the generator rotational speeds during MPPT mode is estimated based on the optimal value of the tip speed ratio.

Parameters	3.2 V, 20 Ah Model	3.2 V, 195 Ah Model
Number of parallel strings	1	3
Number of series cells in the string	1	168
Cell internal resistance $R_i$ ( $\Omega$ )	0.005	0.005
Transient resistance $R_T$ ( $\Omega$ )	0.0052	0.0052
Transient capacitance $C_T$ (F)	0.52	1000/ $R_T$
Full charge zone voltage $E_{full}$ (V)	3.308	3.308
Exponential zone voltage $E_{Exp}$ (V)	3.251	3.251
Nominal zone voltage $E_{Nom}$ (V)	3.122	3.122
Full Capacity $Q$ (Ah)	18	118.8
Exponential zone capacity $Q_{Exp}$ (Ah)	16.44	108.5
Nominal zone capacity $Q_{Nom}$ (Ah)	5.6	37
$A$ (V)	0.057	0.057
$B$ ( $Ah^{-1}$ )	0.1825	0.1825
$K$ (V)	0.331	0.03
$E_o$ (V)	3.632	3.332

Table 3.4 Battery Stack Model Parameters [158], [159], [187], [188].

This relationship is a reformation of (2.3) by applying the modeled system parameters (refer to Appendix A) to be in the form of (3.17) which is a linear relation as shown in Fig. 3.23.

$$\frac{\Omega}{V} = \frac{\lambda_{\text{Optimal}}}{R} = \frac{6.3}{8} = 0.7875 \quad (3.17)$$

Figure 3.24 shows the core losses reduction based on applying the loss minimization strategy at different marine current speeds. Due to the loss minimization control of the generator, a negative d-axis current component provides a little increase in the copper losses of the generator as shown in Fig. 3.25. The percentage reduction of the core and total losses of the generator estimation based on the comparison between the maximum (torque/ampere) and the loss minimization control strategies.

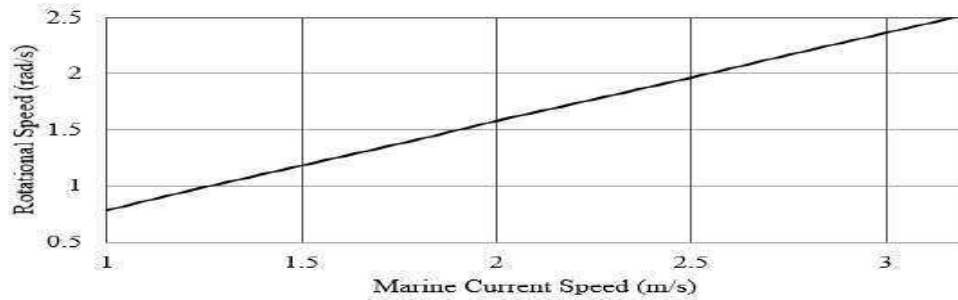


Fig. 3.23. Marine current and PMSG Rotational Speeds in MPPT Mode.

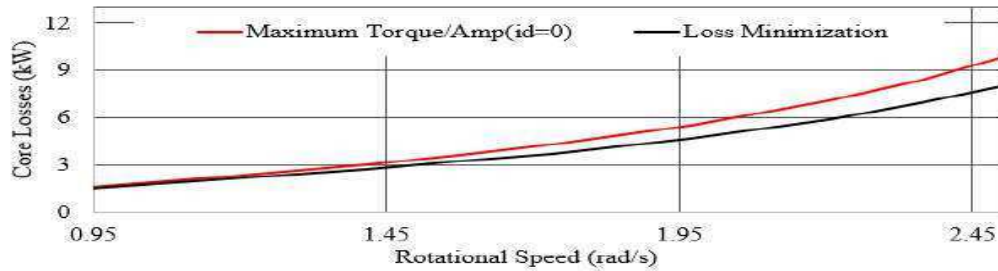


Fig. 3.24. Generator Core Losses at Different Generator Rotational Speeds.

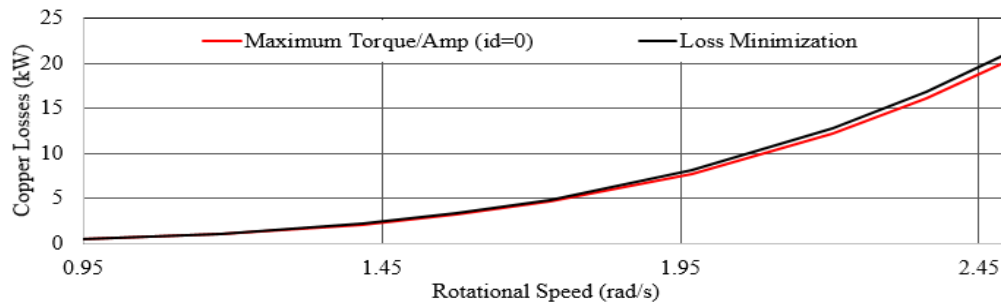


Fig. 3.25. Generator Copper Losses at Different Generator Rotational Speeds.



Figure 3.26 exhibits these percentages reduction in the PMSG core and total losses and Fig. 3.27 shows the improvement in the generator efficiency. It is clear that the average percentage reduction in the generator total and core losses are 3.33% and 11.56%, respectively. The value of the decrease in total losses seems low, but the evaluation of this reduction or saving is more powerful from the energy saving point of view. The total annual energy production estimation of the MCT under particular control strategy has been presented in [118]. This estimation has been performed for the site of Raz de Sein, France. This study has introduced the relationship between the power and the extracted energy limitations for a turbine of 1.245 MW as a case study. This turbine has a cut-in marine current speed of 1m/s and diameter of 12 m. This study concludes that 30% of the rated power limitation provides 7864 hours per year turbine operation in MPPT mode to produce 656 MWh while it operates 560 hours in power limitation mode to produce 228 MWh [118]. Based on this study and by applying the loss minimization control strategy during MPPT mode, the amount of energy saving per year is 3.33% of the PMSG total losses (15 kW as a linear average of the nominal power losses) for 7864 hours, which is 4 MWh. As an evaluation, the amount of energy conservation is used to determine the number of households that fed per year. The World Energy Council determines the average household energy consumption be about 4000 kWh per year [157]. Thus, the loss minimization strategy adapted for one MCT (1.245 MW nominal power) provides energy saving sufficient to feed averagely one house per year. With considering the hydrogen higher heating value (HHV) of 141.88 MJ (0.0392 MWh) [102], the loss minimization strategy for one MCT turbine provides an increase of the annual hydrogen production about 100 kg (due to annual energy saving of 3.93 MWh).

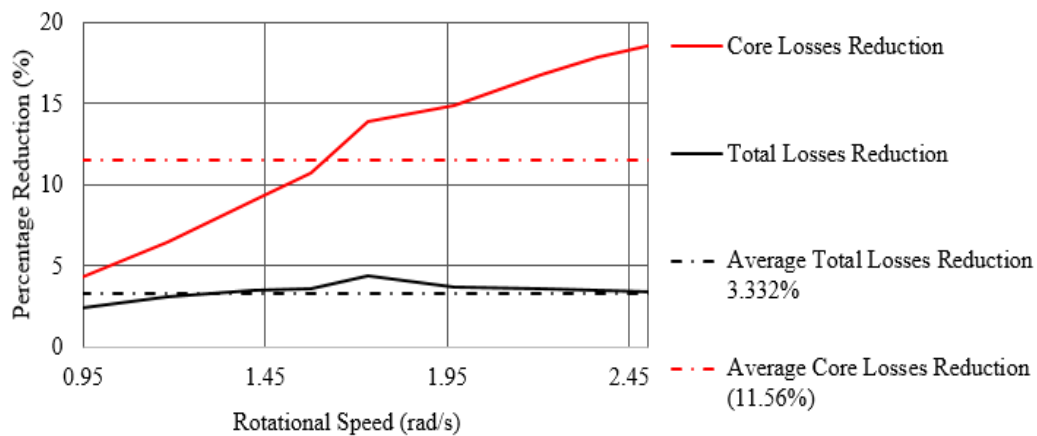


Fig. 3.26. Percentage Reduction of the Generator Core and Total Losses.

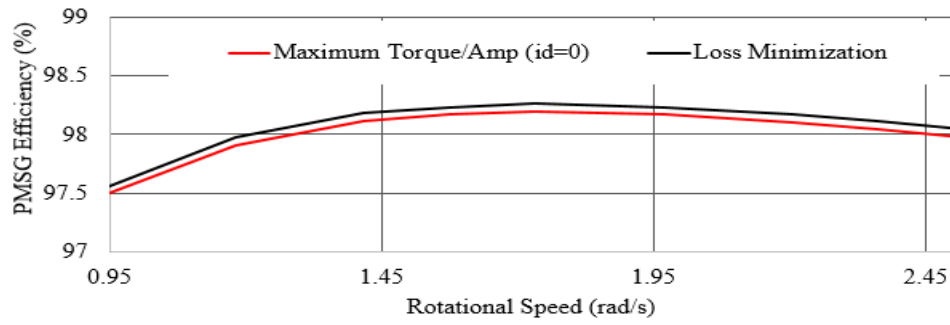


Fig. 3.27. Generator Efficiency at Different Rotational Speeds.

#### 4.2. System Performance with Variable Marine Current Speed

The system model has been tested with a real data of the marine current speed as shown in Fig. 3.28. The marine current speed values and their time ranges represent the actual measurements of the Alderney Race marine site. The modeled time intervals are smaller than the real-time range (a half cycle of the marine current speed profile in the selected site takes about 6 hours). The simulation time is one of the system model parameters (refer to Appendix A) [173]. The point of measurement in the site can be considered as a bidirectional model based on its hydrodynamic model [189]. Due to the model, the measurement of 15 September 2005 is selected as it is the day of the highest tide during the year. The PMSG rotational speed follows the marine current speed in a linear regime under the rated value while the relation is changed above the base speed to limit the power at the rated value [from hours of 8.4 to 9.6 and 20.4 to 21.6]. The MPPT control mode is effective as the power coefficient is kept at its maximum value of 0.45 when the speed is below the rated value. The turbine power coefficient reduces when the speed increases above the rated speed (3.2 m/s). This reduction to keep the power at its rated value of 1.52 MW based on the power limitation mode (From hours of 8.4 to 9.6 and 20.4 to 21.6) as illustrated in Fig. 3.29 and Fig. 3.30.

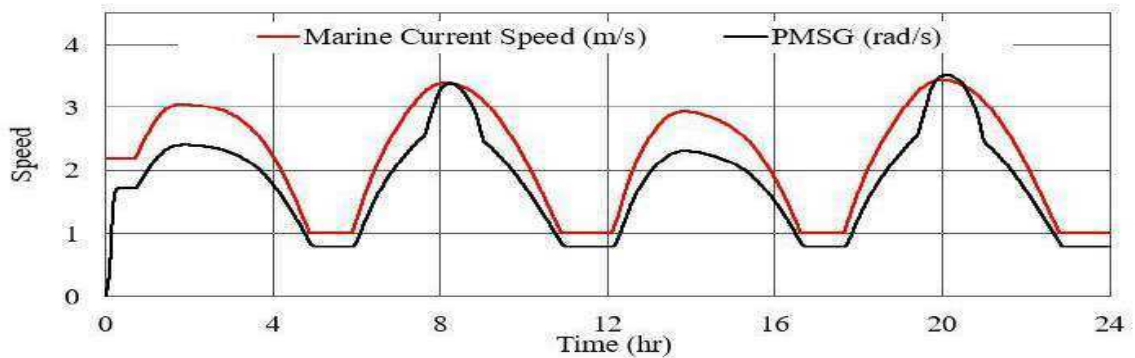


Fig. 3.28. Daily Marine Current and PMSG Rotational Speed Profiles

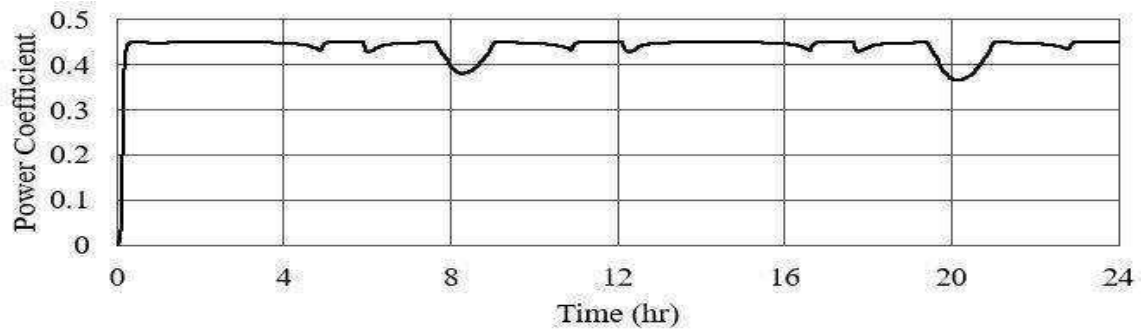


Fig. 3.29. Marine Current Turbine Power Coefficient.

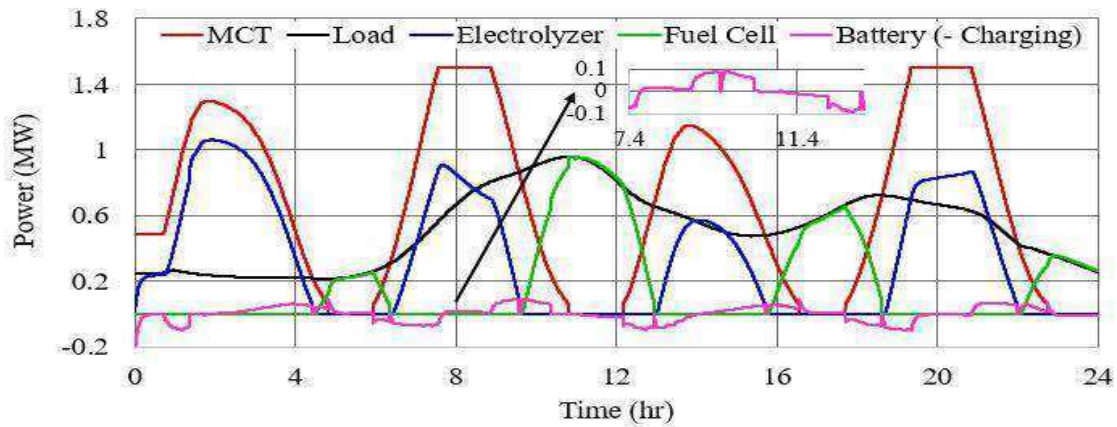


Fig. 3.30. Active Hybrid MCT/Hydrogen System Power Profiles.

While the other reductions (e.g., from hours of 4 to 5) represent the marine current speed below the cut-in speed (1m/s) intervals at which the turbine cannot generate any power. When the generated power is higher than the load demand, the electrolyzer is switched on to consume the surplus power and generate hydrogen [from hours of 1 to 4.5, from 6.5 to 9.5, from 13 to 15.6 and from 18.5 to 22]. Otherwise, the fuel cell is switched on to compensate the shortage of the power [the complementary period]. The battery covers all the times the fast dynamic power variations by changing from charging to discharging modes. The MSC flux control system limits the PMSG current and voltage under their rated values when it runs above the rated speed [from hours of 7.6 to 9 and from 19.5 to 21] to protect the generator from over current and over potential as shown in Fig. 3.31 and Fig 3.32. The generalized average model of the power electronic converters as discussed earlier is used to study the power flow and represents only the fundamental components of the voltage and current sine waves even for the generator or the load. The load-side converter control feeds a fixed AC voltage on the load terminals while the current changes with the load profile during the day as shown in Fig 3.33 and Fig. 3.34.

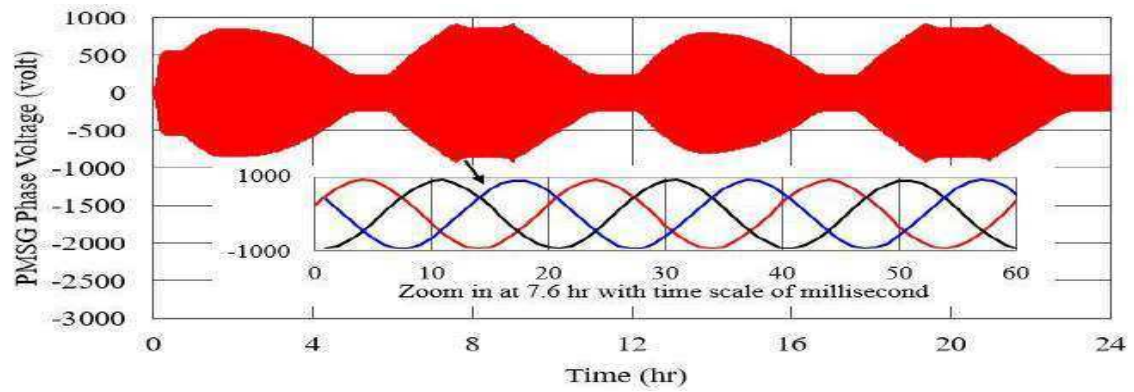


Fig. 3.31. PMSG Instantaneous Phase Voltage.

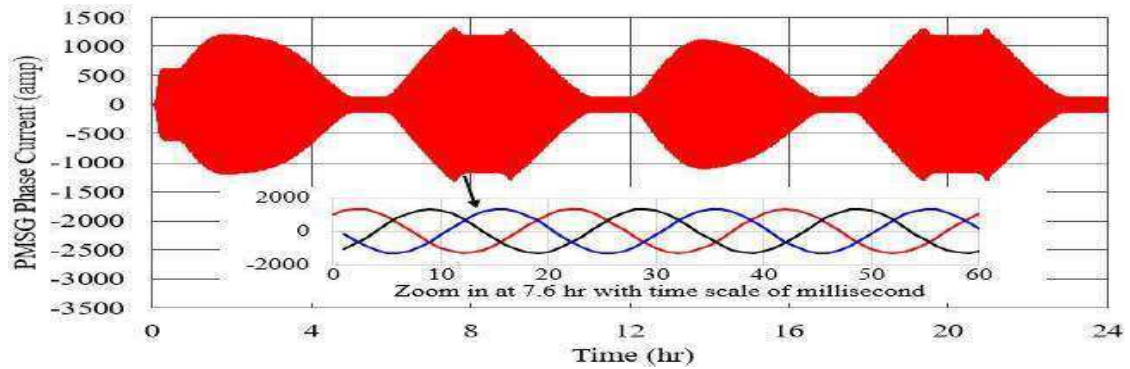


Fig. 3.32. PMSG Instantaneous Phase Current.

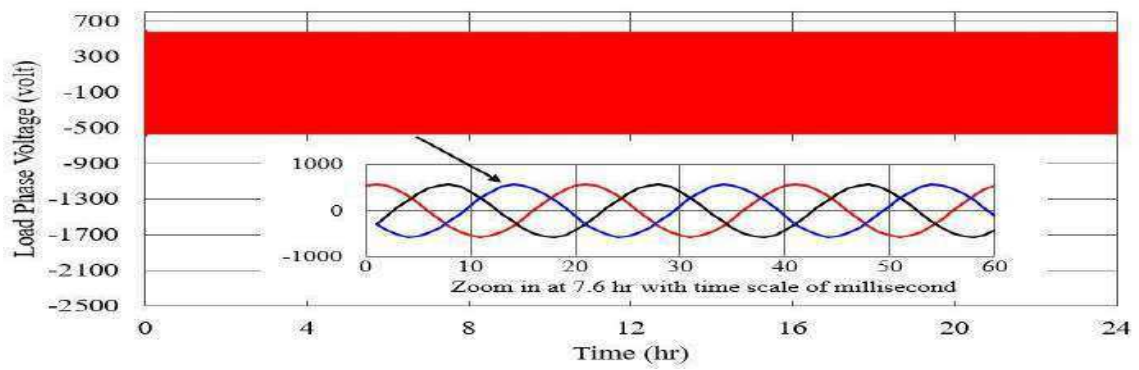


Fig. 3.33. Load Instantaneous Phase Voltage.

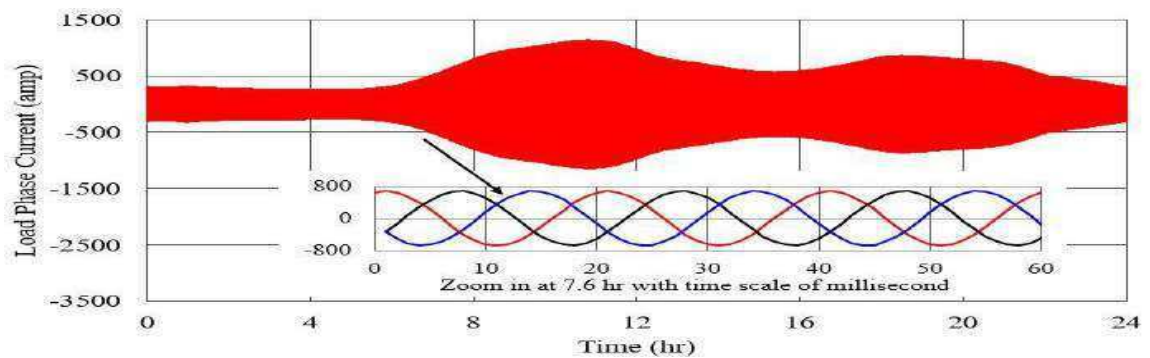


Fig. 3.34. Load Instantaneous Phase Current.

The DC-link voltage control regards the voltage fixed under the generation and consumption variations as shown in Fig. 3.35. The DC voltage of the electrolyzer, the fuel cell, and the battery systems varies due to the control action with a broad range of power duties from no-load to full load as shown in Fig. 3.36. The fuel cell and the electrolyzer dynamics under current step variation are estimated in the range of millisecond (50 ms for electrolyzer and 400 ms maximum for fuel cell) [178], [190]. The currents of the fuel cell, the electrolyzer and the battery measured at the DC-link side of the DC-DC converters are shown in Fig. 3.37. The figure exhibits the dynamic response of the PEM fuel cell and the electrolyzer while the battery current supports the DC-link voltage stabilization. The hydrogen volume at the storage tank is estimated during the day based on the volume flow rates as shown in Fig. 3.38. The hydrogen volume negative values indicate that the amount of produced hydrogen this day (based on the marine current speed and load profiles) is not sufficient to have the energy balance and it is required to have a hydrogen storage reserve from previous days.

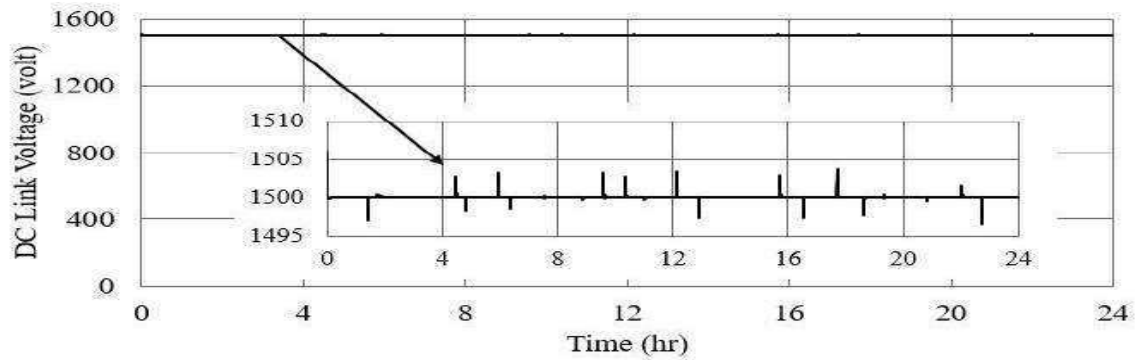


Fig. 3.35. DC-Link Voltage.

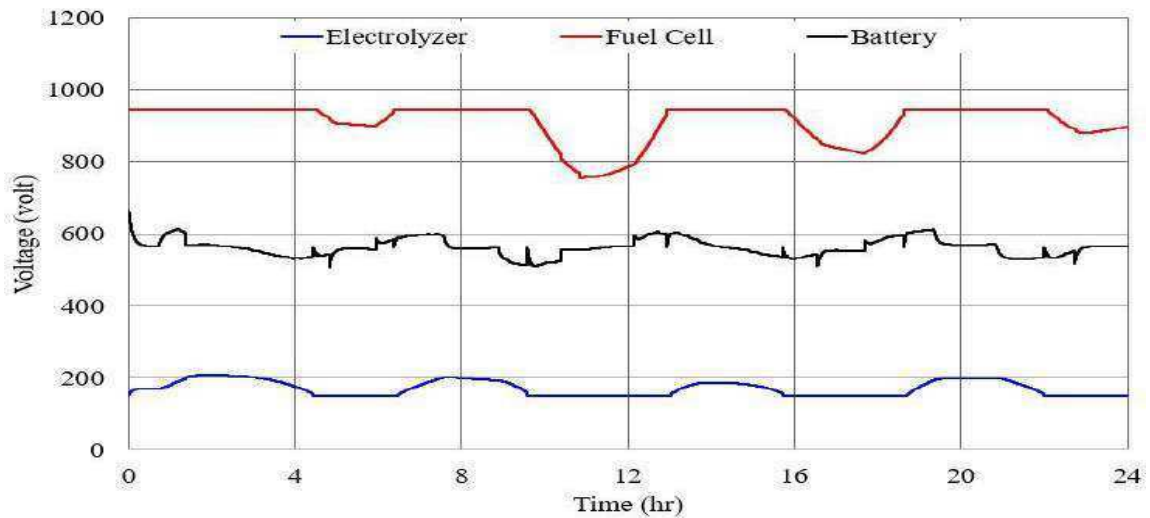


Fig. 3.36. PEM Fuel Cell, Electrolyzer and Battery Voltages.



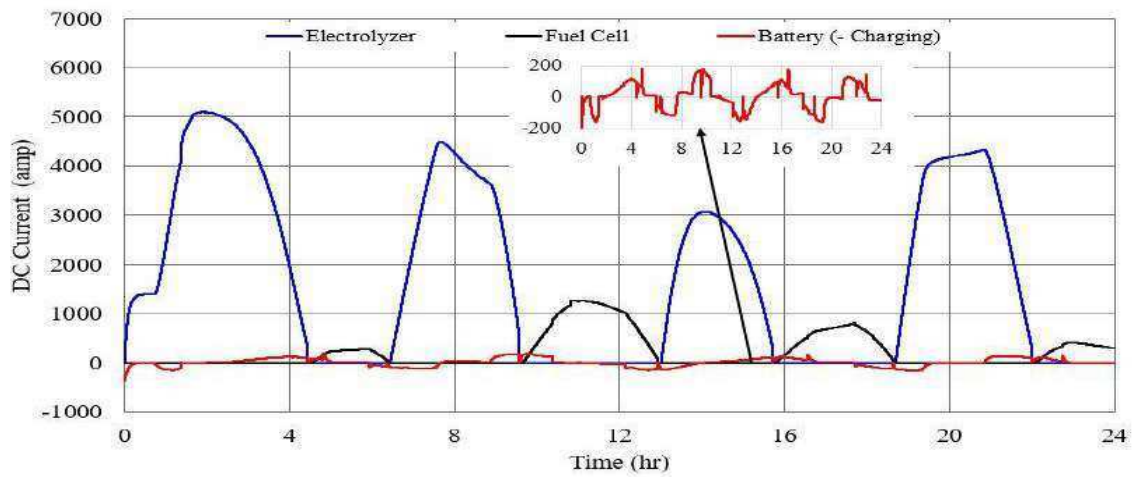


Fig. 3.37. PEM Fuel Cell, Electrolyzer and Battery Currents.

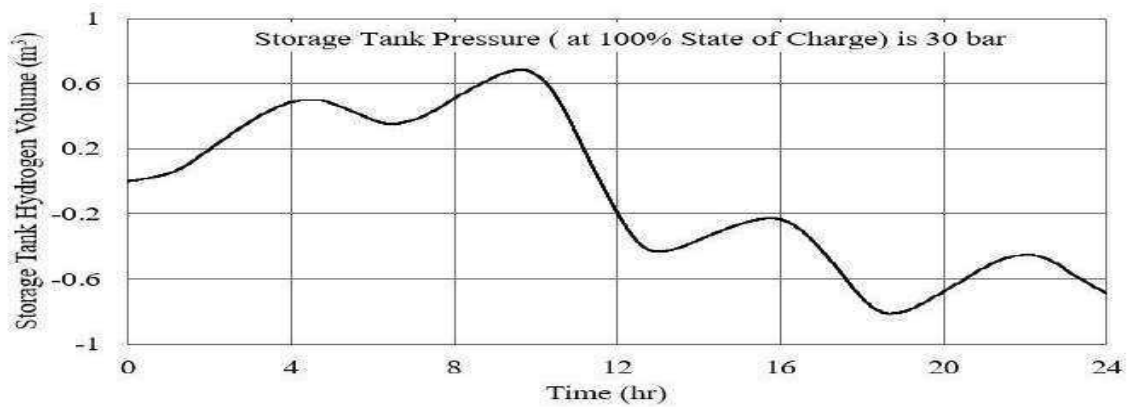


Fig. 3.38. Hydrogen Volume at the Storage Tank.

The energy management system considers the safe operation of the battery by respecting the SOC limits as shown in Fig. 3.39. The proposed model of the active MCT/hydrogen power generation system can be used to study and to analyze the hydrogen energy storage system with the marine current energy for feeding the stand-alone loads, especially for islands.

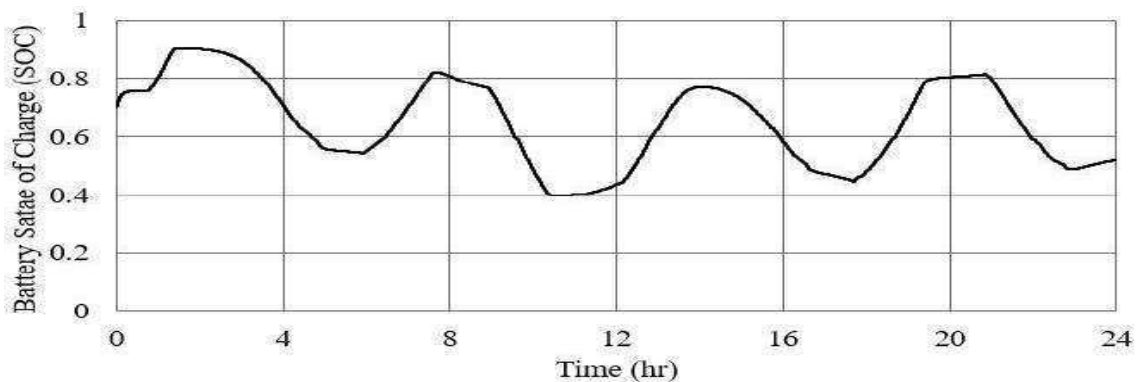


Fig. 3.39. Battery State-of-Charge (SOC).

## 5. Conclusion

This chapter discusses the centralized energy management system of the hybrid marine-hydrogen power generation system. The proposed energy management system provides the low-level controllers by the reference values. The controllers have been designed due to the inversion control principal of the energetic macroscopic representation for designing the practical control structure of the system. Due to the inversion control principal, each control system has a tuning chain that must be defined to enable the effective and powerful controllers design. The hybrid marine-hydrogen system has five tuning chains related to the integrated power electronic converters. The machine (PMSG) side converter has two control strategies. The first is the active power control that tracks the point of the maximum power under the base speed and limits the power at the rated value above it. The second is the flux weakening that protects the machine from overcurrents and overvoltages above the base speed. One of this work novelty is the adaptation of the flux control to maximize the generated power (loss minimization) when the machine runs below the base speed. The load side converter is controlled to feed a fixed voltage and fixed frequency at the load terminals as the system operates in the stand-alone mode. The PEM electrolyzer and fuel cell converters are controlled as a current source to follow the reference values provided by the energy management system. The battery side converter is controlled to stabilize the DC-link voltage and covers the fast dynamics of the electrical energy. The centralized energy management system is designed to balance the energy between the generation (tidal turbine) and the demand (residential loads). The safe and the recommended dynamic response of the PEM electrolyzer and fuel cell has been considered during the energy management system design to provide the healthy and the safe operation. Also, the energy management system considers the battery safe operation that represents the rated current limit (considered during the battery sizing) and the maximum and the minimum state of charge limits.

Moreover, the small-scale PEM electrolyzer and fuel cell models have been adapted to represent the MW scale models. The model's adaptation depends on the reverse engineering by estimating the main model's parameters to provide the same MW scale systems characteristics and key performance indicators.

The annual energy saving of one marine current turbine is considered to evaluate the effectiveness of the PMSG losses minimization (output maximization) strategy. The results indicate that the annual energy saving of the considered tidal turbine is equivalent to the

annual energy consumption of one residential load (household profile). From another point of view, it is sufficient to generate about 100 kg of hydrogen.

The real data of the Alderney Race marine site is used to investigate and analyze the global performance of the system. The selected marine current speed profile represents the turbine input at the day of the highest tides in 2005. The maximum power point tracking technique is powerful to keep the turbine power coefficient at the maximum value when the turbine runs below the rated value. The power limitation and the flux weakening strategies protect the machine from overload and overvoltages when it runs above the base speed. The control system of the battery side converter stabilizes the DC-link voltages during all the daily variations. The designed energy management system sustains the balance between the generation and the consumption besides the protection of the electrolyzer, the fuel cell, and the battery by considering the PEM systems dynamics and the battery state of charge limits.

Generally, the proposed centralized management system merits the powerful operation but suffers from the lack of the scalability, the flexibility, and the redundancy. In case of an outage or failure of one of the system components or even the management system itself, all the system will be out of step that is called the single point of common failure. Moreover, the system during specific operating conditions requires the connection with the main grid. The centralized energy management system is unable to fulfill all these requirements. Thus, the migration into the decentralized energy management system is one of the best solutions. The following chapter discusses the JADE based multi-agent energy management system (as a paradigm of the decentralized energy management system).





## **Chapter 4**

# **JADE Based Multi-Agent Decentralized Energy Management System**



## 1. Introduction

A MATLAB/Simulink model has been built to simulate the component layer (hybrid marine-hydrogen active power generation system) presented in the previous two chapters with a simple energy balance strategy included in the model as a centralized management system. The migration into a decentralized management topology based on the MAS (Multi-Agent System) requires interfacing the MATLAB/Simulink model with the MAS platform.

As aforementioned in Chapter 1 (section 2.1.2, Fig. 1.9), there are centralized, hierarchical and decentralized management and control systems. The main difference between these systems is the responsibility of the optimization and management duties. The centralized systems have a master unit that feeds all the set points to the lower level control entities. The hierarchical system distributes the management duties over the different control entities with regarding the master unit for general survey and monitoring. The decentralized is the same topology like the hierarchical with removing the master unit due to sharing the survey and monitoring duties between the control entities based on peer-to-peer communication. The main merit of the decentralized system is the redundancy and flexibility deduced from avoiding the single point of failure as a main disadvantage of the centralized system.

The MAS is a paradigm of the decentralized system that is used for energy management and control of the hybrid marine-hydrogen active power generation system. The marine-hydrogen system has a heterogeneous nature including electromechanical (tidal turbine, generator), electrochemical (PEM electrolyzer, PEM fuel cell, and the Li-FePO<sub>4</sub> battery) and the electrical (power electronic converters) systems. Many parameters must be taken into consideration for managing the system. Moreover, the system runs in the stand-alone operating mode (for feeding the residential loads of an island). Consequently, the management system must have the capability of dealing with each system independently and reliably. Thus, the MAS decentralized is selected to perform the control and the management of the system under the different operating conditions and scenarios as discussed later. As aforementioned in chapter 1, there is no clear definition of the agent while the Wooldridge's definition is the more accepted worldwide. Due to this definition, the agent is an entity of software or hardware (or both) that can react autonomously to the environment changes with definite characteristics:

- Reactivity
- Pro-activeness
- Social ability

As a result, the multi-agent system consists of several agents working together in harmony and synchronization for achieving the main task.

This chapter covers the migration of the marine-hydrogen energy management and control system from the centralized to the decentralized topology. The following sections discuss the MAS platforms features and comparison to facilitate the selection, which is the JADE (Java Agent Development Environment) platform. Hence, the JADE main features and programming are covered. The JADE is a Java-based multi-threading platform. The interface between MATLAB/Simulink and JADE requires a work-round for adding the agent options in the Simulink. The MACSimJX (Multi-Agent Control for Simulink Java Extension) enables the MATLAB/Simulink-JADE interface that is briefly described in the following sections. The development of the MAS for energy management of the marine-hydrogen system with different agent's definition and programming is analyzed by investigating the system effectiveness under different operation conditions and scenarios. Finally, the proposed MAS system is scoped from the SGAM (Smart Grid Architecture Model) view to keep following the harmony of the manuscript ideas.

## **2. Multi-Agent Platform Selection**

The MAS has been applied for many applications due to the survey of the decentralized energy management system presented in chapter 1 (section 2.1.2). There are many platforms or even the MATLAB itself can be used for developing the MAS. The most important question is the selection of the platform to be used for developing the MAS. There are many studies [191]–[199] that presented the different evaluation criteria's of the MAS platforms for facilitating the platform selection for a specific application. The more detailed and comprehensive comparison of the MAS platforms has been presented in [200]. The proposed comparison based on definite evaluation criteria as follows:

- Platform properties: represent the main characteristics to understand the main scope and domain of the platform.
- Usability is the estimation of the difficulty of developing the application by using the platform.
- Operating ability is the quality of the platform.
- Pragmatics is the factors of the application running and getting started using the platform.
- Security Management is the platform safety.

Each one of these criteria has sub-categories as shown in Table 4.1 while their detailed description has been presented in [200]. One of the most important sub-criteria the standard computability which is the ability of the platform to follow the agent system international standard. One of the IEEE societies specified on agent standards definition is the FIPA (Foundation for the Intelligent Physical Agent. Moreover, the source nature of the platform is the main factor of the selection; it is preferable to select an open source platform. The platform programming plays an important role in the interface or gaping between the MAS and the system-modeling platform (MATLAB/Simulink in this study). The system stability defines the ability of the platform to be integrated into many applications (trusted platform to run all the times). Based on the defined evaluation criteria, twenty-four platforms were compared in this study as shown in Table 4.2.

Criteria	Sub-Criteria				
Platform Properties	Developer/ Organization	Primary domain	Latest release	License	Open Source
Usability	Simplicity	Learnability	Scalability	Standard compatibilities	Communication
Operating ability	Performance	Stability	Robustness	Programming languages	Operating systems
Pragmatics	Installation	User support	Popularity	Technological maturity	Cost
Security management	End-to-end security		Fairness	Platform security	

Table 4.1. Multi-Agent System Platforms Evaluation Criteria [200].

No.	Platform name	Developer/ Organization	Primary domain	Latest release	License	Open Source
1	Agent Factory	University College Dublin	General purpose agent-based	AFSE v3.0 (07/12/2011)	LGPL	YES
2	AgentBuilder	Acronymics Inc.	General Purpose multi-agent systems	AgentBuilder Lite/Pro v1.4 (06/11/2004)	Proprietary Discounted academic licenses	NO
3	AgentScape	Delft University of Technology	Large-scale distributed agent systems	AgentScape2 M5 (r6343) (06/11/204	BSD	YES
4	AGLOBE	Czech Technical University	Real-world simulations	AGLOBE v5.5 (01/01/2008)	LGPL	YES
5	AnyLogic	AnyLogic Company	General purpose distributed agent-based simulations	AnyLogic 8.2 (27/10/2017)	Commercial Academic License	NO

6	Cormas	Cirad research Centre	Natural resources and agent-based simulations	Cormas2017 (09/11/2017)	GPL	YES
7	Cougaar	Raytheon BBN Technologies	Complex, large-scale, distributed applications	Cougaar 12.7 (27/07/2012)	Cougaar Open Source License COSL	YES
8	CybelePro	Intelligent Automation Inc.	Large-scale distributed systems	CybelePro 3.1.3 (2013)	Commercial Academic license	NO
9	EMERALD	LPIS Group, Aristotle University of Thessaloniki	Distributed applications composed of autonomous entities	EMERLAD v1.0 (23/01/201)	LGPL	YES
10	GAMA	IRD/UPMC International Research Unit UMMISCO	Large-scale distributed spatially explicit agent-based simulations	GAMA 1.7 v2 (22/04/2017)	GPL	YES
11	INGENIAS Development Kit	Grasia research group	General purpose agent-based	IDK 2.8 (04/11/2013)	CC By-SA GPLv2	YES
12	JACK	AOS	Dynamic and complex environments	JACK 5.5 (02/09/2010)	Commercial Academic license	NO
13	JADE	Telecom Italia (TILAB)	Distributed applications composed of autonomous entities	Jade 4.5 (08/06/2017)	LGPLv2	YES
14	Jadex	Hamburg University	Distributed applications composed of autonomous BDI entities	Jadex 3.0.86 (19/01/2018)	LGPLv2	YES
15	JAMES II	University of Rostock	General purpose agent-based modeling and simulations	JAMES II 0.9.7 (25/09/2014)	JAMESLIC (Compatible with GPL)	YES
16	JAS	University of Torino	General purpose agent-based	JAS 1.2.1 (21/06/2005)	LGPL; 3 <sup>rd</sup> PARTY LICENSES	YES
17	Jason	Universities of Rio Grande do Sul and Santa Catarina	Distributed applications composed of autonomous BDI entities	Jason 2.3 (19/12/2017)	LGPLv2	YES
18	JIAC	Technische Universität Berlin	Large-scale distributed systems	JIAC 5.2.4 (07/12/2017)	Apache Licenses V2	YES
19	MaDKit	Institut Universitaire de Technologie	Multi-agent systems with agent-based simulation	MaDKit 5.2 (18/07/2017)	GPL	YES

20	MASON	George Mason University	Event-driven multi-agent simulations	MASON v18 (01/08/2014)	Academic Free License version 3.0	YES
21	NetLogo	Center for connected Learning (CCL) and Computer Based Modeling, Northwestern University	Agent-based simulations	NetLogo 6.0.2 (11/08/2017)	GPL	NO
22	Repast	University of Chicago	Agent-based simulations	Repast Symphony2.4 (30/09/2016)	New BSD	YES
23	SeSAM	Örebro University	Agent-based simulations	SeSAM 2.5.2 (06/02/2017)	LGPL	YES
24	Swarm	Swarm Development Group	General purpose agent-based	Swarm 2.4.1 (03/08/2011)	GPL	YES

Table 4.2. Multi-Agent Platforms Properties.

The different multi-agent platforms have been compared based on the evaluation criteria tables of usability, operating ability, pragmatics and the security management that have been comprehensively discussed in [200]. The platform classification provides the clear vision of different platforms and makes the selection easier. The platforms have been classified based on the programming language that estimates the difficulty of programming and the ability to interface the Physical layer models (MATLAB/Simulink in this study) with the multi-agent platform domain. Table 4.3 shows the different programming languages of the multi-agent platforms. The Java and C++ are the preferred programming languages to be interfaced with the MATLAB, in which they are already integrated. The application domains are the second factor of platform selection as it defines the scope for which the platform is applied. The general-purpose platform is the more suitable candidate due to its ability to manage and control any application without specified limits as Table 4.4 exhibits. Last, not least the FIPA standard compliance is the keystone of selection. FIPA was established in 1996 as a non-profitable association for developing the standards of the software agent technology considering definite core principles:

- Proposing a new agent paradigm Solving the agent technology problems;
- The consideration of the agent technology maturity;
- Studying the possibility of agent technology Standardization;
- Considering the internal agent mechanisms as the main objective of the standardization [201].



<b>Programming Language</b>	<b>Multi-Agent Platforms</b>
Java	JADE, SeSAM, Jadex, JAS, AgentBuilder, EMERALD, Repast, MaDKit, CybelePro, Cormas, AGLOBE, Cougaar, Swarm, MASON, INGENIAS Development Kit, AnyLogic, JAMES II
C/C++	AgentBuilder, Swarm (Objective C), Repast (plus C#), MaDKit
Declarative/rule programming	Repast (Lisp, Prolog), JADE (JESS), EMERALD (JESS)
Python	Repast, MaDKit
AgentSpeak	Jason, Agent Factory (AFSE)
SmallTalk	Cormas
JAL	JACK
NetLogo	NetLogo
GAML	GAMA
XML	AgentScape, EMERALD, INGENIAS Development Kit, JACK, Jadex, JIAC
Multiple languages	AgentScape, EMERALD, INGENIAS Development Kit, JACK, Jadex, JIAC, Jason, MaDKit, Repast, AgentBuilder, AgentFactory

Table 4.3. Multi-Agent Platforms Programming Languages [200].

<b>Purpose</b>	<b>Multi-agent Platforms</b>
General purpose distributed simulations	JADE, Jadex, Jason, EMERALD, MaDKit, CybelePro, JIAC, AgentScape, AnyLogic, GAMA
General purpose agent-based simulations	JAS, AgentBuilder, Agent Factory (AFSE), Swarm, MASON, INGENIAS Development Kit, Repast, MaDKit, AgentScape, SeSAM, AnyLogic, NetLogo, GAMA, JAMES II
Scientific simulations	Swarm, MASON, Cormas, Repast (Social Sciences), MaDKit, CybelePro, SeSAM, AnyLogic, GAMA, JAMES II
Dynamic and complex environments	JACK, Cougaar, CybelePro, AnyLogic
Real-World-GIS	AGLOBE, Cougaar (integrated with OpenMap), Repast, CybelePro, SeSAM, AnyLogic, GAMA
Large scale simulations	Cougaar, CybelePro, JIAC, AgentScape, GAMA, JAMES II
Scheduling & Planning	Jadex, CybelePro, SeSAM, AnyLogic, NetLogo, GAMA
Mobile computing	JADE, Jadex, Agent Factory
Multiple domains	JADE, Jadex, MaDKit, CybelePro, Cougaar, JIAC, AgentScape, Agent Factory, Repast, SeSAM, AnyLogic, GAMA, JAMES II
Artificial life and behavioral observation	JADE, Jadex, Jason, SeSAM, EMERALD, JACK, Cougaar, CybelePro, AnyLogic, NetLogo, GAMA
Biological & Social studies	JADE, SeSAM, Jadex, Jason, EMERALD, JACK, Cougaar, CybelePro, MaDKit, Repast, AnyLogic, NetLogo, GAMA, JAMES II
Economics/ e-Commerce	JADE, EMERALD, JACK, Cougaar, CybelePro, MaDKit, AnyLogic
Natural resources & environment	Cormas, Swarm, SeSAM, AnyLogic, NetLogo, GAMA, JAMES II

Table 4.4. Multi-Agent Platforms Domains [200].

Since then, it was developed with integrating new committees and societies to provide more specified standards of agent technology until it was reincorporated by the mid of 2005 as a standards activity of the IEEE known as FIPA-IEEE. The FIPA core consists of many ideas that are partially reached to maturity while another group is incomplete and the rest stopped. The main principals of the FIPA core are discussed in the following paragraphs [201].

- Agent Communication

The multi-agent system consists of a distributed entities with definite function programmed on their codes that work in harmony with internal communication to achieve the main system goal. Thus, the agent communication is an essential part that must be well defined and standardized. The FIPA-ACL message structure specification (SC00061) defines a set of parameters for the message shared between the different agents as shown in Table 4.5. The main parameters are the sender, the receiver, and the content. The most important parameter is the performative that describes the function or the action to be performed. FIPA-ACL Communicative Action library specification (SC00037) is a set of 22 CA (Communicative Actions) as shown in Table 4.6. These actions define the semantics of the communication between the sender and the receiver. Moreover, it is required to define the procedure of the communication between the agents that is called the communication protocol. The FIPA defined some forms of the communication protocols while the most applied and important protocol is the FIPA contract net protocol defined by specification SC 00026 as shown in Fig. 4.1.

- Agent Management

The agent management represents the main rules of agent creation, registration, location, communication, migration, and operation. Figure 4.2 exhibits the proposed FIPA model of the agent management that consists of the AP (Agent Platform), the DF (Directory Facilitator), the AMS (Agent Management System) and the MTS (Message Transport Service). The AP is the physical infrastructure of developing the agents that consist of the machine, the operating system and the agents with their management and additional services. The agent is the software code that represents one autonomous entity of the multi-agent system. The agent, due to the FIPA, must have an identity called AID (Agent Identifier) that is used for distinguishing and addressing it. The directory facilitator is the yellow page service of the agent platform in which all the agents register to announce their services. The AMS is the main core of the AP that manages the operation of the AP to provide the capabilities of agent's creation, delete and migration from AP to another. The MTS is the service of transporting the FIPA-ACL messages between the different agents. Due to the FIPA, the message must have the definite structure as shown in Fig. 4.3 to simplify its broadcasting.

Parameter	Description
Performative	Communication Act (CA) type
Sender	Sender identity
Receiver	Receiver identity
Reply-to	The identity of the agent that receives a subsequent of messages concerning a conversation
Content	The content of the message (communicative act data to be processed)
Language	The message content (data) language
Encoding	The message content encoding
Ontology	Message content symbols ontology meaning references
Protocol	The communication protocol concerning the message
Conversation-ID	The unique identity of the conversation
Reply-with	Identifying expression concerning the conversation to be used by the responding agents
In-reply-to	Message communication act reference
Reply-by	Response deadline time interval

Table 4.5. FIPA-ACL Message Parameters [201].

Communication Act	Description
Accept Proposal	Accept the previously received proposal concerning the CA
Agree	Agree to perform definite CA, maybe now or in the future
Cancel	The initiator agent inform the participant (with the accepted proposal) to cancel the CA it is performing
Call for Proposal	The initiator agent asks the different agent for proposal concerning definite CA
Confirm	The sender confirms (true) the receiver a definite proposition that is uncertain for the sender
Disconfirm	The sender disconfirms (false) the receiver a definite proposition that is uncertain for the sender
Failure	The sender informs the receivers that a definite CA that it fails to perform this action
Inform	The sender informs the receiver that a definite proposition is true
Inform If	The sender informs the receiver whether a definite proposition is true or not
Inform Ref	The sender informs the receiver a specific description
Not Understood	The sender informs the receiver that the received message is not understood
Propagate	The sender informs the receiver to share the received message with the agents that it identifies
Propose	Submitting a proposal to perform definite action considering specific conditions
Proxy	The sender informs the receiver to send an embedded message to targeted agents with a specific description
Query If	The sender inquiries from another agent whether a specific proposition is true or not
Query Ref	The sender inquiries from another agent to consider a specific object as a reference
Refuse	Refusal of performing a specific action with an explanation
Reject Proposal	Refusal of performing a specific action during the negotiation
Request	The sender asks the receiver to perform a specific action
Request When	The sender asks the receiver to perform a specific action when specific propositions are true
Request Whenever	The sender asks the receiver to perform a specific action periodically when specific propositions are true
Subscribe	The sender asks the persistent intention to notify a reference value object continuously

Table 4.6. FIPA-ACL Communication Act [201].

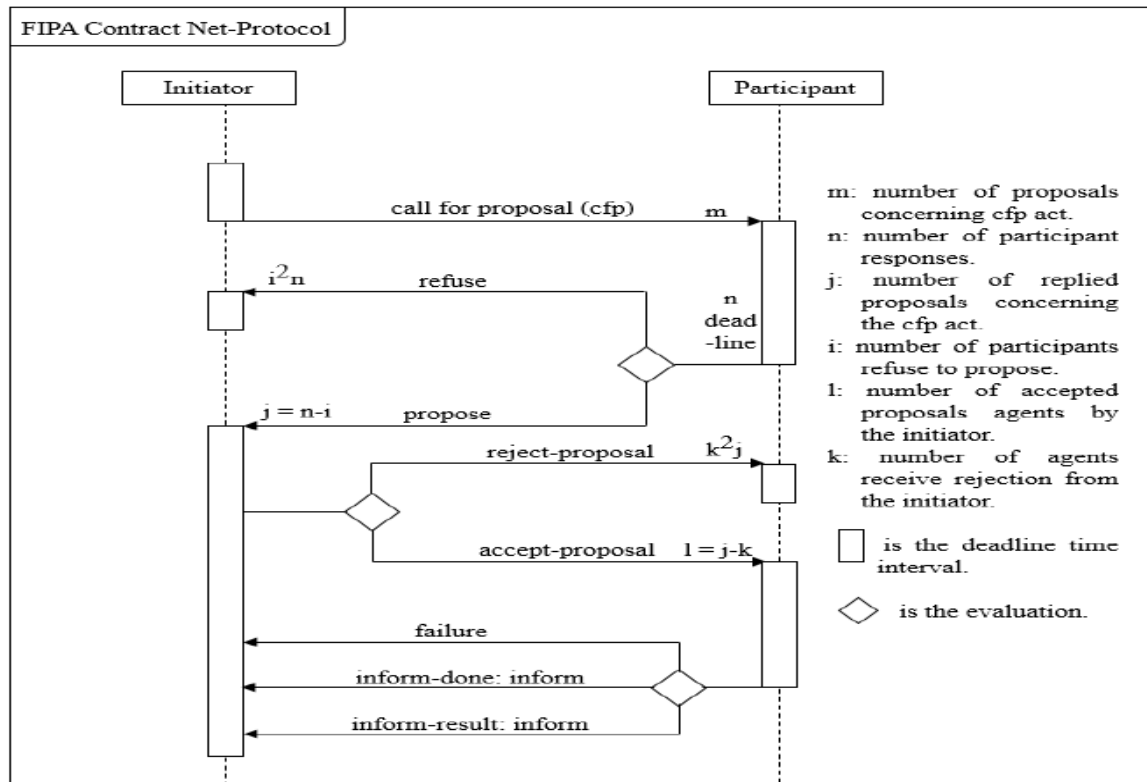


Fig. 4.1. FIPA Contract Net Interaction Protocol [201].

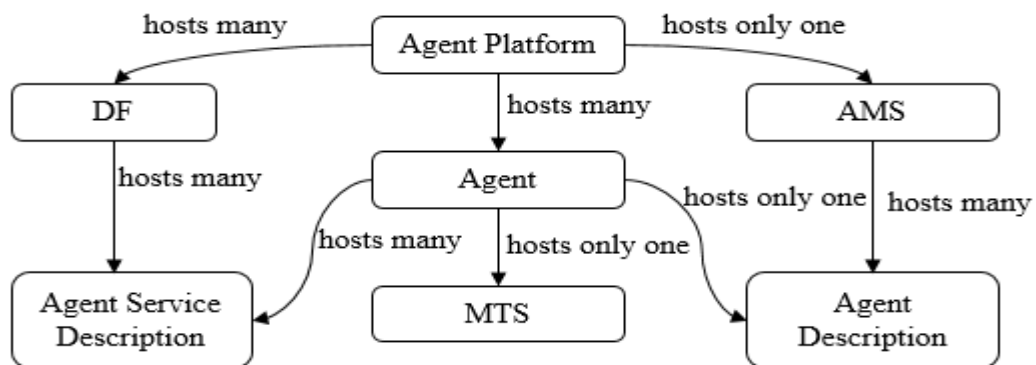


Fig. 4.2. FIPA Agent Management Model [201].

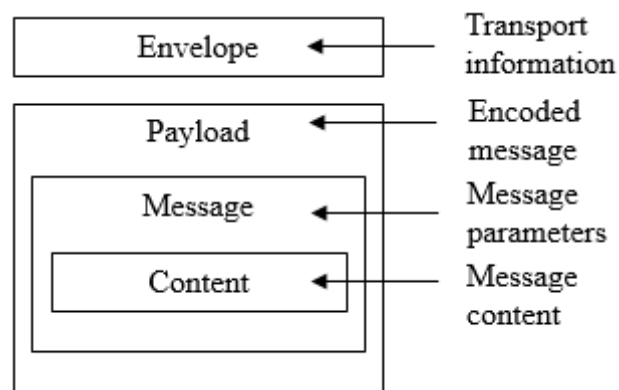


Fig. 4.3. FIPA Message Structure [201].

Some of the reviewed Multi-Agent platforms are completely compliant with FIPA specifications as shown in Table 4.7. Based on all the above, the required MAS platform must be compliant with the FIPA standards and fulfill the evaluation criteria's. It is possible to use the system-modeling platform (e.g., MATLAB) to develop the MAS system that requires much time-consuming groundwork for adapting the developed AP with the FIPA standards and follow the evaluation criteria's. Otherwise, one of the directly applicable MAS platforms (refer to Table 4.2) can be used. The JADE platform is selected to apply the decentralized energy management of the hybrid marine-hydrogen system. It has many advantages; an open source Java-based software, general-purpose application, more widely applied in many applications and the most important feature is the FIPA compliance. The following section discusses the main architecture and features of JADE platform for developing the MAS.

FIPA Compliance	MAS Platforms
Full Compliance	JADE, Jadex, JACK, EMERALD
Partial Compliance	JAS, Jason, AGLOBE, Agent Factory, SeSAM, GAMA
No Compliance	Cougaar, Swarm, MASON, INGENIAS Development Kit, Cormas, Repast, MaDKit, CybelePro, JIAC, AgentScape, AnyLogic, NetLogo, JAMES II

Table 4.7. MAS Platforms FIPA Compliance Overview [200].

### 3. JADE Platform

JADE was initially developed in late 1998 by Telecom Italia to validate the early FIPA specifications. By 2000, the JADE platform became an open source software distributed under the Library Gnu Public License (LGPL). The LGPL provides completely the rights to use the software in commercial products, to make and distribute software copies and the software source codes access and modifications with a return back to the JADE community as a condition. The main core of JADE is a Java-based set of software abstractions and tools that hid the FIPA specifications and enables the widespread of these specifications by its direct implementation. The agent paradigm in JADE is an autonomous and proactive entity that has its thread of execution and works in harmony with the other agents based on peer-to-peer communication. The following paragraphs present the main architecture of the JADE platform and its classes. JADE is a fully distributed platform consists of autonomous entities called the agents. The agent lives in a container that provides the JADE run-time and the

agents hosting and execution services as a Java process. There is only one container created automatically by launching the software that is called the main container. The main container hosts the directory facilitator agent (DF) and the agent management service (AMS). The main container is the platform hub that all the other programmed containers must register with it. Consequently, it manages the container table (CT) in which all the containers register. As long as, it manages the global agent descriptor table (GADT) in which all the agents register as shown in Fig. 4.4. The main container has a default name of (Main Container), and the others have the names of (Container-1, Container-2, etc.) while the relation in between as Figure 4.5 exhibits [202]. The JADE platform has main java classes and interfaces that implement specific and principal functions and arranged hierarchically in the form of packages and sub-packages as shown in Fig. 4.6.

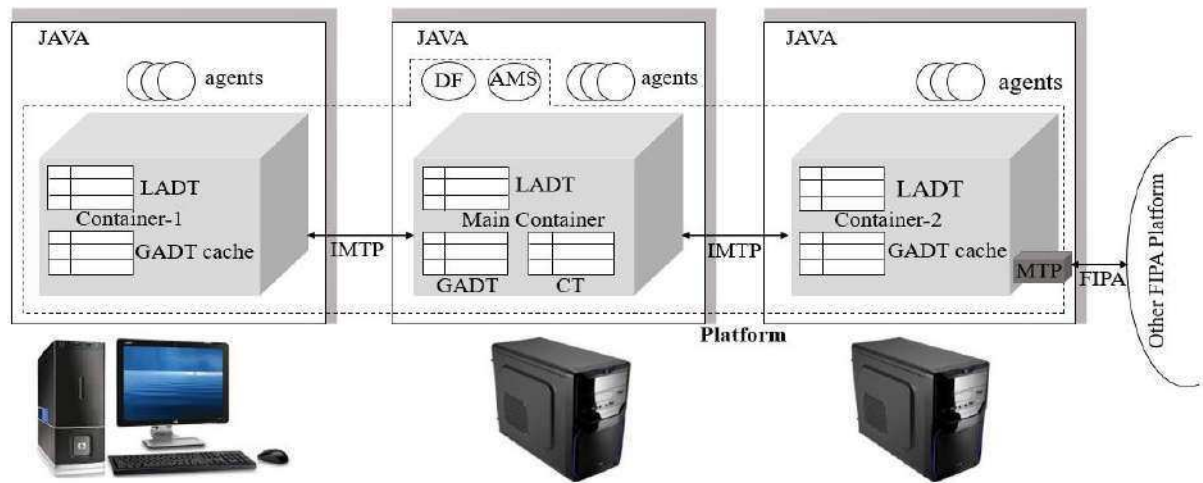


Fig. 4.4. JADE Main Architecture[202].

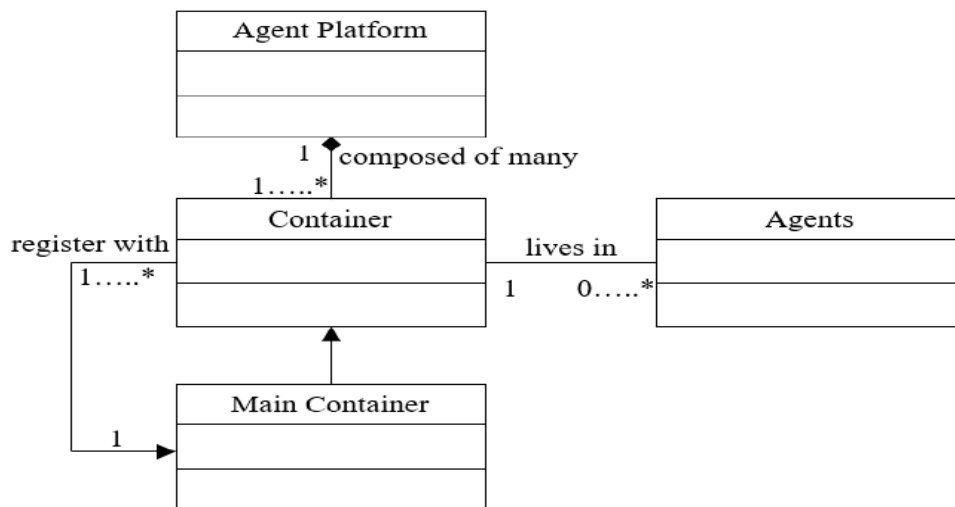


Fig. 4.5. Relationship between Main JADE Architectural Components

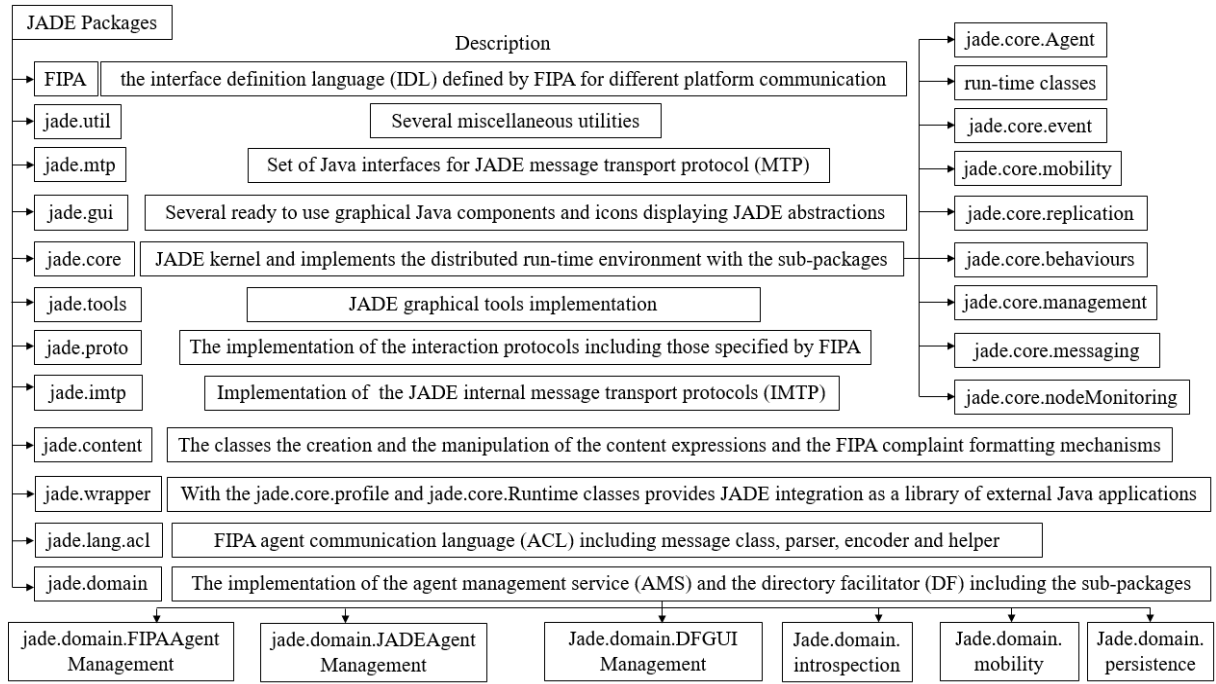


Fig. 4.6. JADE Packages Hierarchical Architecture.

The detailed description of the JADE different services and classes are presented in [202]. One of the most important JADE services is the admin and the debugging tools as shown in Fig. 4.7. The sniffer agent is one of the debugging tools that surveys and monitors the conversations and the messages (agent's communication) exchanged between a set of specified agents defined by the programmer. The jade.tools. Sniffer class implements the sniffer agent that register with the AMS to keep tracking all the platform events and messages exchanged between the specified agents. The sniffer agent has a GUI that consists of the sniffed agents set with canvas represent the messages exchanged in between including each message as an arrow with a definite color indicates the conversation (as shown later in the results).

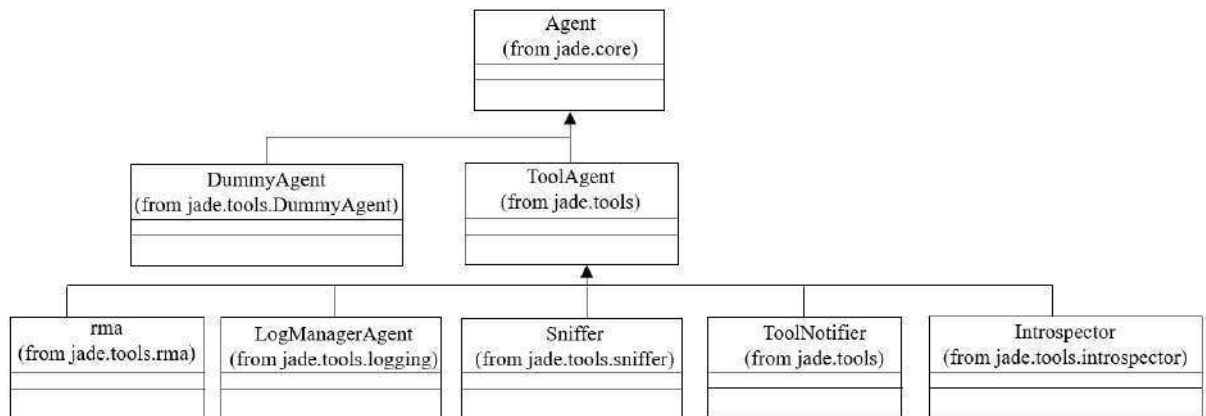


Fig. 4.7. JADE Admin and Debugging Tools Diagram [202].

After the brief description of the JADE main architecture and its different packages that, represent the groundwork of the platform inherited directly by the programmer. The following paragraphs present briefly the main programming features of the MAS development with JADE. The MAS development consists of basic features: agent creation, agent tasks, agent communication and the DF services that have been described in details in [203]. It is important to mention that these services represent 10% of the platform classes. Moreover, the JADE depends on the “pay as you go” philosophy that means call the advanced platform features when they are required. The agent tasks are the main function that the agent must perform represented in the form of behaviors. Figure 4.8 shows the behavior scheduling and execution in the JADE agent thread, and it is clear that the action method of the behavior is running continuously until it provides a return. Generally, there are four main types of JADE agent behaviors: one-shot, cyclic, generic and the scheduled that can be repeated or joined together based on the application requirements [203]. The directory facilitator (DF) provides the yellow pages service in which all the agent register to publish their services or searching services announced by the other agents as shown in Fig. 4.9. The agent interaction with the DF consists mainly of two methods publishing service and searching a service that has been presented in details.

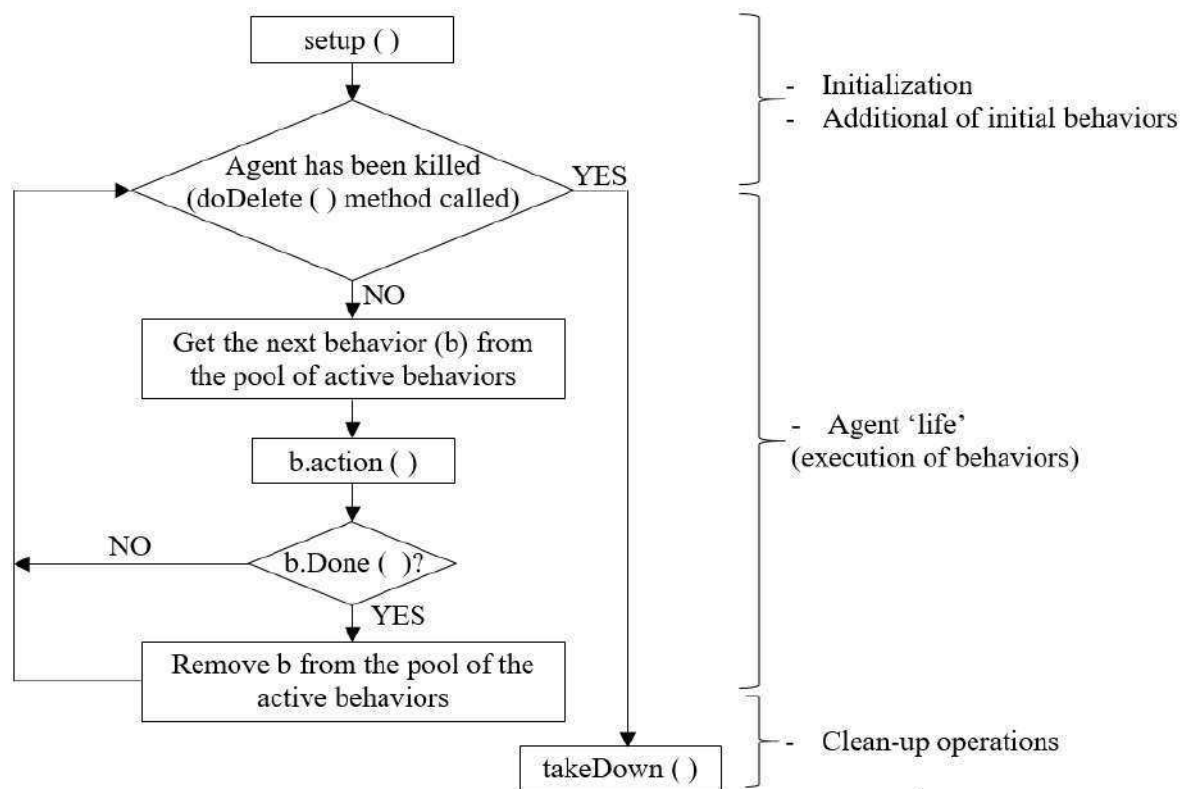


Fig. 4.8. Agent Thread Execution [203].



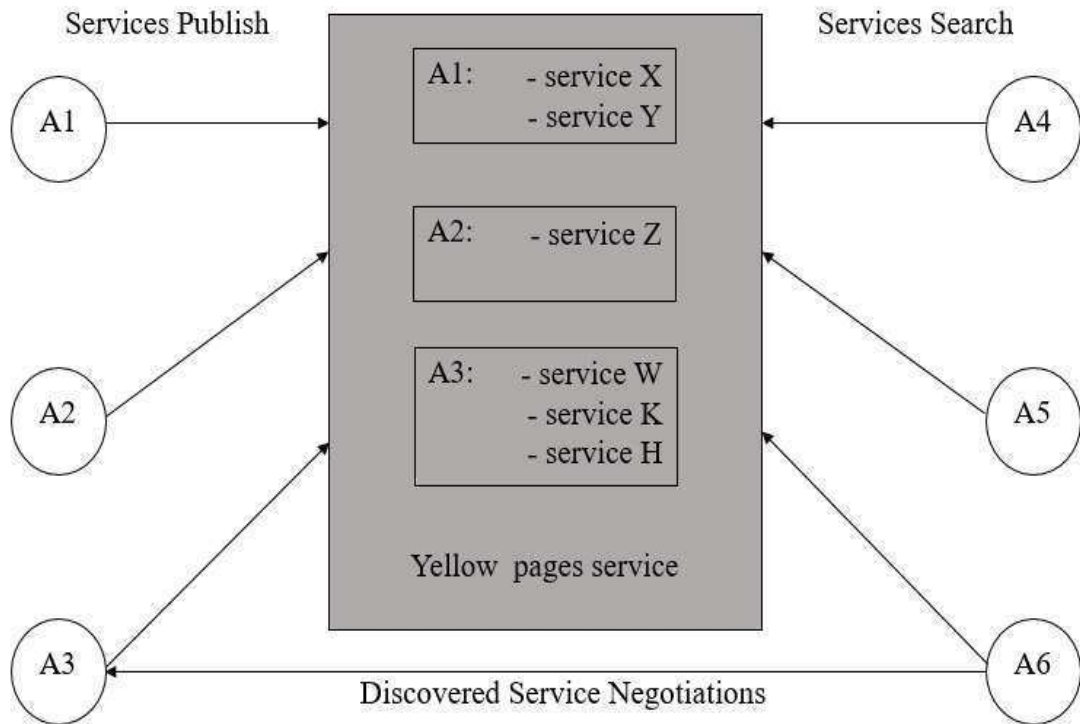


Fig. 4.9. Directory Facilitator Interaction [203].

#### 4. MATLAB/SIMULINK-JADE Interface

I have built a MATLAB/Simulink model of the component layer (hybrid marine-hydrogen active power generation system) that has been presented in the second and the third chapters with a simple energy balance strategy (included in the Simulink model) as a centralized management system. The migration into a decentralized management topology based on the MAS requires interfacing the MATLAB/Simulink model with the MAS platform. As aforementioned, the Java-based multi-threading JADE platform is selected to develop the decentralized MAS energy management system. The interface between MATLAB/Simulink and JADE requires a work-round for adding the agent options in the Simulink. The S-function Simulink block is the best candidate for this mission due to the possibility of writing any language program (mainly C++ or Java) and encapsulating it as a Simulink block. The obstacle of this scenario is the S-function instability of processing a multi-threading program, which is a fundamental principle in Java. A special program was created to overcome this obstacle (MATLAB/Simulink-JADE interface) that is called MACSim (Multi-Agent Control for Simulink) [204]. The MACSim depends mainly on the Server-Client architecture where the client is the MATLAB/Simulink S-function and the server is the Multi-threading program (JADE). The communication in between the client and the server is named a windows pipe as shown in Fig. 4.10. The MACSim is a C++ based program

with a Java wrapper for enabling JADE interaction. The MACSim has been extended to include Java extension (MACSimJX) that was presented for the first time in [205] to be used for the Boeing aircraft data mining and fusion. The MACSimJX program contains two main parts: the AE (Agent Environment) and the ATF (Agent Task Force) as shown in Fig. 4.11. The AE represents the main interface for transferring data between Simulink and JADE. The AE consists of many classes that are already programmed in a package named macsimagent to perform the following functions:

- Continuous track of the different agents with enabling their birth and death.
- Simulink synchronization
- Handling the requested input and time step data.
- Message manipulation between the different agents.
- Output data (directed to Simulink) storage with online updating.

Generally, the MACSimJX is an open source program that has been utilized for many applications from the Boeing 747 data fusion and mining to the renewables (PV, wind) MAS based energy management systems [205], [33], [206]–[209]. The software getting started, and detailed description are provided in [210], [211]. The following two sections describe the work novelty of developing the JADE based energy management MAS of the hybrid marine-hydrogen system in a stand-alone and grid-connected mode using the MACSimJX.

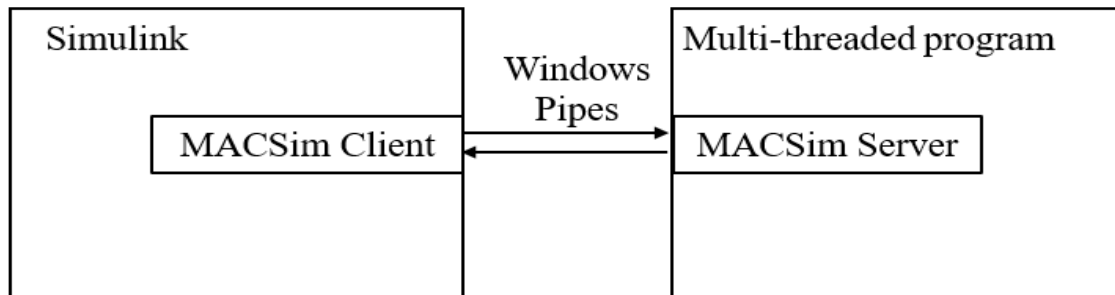


Fig. 4.10. MACSim Architecture [204].

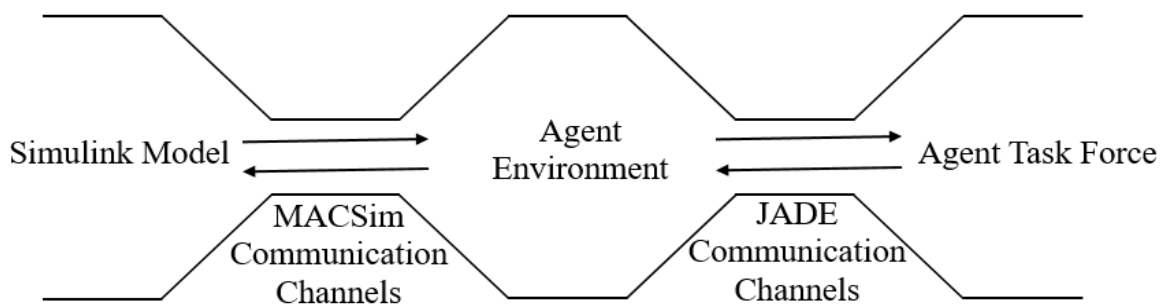


Fig. 4.11. MACSim Complete Model [205].

## 5. JADE based Multi-Agent Energy Management System of the Hybrid Marine-Hydrogen Power Generation System.

The main objective of the proposed decentralized energy management system is the energy balance between the marine current system generation and the load consumption (residential load). The main advantages of the JADE based MAS over the centralized topology is the redundancy (by avoiding the single point of common failure). Each agent is responsible for managing and controlling its subsystem and communicate peer to peer to the neighbor agent for negotiation based on the JADE agent paradigm. The results are discussed in the form of describing the agent's functions and the communication in between while the source code files are presented in Appendix B. The proposed scenarios are oriented mainly to emphasize the flexibility and the redundancy of the management systems. Firstly, the MAS system is proposed to manage the energy balance of the stand-alone system topology for investigating the decentralized energy management system ability compared to the centralized one discussed in chapter 3 (section 3.3). Then, a grid-connected topology is analyzed to exhibit the MAS system flexibility considering the transition from the grid connected to the stand-alone modes and vice versa. The mode transition provides mainly two challenges for the management system as follow:

- The isolated mode considers the battery as a dual loop controlled system for the DC-link voltage stabilization besides the fast dynamics power smoothing. The transition to the grid-connected mode changes the control duties of the battery to the power smoothing only while the DC-link voltage stabilization is the grid responsibility (as the reference node with the biggest ratings).
- The transition from the grid connected to isolated mode means the activation/deactivation of the grid agent during the system management. The flexibility or the scalability of the management system that can be applied not only to the grid agent but also for all the other subsystems (e.g., electrolyzer, fuel cell, battery). The system components can be disconnected at any time due to their operating conditions (e.g., failure or maintenance).

### 5.1. Isolated Mode MAS Energy Management

Figure 4.12 shows a simplified Simulink model of the isolated system described in the second and the third chapters considering the MACSimJX client as an S-function. The main objective of the JADE based MAS system is the assurance of the energy balance between the generation and the consumption. Consequently, the MACSimJX client (S-

function) forwards the generated marine current and the demand side powers. Moreover, it is important to consider the battery and the hydrogen storage tank SOC (State Of Charge) as main parameters of the energy management system. The battery SOC limits, as aforementioned, represents the safe and healthy operation. The proposed energy management system of the stand-alone mode does not consider the hydrogen tank SOC to evaluate the system performance. The performance evaluation represents the estimation of the produced hydrogen with the marine and demand profiles variations as discussed the following paragraphs. The MAS different agents are programmed to perform cooperatively a management procedure shown in Fig. 4.13. One of the most important modifications is that the proposed decentralized procedure considers the demand side management based on two strategies; load shedding (valley filling) and load shifting (refer to Fig. 1.8). The proposed centralized energy management system in chapter 3 does not consider the demand side management. The proposed MAS consists of five main agents that provide the low-level control system of the SIMULINK model by the reference values to be tracked. The marine energy conversion system is completely controlled by the low-level control system considering the different operation modes (discussed in Chapter 3 section 3.1). It is important to emphasize that the MAS can be programmed to integrate another agent for the marine energy conversion system to provide its control system by the references.

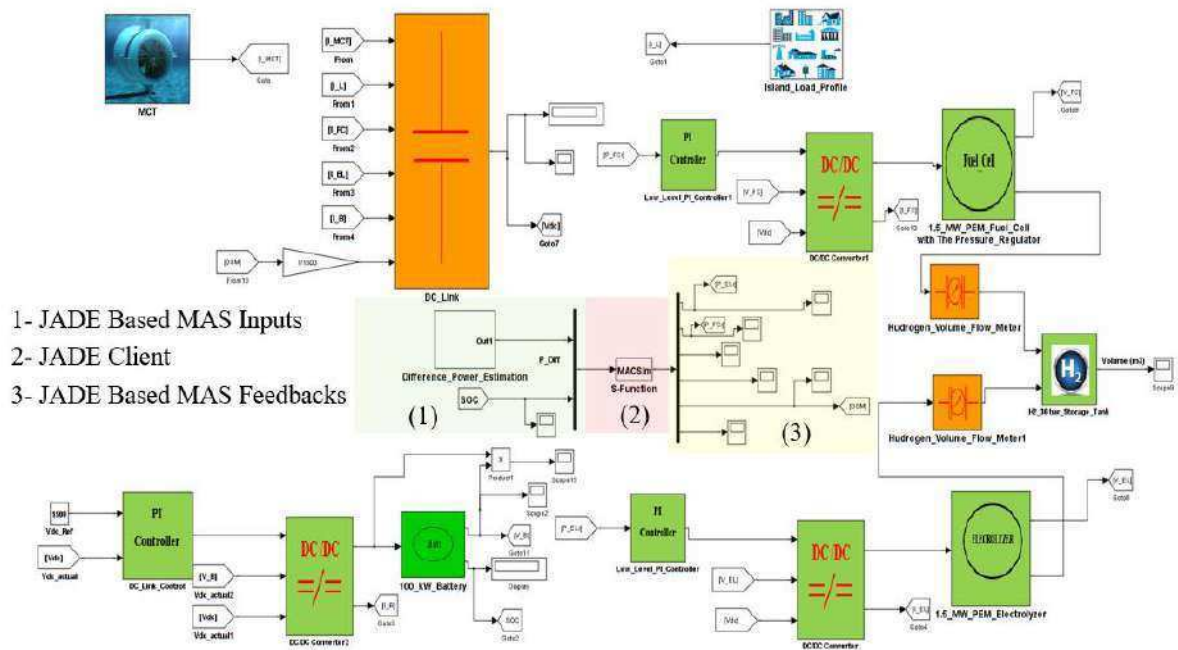


Fig. 4.12. Simplified Marine-Hydrogen Simulink Model.

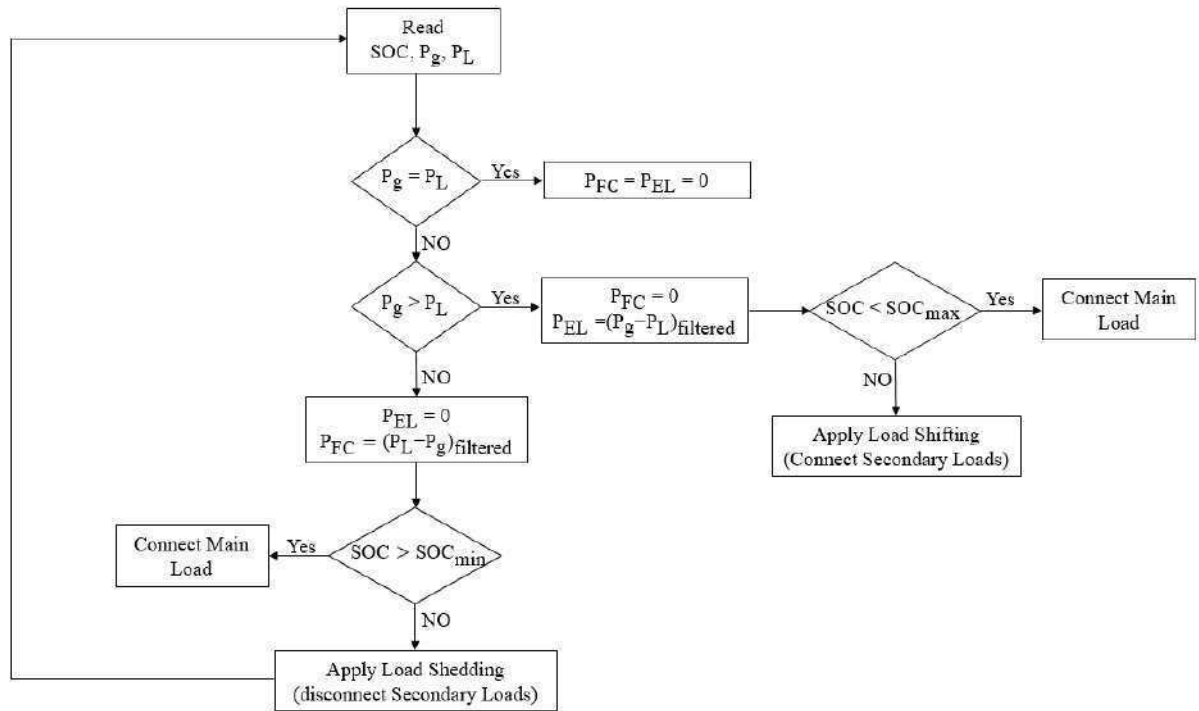


Fig. 4.13. JADE Based Isolated Mode Energy Management System Flow Chart.

The following paragraphs describe the different agents and their functions as follow:

- Electrolyzer Agent

It is responsible for the energy management of the electrolyzer system. Firstly, it communicates with the MACSimJX Agent Environment (AE) to search the generation-consumption power difference. Based on the updated values of the power difference (power surplus), it filters the power difference considering the electrolyzer dynamic response that is stored in the agent arguments (its value depends on the manufacturer operation recommendations). It continuously estimates the electrolyzer operating point and feeds it back to the AE that feeds it to the SIMULINK model as the electrolyzer control system updated reference value. Thus, it manages the electrolyzer-consumed energy, which means the amount of the produced hydrogen, and at the same time protect the electrolyzer components from lifetime degradation.

- Fuel Cell Agent

It is responsible for the energy management of the fuel cell system. It communicates with the MACSimJX Agent Environment (AE) to search the generation-consumption power difference. Based on the updated values of the power difference (power shortage), it filters the power difference considering

the fuel cell dynamic response that is stored in the agent arguments (its value depends on the manufacturer operation recommendations). It continuously estimates the fuel cell operating point and feeds it back to the AE that feeds it to the SIMULINK model as the fuel cell control system updated reference value. Thus, it manages the fuel cell-produced energy, which means the amount of the consumed hydrogen, and at the same time protect the fuel cell components from lifetime degradation.

- **Battery Agent**

It provides the battery SOC to the JADE platform by the communication with the AE of the MACSimJX. Then, it communicates with the DSM to share the SOC and receives the power difference.

- **Demand Side Management (DSM) Agent**

It is responsible for implementing the demand side management strategies [Load shifting and the Load shedding (Filling Valley)]. It communicates with the AE of the MACSimJX to receive the power difference and shares it with the battery agent to receive its SOC based on peer-to-peer communication. Consequently, it filters the power difference based on the electrolyzer and the fuel cell dynamic responses and defines the operating condition (power surplus or shortage). Based on the operation condition, it selects the DSM strategy (load shifting for power surplus and load shedding for power shortage). The amount of the shaded or shifted power is estimated based on the battery SOC to protect it from overcharging or under discharging.

- **Hydrogen (H<sub>2</sub>) Storage Tank Agent**

The storage tank agent is a vital member of the proposed energy management system. It communicates with the MACSimJX AE to keep monitoring the hydrogen volume in the storage tank. Then, it starts to announce its value in the form of a periodical message (as exhibited in the system results). The hydrogen volume announcement (the periodical message) provides the system operators an alarm about the stored energy levels. Thus, it enables the decision-making even by the migration into another storage tank or changes the system configuration (grid-connected mode).

Figure 4.14 exhibits the communication between these agents that is governed by the DF services registration and discovering (refer to Fig. 4.9). The different agent's source codes are programmed to perform the described functions and then compiled into Java

class files that are added to the MACSimJX ATF (Agent Task Force) folder. The proposed decentralized energy management system has been tested under the same profile of the marine current speed that used in Chapter 3 (Fig. 3.28). The MAS system can manage the energy between the marine-hydrogen different components based on the operating conditions as shown in Fig. 4.15. When the marine current generated energy is higher than the load demand; the electrolyzer is switched on converting the surplus energy in hydrogen stored in the tank. Otherwise, the fuel cell is switched on compensating the power shortage. The battery is controlled to cover the fast dynamics power for fuel cell and electrolyzer protection.

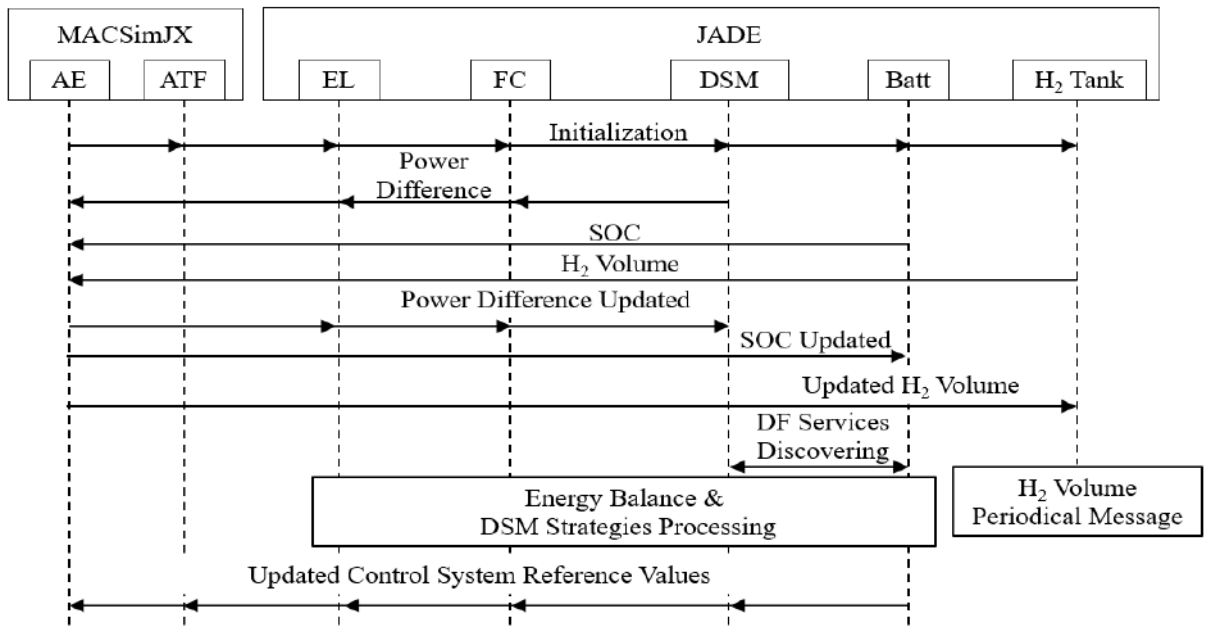


Fig. 4.14. JADE Based Isolated Mode Energy Management System Agent's Interaction.

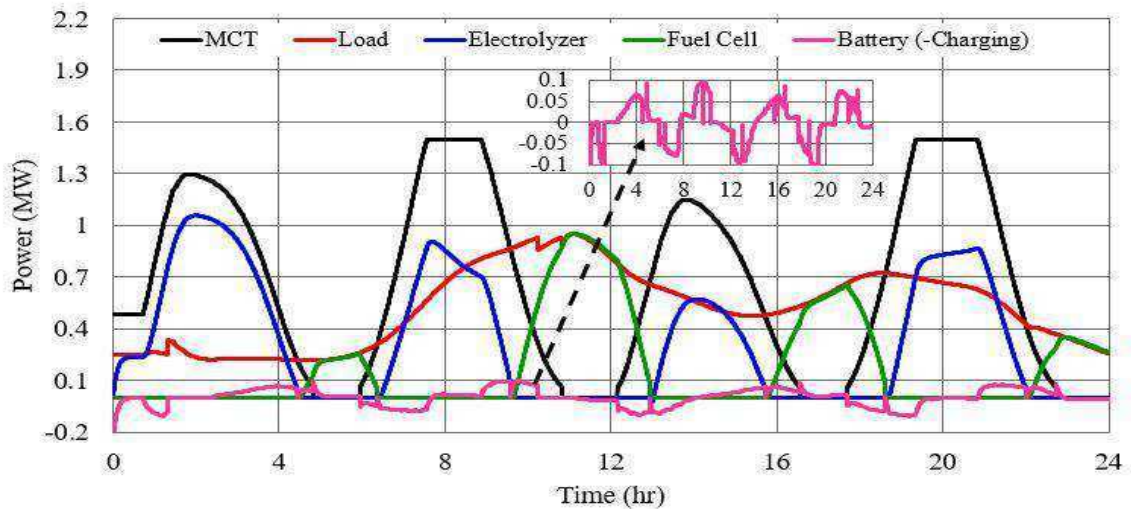


Fig. 4.15. Power Profiles under Isolated Mode Energy Management System.

The DSM agent is powerful to implement the strategies of the demand side management (load shifting and load shedding) as shown in Fig. 4.16. The DSM strategies are effective to protect the battery from the overcharging and the under discharging by limiting the battery SOC within certain limits as shown in Fig. 4.17. Generally, the JADE MAS energy management system is effective to equilibrate the energy between the generation and the consumption under the different operating conditions considering the DC-link voltage stabilization (shown in Fig 4. 18) as an indicator. The hydrogen tank agent provides the command prompt by hydrogen volume periodical messages as shown in Fig. 4.19. The messages are compatible with the volume of the hydrogen deduced from the Simulink model of the storage tank shown in Fig. 4.20. The periodical messages provide the hydrogen storage tank SOC and when it is required to search a storage reserve or changing the system configuration into the grid-connected mode.

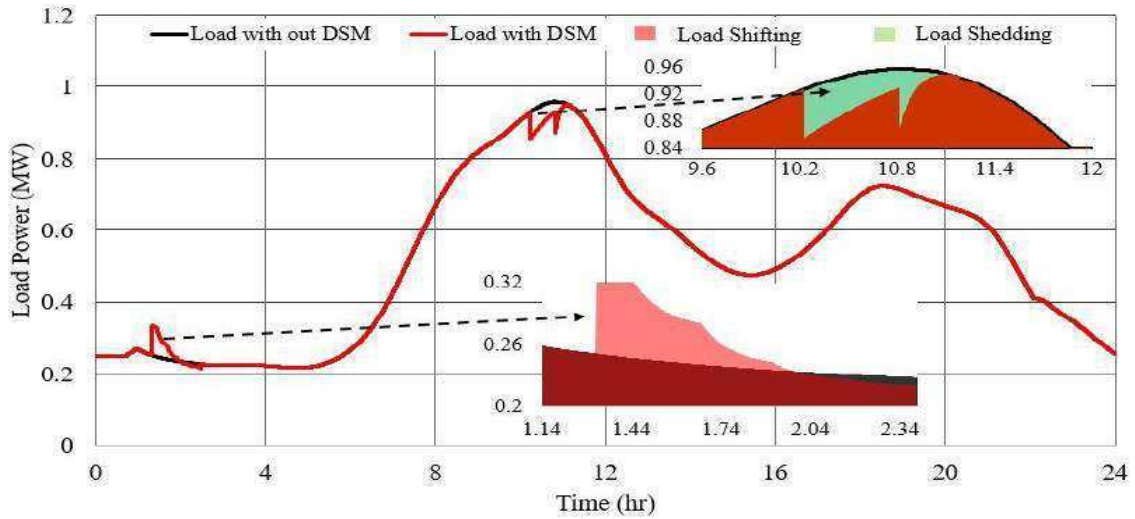


Fig. 4.16. Isolated Mode Demand Side Management Strategies.

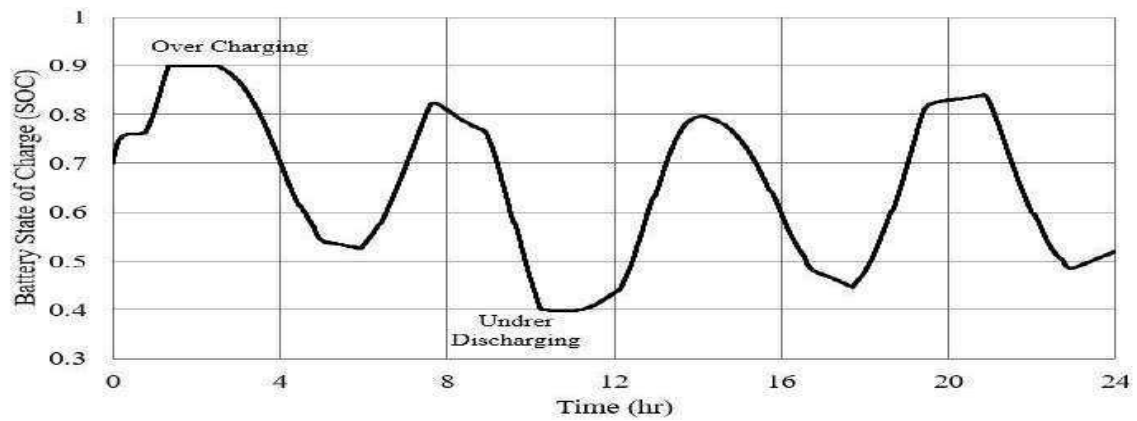


Fig. 4.17. Battery State of Charge (SOC).



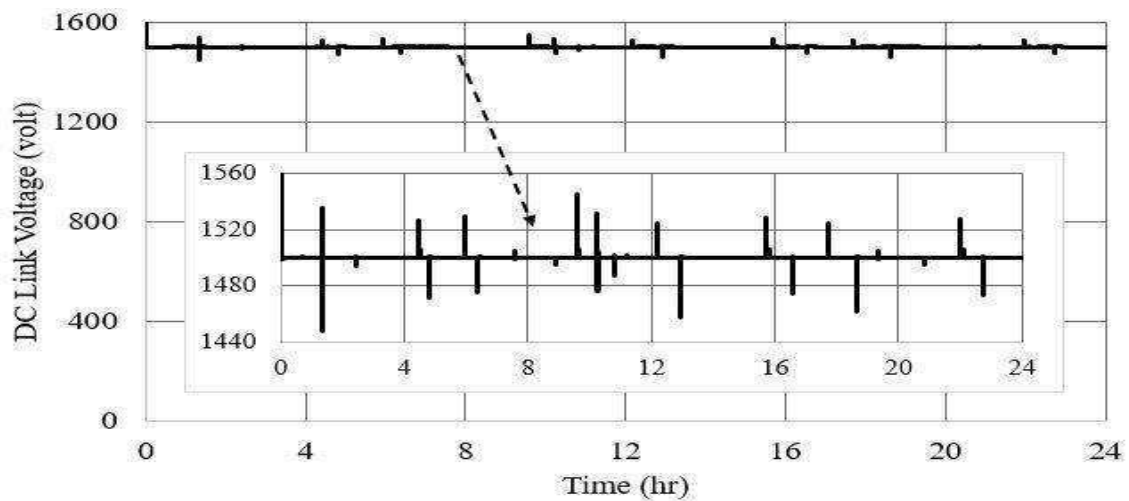


Fig. 4.18. DC-Link Voltage.

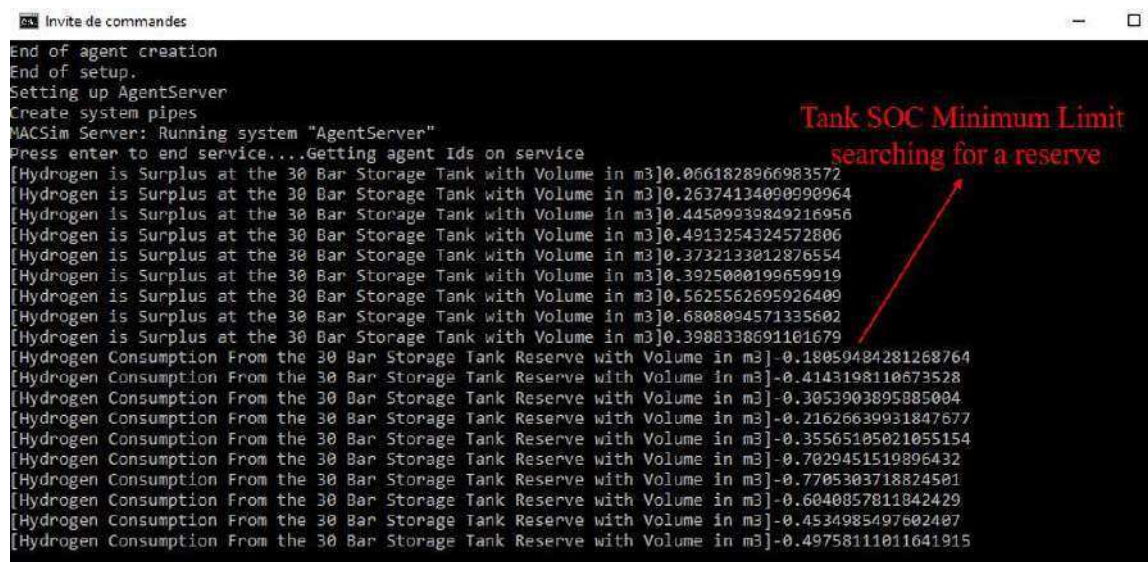


Fig. 4.19. Hydrogen Volume Periodical Messages of the MACSimJX Command Prompt.

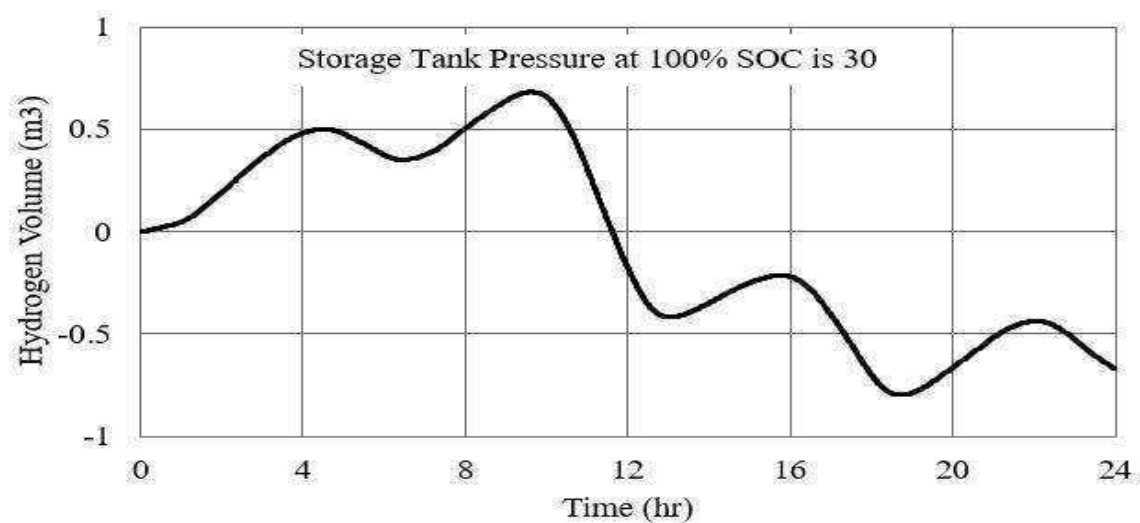


Fig. 4.20. Hydrogen Volume of the Storage Tank Simulink Model.

Figure 4.21 exhibits the Sniffer agent (described in section 3.4) of the proposed JADE based MAS system. The canvas of the Sniffer is the different agents described in Fig. 4.14. The arrows represent the different communications indicating the CA of the communication. Each arrow has a definite color related to its definite conversation.

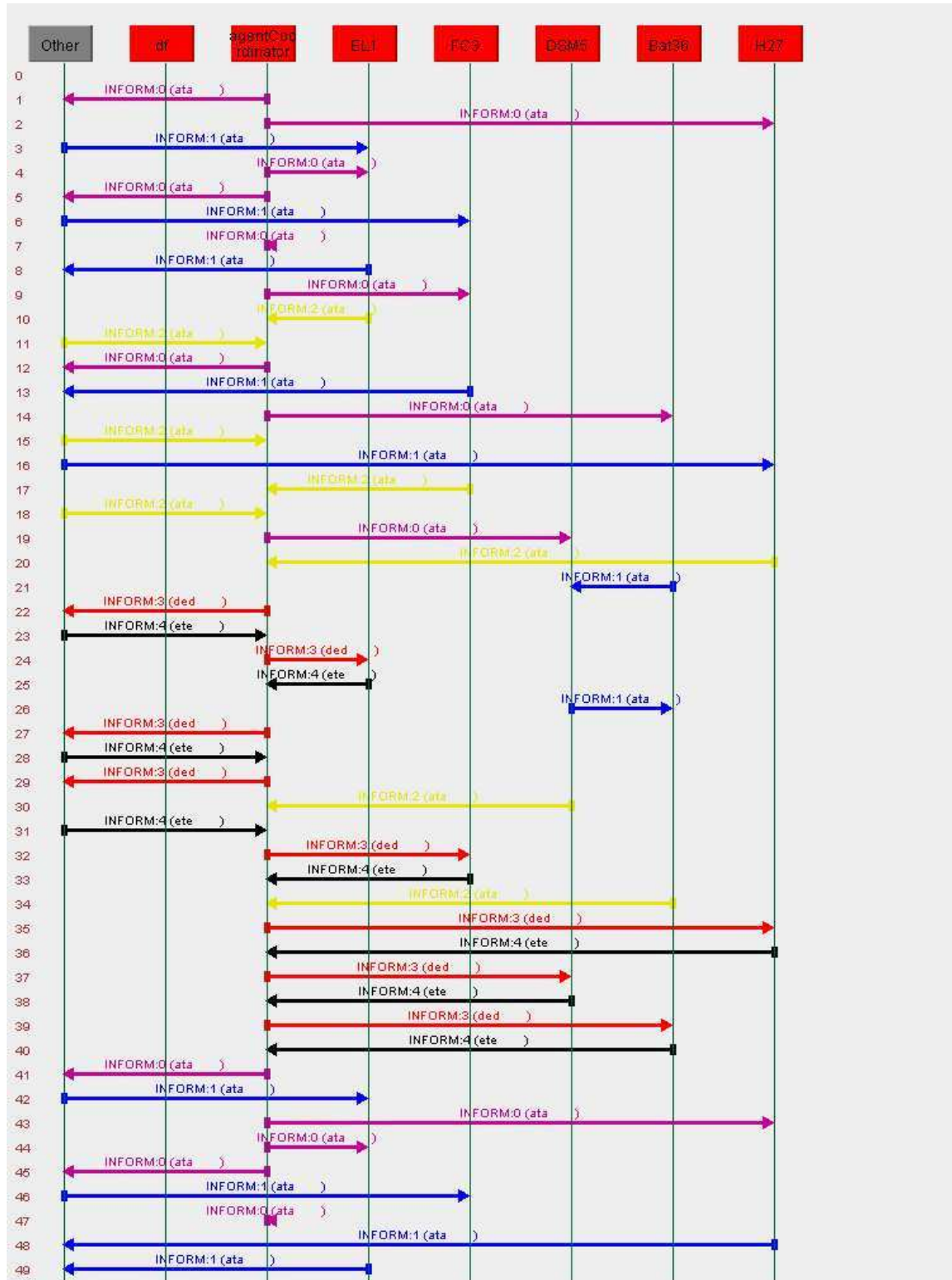


Fig. 4.21. The Sniffer Agent of the Proposed JADE Based MAS System.

## 5.2. Grid-Connected Mode MAS Energy Management System

The Simulink model of the hybrid marine-hydrogen power generation system is modified to integrate the grid as shown in Fig. 4.22. The energy management strategy of the grid-connected mode depends mainly on the operation mode transition in the case of the stored hydrogen shortage. When the storage tank SOC reaches the minimum limit, the PCC (Point of Common Coupling) is switched on to integrate the grid in the system, and the fuel cell is switched off as shown in Fig. 4.23.

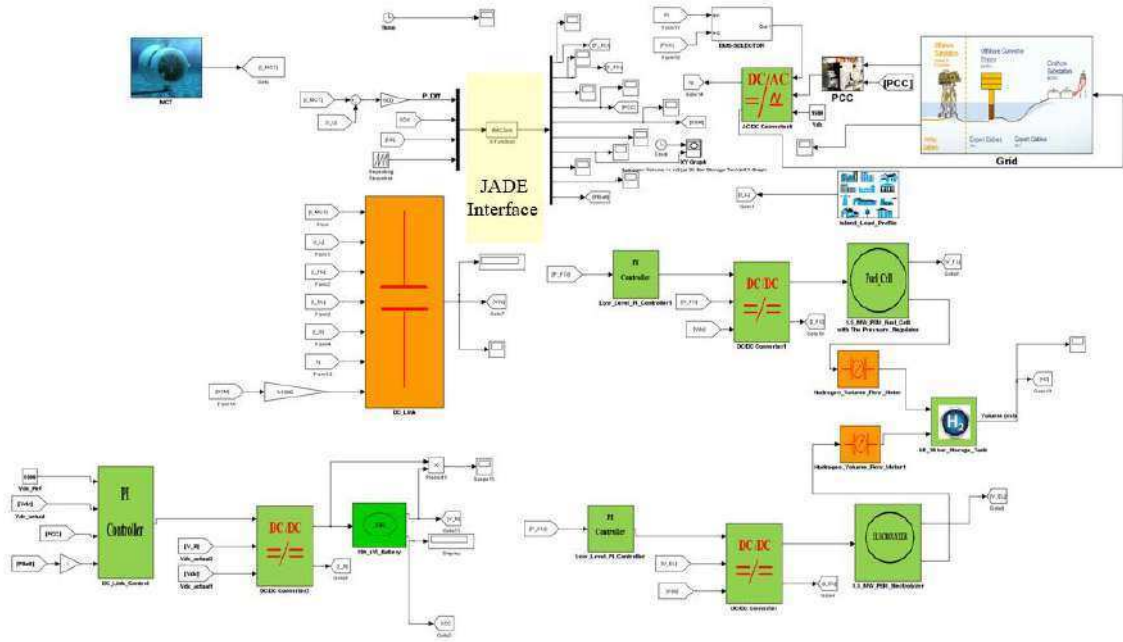


Fig. 4.22. Grid-Connected Hybrid Marine-Hydrogen Simulink Model.

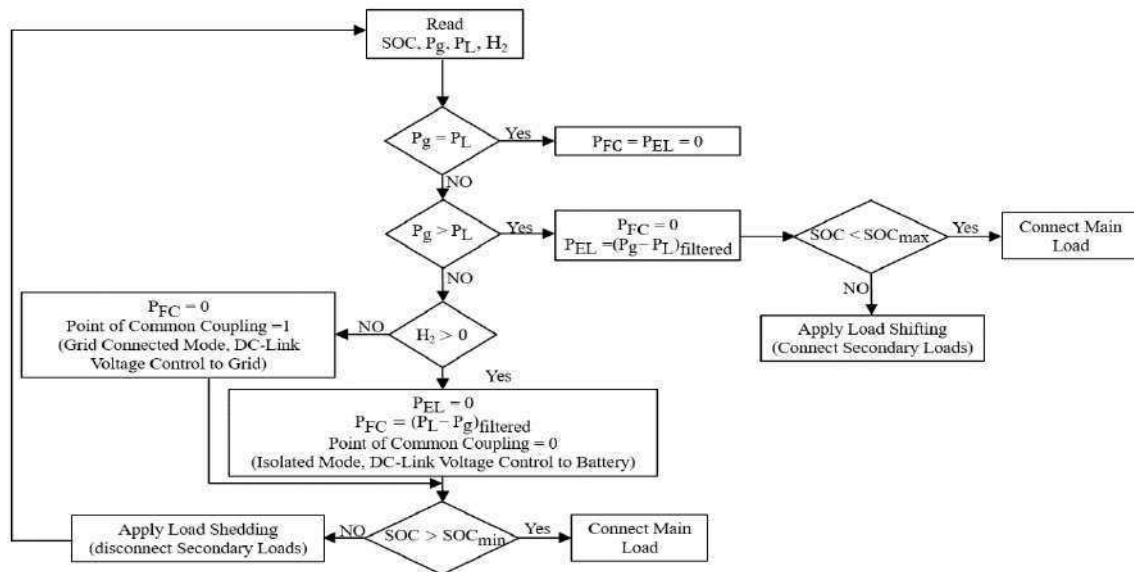


Fig. 4.23. Grid-Connected Mode JADE Based Energy Management Flow Chart.

The MAS energy management system of the grid-connected mode consists of the same isolated system agents performing the same functions with adding another agent for the grid. The grid agent exchanges messages with the hydrogen storage tank to control the PCC based on the storage tank SOC. The fuel cell agent exchanges the messages with the agent of the hydrogen storage tank to control its connection based on its SOC. The messages exchange depends on the DF services discovering while the interaction between the different agents performs the main system function and updates the Simulink model reference values as shown in Fig. 4.24. The designed MAS manages the energy between the different system components effectively with more flexibility. The effectiveness of the system means the ability to keep the balance under the marine current and demand side variations by controlling the operating conditions of the fuel cell, the electrolyzer, the battery and the grid as shown in Fig. 4.25. Due to the operating conditions, the system architecture and topology must be changed in a flexible manner of different components connection/disconnection. In another word, the system scalability that is one of the most important features of MAS decentralized system. When the storage tank SOC is at the minimum limit, the fuel cell is isolated, and the grid is connected (by controlling the PCC as shown in Fig. 4.26) to operate in the grid-connected mode (periods of hours from 11.5 to 13 and from 17 to 19).

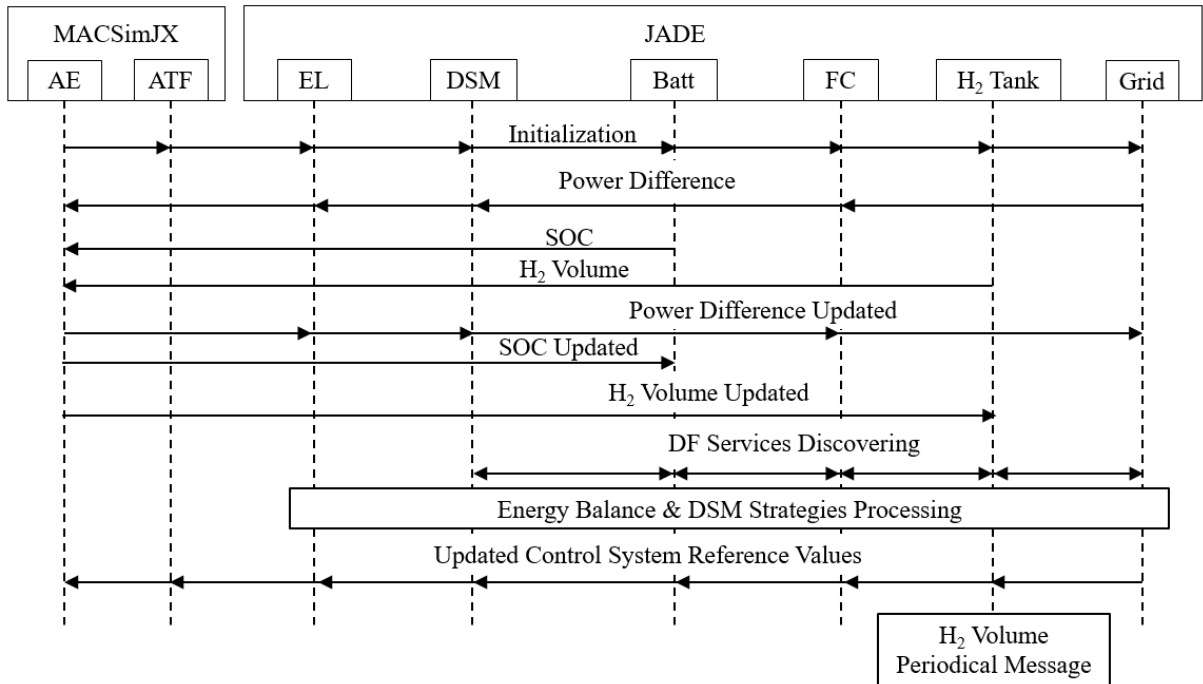


Fig. 4.24. JADE Based Grid-Connected Mode Energy Management System Agent's Interaction.

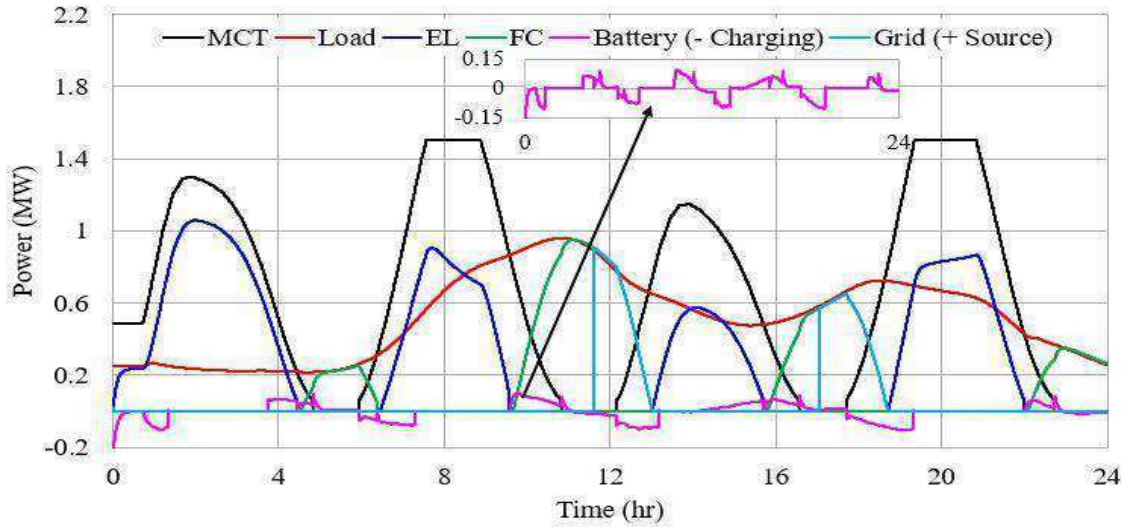


Fig. 4.25. Power Profiles under Grid-Connected Mode Energy Management System.

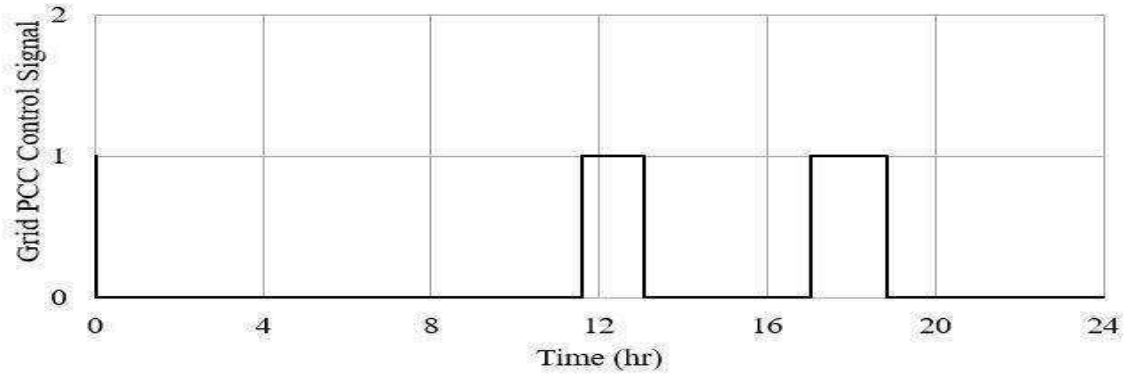


Fig. 4.26. PCC Control Signal.

In the case of energy shortage and the storage tank SOC in between the minimum and maximum limits, the fuel cell is switched on to cover the shortage. Moreover, the grid is disconnected to be in the stand-alone mode (periods of hours from 4.5 to 6, from 10 to 11.5, from 15.5 to 17 and from 22 to 24). Consequently, the decentralized JADE based MAS is a scalable and more flexible than the centralized one proposed in the third chapter that is subjected to the complete failure in case of one component outage or failure. Moreover, it is capable of migrating between the grid connected and the stand-alone operation modes efficiently. The proposed DSM strategy (shown in Fig. 4.27) provides the battery with the more secure and safe operation avoiding the under discharging by increasing the SOC minimum limit as shown in Fig. 4.28. The DC-link voltage control depends on the operation mode that is the responsibility of the battery during the stand-alone mode while it is transferred to the grid during the grid-connected mode.



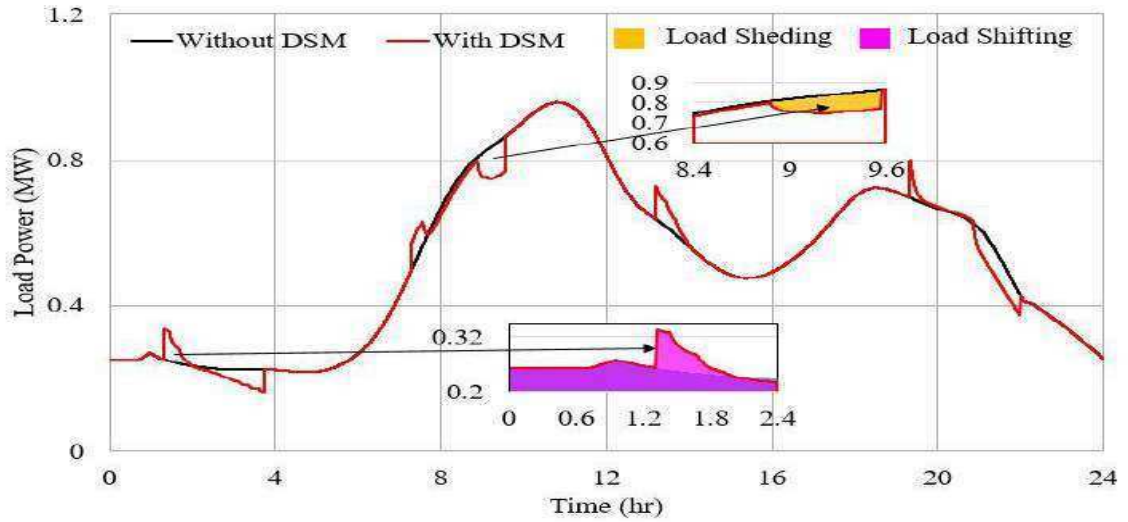


Fig. 4.27. Grid-Connected Mode DSM Strategies.

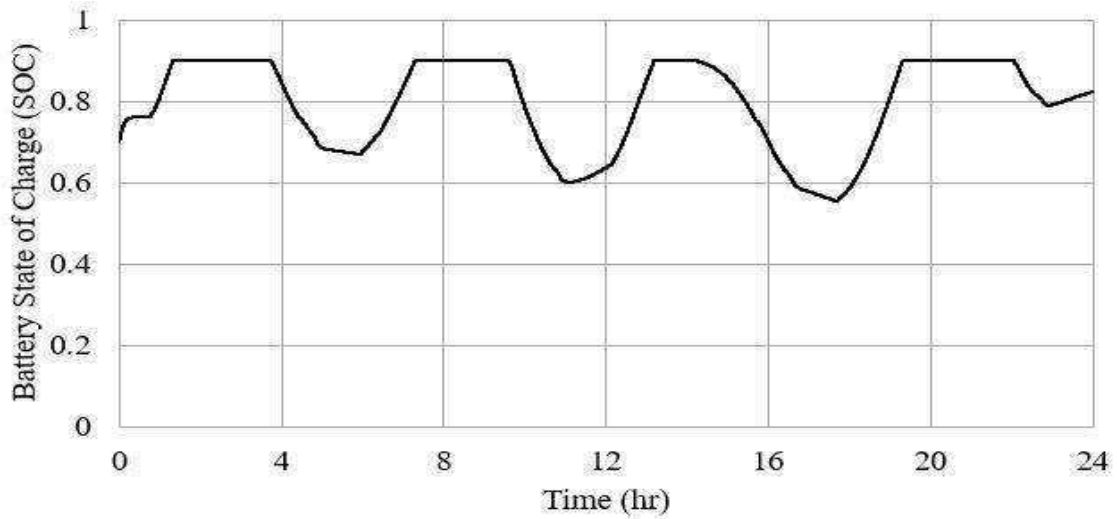


Fig. 4.28. Battery State of Charge (SOC) during Grid-Connected Mode.

The MAS shares the responsibility of the DC-link between the grid and the battery by exchanging the messages between the concerned agents. The sampling frequency of the proposed MACSimJX ATF is 100 Hz (it can be increased) that is selected based on the recommendations of the software package. The transition between the grid connected and the stand-alone modes consumes at least 0.01 sec that provides a slow response to the DC-link voltage control and as a result high over or undershoot as shown in Fig. 4.29. This effect represents the communication system effect on the system performance that requires a high speed system for minimizing the delay of the signals transmission and sustaining the accepted performance of the control systems.

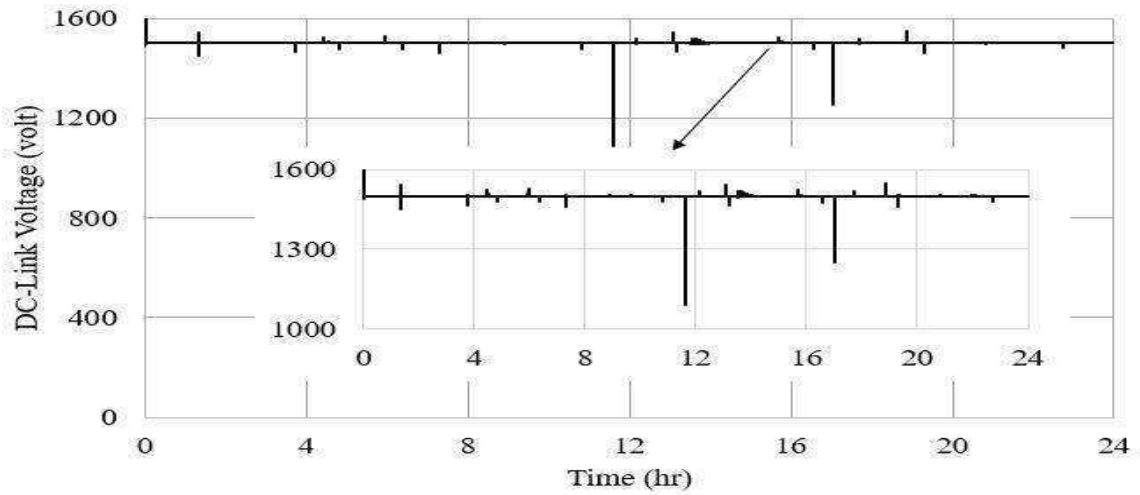


Fig. 4.29. DC-Link Voltage.

By integrating the grid during the hydrogen shortage (minimum limit of the tank SOC), the amount of the stored hydrogen in the tank is to be increased without negative value as shown in Fig. 4.30. The hydrogen tank agent is programmed to provide the periodical messages of the hydrogen volume that is compatible with the Simulink model results as Fig 4.31.

Figure 4.32 shows the interaction between different agents by the Sniffer GUI that is compatible with the designed procedure (Fig. 4.24).

## 6. SGAM Scope of the Proposed JADE Based MAS

The previous chapters describe the representation and the modeling of the SGAM component layer. This chapter presents the JADE based MAS decentralized energy management system. The proposed MAS is consistent with the SGAM considering its different layers definition presented in [212], [213] as follow:

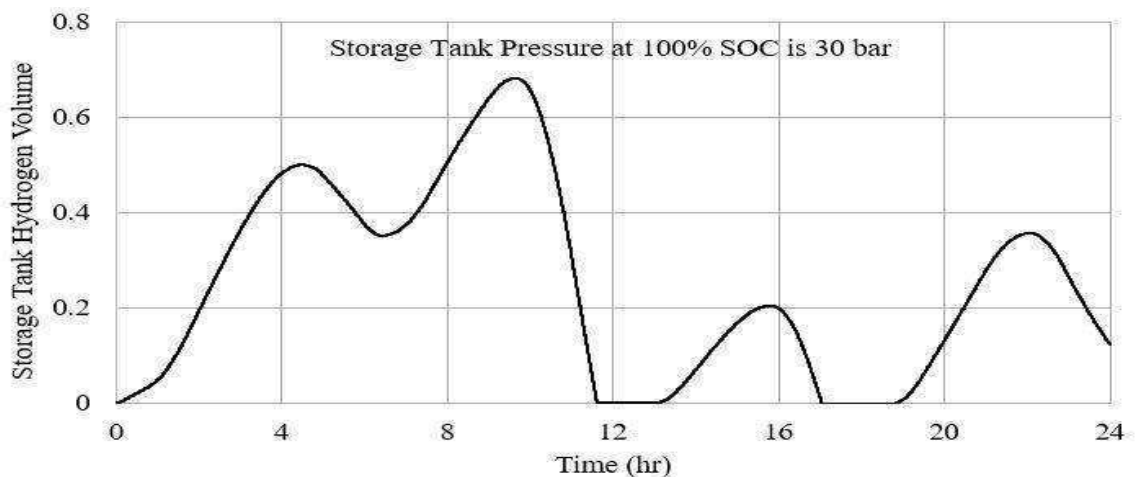


Fig. 4.30. Hydrogen Volume of the Storage Tank Simulink Model.

```

Invite de commandes
End of agent creation
End of setup.
Setting up AgentServer
Create system pipas
MACSim Server: Running system "AgentServer"
Press enter to end service....Getting agent Ids on service
[Hydrogen is Surplus at the 30 Bar Storage Tank with Volume in m3]0.0661828966983572
[Hydrogen is Surplus at the 30 Bar Storage Tank with Volume in m3]0.26374134090990964
[Hydrogen is Surplus at the 30 Bar Storage Tank with Volume in m3]0.44509939849216956
[Hydrogen is Surplus at the 30 Bar Storage Tank with Volume in m3]0.4913254324572806
[Hydrogen is Surplus at the 30 Bar Storage Tank with Volume in m3]0.3732133012876554
[Hydrogen is Surplus at the 30 Bar Storage Tank with Volume in m3]0.3925000199659919
[Hydrogen is Surplus at the 30 Bar Storage Tank with Volume in m3]0.5625562695926409
[Hydrogen is Surplus at the 30 Bar Storage Tank with Volume in m3]0.6808094571335602
[Hydrogen is Surplus at the 30 Bar Storage Tank with Volume in m3]0.3988338691101679
[Hydrogen Consumption From the 30 Bar Storage Tank Reserve with Volume in m3]-0.18059484281268764
[Hydrogen Consumption From the 30 Bar Storage Tank Reserve with Volume in m3]-0.4143198110673528
[Hydrogen Consumption From the 30 Bar Storage Tank Reserve with Volume in m3]-0.3053903895885004
[Hydrogen Consumption From the 30 Bar Storage Tank Reserve with Volume in m3]-0.21626639931847677
[Hydrogen Consumption From the 30 Bar Storage Tank Reserve with Volume in m3]-0.35565105021055154
[Hydrogen Consumption From the 30 Bar Storage Tank Reserve with Volume in m3]-0.7029451519896432
[Hydrogen Consumption From the 30 Bar Storage Tank Reserve with Volume in m3]-0.7705303718824501
[Hydrogen Consumption From the 30 Bar Storage Tank Reserve with Volume in m3]-0.6040857811842429
[Hydrogen Consumption From the 30 Bar Storage Tank Reserve with Volume in m3]-0.4534985497602407
[Hydrogen Consumption From the 30 Bar Storage Tank Reserve with Volume in m3]-0.49758111011641915
done.
Shutting down agents
Deregistering and closing Testnew.Bat1@1de0675

```

Fig. 4.31. Hydrogen Tank Agent Periodical Messages.

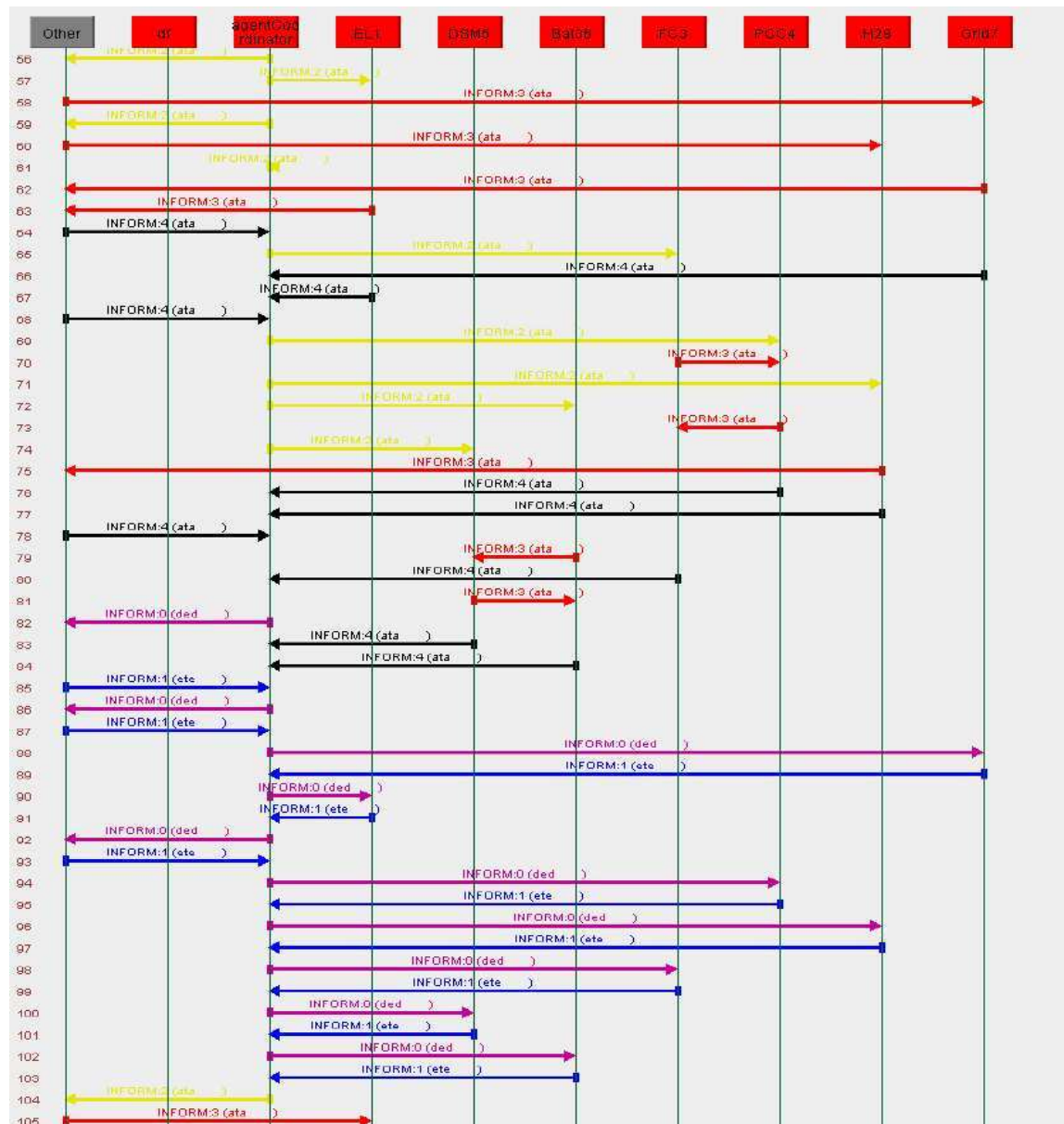


Fig. 4.32. Sniffer Agent of the Grid Connected Mode JADE Based MAS.



- **Communication Layer**

This layer represents the protocol and the mechanisms of information exchanging between the system components and layers. The proposed model utilizes the MACSimJX for interfacing the component layer model (MATLAB/Simulink model) with the JADE platform. As aforementioned, the MACSimJX depends mainly on the asynchronous message exchange between the client and the server using the TCP/IP protocol as a windows pipe.

- **Information Layer**

The information layer describes the information and the data models exchanged between the different system functions and services. The information must be reformed in a standard form of semantics to be understood and easily exchanged between all the system layers. The main information required for the proposed energy management system consists of the power difference, the hydrogen volume and the battery state of charge. These parameters are shared between the different agents using a FIPA compliant message structure (Fig. 4.3) and the DF service registration and discovery (Fig. 4.9).

- **Function Layer**

This layer considers architectural interconnection between the different system functions and services. The functions and services are deduced without considering or thinking about the physical components performing them. The main function of the proposed MAS is the energy management and balance between the marine current generation and the demand-side consumption considering the generation intermittency and the consumption profile. The energy management is performed during two modes of operation (grid-connected and stand-alone). The proposed strategies and functions (Fig. 4.13, Fig. 4.23) are generally designed without considering the different system components, the required number of agents performing them and the responsibilities of each agent.

- **Business Layer**

The business layer considers all the economic structures and the policies that regulate the information exchange in the smart grid. This layer supports the decision making related to the implementation of the different business models. The proposed MAS system has many high-level programmed agents (Java-based) due to the JADE agent paradigm. The agent is an autonomous entity that has the ability

of peer-to-peer communication and negotiation with the other agents. The interaction between the different agents (Fig. 4.14, Fig. 4.24) depends on each agent policies and conditions. For example, the hydrogen tank agent is programmed to perform the online monitoring of the hydrogen volume that enables the system operator to decide on the operation mode selection. The energy balance is programmed as a market model (without considering the economic model) in which each agent has a decision of energy mix share based on its operating conditions.

## **7. Conclusion**

This chapter presents the decentralized JADE based MAS oriented to the energy management and balance of the hybrid marine-hydrogen power generation system. Firstly, the centralized and the decentralized system has been briefly compared with defining the MAS main characteristics. The different MAS platforms have been up to date compared to select one for the decentralized management system implementation. The JADE is a Java-based open source software with a free license. The JADE is a general domain platform that can be applied to any application while the most important feature is the fully compliant with FIPA standard. Consequently, The JADE basic architecture and the main programming features have been briefly discussed. The JADE based MAS developments steps are the main function definition, the system agents' definition, the agents' interaction and finally the agents' source codes programming and compiling. The stand-alone mode of operation is programmed first to evaluate the MAS capability of the energy management and balance considering the marine current intermittency and the demand-side variations. Secondly, the MAS has been modified to consider the operation mode transition (from grid connected to a stand-alone and vice-versa). The MAS is flexible and scalable due to the dynamic nature of the agent (e.g., appearing, registration, deregistration, freezing). The proposed JADE based MAS performance has been tested by disconnecting the fuel cell from the system when the reserve of the stored hydrogen is insufficient. Otherwise, the fuel cell is connected to the system as the main source of the power shortage. The DC-link voltage stabilization has been migrated between the battery during the stand-alone mode to the grid during the grid connected mode and vice-versa. The proposed MAS has the ability of the DC-link voltage control and the operation mode transition. The MAS provides an option of the system online monitoring that enables the system operator of decision making. The last section of this chapter discusses the proposed MAS system from the SGAM point of view. Each layer of the proposed JADE based MAS system and its MACSimJX interface with the

MATLAB/Simulink model of the physical components have been defined and compared with the SGAM. Generally, the designed MAS is compatible with the SGAM and can be considered as a pilot case study of this model.

## **Conclusion and Future Work**



Worldwide, there is no specific definition of the smart grid that is defined locally due to each country energy policies, strategies, and future trends. Otherwise, the SGAM (Smart Grid Architecture Mode) provides the clear and the coherent vision of the general smart grid architecture and its research directions. Thus, the thesis presents the state of the art of the different research directions of the smart grid. The hybrid marine-hydrogen active power generation system has been modeled to represent the component layer of the SGAM. The system integrates the MW scale PEM electrolyzer and fuel cell systems as the main energy balance components. The  $\text{LiFePO}_4$  battery is used to cover the fast dynamics of the electrical energy. Moreover, the thesis analyzes the centralized and the decentralized energy management system. The MAS (Multi-Agent Systems) represents the paradigm of the decentralized system. The JADE platform is used to develop the MAS due to its general domain of application, open source and free license software, interface with MATLAB and the computability with the FIPA (Foundation of Intelligent Physical Agent) standards. The JADE based energy management system balances the energy between the generation (marine-current energy conversion system) and the demand side (residential load profile) during the stand-alone and the grid-connected modes of operation. The novelty of this work is represented in the following points:

- The development of the EMR (Energetic Macroscopic Representation) of the marine current power generation system that, up to my best information, has not been formalized yet. The EMR of the marine system facilitates the understanding of the interactions between the different subsystems (e.g., tidal turbine, permanent magnet synchronous generator, the power electronic converters and the demand side). Moreover, it makes the system model more readable to be integrated easily in any future work. Finally, it enables the design of the effective control strategies under the different operating modes of the system.
- The analysis and the development of the loss minimization (output maximization) flux control strategy of the PMSG (Permanent Magnet Synchronous Generator) directly driven by the tidal turbine. The strategy depends on the injection of a current into the machine windings based on the vector control to reduce the machine core losses and generally the total losses. The proposed strategy has been applied to a marine current turbine system of 1.5 MW rated power to evaluate the annual energy saving. The results indicate the provided energy saving is sufficient to feed one more residential load with an average consumption of 4000 kWh. From another point of view, the energy saving is sufficient to generate about 100 kg of hydrogen from the PEM (Proton Exchange Membrane) electrolyzer system based on The

HHV (Higher Heating Value) without considering the electrolyzer system efficiency. If the electrolyzer system is considered in the range of 40% to 50%, the energy saving can provide surplus generation from 40 to 50 kg annually.

- The model development of the MW scale PEM electrolyzer system that, up to our best information, has been presented before. The PEM electrolyzer state of the art indicates that the MW scale is developed based on the increase of the operating current density in the range of two  $A/cm^2$ . A model of a small-scale PEM electrolyzer with the help of the EMR has been used and adapted to represent the MW scale system. The reverse engineering has adapted the model for estimating the main model parameters (another, cathode exchange current densities, and the membrane conductivity) to provide characteristics and the KPI (Key Performance Indicators) of the MW scale system.
- The development of the JADE based MAS (Multi-Agent System) for the energy management of the hybrid marine-hydrogen active power generation system. The system model has been built in MATLAB/Simulink with the help of the global system EMR. The MACSimJX (Multi-Agent Control for Simulink Java Extension) program has been used to interface the Simulink model with the JADE platform. The JADE based MAS energy management system consists of many agents that perform definite functions and work together in harmony based on the JADE peer-to-peer communication. Each physical system (PEM electrolyzer, PEM fuel cell, battery and the demand side) has an agent that manages its operation due to its healthy and safe operating limits and recommendations. The different agents Java source codes have been programmed to perform their functions, and hence, the codes have been compiled to be integrated into the JADE platform containers. The effectiveness of the proposed JADE based MAS system has been evaluated during the stand-alone and the grid-connected modes. The results indicate that the proposed JADE based energy management system is powerful, scalable and redundant under the different operating conditions. Moreover, the system provides the option of the marine-hydrogen system online monitoring and surveying that enables the operator decision making.
- The whole system integrating the marine-hydrogen active power generation system with the JADE based MAS energy management system represents a novel case study of the SGAM. The study has modeled and represented each layer of the SGAM. Firstly, the component layer with the high renewables integration objective

has been represented by the marine-hydrogen system. Hence, the MACSimJX models the communication and the data layers by interfacing the MATLAB/Simulink model of the marine-hydrogen system with the JADE based MAS. Finally, the JADE based energy management system that represents function and the business layers. Generally, the proposed system presents a model the SGAM that can be utilized for the detailed analysis of the smart grid research directions.

Two directions can expand this work in the future considering the modeling and the experimental validation as illustrated in the following points:

- The proposed marine current energy conversion system can be modified and adapted to model a complete tidal farm. The modification represents the turbines and the machines aggregation method to model the whole farm. The adaptation considers the results accuracy level mainly that are concerning the harnessed energy evaluation.
- The JADE based MAS energy management system can be expanded to include the optimization of the energy market economics. The proposed management model considers only the energy balance between the generation and the consumption as the main objective. Moreover, the JADE based MAS system can integrate the EV (Electric Vehicle) with considering its V2G (Vehicle to Grid) and G2V (Grid to Vehicle) operating modes. The agent (due to the JADE paradigm) is a dynamic entity that can appear and disappear flexibly that is more compatible with the EV.
- The adaptation of the MW scale PEM electrolyzer model can be more analyzed based on the same procedure followed for the small-scale model. A small-scale stack adopted for the MW scale systems can be tested experimentally to estimate precisely the model parameters that provide the same polarization curve and to evaluate the high current density operation hypothesis.
- The JADE based decentralized energy management system can be evaluated experimentally by developing a test-bench that emulates the performance of the physical components (marine system, PEM electrolyzer, PEM fuel cell and the battery) in addition to their power electronic converters. The JADE based can be programmed to perform the required energy management strategies. The interface between the JADE platform and the physical components depends on two stages. The first is the MACSimJX interface that exchanges the signals between JADE and MATLAB/Simulink. The second stage is the interface between the physical



components and MATLAB that can be performed by many procedures. One of the procedure is the dSPACE cards that interact directly with the physical components by the signal processing cards and interface with the MATLAB/Simulink by one of the software libraries (e.g., mLib and mTrace). The test bench will represent the pilot case study for experimentally designing, testing and investigating the present and the future research directions of the smart grid.

## **Extended French Abstract**



## 1. Introduction

Les réseaux électriques traditionnels souffrent de plusieurs problèmes et inconvénients tels que les coupures, un fonctionnement non économique, les impacts environnementaux, etc... Le smart grid est une nouvelle topologie du réseau électrique qui dépend des sources d'énergie renouvelables au lieu des traditionnelles sources d'énergie fossiles. Le smart grid nécessite un fort management avec une communication mutuelle entre la partie génération et la partie consommation. Ce type de réseau présente plusieurs défis et problèmes scientifiques qui doivent être étudiés et analysés comme suit :

- L'infrastructure du réseau traditionnel doit être adaptée aux taux de pénétration élevés des énergies renouvelables,
- Le choix technique et économique d'un système de stockage d'énergie convenable est essentiel dans un smart grid pour assurer un fonctionnement stable, sécurisé sous différentes conditions,
- La gestion et l'optimisation d'énergie en considérant les contraintes et les conditions des parties génération et consommation,
- Un système de communication puissant, redondant et entièrement protégé est essentiel,
- La modélisation et la représentation du smart grid (avec les interactions entre les différentes couches) sont nécessaires pour une meilleure compréhension des interactions entre les couches (puissance, communication, gestion, etc.).

La modélisation du smart grid permet l'étude, l'analyse et la conception de nouvelles solutions pour relever tous ces défis. Cette étude présente la modélisation et la gestion d'un système actif de génération de puissance hybride courant marin- hydrogène. L'énergie des courants marins est choisie à cause de l'objectif d'une forte intégration des sources renouvelables dans le smart grid. L'énergie des courants marins est une technologie qui n'est pas encore mature et qui présente plusieurs défis économiques et technologiques qui doivent être étudiés. Le choix de la machinerie électrique et le système de transmission de puissance sont les principaux défis que rencontre l'intégration des systèmes de courants marins dans le smart grid. L'énergie marémotrice souffre de variations mensuelles et saisonnières qui nécessitent un système de stockage capable d'assurer une alimentation énergétique continue. Le système à hydrogène est choisi en se basant sur l'état de l'art des technologies de stockage d'énergie. Le système à hydrogène a un long cycle charge/décharge (à l'échelle de jours ou semaines) ; ce qui est plus convenable aux variations quotidiennes et hebdomadaires des

courants marins. En plus, la chaîne à hydrogène supporte plusieurs formes d'utilisations finales (p. Ex. production d'électricité par une pile à combustible, alimentation des véhicules électriques à pile à combustible ou directement transmis dans les réservoirs de stockage). Les électrolyseurs PEM (Proton Exchange Membrane) à l'échelle de mégawatt sont des systèmes de nouvelle technologie pour l'amélioration de l'intermittence des sources renouvelables sur le long terme. Les électrolyseurs et la pile à combustible ont une réponse dynamique spécifique qui doit être respectée pour éviter le vieillissement du système et la dégradation des composants. La batterie LiFeO<sub>4</sub> est choisie pour couvrir les dynamiques rapides de la puissance électrique. Cette technologie de batterie combine les avantages de la densité d'énergie élevée des batteries et la densité de puissance élevée des super-condensateurs. La configuration du système hybride courants marins-hydrogène nécessite un système efficace de gestion de l'énergie. Ce système doit avoir la capacité de pilotage et de surveillance des différents composants (mécanique, électromécanique, électrochimique et électrique). Une des techniques d'optimisation et de gestion de puissance est le MAS (Multi-Agent System) qui est un type de système de gestion décentralisé. Cette étude présente le MAS pour contrôler et gérer la totalité du système dans le cadre du smart grid. La REM (Représentation Énergétique Macroscopique) est choisie comme représentation technique du système pour une meilleure compréhension des interactions entre ses différents composants physiques.

## **2. Représentation et Modélisation Énergétique Macroscopique d'un Système Actif de Génération de Puissance Actif Hybride Marine-Hydrogène**

L'expression de système actif de génération de puissance a été utilisée dans la littérature pour décrire un système hybride éolienne-électrolyseur-pile à combustible-super condensateur. Le système actif de génération de puissance consiste à convertir la nature intermittente et statique d'une énergie renouvelable en un système dynamique qui peut survivre dans toutes les conditions de fonctionnement. Ceci en intégrant des systèmes de stockage d'énergie pour équilibrer la différence de production-consommation. L'étude de cas envisagée comprend un système de génération de puissance à partir de l'énergie marine renouvelable de type FFDD-MCT (Fixed Pitch Direct Drive – Marine Current Turbine, un électrolyseur PEM, une pile à combustible PEM qui sont les deux à l'échelle du MW, et des charges résidentielles. Un profil de charge domestique standard est sélectionné pour modéliser une variation de charges résidentielles insulaires ; ce qui fournit une configuration de système d'alimentation autonome. Cette architecture présente l'avantage d'avoir le système de génération proche de la charge et permet ainsi d'éviter le principal défi technique et économique que représente

la transmission de la puissance produite. Le système de génération de puissance utilise un générateur synchrone à aimants permanents (GSAP) pour convertir l'énergie mécanique en énergie électrique et alimenter un bus DC via un redresseur triphasé entièrement commandé. L'électrolyseur et la pile à combustible sont reliés à bus DC par des convertisseurs DC-DC pour équilibrer le flux de puissance entre la charge et le système de génération en tant que sources de courant contrôlées. La charge est connectée au système via un onduleur et un transformateur triphasés. L'onduleur est commandé de manière à garder constantes la valeur efficace et la fréquence de la tension aux bornes de la charge.

La réponse de l'électrolyseur et de la pile à combustible doit être respectée pour éviter leur vieillissement prématuré et assurer un fonctionnement sécurisé. Ainsi, un système de stockage d'énergie auxiliaire doit être intégré pour « lisser » la dynamique rapide. Une batterie Lithium-Ion LiFePO<sub>4</sub> est connectée au bus DC par l'intermédiaire d'un convertisseur DC-DC bidirectionnel en tant que source régulée en tension pour stabiliser la tension de la liaison DC. Ceci peut être considéré comme une technique indirecte de lissage de puissance. Le système comprend de nombreux composants de domaines hétérogènes (mécaniques, électromécaniques, électriques et électrochimiques). La conception du système de contrôle nécessite une bonne compréhension des relations entre tous les sous-systèmes. La représentation énergétique macroscopique (REM) est utilisée pour représenter chaque sous-système et pour concevoir les stratégies de contrôle appropriées de l'ensemble. La REM a été développée en 2000 à l'Université de Lille en France pour décrire des systèmes électromécaniques complexes. C'est une technique de représentation très simple avec un ensemble de principes et d'éléments. Depuis, la REM est devenu un outil plus générique pour la représentation des systèmes multi-physiques. La REM suit une procédure spécifique pour la modélisation du système et se déroule comme suit :

- Développement de la REM de chaque sous-système individuellement,
- Développer la REM général de l'ensemble du système en intégrant les REM des sous-systèmes en se basant sur les principes de causalité intégrale et physique,
- Définition des chaînes de réglage du système en utilisant le principe de la représentation inverse,
- Conception des stratégies de contrôle appropriées en se basant sur les chaînes de réglage définies,
- Développement du modèle du système en utilisant la plate-forme de modélisation appropriée.

Chaque sous-système REM est présenté en premier pour faciliter la compréhension du comportement physique et rendre les équations plus lisibles. Le système de courant marin se compose principalement de la turbine marémotrice et de la GSAP à entraînement direct. Chaque composant a des équations qui décrivent ses performances. Une nouvelle approche a été proposée pour représenter les pictogrammes REM multiports dans un nouveau modèle REM de l'électrolyseur en considérant les deux domaines (thermique-fluidique ou thermique-pneumatique) comme des domaines porteurs et portés. La REM globale de la pile à combustible PEM proposée peut être considérée comme identique à celui de l'électrolyseur PEM en considérant les tensions d'activation, ohmique, de diffusion et de concentration comme des chutes de tension. L'électrolyseur et la pile à combustible ne fonctionnent pas simultanément pour éviter des cycles électricité-électricité en utilisant un système de stockage électrique alors qu'il s'agit d'un système de génération d'hydrogène. La pression de l'hydrogène produit par l'électrolyseur est de 30 bars alors que la pression d'entrée de la pile à combustible est légèrement supérieure à un bar. Par conséquent, un régulateur de pression est utilisé pour abaisser la pression d'hydrogène du réservoir au niveau de la pile à combustible. Ainsi, la REM du régulateur de pression est un élément de conversion mono-physique alors que la REM du réservoir de stockage est constitué d'un élément d'accumulation. L'onduleur complet alimentant la charge est commandé comme on le verra plus loin pour fournir une tension alternative triphasée de valeur efficace et de fréquence fixes ; il peut être représenté par un pictogramme de source d'énergie. Les caractéristiques de la charge dépendent de la combinaison des types de consommateurs (ménages, bureaux et bâtiments publics, installations commerciales ou industrielles et agricoles) ainsi que de la densité de population. Le profil de charge standardisé représente les petits consommateurs en général. Vingt-sept profils normalisés différents ont été développés en Europe pour les différents types de charges. Tous les profils sont estimés par pas d'un quart d'heure pendant une année eu PU, sur la base d'une consommation unitaire de 1000 kWh. Le Conseil mondial de l'énergie estime que la consommation d'énergie moyenne des ménages est d'environ 4000 kWh par an. Par conséquent, le profil de charge des ménages représente quatre fois le profil de charge des ménages standard. La REM de la batterie est une source et des éléments d'accumulation avec la tension en circuit ouvert et le courant comme action et réaction respectivement. Le modèle dynamique de la cellule de batterie LiFePO<sub>4</sub> est basé sur un circuit équivalent décrivant la dynamique de charge / décharge. Il y a cinq convertisseurs dans le système; le redresseur commandé interfacé avec le PMSG, l'onduleur interfacé avec la charge, le convertisseur élévateur interfacé avec la pile à combustible, le convertisseur

abaisseur interfacé avec l'électrolyseur et le convertisseur bidirectionnel DC-DC interfacé avec la batterie. Tous les convertisseurs ont des connexions communes avec la liaison DC en tant qu'entrée ou sortie. Il existe différentes procédures de modélisation des convertisseurs électroniques de puissance. L'objectif principal de la modélisation du système est l'étude du flux d'énergie. La représentation des différents convertisseurs est un élément de conversion mono-physique avec comme fonction des conversions AC-DC, DC-AC ou DC-DC. Les paramètres de réglage de ces éléments sont les indices de modulation ou les rapports cycliques. La représentation de la dynamique de du bus DC est un élément d'accumulation connecté à un élément de couplage mono-physique. Les dynamiques de la charge, du transformateur et des câbles de connexion (avec le filtre) sont représentées respectivement par un élément source, un élément de conversion mono-physique et un élément d'accumulation. Le système global REM est synthétisé en intégrant tous les sous-systèmes en considérant le principe de causalité physique. La REM globale rend le système plus lisible et aide à concevoir les stratégies de contrôle et de gestion de l'alimentation, comme indiqué dans la section suivante.

### **3. Systèmes de Gestion Centralisée d'Énergie et du Contrôle Niveau-Bas**

La conception des stratégies de contrôle efficaces à l'aide de la REM nécessite une analyse détaillée du système, qui est appelée la définition de la chaîne de réglage. Selon le principe de causalité physique de la REM, le paramètre de réglage de chaque système est défini pour visualiser son effet sur les paramètres du système.

Le système de contrôle niveau-bas consiste en le contrôle des entités qui sont conçues en se basant sur les chaînes de réglage et attachées aux composants physique pour recevoir leurs valeurs de référence de la part du système de management. Un paradigme du système centralisé de gestion d'énergie est présenté afin d'évaluer les performances du système globale dans un mode de fonctionnement autonome. Un modèle du sur MATLAB/Simulink analyse les performances du système. Le système actif de génération de puissance hybride marine-hydrogène intègre cinq chaînes de réglage : une pour le convertisseur côté machine (AC-DC)) et la deuxième pour le convertisseur côté charge (DC-AC) pendant que chaque convertisseur DC-DC possède une chaîne de réglage basée sur son rôle et son mode de fonctionnement. Les stratégies de contrôle convertisseur côté machine sont la FCS (Flux Control Strategy) et la PCS (Power Control Strategy). Le but principal de la PCS est le contrôle de la puissance active à la sortie de GSAP. Cette stratégie a deux modes: le mode de suivi du point de puissance maximale lorsque la machine tourne en-dessous de la vitesse



de base et le mode de limitation de puissance lorsque la vitesse de la machine dépasse la vitesse de base. De même, la FCS a deux modes. Le premier mode est le mode de couple/courant maximum qui maintient la composante de courant (axe d) à zéro lorsque la machine tourne en-dessous de la vitesse nominale. Le deuxième mode est la stratégie du defluxage qui maintient la tension et le courant de la machine sous leurs valeurs nominales lorsqu'elle tourne au-dessus de sa vitesse de référence. Une des nouveautés de ce travail est l'adaptation de la méthode de la maximisation de la puissance de sortie (minimisation des pertes) pour le système de génération de puissance à partir de l'énergie marine renouvelable. Se basant sur toutes les stratégies de contrôle sus-citées, le système de contrôle du convertisseur côté machine est conçu. Le système étudié est autonome et doit en fournir une tension alternative de valeur efficace constante aux bornes de charge avec un facteur de puissance unitaire. Le contrôle d'un onduleur dans un système de conversion d'énergie éolienne en mode de fonctionnement autonome a été présenté dans la littérature. En se basant sur la même stratégie de contrôle, le système de contrôle du convertisseur côté charge est conçu. Les convertisseurs de l'électrolyseur et de la pile à combustible sont contrôlés pour gérer l'équilibrage d'énergie entre la génération et la consommation.

L'électrolyseur et la pile à combustible ont une réponse dynamique qui doit être respectée afin d'éviter l'altération des composants. Le système de gestion de l'énergie doit également prendre en compte les limites de fonctionnement de la batterie que sont le courant et le SOC (State of Charge). Le système de gestion d'énergie proposé estime le point de fonctionnement de l'électrolyseur en décomposant la puissance en deux composantes de dynamiques lente et rapide. La constante de temps du filtre dépend de la réponse dynamique sûre et recommandée de l'électrolyseur. Le système d'électrolyseur considéré a une réponse dynamique de démarrage de cinq minutes ; ce qui est compatible avec la dynamique des systèmes de stockage d'énergie PEM. Ainsi, le système de gestion de l'énergie fournit les points de fonctionnement de la pile à combustible et de l'électrolyseur en tant que sortie d'un filtre passe-bas avec une constante de temps de 5 minutes en respectant les limites minimales et maximales de l'état de charge de la batterie. Les convertisseurs de la l'électrolyseur et de la pile à combustible sont des sources de courant contrôlées suivant la puissance des points de fonctionnement qui est réinjectée en valeurs de courant de référence (en supposant une tension du bus DC constante).

Le convertisseur côté batterie est contrôlé suivant des fonctions de contrôle définies qui stabilisent la tension du bus DC et couvre la dynamique rapide des variations de puissance. En contrôlant l'électrolyseur et le point de fonctionnement de la pile à combustible, la batterie

peut couvrir la dynamique rapide si son état de charge permet la charge ou la décharge. Sinon, il stabilise la tension du bus continu en considérant la batterie comme une source de tension. Le contrôleur du convertisseur côté batterie est constitué d'une double boucle. Se basant sur REM de l'ensemble du système et de la définition des chaînes de commande, la structure de commande pratique du système actif de génération de puissance hybride marine-hydrogène est conçue. Un modèle Matlab / Simulink est construit en considérant toutes les équations du système et de contrôle pour analyser et étudier le processus de production d'hydrogène sous une vitesse du courant marin et un profil de charge variables. Les paramètres du système de génération de puissance englobent les paramètres de la turbine, du GSAP, du bus DC et du convertisseur côté charge (y compris les câbles, le filtre et le transformateur). De nombreux manuels et publications ont présenté les premiers détails d'un stack électrolyseur de 250 kW qui est sélectionné pour être utilisé et modélisé. Le modèle d'un électrolyseur PEM de 50W a été modifié en fonction des paramètres disponibles pour représenter un stack de 250 kW. La puissance nominale du système marine modélisé est de 1,52 MW. Lorsque la vitesse du courant marin est à sa valeur nominale, et qu'il n'y a pas de demande de charge, presque toute la puissance générée doit être convertie en hydrogène. Ainsi, l'électrolyseur à l'échelle du MW est conçu pour avoir six stacks en parallèles. Le modèle a été adapté en changeant les paramètres principaux (les densités de courant d'échange, la conductivité de la membrane et les coefficients de transfert de charge de l'anode et de la cathode). L'estimation des paramètres est obtenue grâce à la technique de la rétro-ingénierie. Cette technique exige la connaissance de la courbe de polarisation, la densité de courant, le nombre de cellules et la surface de cellule (disponibles dans les manuels de la pile). Les indicateurs clés des performances de l'électrolyseur sont le taux de production d'hydrogène, la puissance électrique, la pression d'hydrogène, le rendement, la pureté de l'hydrogène, la durée de vie, la dégradation et le coût de production de l'hydrogène. Les quatre premiers indicateurs sont les plus appropriés pour être également utilisés pour vérifier la précision du modèle. Le modèle fournit des taux de production d'hydrogène et de consommation d'eau de 51 Nm<sup>3</sup>/h et 46l/h respectivement qui sont approximativement les mêmes taux réels du stack. Les caractéristiques de tension, de courant et de puissance montrent la convergence du modèle avec la performance réelle de la pile alors que la tension de fonctionnement du modèle est presque la même que celle de la pile, ce qui offre le même niveau de rendement.

Le modèle d'une petite pile à combustible a été modifié et adapté pour être à l'échelle du MW en empilant 6 stacks 250 kW. Le modèle des batteries, de puissance de 100kW, est obtenu en se basant sur le modèle d'une cellule de 3,2V-195Ah.

Les résultats sont divisés en deux parties: la première présente la minimisation des pertes tandis que la seconde discute des performances du système avec un profil journalier de la vitesse du courant marin pour évaluer l'efficacité des différentes stratégies de contrôle. Pour la deuxième partie, nous avons utilisé des données réelles du Raz-Blanchard. Ce site est situé entre l'île d'Alderney et le cap de La Hague et capitalise environ la moitié de la ressource nationale. Deux stratégies de contrôle du FCS (Flux Control Strategy ; au dessous de vitesse nominale) ont été testées: une avec le maximum (couple / courant) et l'autre avec le courant de référence de l'axe-d estimé sur la base des calculs de minimisation des pertes.. Ces tests ont montré que, en fonction de la vitesse de rotation, les pertes totales et les pertes fer dans la génératrice sont réduites en moyenne de 3,33% et de 11,56% respectivement. La diminution des pertes totales semble faible, mais il serait plus judicieux de raisonner en terme d'économie d'énergie.

En appliquant la stratégie de contrôle de minimisation des pertes en mode MPPT (Maximum Power Point Tracking), la quantité d'énergie économisée par an est de 3,33% de la moyenne des pertes totales de la GSAP qui sont de 15 kW pour 7864 heures ; soit 4 MWh. Le Conseil Mondial de l'Energie estime que la consommation moyenne d'un ménage est d'environ 4000 kWh par an. Ainsi, la stratégie de minimisation des pertes adaptée à une Génératrice (cas d'étude : 1,245 MW) permet une économie d'énergie suffisante pour alimenter un foyer par an. En considérant la HHV (Higher Heating Value) l'hydrogène de 141,88 MJ (0,0392 MWh), cette stratégie permettrait aussi une augmentation de la production annuelle d'hydrogène d'environ 100 kg.

Le modèle du système a été testé avec des données réelles de la vitesse d'un courant marin. Les valeurs de vitesse du courant marin et leurs plages horaires représentent les mesures réelles du Raz Blanchard. Les intervalles de temps modélisés sont plus petits que la plage en temps réel (un demi-cycle du profil de vitesse du courant marin dans le site sélectionné dure environ 6 heures). La mesure du 15 septembre 2005 est choisie pour effectuer les simulations car c'est le jour de la marée la plus haute au cours de l'année. La vitesse de rotation de la GSAP suit la vitesse du courant marin en dessous la valeur nominale alors que la relation est modifiée au-dessus de la vitesse de base pour limiter la puissance à sa valeur nominale. Le mode de contrôle MPPT est efficace car le coefficient de puissance est maintenu à sa valeur maximale de 0,45 lorsque la vitesse est inférieure à la valeur nominale. Le coefficient de

puissance de la turbine diminue lorsque la vitesse augmente au-dessus de la vitesse nominale (3,2 m/s). Cette réduction permet de maintenir la puissance à sa valeur nominale de 1,52 MW grâce au mode de limitation de puissance..

Le FCS (Flux Control System) limite bien le courant et la tension de la GSAP à leurs valeurs nominales lorsqu'elle dépasse la vitesse nominale pour protéger la génératrice. La commande du convertisseur côté charge fournit bien une tension alternative de valeur efficace constante aux bornes de la charge alors que le courant change avec le profil de charge pendant la journée.

#### **4. Système de gestion de l'énergie décentralisée multi-agents basé sur JADE**

La migration vers une topologie de gestion décentralisée basée sur le MAS (Multi-Agent System) nécessite l'interfaçage du modèle MATLAB / Simulink avec la plate-forme MAS. Le MAS est un paradigme du système décentralisé utilisé pour la gestion de l'énergie et le contrôle du système de production d'énergie hybride marine-hydrogène actif. Le système marin-hydrogène a une nature hétérogène comprenant l'électromécanique (turbine marémotrice, générateur), l'électrochimie (électrolyseur, pile à combustible, et la batterie Li-FePO<sub>4</sub>) et les systèmes électriques (convertisseurs électroniques de puissance). De nombreux paramètres doivent être pris en compte pour la gestion du système. De plus, le système fonctionne en mode autonome (pour alimenter les charges résidentielles d'une île). Par conséquent, le système de gestion doit avoir la capacité de traiter chaque système de façon indépendante et fiable. Ainsi, le MAS décentralisé est sélectionné pour effectuer le contrôle et la gestion du système dans les différentes conditions de fonctionnement et différents scénarios. Il n'y a pas de définition claire de l'agent alors mais la définition de Wooldridge est la plus acceptée. En raison de cette définition, l'agent est une entité de logiciel ou de matériel (ou les deux) qui peut réagir de manière autonome aux changements d'environnement avec des caractéristiques définies:

- Réactivité,
- Pro-activité,
- « Capacité sociale »,

En conséquence, le système multi-agent consiste en plusieurs agents travaillant ensemble en harmonie et en synchronisation pour accomplir la tâche principale. Il existe de nombreuses plates-formes ou même le MATLAB lui-même peut être utilisé pour développer le MAS. La

question la plus importante est la sélection de la plate-forme à utiliser pour développer le MAS. De nombreuses études ont présenté les différents critères d'évaluation des plateformes MAS pour faciliter la sélection d'une plate-forme pour une application spécifique. Il est possible d'utiliser une plate-forme de modélisation de systèmes (par exemple, MATLAB) pour développer le MAS mais cela nécessiterait beaucoup de temps pour adapter le paradigme développé aux normes FIPA et suivre les critères d'évaluation. Sinon, l'une des plates-formes MAS directement applicables peut être utilisée. La plate-forme JADE est sélectionnée pour appliquer la gestion décentralisée de l'énergie du système hybride marin-hydrogène. Cette plate-forme a beaucoup d'avantages : un logiciel open-source basé sur Java, une application polyvalente, plus largement appliqué dans de nombreuses applications et la caractéristique la plus importante est la conformité avec les standards FIPA. JADE est une plate-forme entièrement distribuée composée d'entités autonomes appelées les agents. L'agent réside dans un conteneur qui fournit l'exécution JADE et les services d'hébergement et d'exécution des agents en tant que processus Java. Un seul conteneur, appelé conteneur principal, est créé automatiquement en lançant le logiciel. Nous avons construit un modèle MATLAB / Simulink de la couche de composants (système actif de génération de puissance hybride marine-hydrogène avec une simple stratégie d'équilibre énergétique (incluse dans le modèle Simulink) en tant que système de gestion centralisé. La migration vers une topologie de gestion décentralisée basée sur le MAS nécessite l'interfaçage du modèle MATLAB / Simulink avec la plate-forme MAS. Comme mentionné précédemment, la plate-forme JADE multithreading basée sur Java est sélectionnée pour développer le système de gestion d'énergie MAS décentralisé. L'interface entre MATLAB / Simulink et JADE nécessite un travail autour pour ajouter les options d'agent dans Simulink. Le bloc fonction-S du Simulink est le meilleur candidat pour cette mission en raison de la possibilité dans n'importe quel langage (principalement C ++ ou Java) et de l'encapsuler comme un bloc Simulink. L'obstacle de ce scénario est l'instabilité de la fonction S du traitement d'un programme multithreading, qui est un principe fondamental en Java. Il existe un programme spécial qui permet de surmonter cet obstacle (interface MATLAB / Simulink-JADE) appelé MACSim (Contrôle multi-agent pour Simulink). Le MACSim dépend principalement de l'architecture Serveur-Client où le client est la fonction MATLAB / Simulink S fonction et le serveur est le programme Multi-threading (JADE). Généralement, le MACSimJX est un programme de licence libre.

Les paragraphes suivants décrivent la nouveauté du travail de développement du système MAS de gestion de l'énergie basé sur JADE du système hybride marin-hydrogène en mode

autonome et connecté au réseau à l'aide du MACSimJX. L'objectif principal du système de gestion de l'énergie décentralisé proposé est l'équilibrage de l'énergie entre la génération et la consommation de la charge. Le principal avantage du MAS basé sur JADE par rapport à la topologie centralisée est la redondance. Chaque agent est responsable de la gestion et du contrôle de son sous-système et de la communication d'égal à égal avec l'agent voisin pour la négociation basée sur le paradigme de l'agent JADE. Le système MAS est proposé pour gérer le bilan énergétique de la topologie du système autonome afin d'étudier la capacité décentralisée du système de gestion de l'énergie par rapport à celle centralisée. Par conséquent, le client MACSimJX (fonction S) transmet le courant marin généré et les puissances côté demande (charge). De plus, il est important de considérer l'état de charge de la batterie et du réservoir de stockage d'hydrogène comme les principaux paramètres du système de gestion de l'énergie. Les limites de l'état de charge de la batterie représentent le fonctionnement sûr et sain. Le système de gestion d'énergie proposé du mode autonome ne considère pas l'état de charge du réservoir d'hydrogène pour évaluer la performance du système. L'évaluation des performances représente l'estimation de l'hydrogène produit avec les profils des courants marins et de demande. Les différents agents du MAS sont programmés pour réaliser une gestion d'énergie en mode isolé. L'une des modifications les plus importantes est que la procédure décentralisée proposée considère la gestion de la demande sur la base de deux stratégies: le délestage et le déplacement de la charge. Le MAS proposé se compose de cinq agents principaux qui fournissent au système de contrôle de bas niveau du modèle SIMULINK les valeurs de référence à suivre. Le système de gestion de l'énergie décentralisé proposé a été testé et validé. Lorsque la puissance produite par le courant marin est supérieure à la demande de la charge; l'électrolyseur est activé en convertissant l'énergie excédentaire en hydrogène stocké dans le réservoir. Sinon, la pile à combustible est activée pour compenser le manque de puissance. La batterie est contrôlée pour couvrir dynamique rapide des variations de puissance pour la protection de la pile à combustible et de l'électrolyseur.

Généralement, le système de gestion de l'énergie MAS sous JADE est efficace pour équilibrer l'énergie entre la production et la consommation dans les différentes conditions de fonctionnement. Quand l'hydrogène stocké n'est pas suffisant, le MAS fait passer le système du mode isolé en mode connecté au réseau. Lorsque l'état de charge du réservoir de stockage atteint la limite minimale, le PCC (Point of Common Coupling) est commuté pour intégrer le réseau dans le système, et la pile à combustible est désactivée. Le système de gestion

d'énergie MAS du mode connecté au réseau est constitué des mêmes agents que le système isolé remplissant les mêmes fonctions avec l'ajout d'un autre agent pour le réseau. L'agent du réseau échange des messages avec le réservoir de stockage d'hydrogène pour commander le PCC sur la base de l'état de charge réservoir de stockage. L'agent de pile à combustible échange les messages avec l'agent du réservoir de stockage d'hydrogène pour contrôler sa connexion en fonction de son état de charge. Le MAS conçu gère efficacement l'énergie entre les différents composants du système avec plus de flexibilité. L'efficacité du système signifie la capacité de maintenir l'équilibre sous les variations du courant marin et de la demande en contrôlant les conditions de fonctionnement de la pile à combustible, de l'électrolyseur, de la batterie et du réseau. En raison des conditions de fonctionnement, l'architecture et la topologie du système doivent être modifiées de manière flexible pour la connexion/déconnexion de différents composants. En d'autres termes, l'évolutivité du système est l'une des caractéristiques les plus importantes du système décentralisé MAS.

### **Conclusions et perspectives**

Dans cette thèse, nous avons présenté l'état de l'art des différents axes de recherche dans le smart grid. Le système actif hybride de génération de puissance marine-hydrogène a été modélisé. Le système intègre un électrolyseur PEM à l'échelle du mégawatt et un système de pile à combustible en tant que composants principaux du bilan énergétique.

La batterie LiFePO<sub>4</sub> est utilisée pour couvrir la dynamique rapide de l'énergie électrique. En outre, la thèse analyse le système de gestion de l'énergie centralisé et décentralisé. Le MAS représente le paradigme du système décentralisé. La plate-forme JADE est utilisée pour développer le MAS en raison de son domaine d'application général, des logiciels open source et de licences libres, de l'interface avec MATLAB et de la compatibilité avec les standards FIPA. Le système de gestion d'énergie basé sur JADE équilibre l'énergie entre la génération (système de conversion d'énergie marine-courant) et la demande (profil de charge résidentielle) pendant les modes de fonctionnement autonome et connecté au réseau. Les nouveautés apportées par ce travail est représentée dans les points suivants :

- Le développement de la REM du système actif de génération de puissance électrique maritime qui, à notre connaissance, n'a pas encore été formalisé. La REM du système marin facilite la compréhension des interactions entre les différents sous-systèmes. De plus, il rend le modèle du système plus lisible pour s'intégrer

facilement dans tout travail futur. Enfin, il permet la conception des stratégies de contrôle efficaces dans les différents modes de fonctionnement du système.

- L'analyse et le développement de la stratégie de contrôle de flux pour la minimisation des pertes du GSAP directement entraîné par l'hydrolienne. La stratégie est basée sur l'injection d'un courant dans les enroulements de la machine basée sur le contrôle vectoriel pour réduire les pertes fer de la machine et généralement les pertes totales. La stratégie proposée a été appliquée à un système de turbine à courant marin d'une puissance nominale de 1.5 MW afin d'évaluer les économies d'énergie annuelles. Les résultats indiquent que les économies d'énergie fournies sont suffisantes pour alimenter une charge résidentielle supplémentaire avec une consommation moyenne de 4 000 kWh. D'un autre point de vue, l'économie d'énergie est suffisante pour générer environ 100 kg d'hydrogène à partir du système d'électrolyseur basé sur la valeur de chauffage la plus élevée sans tenir compte du rendement du système d'électrolyseur. Si le système d'électrolyseur est considéré dans la plage de 40% à 50% de rendement, l'économie d'énergie peut fournir une production excédentaire de 40 à 50 kg par an.
- Le développement du modèle du système d'électrolyseur PEM à l'échelle mégawatt qui, à notre connaissance, n'a pas été présenté auparavant. Un modèle d'électrolyseur à petite échelle, avec l'aide de la REM, a été utilisé et adapté pour représenter le système à l'échelle mégawatt. A rétro-ingénierie a été utilisée pour en estimer les principaux paramètres pour fournir des caractéristiques et les indicateurs clés de la performance du système d'échelle mégawatt.
- Le développement du MAS basé sur JADE pour la gestion de l'énergie du système actif de production d'énergie hybride marine-hydrogène. Le modèle du système a été construit dans MATLAB / Simulink avec l'aide de la REM globale du système. Le programme MACSimJX (Contrôle multi-agent pour l'extension Java Simulink) a été utilisé pour interfacer le modèle Simulink avec la plate-forme JADE. Le système de gestion d'énergie MAS basé sur JADE se compose de nombreux agents qui exécutent des fonctions définies et travaillent ensemble en harmonie sur la base d'une communication pair-à-pair. Chaque système physique (électrolyseur, pile à combustible, batterie et côté demande) dispose d'un agent qui gère son fonctionnement grâce à ses limites et recommandations pour avoir un fonctionnement sûr. Les différents codes source des agents Java ont été programmés. L'efficacité du système MAS basé sur JADE a été évaluée en mode



autonome et en mode connecté au réseau. Les résultats indiquent que le système de gestion de l'énergie proposé sur JADE est puissant, évolutif et redondant dans les différentes conditions d'exploitation. De plus, le système offre l'option de la surveillance et le suivi en ligne du système marin-hydrogène qui permet à l'exploitant de prendre des décisions.

- L'ensemble du système intégrant le système actif de génération de puissance hybride marine-hydrogène avec le système de gestion d'énergie MAS basé sur JADE représente une nouvelle étude de cas du SGAM (Smart Grid Architecture Model). L'étude a modélisé et représenté chaque couche du SGAM. Premièrement, la couche de composants avec l'objectif d'intégration des énergies renouvelables a été représentée par le système marin-hydrogène. Ensuite, le MACSimJX modélise les couches de communication et de données en interfaçant le modèle MATLAB / Simulink du système marin-hydrogène avec le MAS basé sur JADE. Enfin, le système de gestion de l'énergie basé sur JADE qui représente la fonction et les couches de gestion. Généralement, le système proposé présente un modèle SGAM qui peut être utilisé pour l'analyse détaillée des directions de recherche du smart grid.

Deux directions peuvent étendre ce travail à l'avenir en considérant la modélisation et la validation expérimentale comme illustré dans les points suivants:

- Le système de conversion d'énergie du courant marin proposé peut être modifié et adapté pour modéliser une ferme d'hydroliennes complète. La modification représente la méthode d'agrégation des turbines et des machines pour modéliser l'ensemble de la ferme..
- Le système de gestion d'énergie SMA basé sur JADE peut être étendu pour inclure l'optimisation de l'économie du marché de l'énergie. Le modèle de gestion proposé considère uniquement l'équilibre énergétique entre la production et la consommation comme objectif principal. De plus, le système MAS à base de JADE peut intégrer le VE (Electric Vehicle) en considérant ses modes de fonctionnement V2G (Véhicule to Grid) et G2V (Grid to Vehicle). L'agent (du fait du paradigme JADE) est une entité dynamique qui peut apparaître et disparaître de manière flexible, plus compatible avec le VE.
- L'adaptation du modèle de l'électrolyseur PEM à l'échelle du mégawatt peut être plus analysée sur la base de la même procédure que pour le modèle à petite échelle.

- Le système de gestion d'énergie décentralisée basé sur JADE peut être évalué expérimentalement en développant un banc d'essai qui émule les performances des composants physiques (système marin, électrolyseur, pile à combustible et batterie) en plus de leurs convertisseurs électroniques de puissance. La base JADE peut être programmée pour exécuter les stratégies de gestion d'énergie requises. L'interface entre la plate-forme JADE et les composants physiques dépend de deux étapes. La première est l'interface MACSimJX qui échange les signaux entre JADE et MATLAB / Simulink. La deuxième étape est l'interface entre les composants physiques et MATLAB qui peut être effectuée par de nombreuses procédures. L'une des procédures repose sur l'utilisation des cartes dSPACE qui interagissent directement avec les composants physiques par les cartes de traitement de signal et qui sont en interface avec MATLAB / Simulink par l'une des bibliothèques logicielles (par exemple, mLib et mTrace). Le banc d'essai représentera l'étude de cas pilote pour la conception expérimentale, l'expérimentation et l'étude des axes de recherche actuelles et futures du smart grid.



**Appendix A**  
**Active Marine-Hydrogen Hybrid Power Generation**  
**System Model Parameters**



Parameter	Value
<b>Marine Current Power Generation System Model</b>	
Turbine Blade Radius	8 m
System Total Inertia	$1.3131 \times 10^6$ kg.m <sup>2</sup>
Generator Rated Power	1.52 MW
Rated Marine Current Speed	3.2 m/s
Generator Nominal Phase Voltage	649 V (RMS)
Generator Nominal Phase Current	928 A (RMS)
DC Bus Voltage	1500 V
Rated Rotational Speed	24 rpm
Pole Pair Number	125
Permanent Magnet Flux	2.458 Wb
Generator Stator Resistance	0.0081 $\Omega$
Generator Inductance (d-q axis)	1.2 mH
DC Link Capacitance	13 mF
DC Link resistance	0.2 m $\Omega$
Load – Side Resistance (including filter and transformer)	0.1 m $\Omega$
Load – Side Inductance (including filter and transformer)	1.5 mH
Load Frequency	50 Hz
Load Phase - Phase Voltage	690 V (RMS)
<b>MW Scale PEM Electrolyzer System Model (Proton Onsite Stack)</b>	
Number of Stacks	6
Power per Stack	250 kW
Number of Cells per Stack	100
MEA Active Area	650 cm <sup>2</sup>
Current Density	1.9231 A/cm <sup>2</sup>
Anode Exchange Current Density	$8 \times 0.1548 \times 10^{-2}$ A/cm <sup>2</sup>
Cathode Exchange Current Density	$8 \times 0.3539 \times 10^{-1}$ A/cm <sup>2</sup>
Membrane Conductivity	$8 \times 0.9322 \times 10^{-2}$ S/cm
Anode Charge Transfer Coefficient	0.7178
Cathode Charge Transfer Coefficient	0.6395
Output Pressure	30 bar
Hydrogen Production Rate	50 Nm <sup>3</sup> /hr.
Reactant Water Consumption Rate	45 L/hr.
<b>MW Scale PEM Fuel Cell System Model</b>	
Number of stacks	6
Rated Power per Stack	250 kW
Number of Cells per Stack	1050
Active Area	1200 cm <sup>2</sup>

Current Density	0.8 A/cm <sup>2</sup>
Concentration and Activation Voltages Coefficients (A,B)	6*10 <sup>-5</sup> , -1.5*10 <sup>-4</sup> K/V respectively
Nernst Voltage Coefficients (A <sub>cd</sub> , B <sub>cd</sub> )	300*10 <sup>-4</sup> , 57*10 <sup>-5</sup> K/V respectively
Reversible Voltage Coefficients (α, β, γ, δ, ν)	1.4629, -4.5*10 <sup>-4</sup> , 1.0285*10 <sup>-8</sup> , 9.519*10 <sup>-13</sup> , -5.989*10 <sup>-5</sup> respectively
Cell Ohmic Resistance	150 mΩ
Cell Impedance Electrode Resistance	150 mΩ
Double Layer Capacitance	20 mF
Exchange Current	0.03 mA
Current Limit	1 A
Internal Current	3 mA
Standard Pressure	0.1*10 <sup>6</sup> Pa
Hydrogen Pressure	0.1*10 <sup>6</sup> Pa
Oxygen Pressure	0.21*10 <sup>6</sup> Pa
Fuel Cell Temperature	50° C
<b>LiFePO4 Battery System Model</b>	
Cell Voltage	3.2 V
Rated Capacity	195 Ah
Number of Parallel Strings	3
Number of Series Cells per String	168
Cell Internal Resistance	0.005 Ω
Transient Resistance	0.0052 Ω
Transient Capacitance	1000/R <sub>T</sub> F
Full Charge Zone Voltage	3.308 V
Exponential Zone Voltage	3.251 V
Nominal Zone Voltage	3.122 V
Full Capacity	118.8 Ah
Exponential Zone Capacity	108.5 Ah
Nominal Zone Capacity	37 Ah
A	0.057 V
B	0.1825 Ah <sup>-1</sup>
K	0.03 V
E <sub>o</sub>	3.332 V

**Appendix B**  
**Source Codes of the Hybrid Marine-Hydrogen JADE**  
**Based MAS Management System**





### **/\*\* Battery Agent**

\* <p>Title: Example to manage the Hybrid MCT-Hydrogen System Energy Balance from Simulink via JADE agents.</p>

\* \* <p>Description: This JADE agent is used to demonstrate how one can be set up in order  
\* to receive data from Simulink via the Agent Environment(that is the Agent Coordinator  
\* and AgentServer). It also shows the exchange of data between agents and then how  
\* the data is finally returned back to Simulink.</p>\*/

```
package Testnew;
import macsimjx.*;
import jade.lang.acl.ACLMessage;
import jade.domain.FIPAEException;
import jade.domain.DFService;
import jade.core.behaviours.CyclicBehaviour;
import jade.core.Agent;
import jade.core.AID;
public class Bat1 extends UsefulAgentMethods {
    Agent thisAgent = (Agent)this;
    int agentNumber = 0;
    /** These determine which elements of the input data that this agent
     * is interested in, and which element of the outgoing data it is changing.*/
    int[] inputPortsOfInterest = { 1 }; // I.e. top signal input to MACSim block.
    int[] outputPorts = { 2 }; // Set which ports in simulink data is shown on.
    // Set to true for helpful output.
    boolean debug = false;
    // Keep track of number of information agents.
    private int agentsSubscribed = 0;
    private int agentsLeftToRespond = 0;
    boolean firstRun = true;
    boolean dataUpdated = false;
    AID[] agentIDs = null;
    AID agentID = null;
    AID AgentCoordinatorID = null;
    TimeStepData tsd = new TimeStepData();
    double SOC = 0;
    double Out = 0;
    public void setup() {
        addBehaviour(new filterBehaviour());
        /** Register agent with directory facilitator of JADE along with the
         * services it provides (in this case, ELBatt and generic agent services).
         * NB - To change properties after registering use the JADE 'modify' method. */
```

```

String[] services = {"ELBatt", "Agent"};
registerAgent(thisAgent, services, services);
// Get agent number from argument provided by instantiator of this agent.
Object[] args = getArguments();
if (args != null && args.length > 0) {
    String firstArg = args[0].toString();
    agentNumber = new Integer(firstArg).intValue();
} else {
    // Terminate agent.
    System.out.println("No agent id");
    doDelete(); }
try {
    // Locate data provider.
    AgentCoordinatorID = getAgentIDsOfService(thisAgent,
        "InputsUpdate")[0];
    // Find agents that are interested in this agent's data.
    agentIDs = getAgentIDsOfService(thisAgent, "ELBatt");
    /* * N.B. If environment is dynamic would need to perform these
    * searches either more than once to check for new agents, or
    * implement some service subscription method to receive a message
    * when new agents enter environment.*/
} catch (Exception e) {
    System.out.println("Error finding service: " + e); }
agentsSubscribed = countSubscribingAgents(thisAgent, "ELBatt");
if (debug)
    System.out.println("agentsSubscribed to ELBatt service:"
        + agentsSubscribed);
agentsLeftToRespond = agentsSubscribed - 1; }
class filterBehaviour extends CyclicBehaviour {
    public void action() {
        TimeStepData tsd = new TimeStepData();
        double[] dataArray;
        int length;
        ACLMessage msg = receive();
        if (msg != null) {
            String message = msg.getConversationId();
            // If new data from AgentCoordinator (ie Simulink).
            if (message.equals("UpdateData")) {
                try {
                    tsd = (TimeStepData) msg.getContentObject();

```

```

    } catch (Exception e) {
        System.out.println("Exception with content object" + e);}
// Extract data from incoming array.
length = tsd.getData().length;
dataArray = new double[length];
for (int i = 0; i < length; i++)
    dataArray[i] = tsd.getData()[i];
if (debug) {
    System.out.println("(Debug)Incoming data: ");
    for (int j = 0; j < length; j++) {
        System.out.print(j + ": " + dataArray[j] + " ");
    }
    System.out.printf("\n");}
/** Agent particular aspects begin here. *****/
// Extract the relevant data.
SOC = dataArray[inputPortsOfInterest[0]];
/* Perform here any calculations required before using data from
   * other agents. In this case no calculations as it is a DC Link Voltage Control.*/
/** Block ends here *****/
if (debug) {
    System.out.println(getLocalName() +
        " awaiting info from "
        + agentsLeftToRespond + " agent(s)");}
dataUpdated = true;
/** Pass information about the new data to the other agents.*/
if (agentsSubscribed > 1) {
    try {
/** Set information in dataStructure to be passed to other agents *****/
        double [] dataToShare = {SOC};
        int [] elementToChange={0};
        TimeStepData tsdInner= new TimeStepData();
        // Populate data structure with required data to exchange.
        tsdInner.setData(dataToShare);
        tsdInner.setElementsToChange(elementToChange);
        // Send information off to other agents.
        for (int i = 0; i < agentIDs.length; i++) {
            if (!agentIDs[i].getLocalName().equals(
                thisAgent.getLocalName())) {
                sendObject(agentIDs[i], "agentData",
                    tsdInner);} }

```

```

/** Block ends here *****/
    } catch (Exception e) {
        System.out.println("Exception: " + e); }}
    if (agentsLeftToRespond == 0) {
        finishCalculationsThenSend();}}
// Additional information from another agent.
if (message.equals("agentData")
    && !msg.getSender().getLocalName().equals(
        thisAgent.getLocalName())) {
    try {
        tsd = (TimeStepData) msg.getContentObject();
    } catch (Exception e) {
        System.out.println("Exception getting content object: "
            + e); }
        length = tsd.getData().length;
        dataArray = new double[length];
        for (int i = 0; i < length; i++)
            dataArray[i] = tsd.getData()[i];
/** Agent specific task inside this block *****/
        int [] elementsToUse = tsd.getElementsToChange();
        double Pdiff = dataArray[elementsToUse[0]];
        // Perform calculations with data from other agents.
        //In this case no calculations as it is a DC Link Voltage Control.
        Out = Pdiff;
/** Block ends here *****/
        agentsLeftToRespond--;
        if (debug)
            System.out.println(getLocalName() + " recieved info "
                + " awaiting "
                + agentsLeftToRespond + " more.");

        if (agentsLeftToRespond == 0 && dataUpdated) {
            finishCalculationsThenSend();}}
        if (message.equals("DataAmended")) {
            if (debug)
                System.out.println("Agent " + agentNumber + " finished.");
            replyToAgent(msg.getSender(), "ProcessingComplete");}
        if (message.equals("Shutting Down")) {
            takeDown(msg.getSender());}
    } else {

```

```

        block();}}}}
    /** Finalise calculations and return to AgentCoordinator and Simulink. */
    public void finishCalculationsThenSend() {
    /** Agent specific task inside this block *****/
        // Carry out any final calculation before returning back to Simulink and
        // specified port.
        double[] dataOut = new double[outputPorts.length];
        dataOut[0] = Out;
    /** Block ends here *****/
        tsd.setData(dataOut);
        tsd.setElementsToChange(outputPorts);
        // Send modified data back to Simulink.
        ACLMessage reply = new ACLMessage(ACLMessage.INFORM);
        reply.setConversationId("ProcessedData");
        try {
            reply.setContentObject(tsd);
        } catch (Exception e) {
            System.out.println("Exception setting tsd: " + e);}
        if (debug)
            System.out.println(getLocalName() + " finished, sending data to "
                               + AgentCoordinatorID.getLocalName());
        reply.addReceiver(AgentCoordinatorID);
        send(reply);
        agentsLeftToRespond = agentsSubscribed - 1;
        dataUpdated = false;}
    /** Terminate agent. * @param senderAID AID*/
    protected void takeDown(AID senderAID) {
        try {
            System.out.println("Deregistering and closing " + thisAgent);
            DFService.deregister(thisAgent);
        } catch (FIPAException fe) {
            System.out.println("Problem deregistering " + fe);}
        if (senderAID != null)
            contactAgent(senderAID, "Agent Deregistered");
        doDelete();}}

```

#### **/\*\* Demand Side Management Agent**

\* <p>Title: Example to manage the Hybrid MCT-Hydrogen System Energy Balance from Simulink via JADE agents.</p>

\* <p>Description: This JADE agent is used to demonstrate how one can be set up in order

\* to receive data from Simulink via the Agent Environment(that is the Agent Coordinator

\* and AgentServer). It also shows the exchange of data between agents and then how  
 \* the data is finally returned back to Simulink.</p>\*/

```
package Testnew;
import macsimjx.*;
import jade.lang.acl.ACLMessage;
import jade.domain.FIPAAException;
import jade.domain.DFService;
import jade.core.behaviours.CyclicBehaviour;
import jade.core.Agent;
import jade.core.AID;
public class dsm extends UsefulAgentMethods {
    Agent thisAgent = (Agent) this;
    int agentNumber = 0;
    /** These determine which elements of the input data that this agent
    *is interested in, and which element of the out going data it is changing.*/
    int[] inputPortsOfInterest = {0}; // I.e. Second to top signal input to MACSim block.
    int[] outputPorts = {4}; // Set which ports in simulink data is shown on.
    // Set to true for helpful output.
    boolean debug = false;
    // Keep track of number of information agents.
    private int agentsSubscribed = 0;
    private int agentsLeftToRespond = 0;
    boolean firstRun = true;
    boolean dataUpdated = false;
    AID[] agentIDs = null;
    AID agentID = null;
    AID AgentCoordinatorID = null;
    TimeStepData tsd = new TimeStepData();
    double Pdiff = 0;
        double PdiffL;
        double Pdsm;
    public void setup() {
        addBehaviour(new filterBehaviour());
        /** Register agent with directory facilitator of JADE along with the services it provides (in this case,
DSMBatt and generic agent services).
NB - To change properties after registering using the JADE 'modify' method. */
        String[] services = {"DSMBatt", "Agent"};
        registerAgent(thisAgent, services, services);
        // Get agent number from argument provided by instantiator of this agent.
        Object[] args = getArguments();
```

```

if (args != null && args.length > 0) {
    String firstArg = args[0].toString();
    agentNumber = new Integer(firstArg).intValue();
} else {
    // Terminate agent.
    System.out.println("No agent id");
    doDelete();}
try {
    // Locate data provider.
    AgentCoordinatorID = getAgentIDsOfService(thisAgent,
        "InputsUpdate")[0];
    // Find agents that are interested in this agent's data.
    agentIDs = getAgentIDsOfService(thisAgent, "DSMBatt");
    /** N.B. If environment is dynamic would need to perform these searches either more than once to check
        for new agents, or implement some service subscription method to receive a message when new agents
        enter environmen */
} catch (Exception e) {
    System.out.println("Error finding service: " + e); }
    agentsSubscribed = countSubscribingAgents(thisAgent, "DSMBatt");
if (debug)
    System.out.println("agentsSubscribed to DSMBatt service:"
        + agentsSubscribed);
    agentsLeftToRespond = agentsSubscribed - 1;}
class filterBehaviour extends CyclicBehaviour {
    public void action() {
        TimeStepData tsd = new TimeStepData();
        double[] dataArray;
        int length;
        ACLMessage msg = receive();
        if (msg != null) {
            String message = msg.getConversationId();
            // If new data from AgentCoordinator (ie Simulink).
            if (message.equals("UpdateData")) {
                try {
                    tsd = (TimeStepData) msg.getContentObject();
                } catch (Exception e) {
                    System.out.println("Exception with content object" + e);}
                // Extract data from incoming array.
                length = tsd.getData().length;
                dataArray = new double[length];

```



```

for (int i = 0; i < length; i++)
    dataArray[i] = tsd.getData()[i];
if (debug) {
    System.out.println("(Debug)Incoming data: ");
    for (int j = 0; j < length; j++) {
        System.out.print(j + ": " + dataArray[j] + " ");
    }
    System.out.printf("\n");
}
/** Agent particular aspects begin here. *****/
// Extract the relevant data.
Pdiff = dataArray[inputPortsOfInterest[0]];
/* Perform here any calculations required before using data from
 * other agents. (Low pass filter to avoid feeding electrolyzer with high dynamics) */
int a = 755; /* Low pass filter constant-sample time 0.01 sec and cut off frequency 7 Hz */
PdiffL += (Pdiff - PdiffL) / a;

/** Block ends here *****/
if (debug) {
    System.out.println(getLocalName() +
        " awaiting info from "
        + agentsLeftToRespond + " agent(s)");
}
dataUpdated = true;
/** Pass information about the new data to the other agents. */
if (agentsSubscribed > 1) {
    try {
        /** Set information in dataStructure to be passed to other agents *****/
        double [] dataToShare = {PdiffL};
        int [] elementToChange = {0};
        TimeStepData tsdInner= new TimeStepData();
        // Populate data structure with required data to exchange.
        tsdInner.setData(dataToShare);
        tsdInner.setElementsToChange(elementToChange);
        // Send information off to other agents.
        for (int i = 0; i < agentIDs.length; i++) {
            if (!agentIDs[i].getLocalName().equals(
                thisAgent.getLocalName())) {
                sendObject(agentIDs[i], "agentData", tsdInner);
            }
        }
        /** Block ends here *****/
    } catch (Exception e) {
        System.out.println("Exception: " + e);
    }
}
if (agentsLeftToRespond == 0) {
    finishCalculationsThenSend();
}

```

```

// Additional information from another agent.
if (message.equals("agentData"))
    && !msg.getSender().getLocalName().equals(
        thisAgent.getLocalName())) {
    try {
        tsd = (TimeStepData) msg.getContentObject();
    } catch (Exception e) {
        System.out.println("Exception getting content object: " + e); }
    length = tsd.getData().length;
    dataArray = new double[length];
    for (int i = 0; i < length; i++)
        dataArray[i] = tsd.getData()[i];
    /** Agent specific task inside this block *****/
    int [] elementsToUse = tsd.getElementsToChange();
    double SOC = dataArray[elementsToUse[0]];
    // Perform calculations with data from other agents.
    //In this case and due to power state (Surplus or Scarcity) AND the battery SOC, the fuel cell power
    setting is estimated.
    if (Pdiff > 0 && SOC >= 0.9){
        Pdsm = Pdiff - PdiffL; }
    else if (Pdiff < 0 && SOC <= 0.4){
        Pdsm = Pdiff - PdiffL; }
    else{
        Pdsm = 0; }
    /** Block ends here *****/
    agentsLeftToRespond--;
    if (debug)
        System.out.println(getLocalName() + " recieved info "
            + " awaiting "
            + agentsLeftToRespond + " more.");
    if (agentsLeftToRespond == 0 && dataUpdated) {
        finishCalculationsThenSend();}
    if (message.equals("DataAmended")) {
        if (debug)
            System.out.println("Agent " + agentNumber + " finished.");
        replyToAgent(msg.getSender(), "ProcessingComplete"); }
    if (message.equals("Shutting Down")) {
        takeDown(msg.getSender());}
    else {
        block();}}

```

```

/** Finalise calculations and return to AgentCoordinator and Simulink. */
public void finishCalculationsThenSend() {
/** Agent specific task inside this block *****/
    // Carry out any final calculation before returning back to Simulink and
    // specified port.
    double[] dataOut = new double[outputPorts.length];
    dataOut[0] = Pdsm;
/** Block ends here *****/
    tsd.setData(dataOut);
    tsd.setElementsToChange(outputPorts);
    // Send modified data back to Simulink.
    ACLMessage reply = new ACLMessage(ACLMessage.INFORM);
    reply.setConversationId("ProcessedData");
    try {
        reply.setContentObject(tsd);
    } catch (Exception e) {
        System.out.println("Exception setting tsd: " + e);
    }
    if (debug)
        System.out.println(getLocalName() + " finished, sending data to "
            + AgentCoordinatorID.getLocalName());
    reply.addReceiver(AgentCoordinatorID);
    send(reply);
    agentsLeftToRespond = agentsSubscribed - 1;
    dataUpdated = false;
}
/** Terminate agent. @param senderAID AID */
protected void takeDown(AID senderAID) {
    try {
        System.out.println("Deregistering and closing " + thisAgent);
        DFService.deregister(thisAgent);
    } catch (FIPAException fe) {
        System.out.println("Problem deregistering " + fe);
    }
    if (senderAID != null)
        contactAgent(senderAID, "Agent Deregistered");
    doDelete();}
}

```

### **Electrolyzer Agent**

\* <p>Title: Example to manage the Hybrid MCT-Hydrogen System Energy Balance from Simulink via JADE agents.</p>

\* <p>Description: This JADE agent is used to demonstrate how one can be set up in order

\* to receive data from Simulink via the Agent Environment(that is the Agent Coordinator

\* and AgentServer). It also shows the exchange of data between agents and then how

```

    * the data is finally returned back to Simulink.</p>*/
package Testnew;
import macsimjx.*;
import jade.lang.acl.ACLMessage;
import jade.domain.FIPAEException;
import jade.domain.DFService;
import jade.core.behaviours.CyclicBehaviour;
import jade.core.Agent;
import jade.core.AID;
public class EL extends UsefulAgentMethods {
    Agent thisAgent = (Agent)this;
    int agentNumber = 0;
    /** these determine which elements of the input data that this agent is interested in, and which element of the
        outgoing data it is changing. Which are the power difference between generation and consumption as an
        input and the Electrolyzer setting power as an output*/
    int[] inputPortsOfInterest = {0}; // I.e. top signal input to MACSim block.
    int[] outputPorts = {0}; // Set which ports in simulink data is shown on.
    // Set to true for helpful output.
    boolean debug = false;
    // Keep track of number of information agents.
    private int agentsSubscribed = 0;
    private int agentsLeftToRespond = 0;
    boolean firstRun = true;
    boolean dataUpdated = false;
    AID[] agentIDs = null;
    AID agentID = null;
    AID AgentCoordinatorID = null;
    TimeStepData tsd = new TimeStepData();
    double Pdiff = 0;
    double PdiffL;
        double PEL;
    public void setup() {
        addBehaviour(new filterBehaviour());
        /** Register agent with directory facilitator of JADE along with the
            * services it provides (in this case, ELBatt and generic agent services).
            * NB - To change properties after registering use the JADE 'modify' method. */
        String[] services = {"ELBatt", "Agent"};
        registerAgent(thisAgent, services, services);
        // Get agent number from argument provided by instantiator of this agent.
        Object[] args = getArguments();

```

```

if (args != null && args.length > 0) {
    String firstArg = args[0].toString();
    agentNumber = new Integer(firstArg).intValue();
} else {
    // Terminate agent.
    System.out.println("No agent id");
    doDelete();
}
try {
    // Locate data provider.
    AgentCoordinatorID = getAgentIDsOfService(thisAgent,
        "InputsUpdate")[0];
    // Find agents that are interested in this agent's data.
    agentIDs = getAgentIDsOfService(thisAgent, "ELBatt");
    /** N.B. If environment is dynamic would need to perform these searches either more than once to check
    for new agents, searches either more than once to check for new agents, or implement some service
    subscription method to receive a message when new agents enter environment. */
} catch (Exception e) {
    System.out.println("Error finding service: " + e);
}
agentsSubscribed = countSubscribingAgents(thisAgent, "ELBatt");
if (debug)
    System.out.println("agentsSubscribed to ELBatt service:"
        + agentsSubscribed);
    agentsLeftToRespond = agentsSubscribed - 1;
}
class filterBehaviour extends CyclicBehaviour {
    public void action() {
        TimeStepData tsd = new TimeStepData();
        double[] dataArray;
        int length;
        ACLMessage msg = receive();
        if (msg != null) {
            String message = msg.getConversationId();
            // If new data from AgentCoordinator (ie Simulink).
            if (message.equals("UpdateData")) {
                try {
                    tsd = (TimeStepData) msg.getContentObject();
                } catch (Exception e) {
                    System.out.println("Exception with content object" + e);
                }
                // Extract data from incoming array.
                length = tsd.getData().length;
                dataArray = new double[length];
            }
        }
    }
}

```

```

    for (int i = 0; i < length; i++)
        dataArray[i] = tsd.getData()[i];
    if (debug) {
        System.out.println("(Debug)Incoming data: ");
        for (int j = 0; j < length; j++) {
            System.out.print(j + ": " + dataArray[j] + " ");
            System.out.printf("\n");
        }
    }
    /** Agent particular aspects begin here. *****/
    // Extract the relevant data.
    Pdiff = dataArray[inputPortsOfInterest[0]];
    /* Perform here any calculations required before using data from other agents. (Low pass filter to avoid
    feeding electrolyzer with high dynamics) */
    int a = 755; /* Low pass filter constant-sample time 0.01 sec and cut off frequency 7 Hz */
    PdiffL += (Pdiff - PdiffL) / a;
    /** Block ends here *****/
    if (debug) {
        System.out.println(getLocalName() +
            " awaiting info from "
            + agentsLeftToRespond + " agent(s)");
    }
    dataUpdated = true;
    /** Pass information about the new data to the other agents. */
    if (agentsSubscribed > 1) {
        try {
            /** Set information in dataStructure to be passed to other agents *****/
            double [] dataToShare = {Pdiff};
            int [] elementToChange = {0};
            TimeStepData tsdInner= new TimeStepData();
            // Populate data structure with required data to exchange.
            tsdInner.setData(dataToShare);
            tsdInner.setElementsToChange(elementToChange);
            // Send information off to other agents.
            for (int i = 0; i < agentIDs.length; i++) {
                if (!agentIDs[i].getLocalName().equals(
                    thisAgent.getLocalName())) {
                    sendObject(agentIDs[i], "agentData", tsdInner);
                }
            }
            /** Block ends here *****/
        } catch (Exception e) {
            System.out.println("Exception: " + e);
        }
    }
    if (agentsLeftToRespond == 0) {
        finishCalculationsThenSend();
    }

```

```

// Additional information from another agent.
if (message.equals("agentData")
    && !msg.getSender().getLocalName().equals(
        thisAgent.getLocalName())) {
    try {
        tsd = (TimeStepData) msg.getContentObject();
    } catch (Exception e) {
        System.out.println("Exception getting content object: "
            + e); }
        length = tsd.getData().length;
        dataArray = new double[length];
        for (int i = 0; i < length; i++)
            dataArray[i] = tsd.getData()[i];
        /** Agent specific task inside this block *****/
        int [] elementsToUse = tsd.getElementsToChange();
        double SOC = dataArray[elementsToUse[0]];
        // Perform calculations with data from other agents.
        //In this case and due to power state ( Surplus or Scarcity) AND the battery SOC, the electrolyzer
power seting is estimated.
        if (Pdiff > 0){
                                PEL = PdiffL; }
                                else {
                                PEL = 0; }

        /** Block ends here *****/
        agentsLeftToRespond--;
        if (debug)
            System.out.println(getLocalName() + " recieved info "
                + " awaiting "
                + agentsLeftToRespond + " more.");
        if (agentsLeftToRespond == 0 && dataUpdated) {
            finishCalculationsThenSend();}
        if (message.equals("DataAmended")) {
            if (debug)
                System.out.println("Agent " + agentNumber + " finished.");
            replyToAgent(msg.getSender(), "ProcessingComplete");}
        if (message.equals("Shutting Down")) {
            takeDown(msg.getSender());}
    } else {
        block();} } }

/** Finalise calculations and return to AgentCoordinator and Simulink. */

```

```

public void finishCalculationsThenSend() {
/** Agent specific task inside this block *****/
    // Carry out any final calculation before returning back to Simulink and specified the port.
    double[] dataOut = new double[outputPorts.length];
    dataOut[0] = PEL;
/** Block ends here *****/
    tsd.setData(dataOut);
    tsd.setElementsToChange(outputPorts);
    // Send modified data back to Simulink.
    ACLMessage reply = new ACLMessage(ACLMessage.INFORM);
    reply.setConversationId("ProcessedData");
    try {
        reply.setContentObject(tsd);
    } catch (Exception e) {
        System.out.println("Exception setting tsd: " + e);
    }
    if (debug)
        System.out.println(getLocalName() + " finished, sending data to "
            + AgentCoordinatorID.getLocalName());
    reply.addReceiver(AgentCoordinatorID);
    send(reply);
    agentsLeftToRespond = agentsSubscribed - 1;
    dataUpdated = false;
}

/** Terminate agent. @param senderAID AID*/
protected void takeDown(AID senderAID) {
    try {
        System.out.println("Deregistering and closing " + thisAgent);
        DFService.deregister(thisAgent);
    } catch (FIPAException fe) {
        System.out.println("Problem deregistering " + fe);
    }
    if (senderAID != null)
        contactAgent(senderAID, "Agent Deregistered");
    doDelete();
}

/** Fuel Cell Agent
* <p>Title: Example to manage the Hybrid MCT-Hydrogen System Energy Balance from Simulink via JADE
agents.</p>
* <p>Description: This JADE agent is used to demonstrate how one can be set up in order
* to receive data from Simulink via the Agent Environment(that is the Agent Coordinator
* and AgentServer). It also shows the exchange of data between agents and then how
* the data is finally returned back to Simulink.</p>*/
package Testnew;

```



```

import macsimjx.*;
import jade.lang.acl.ACLMessage;
import jade.domain.FIPAException;
import jade.domain.DFService;
import jade.core.behaviours.CyclicBehaviour;
import jade.core.Agent;
import jade.core.AID;
public class FC extends UsefulAgentMethods {
    Agent thisAgent = (Agent)this;
    int agentNumber = 0;
    /** These determine which elements of the input data that this agent is interested in, and which element of the
        out going data it is changing. */
    int[] inputPortsOfInterest = {0}; // I.e. Second to top signal input to MACSim block.
    int[] outputPorts = {1}; // Set which ports in simulink data is shown on.
    // Set to true for helpful output.
    boolean debug = false;
    // Keep track of number of information agents.
    private int agentsSubscribed = 0;
    private int agentsLeftToRespond = 0;
    boolean firstRun = true;
    boolean dataUpdated = false;
    AID[] agentIDs = null;
    AID agentID = null;
    AID AgentCoordinatorID = null;
    TimeStepData tsd = new TimeStepData();
    double Pdiff = 0;
        double PdiffL;
        double PFC;
    public void setup() {
        addBehaviour(new filterBehaviour());
        /** Register agent with directory facilitator of JADE along with the services it provides (in this case, FCBatt
            and generic agent services). NB - To change properties after registering use the JADE 'modify' method.*/
        String[] services = {"FCBatt", "Agent"};
        registerAgent(thisAgent, services, services);
        // Get agent number from argument provided by instantiator of this agent.
        Object[] args = getArguments();
        if (args != null && args.length > 0) {
            String firstArg = args[0].toString();
            agentNumber = new Integer(firstArg).intValue();
        } else {

```

```

// Terminate agent.
System.out.println("No agent id");
doDelete();}

try {
// Locate data provider.
AgentCoordinatorID = getAgentIDsofService(thisAgent,
    "InputsUpdate")[0];
// Find agents that are interested in this agent's data.
agentIDs = getAgentIDsofService(thisAgent, "FCBatt");
/** N.B. If environment is dynamic would need to perform these searches either more than once to check
    for new agents, or implement some service subscription method to receive a message when new agents
    enter environment. */
} catch (Exception e) {
    System.out.println("Error finding service: " + e); }
agentsSubscribed = countSubscribingAgents(thisAgent, "FCBatt");
if (debug)
    System.out.println("agentsSubscribed to FCBatt service:"
        + agentsSubscribed);
    agentsLeftToRespond = agentsSubscribed - 1; }

class filterBehaviour extends CyclicBehaviour {
    public void action() {
        TimeStepData tsd = new TimeStepData();
        double[] dataArray;
        int length;
        ACLMessage msg = receive();
        if (msg != null) {
            String message = msg.getConversationId();
            // If new data from AgentCoordinator (ie Simulink).
            if (message.equals("UpdateData")) {
                try {
                    tsd = (TimeStepData) msg.getContentObject();
                } catch (Exception e) {
                    System.out.println("Exception with content object" + e); }
                // Extract data from incoming array.
                length = tsd.getData().length;
                dataArray = new double[length];
                for (int i = 0; i < length; i++)
                    dataArray[i] = tsd.getData()[i];
                if (debug) {
                    System.out.println("(Debug)Incoming data: ");

```

```

        for (int j = 0; j < length; j++) {
            System.out.print(j + ": " + dataArray[j] + " ");
            System.out.printf("\n");
        }
        /** Agent particular aspects begin here. *****/
        // Extract the relevant data.
        Pdiff = dataArray[inputPortsOfInterest[0]];
        /* Perform here any calculations required before using data from other agents. (Low pass filter to
        avoid feeding Fuel Cell with high dynamics) */
        int a = 755; /* Low pass filter constant-sample time 0.01 sec and cut off frequency 7 Hz */
        PdiffL += (Pdiff - PdiffL) / a;
        /** Block ends here *****/
        if (debug) {
            System.out.println(getLocalName() +
                " awaiting info from "
                + agentsLeftToRespond + " agent(s)");
        }
        dataUpdated = true;
        /** Pass information about the new data to the other agents. */
        if (agentsSubscribed > 1) {
            try {
                /** Set information in dataStructure to be passed to other agents *****/
                double [] dataToShare = {PdiffL};
                int [] elementToChange = {0};
                TimeStepData tsdInner= new TimeStepData();
                // Populate data structure with required data to exchange.
                tsdInner.setData(dataToShare);
                tsdInner.setElementsToChange(elementToChange);
                // Send information off to other agents.
                for (int i = 0; i < agentIDs.length; i++) {
                    if (!agentIDs[i].getLocalName().equals(
                        thisAgent.getLocalName())) {
                        sendObject(agentIDs[i], "agentData",
                            tsdInner);
                    }
                }
                /** Block ends here *****/
            } catch (Exception e) {
                System.out.println("Exception: " + e);
            }
            if (agentsLeftToRespond == 0) {
                finishCalculationsThenSend();
            }
        }
        // Additional information from another agent.
        if (message.equals("agentData"))
            && !msg.getSender().getLocalName().equals(

```

```

        thisAgent.getLocalName())) {
    try {
        tsd = (TimeStepData) msg.getContentObject();
    } catch (Exception e) {
        System.out.println("Exception getting content object: "
            + e); }
    length = tsd.getData().length;
    dataArray = new double[length];
    for (int i = 0; i < length; i++)
        dataArray[i] = tsd.getData()[i];
    /** Agent specific task inside this block *****/
    int [] elementsToUse = tsd.getElementsToChange();
    double SOC = dataArray[elementsToUse[0]];
    // Perform calculations with data from other agents.

        //In this case and due to power state ( Surplus or Scarcity) AND the battery SOC, the fuel
cell power setting is estimated.
        if (Pdiff < 0){

                                PFC = PdiffL; }

                                else {

                                PFC= 0; }

/** Block ends here *****/
    agentsLeftToRespond--;
    if (debug)
        System.out.println(getLocalName() + " recieved info "
            + " awaiting "
            + agentsLeftToRespond + " more.");
    if (agentsLeftToRespond == 0 && dataUpdated) {
        finishCalculationsThenSend();} }
    if (message.equals("DataAmended")) {
        if (debug)
            System.out.println("Agent " + agentNumber + " finished.");
        replyToAgent(msg.getSender(), "ProcessingComplete");}
    if (message.equals("Shutting Down")) {
        takeDown(msg.getSender());}
        } else {
    block();} } }

/** Finalise calculations and return to AgentCoordinator and Simulink.*/
public void finishCalculationsThenSend() {
/** Agent specific task inside this block *****/
    // Carry out any final calculation before returning back to Simulink and

```

```

        // specified port.
double[] dataOut = new double[outputPorts.length];
dataOut[0] = PFC;
/** Block ends here *****/

tsd.setData(dataOut);
tsd.setElementsToChange(outputPorts);
// Send modified data back to Simulink.
ACLMessage reply = new ACLMessage(ACLMessage.INFORM);
reply.setConversationId("ProcessedData");
try {
    reply.setContentObject(tsd);
} catch (Exception e) {
    System.out.println("Exception setting tsd: " + e); }
if (debug)
    System.out.println(getLocalName() + " finished, sending data to "
        + AgentCoordinatorID.getLocalName());
reply.addReceiver(AgentCoordinatorID);
send(reply);
agentsLeftToRespond = agentsSubscribed - 1;
dataUpdated = false; }
/** Terminate agent. @param senderAID AID*/
protected void takeDown(AID senderAID) {
    try {
        System.out.println("Deregistering and closing " + thisAgent);
        DFService.deregister(thisAgent);
    } catch (FIPAException fe) {
        System.out.println("Problem deregistering " + fe); }
    if (senderAID != null)
        contactAgent(senderAID, "Agent Deregistered");
    doDelete();}

```

**Hydrogen Storage Tank Agent**

\* <p>Title: Example to manage the Hybrid MCT-Hydrogen System Energy Balance from Simulink via JADE agents.</p>

\*<p>Description: This JADE agent is used to demonstrate how one can be set up in order to receive data from Simulink via the Agent Environment(that is the Agent Coordinator and AgentServer). It also shows the exchange of data between agents and then how the data is finally returned back to Simulink.</p>\*/

```

package Testnew;
import macsimjx.*;
import jade.lang.acl.ACLMessage;
import jade.domain.FIPAException;

```

```

import jade.domain.DFService;
import jade.core.behaviours.CyclicBehaviour;
import jade.core.Agent;
import jade.core.AID;
public class H2 extends UsefulAgentMethods {
    Agent thisAgent = (Agent)this;
    int agentNumber = 0;
    /** These determine which elements of the input data that this agent is interested in, and which element of the
outgoing data it is changing. Which the hydrogen storage tank online monitoring and survey */
    int[] inputPortsOfInterest = {2}; // I.e. top signal input to MACSim block.
    int[] outputPorts = {6}; // Set which ports in simulink data is shown on.
    // Set to true for helpful output.
    boolean debug = false;
    // Keep track of number of information agents.
    private int agentsSubscribed = 0;
    private int agentsLeftToRespond = 0;
    boolean firstRun = true;
    boolean dataUpdated = false;
    AID[] agentIDs = null;
    AID agentID = null;
    AID AgentCoordinatorID = null;
    TimeStepData tsd = new TimeStepData();
    double H2 = 0;
    int counter = 0;
    public void setup() {
        addBehaviour(new filterBehaviour());
        /** Register agent with directory facilitator of JADE along with the services it provides (in this case, H2Tank
and generic agent services). NB - To change properties after registering using the JADE 'modify' method. */
        String[] services = {"H2Tank", "Agent"};
        registerAgent(thisAgent, services, services);
        // Get agent number from argument provided by instantiator of this agent.
        Object[] args = getArguments();
        if (args != null && args.length > 0) {
            String firstArg = args[0].toString();
            agentNumber = new Integer(firstArg).intValue();
        } else {
            // Terminate agent.
            System.out.println("No agent id");
            doDelete();
        }
        try {

```

```

// Locate data provider.
AgentCoordinatorID = getAgentIDsOfService(thisAgent,
    "InputsUpdate")[0];
// Find agents that are interested in this agent's data.
agentIDs = getAgentIDsOfService(thisAgent, "H2Tank");
/** N.B. If environment is dynamic would need to perform these searches either more than once to check
for new agents, or implement some service subscription method to receive a message when new agents
enter environment.*/
} catch (Exception e) {
    System.out.println("Error finding service: " + e); }
    agentsSubscribed = countSubscribingAgents(thisAgent, "H2Tank");
if (debug)
    System.out.println("agentsSubscribed to H2Tank service:"
        + agentsSubscribed);
    agentsLeftToRespond = agentsSubscribed - 1; }
class filterBehaviour extends CyclicBehaviour {
public void action() {
    TimeStepData tsd = new TimeStepData();
    double[] dataArray;
    int length;
    ACLMessage msg = receive();
    if (msg != null) {
        String message = msg.getConversationId();
        // If new data from AgentCoordinator (ie Simulink).
        if (message.equals("UpdateData")) {
            try {
                tsd = (TimeStepData) msg.getContentObject();
            } catch (Exception e) {
                System.out.println("Exception with content object" + e); }
            // Extract data from incoming array.
            length = tsd.getData().length;
            dataArray = new double[length];
            for (int i = 0; i < length; i++)
                dataArray[i] = tsd.getData()[i];
            if (debug) {
                System.out.println("(Debug)Incoming data: ");
                for (int j = 0; j < length; j++) {
                    System.out.print(j + ": " + dataArray[j] + " ");}
                System.out.printf("\n");}
        }
    }
}
/** Agent particular aspects begin here. *****/

```

```

        // Extract the relevant data.
        H2 = dataArray[inputPortsOfInterest[0]];
        /* Perform here any calculations required before using data from other agents. (Hydrogen Storage Tank
        Volume in m3)*/
        /** Block ends here *****/
        if (debug) {
            System.out.println(getLocalName() +
                " awaiting info from "
                + agentsLeftToRespond + " agent(s)"); }
        dataUpdated = true;

        /** Pass information about the new data to the other agents. */
        if (agentsSubscribed > 1) {
            try {
                /** Set information in dataStructure to be passed to other agents *****/
                double [] dataToShare = {H2};
                int [] elementToChange = {0};
                TimeStepData tsdInner= new TimeStepData();
                // Populate data structure with required data to exchange.
                tsdInner.setData(dataToShare);
                tsdInner.setElementsToChange(elementToChange);
                // Send information off to other agents.
                for (int i = 0; i < agentIDs.length; i++) {
                    if (!agentIDs[i].getLocalName().equals(
                        thisAgent.getLocalName())) {
                        sendObject(agentIDs[i], "agentData",
                            tsdInner); } }
                /** Block ends here *****/
            } catch (Exception e) {
                System.out.println("Exception: " + e); } }
        if (agentsLeftToRespond == 0) {
            finishCalculationsThenSend(); } }
        // Additional information from another agent.
        if (message.equals("agentData")
            && !msg.getSender().getLocalName().equals(
                thisAgent.getLocalName())) {
            try {
                tsd = (TimeStepData) msg.getContentObject();
            } catch (Exception e) {
                System.out.println("Exception getting content object: "

```



```

        + e); }

length = tsd.getData().length;
dataArray = new double[length];
for (int i = 0; i < length; i++)
    dataArray[i] = tsd.getData()[i];
/** Agent specific task inside this block *****/
int [] elementsToUse = tsd.getElementsToChange();
double t = dataArray[elementsToUse[0]];
// Perform calculations with data from other agents.
//In this case and due to power state ( Storage Tank Feed Back).
    if (H2 > 0 && t >= 99.999){
System.out.println("[Hydrogen is Surplus at the 30 Bar Storage Tank with Volume in m3]" + H2); }
        else if (H2 < 0 && t >= 99.999){ System.out.println("[Hydrogen
Consumption From the 30 Bar Storage Tank Reserve with Volume in m3]" + H2); }
        else{;}
/** Block ends here *****/
    agentsLeftToRespond--;
    if (debug)
        System.out.println(getLocalName() + " recieved info "
            + " awaiting "
            + agentsLeftToRespond + " more.");
    if (agentsLeftToRespond == 0 && dataUpdated) {
        finishCalculationsThenSend();}
    if (message.equals("DataAmended")) {
        if (debug)
            System.out.println("Agent " + agentNumber + " finished.");
        replyToAgent(msg.getSender(), "ProcessingComplete");}
    if (message.equals("Shutting Down")) {
        takeDown(msg.getSender());}
    } else {
        block();} } }

/** Finalise calculations and return to AgentCoordinator and Simulink.*/
public void finishCalculationsThenSend() {
/** Agent specific task inside this block *****/
    // Carry out any final calculation before returning back to Simulink and
    // specified port
    double[] dataOut = new double[outputPorts.length];
    dataOut[0] = H2;
/** Block ends here *****/
    tsd.setData(dataOut);

```

```

tsd.setElementsToChange(outputPorts);
// Send modified data back to Simulink.
ACLMessage reply = new ACLMessage(ACLMessage.INFORM);
reply.setConversationId("ProcessedData");
try {
    reply.setContentObject(tsd);
} catch (Exception e) {
    System.out.println("Exception setting tsd: " + e); }
if (debug)
    System.out.println(getLocalName() + " finished, sending data to "
        + AgentCoordinatorID.getLocalName());
reply.addReceiver(AgentCoordinatorID);
send(reply);
agentsLeftToRespond = agentsSubscribed - 1;
dataUpdated = false; }
/** Terminate agent. @param senderAID AID*/
protected void takeDown(AID senderAID) {
    try {
        System.out.println("Deregistering and closing " + thisAgent);
        DFService.deregister(thisAgent);
    } catch (FIPAException fe) {
        System.out.println("Problem deregistering " + fe); */
    if (senderAID != null)
        contactAgent(senderAID, "Agent Deregistered");
    doDelete();} }

```



## References



- [1] M. Eissa, M. Elmesalawy, A. Soliman, A. Shetaya, and M. Shaban, "Egyptian Wide Area Monitoring System (EWAMS) Based on Smart Grid System Solution, " in *Energy Efficiency Improvements in Smart Grid Components*, M. Eissa, M. Elmesalawy, A. Soliman, A. Shetaya, and M. Shaban, INTECH, 2015, pp. 3-19.
- [2] M. Hossain, A. Oo and A. Ali, "Smart grids: Opportunities, developments, and trends," in *Smart Grids, Green Energy and Technology*, M. Hossain, A. Oo and A. Ali, Springer-Verlag London, 2013, pp. 23-44.
- [3] A. Richter, E. Van Der Laan, W. Ketter, and K. Valogianni, "Transitioning from the traditional to the smart grid: Lessons learned from closed-loop supply chains," *Proceedings of the international conference of smart grid technologies, economics. and policies*, 2012, pp1-7.
- [4] G. Shafiullah, A. Oo, A. Ali, and P. Wolfs, "Smart Grid for a Sustainable Future," *Smart Grid Renew. Energy*, vol. 4, pp. 23–34, 2013.
- [5] X. Fang, S. Misra, G. Xue, and D. Yang, "Smart Grid – The New and Improved Power Grid: A Survey," *IEEE Commun. Surv. Tutorials*, vol. 14, no. 4, pp. 944-980, 2011.
- [6] L. Cozzi and F. Gould, "World Energy Outlook," IEA, 2015, 2011, Available online ([https://www.iea.org/publications/freepublications/publication/WEO2015,WEO\\_2011.pdf](https://www.iea.org/publications/freepublications/publication/WEO2015,WEO_2011.pdf)), Last access 30<sup>th</sup> April 2018.
- [7] IEC White Paper, "Grid Integration of Large-capacity Renewable Energy Sources and Use of Large-Capacity Electrical Energy Storage," pp. 1–102, 2011, Available online (<http://www.iec.ch/whitepaper/gridintegration>), Last access 30<sup>th</sup> April 2018.
- [8] Departement of Energy and Climate Change, "UK Renewable Energy Roadmap," 2011, 2013, DECC, London, U.K, Available online (<https://www.gov.uk/government/collections/UK-renewable-energy-roadmap>), Last access 30<sup>th</sup> April 2018.
- [9] M. Dopita and R. Williamson, "Australia's Renewable Energy Future," pp. 1-35, January 2010, Available online (<https://www.science.org.au/files/userfiles/support/reports-and-plans/2015/renewable-energy-future.pdf>), Last access 30<sup>th</sup> April 2018.
- [10] P. Capros et al., "EU Energy, Transport, and GHG Emissions: Trends to 2050," 2016, 2013, Available online (<https://ec.europa.eu/energy/sites/ener/files/documents>), Last access 30<sup>th</sup> April 2018.
- [11] E. Stigson et al., "Energy Scenario for Sweden 2050," 2011, Available online (<http://www.wwf.se/source.php>), Last access 30<sup>th</sup> April 2018.

- [12] IFP Energy Nouvelles, “Marine renewable energy sources : their place in energy policy, projects,” 2014, 2012, Available online (<http://www.ifpenergiesnouvelles.com/Publications/Available-studies/Panorama-technical-reports/Panorama> 2014, 2012), Last access 30<sup>th</sup> April 2018.
- [13] Y. Zheng, Z. Hu, J. Wang, and Q. Wen, “IRSP ( integrated resource strategic planning ) with interconnected smart grids in integrating renewable energy and implementing DSM (demand side management) in China,” *Energy*, vol. 76, pp. 863–874, 2014.
- [14] M. Blanco et al., “Smart Grids Laboratories Inventory,” JRC Science and Policy Report, 2015, Available online (<https://ec.europa.eu/jrc/en/publication/eur-scientific-and-technical-research-reports/smart-grids-laboratories-inventory-2015>), Last access 30<sup>th</sup> April 2018.
- [15] R. Apel, “Smart Grid Architecture Model,” Proceedings of the 12<sup>th</sup> international workshop of electric power control centers, June 2013.
- [16] Departement of Energy Technology, Aalborg University “Smart Energy System Laboratory,” 2013, Available online (<http://www.et.aau.dk/departement/laboratory-facilities/smart-energy-systems-lab>), Last access 30<sup>th</sup> April 2018.
- [17] IEA, “Technology Roadmap-Smart Grids,” 2011, pp. 1-52, Available online ([https://www.iea.org/publications/freepublications/publication/smartgrids\\_roadmap.pdf](https://www.iea.org/publications/freepublications/publication/smartgrids_roadmap.pdf)), Last access 30<sup>th</sup> April 2018.
- [18] M. Macedo, J. Galo, L. Almeida, and A. Lima, “Demand-side management using artificial neural networks in a smart grid environment,” *Renew. Sustain. Energy Rev.*, vol. 41, pp. 128–133, 2015.
- [19] S. Plathottam and H. Salehfar, “Unbiased economic dispatch in control areas with conventional and renewable generation sources,” *Electr. Power Syst. Res.*, vol. 119, pp. 313–321, 2015.
- [20] M. Silvestre and E. Sanseverino, “Modelling energy storage systems using Fourier analysis: An application for smart grids optimal management,” *Appl. Soft Comput. J.*, vol. 14, pp. 469–481, 2014.
- [21] K. Zhou, S. Yang, Z. Chen, and S. Ding, “Optimal load distribution model of microgrid in the smart grid environment,” *Renew. Sustain. Energy Rev.*, vol. 35, pp. 304–310, 2014.
- [22] G. Boukettaya and L. Krichen, “A dynamic power management strategy of a grid connected hybrid generation system using wind, photovoltaic and Flywheel Energy Storage System in residential applications,” *Energy*, vol. 71, pp. 148–159, 2014.

- [23] W. Deng et al., “Battery Matters : Rightsizing Energy Storage for Green Datacenters,” pp. 1–11, 2011, available online (<http://grid.hust.edu.cn/fmliu/Wei2014BatteryMatters.pdf>), Last access 30<sup>th</sup> April 2018.
- [24] M. F. Elsied et al “Analysis , Modeling , and Control of an AC Microgrid System Based on Green Energy Key words,” Proceedings of the international conference on renewable energies and power quality, 2014.
- [25] M. Elsied et al “An Advanced Energy Management of Microgrid System Based on Genetic Algorithm,”, Proceedings of the IEEE 23<sup>rd</sup> international symposium in industrial electronics, 2014, pp. 2541–2547.
- [26] M. Elsied, A. Oukaour, H. Gualous, and R. Hassan, “Energy management and optimization in microgrid system based on green energy,” *Energy*, vol. 84, pp. 139–151, 2015.
- [27] G. Rohbogner and S. Fey, “What the term Agent stands for in the Smart Grid Definition of Agents and Multi-Agent Systems from an Engineer’s Perspective,” Proceedings of the federated conference on computer science and information system, 2012, pp. 1301–1305.
- [28] H. Feroze, “Multi-Agent Systems in Microgrids : Design and Implementation,” M.S. thesis, Virginia Polytechnic Institute and State University, 2009.
- [29] M. Wooldridge, “Introduction,” in *An introduction to multi-agent statistics*, John Wiley & Sons Ltd, 2002, pp. 1-13.
- [30] S. McArthur et al., “Multi-Agent Systems for Power Engineering Applications - Part I: Concepts, Approaches, and Technical Challenges,” *Power Syst. IEEE Trans.*, vol. 22, no. 4, pp. 1743–1752, 2007.
- [31] G. Rohbogner, U. Hahnel, P. Benoit, and S. Fey, “Multi-agent systems’ asset for smart grid applications,” *Comput. Sci. Inf. Syst.*, vol. 10, no. 4, pp. 1799–1822, 2013.
- [32] R. Gupta, D. Jha, V. Yadav, and S. Kumar, “A Multi-Agent Framework for Operation of a Smart Grid,” *Energy Power Eng.*, vol. 5, pp. 1330–1336, 2013.
- [33] Y. Eddy, H. Gooi, and S. Chen, “Multi-agent system for distributed management of microgrids,” *IEEE Trans. Power Syst.*, vol. 30, no. 1, pp. 24–34, 2015.
- [34] T. Logenthiran, D. Srinivasan, A. Khambadkone, and H. Aung, “Multiagent system for real-time operation of a microgrid in real-time digital simulator,” *IEEE Trans. Smart Grid*, vol. 3, no. 2, pp. 925–933, 2012.



- [35] T. Logenthiran, D. Srinivasan, and A. Khambadkone, "Multi-agent system for energy resource scheduling of integrated microgrids in a distributed system," *Electr. Power Syst. Res.*, vol. 81, no. 1, pp. 138–148, 2011.
- [36] H. Shirzeh, F. Naghdy, and P. Ciufo, "Balancing Energy in the Smart Grid Using Distributed Value Function ( DVF )," *IEEE Trans. Smart Grid*, vol. 6, no. 2, pp. 808–818, 2015.
- [37] K. Wu and H. Zhou, "A multi-agent-based energy-coordination control system for grid-connected large-scale wind-photovoltaic energy storage power-generation units," *Sol. Energy*, vol. 107, pp. 245–259, 2014.
- [38] T. Dethlefs, T. Preisler, and W. Renz, "Multi-Agent-based Distributed Optimization for Demand-Side-Management Applications," *Proceedings of the federated conference on computer science and information system*, 2014, pp. 1489–1496.
- [39] P. Palensky and D. Dietrich, "Demand-side management: Demand response, intelligent energy systems, and smart loads," *Ind. Informatics, IEEE Trans.*, vol. 7, no. 3, pp. 381–388, 2011.
- [40] R. Menon, D. Srinivasan, and L. Jain, "Fuzzy logic decision-making in multi-agent systems for smart grids," *Proceedings of the IEEE Symposium on computational intelligence applications in smart grid*, 2013, pp. 44-50.
- [41] J. Lagorse, M. Simoes, and A. Miraoui, "A Multi-Agent Fuzzy Logic Based Energy Management of Hybrid Systems," *IEEE Ind. Appl*, vol. 45, no. 6, pp. 3123-2129, 2009.
- [42] C. Nguyen, A. Flueck, and S. Member, "Agent-Based Restoration With Distributed Energy Storage Support in Smart Grids," *IEEE Trans. Smart Grid*, vol. 3, no. 2, pp. 1029–1038, 2012.
- [43] H. Kim, Y. Lim, and T. Kinoshita, "An intelligent multiagent system for autonomous microgrid operation," *Energies*, vol. 5, pp. 3347–3362, 2012.
- [44] J. Lagorse, D. Paire, and A. Miraoui, "A multi-agent system for energy management of distributed power sources," *Renew. Energy*, vol. 35, pp. 174–182, 2010.
- [45] S. Jin and D. Chassin, "Thread group multithreading: Accelerating the computation of an agent-based power system modeling and simulation tool-GridLAB-D," *Proceedings of the 47<sup>th</sup> annual Hawaii international conference on system sciences*, 2014, pp. 2536–2545.

- [46] M. Narkhede, S. Chatterji, and S. Ghosh, "Multi-Agent Systems (MAS) controlled Smart Grid – A Review," Proceedings of the international conference on recent trends in engineering & technology, 2013, pp. 12-17.
- [47] I. Chung, S. Oh and C. Yoo, "Distributed Intelligent Microgrid Control Using Multi-Agent Systems," Engineering, vol. 5, pp. 1–6, 2013.
- [48] A. Zidan and E. El-Saadany, "A cooperative multiagent framework for self-healing mechanisms in distribution systems," IEEE Trans. Smart Grid, vol. 3, no. 3, pp. 1525–1539, 2012.
- [49] A. Álvarez, A. Subirachs, F. Figuerola, O. Bellmunt, and A. Andreu, "Operation of a utility connected microgrid using an IEC 61850-based multi-level management system," IEEE Trans. Smart Grid, vol. 3, no. 2, pp. 858–865, 2012.
- [50] Y. Xu and W. Liu, "Novel multiagent based load restoration algorithm for microgrids," IEEE Trans. Smart Grid, vol. 2, no. 1, pp. 152–161, 2011.
- [51] Z. Zhou, F. Zhao, and J. Wang, "Agent-Based Electricity Market Simulation With," IEEE Trans. Smart Grid, vol. 2, no. 4, pp. 580–588, 2011.
- [52] Z. Xiao et al., "Hierarchical MAS-based control strategy for microgrid," Energies, vol. 3, pp. 1622–1638, 2010.
- [53] S. Fonseca, M. Griss, and R. Letsinger, "Evaluation of the Zeus MAS Framework," Proceedings of the second international workshop in software agents and workflows for systems interoperability, 2001, pp. 1-8.
- [54] J. Kodama et al., "Multi-agent-based autonomous power distribution network restoration using contract net protocol," Electr. Eng. Japan (English Transl. Denki Gakkai Ronbunshi), vol. 166, no. 4, pp. 56–63, 2009.
- [55] Z. Jiang, "Agent-based power-sharing scheme for active hybrid power sources," J. Power Sources, vol. 177, pp. 231–238, 2008.
- [56] Z. Jiang, "Agent-Based Control Framework for Distributed Energy Resources Microgrids," Proceedings of the IEEE/WIC/ACM international conference on intelligent agent technology, 2006.
- [57] R. Lum, B. Canada, and W. Gruver, "Multi-Agent Coordination of Distributed Energy Systems," Proceedings of the IEEE international conference on systems, man and cybernetics, 2005.
- [58] S. Abras, S. Ploix, S. Pesty, and M. Jacomino, "A multi-agent home automation system for power management," Proceedings of the international conference on informatics in control automation and robotics, 2006, pp 59-68.

- [59] L. Tolbert, H. Qi, and F. Peng, "Scalable multi-agent system for real-time electric power management," Proceedings of the power engineering society summer meeting, 2001, pp. 1676–1679.
- [60] F. Brazier et al., "Agents negotiating for load balancing of electricity use," in Proceedings of the 18th international conference on distributed computing systems, 1998.
- [61] F. Ygge and H. Akkermans, "Power Load Management as a Computational Market," Proceeding of the international conference on multi-agent systems, 1996, pp. 393 - 400.
- [62] T. Ayodele and A. Ogunjuyigbe, "Mitigation of wind power intermittency: Storage technology approach," Renew. Sustain. Energy Rev., vol. 44, pp. 447–456, 2015.
- [63] J. Petinrin and M. Shaaban, "Implementation of Energy Storage in a Future Smart Grid," Aust. J. Basic Appl. Sci., vol. 7, no. 4, pp. 273–279, 2013.
- [64] M. Ismail, M. Moghavvemi, T. Mahlia, K. Muttaqi, and S. Moghavvemi, "Effective utilization of excess energy in standalone hybrid renewable energy systems for improving comfortability and reducing cost of energy: A review and analysis," Renew. Sustain. Energy Rev., vol. 42, pp. 726–734, 2015.
- [65] R. Fares and M. Webber, "Combining a dynamic battery model with high-resolution smart grid data to assess microgrid islanding lifetime," Appl. Energy, vol. 137, pp. 482–489, 2015.
- [66] T. Ma, H. Yang, and L. Lu, "Development of hybrid battery-supercapacitor energy storage for remote area renewable energy systems," Appl. Energy, vol. 153, pp. 56–62, 2015.
- [67] M. Suberu, M. Mustafa, and N. Bashir, "Energy storage systems for renewable energy power sector integration and mitigation of intermittency," Renew. Sustain. Energy Rev., vol. 35, pp. 499–514, 2014.
- [68] N. Hasan, M. Hassan, M. Majid, and H. A Rahman, "Review of storage schemes for wind energy systems," Renew. Sustain. Energy Rev., vol. 21, pp. 237–247, 2013.
- [69] B. Ge et al., "Energy storage system-based power control for grid-connected wind power farm," Int. J. Electr. Power Energy Syst., vol. 44, no. 1, pp. 115–122, 2013.
- [70] S. Koohi-Kamali, V. Tyagi, N. Rahim, N. Panwar, and H. Mokhlis, "Emergence of energy storage technologies as the solution for reliable operation of smart power systems: A review," Renew. Sustain. Energy Rev., vol. 25, pp. 135–165, 2013.

- [71] A. Foley et al., “Electrical Energy Storage & Smart Grid Technologies to Integrate the next generation of Renewable Power Systems,” Proceedings of the 4<sup>th</sup> international conference on sustainable energy & environmental protection, 2010.
- [72] O. Onar, M. Uzunoglu, and M. Alam, “Dynamic modeling, design, and simulation of a wind/fuel cell/ultra-capacitor-based hybrid power generation system,” J. Power Sources, vol. 161, pp. 707–722, 2006.
- [73] A. Aktas, K. Erhan, E. Ozdemir, and S. Ozdemir, “Development of a Hybrid Energy Storage System Composed Battery and Ultracapacitor Supplied from Photovoltaic Power Source for 3- phase 4-wire Smart Micro Grid Structure,” Proceedings of the SOLAR TR 2014 conference.
- [74] F. Mwasilu, J. Justo, E. Kim, T. Do, and J. Jung, “Electric vehicles and smart grid interaction: A review on vehicle to grid and renewable energy sources integration,” Renew. Sustain. Energy Rev., vol. 34, pp. 501–516, 2014.
- [75] L. Drude, L. Junior, and R. Rüther, “Photovoltaics (PV) and electric vehicle-to-grid (V2G) strategies for peak demand reduction in urban regions in Brazil in a smart grid environment,” Renew. Energy, vol. 68, pp. 443–451, 2014.
- [76] R. Arulmurugan and N. Suthanthiravanitha, “Model and design of a fuzzy-based Hopfield NN tracking controller for standalone PV applications,” Electr. Power Syst. Res., vol. 120, pp. 184–193, 2015.
- [77] M. Farhadi, S. Member, and O. Mohammed, “Adaptive Energy Management in Redundant Hybrid DC Microgrid for Pulse Load Mitigation,” IEEE Trans. Smart Grid, vol. 6, no. 1, pp. 54–62, 2015.
- [78] A. Mohamed and O. Mohammed, “Real-time energy management scheme for hybrid renewable energy systems in smart grid applications,” Electr. Power Syst. Res., vol. 96, pp. 133–143, 2013.
- [79] A. Mohamed, M. Elshaer, and O. Mohammed, “Control enhancement of power conditioning units for high quality PV systems,” Electr. Power Syst. Res., vol. 90, pp. 30–41, 2012.
- [80] A. Mohamed, M. Elshaer, and O. Mohammed, “High-quality integration of fuel cells energy into electric grids,” Proceedings of the 4th international symposium on resilient control systems, 2011, pp. 89–94.
- [81] M. Elshaer, A. Mohamed, and O. Mohammed, “Integration of sustainable energy sources into DC zonal electric distribution systems,” Proceedings of the IEEE power and energy society general meeting, 2011.

- [82] A. Mohamed, M. Elshaer, and O. Mohammed, "Bi-directional AC-DC/DC-AC converter for power sharing of hybrid AC/DC systems," *Proceedings of the IEEE power and energy society general meeting*, 2011.
- [83] N. Eghtedarpour and E. Farjah, "Power Control and Management in a Hybrid AC / DC Microgrid," *IEEE Trans. Smart Grid*, vol. 5, no. 3, pp. 1494–1505, 2014.
- [84] J. Vasiljevska, J. Lopes, and M. Matos, "Integrated micro-generation, load and energy storage control functionality under the multi micro-grid concept," *Electr. Power Syst. Res.*, vol. 95, pp. 292–301, 2013.
- [85] M. Saqib and A. Saleem, "Power-quality issues and the need for reactive-power compensation in the grid integration of wind power," *Renew. Sustain. Energy Rev.*, vol. 43, pp. 51–64, 2015.
- [86] R. Kamel, "Three fault ride through controllers for wind systems running in isolated micro-grid and Effects of fault type on their performance: A review and comparative study," *Renew. Sustain. Energy Rev.*, vol. 37, pp. 698–714, 2014.
- [87] M. El Moursi, H. Zeineldin, J. Kirtley, and K. Alobeidli, "A dynamic master/slave reactive power-management scheme for smart grids with distributed generation," *IEEE Trans. Power Deliv.*, vol. 29, no. 3, pp. 1157–1167, 2014.
- [88] M. Sarkhanloo, A. Yazdankhah, and R. Kazemzadeh, "A new control strategy for small wind farm with capabilities of supplying required reactive power and transient stability improvement," *Renew. Energy*, vol. 44, pp. 32–39, 2012.
- [89] M. Kyaw and V. Ramachandaramurthy, "Fault ride through and voltage regulation for grid connected wind turbine," *Renew. Energy*, vol. 36, no. 1, pp. 206–215, 2011.
- [90] F. Guo et al., "Comprehensive real-time simulation of the smart grid," *IEEE Trans. Ind. Appl.*, vol. 49, no. 2, pp. 899–908, 2013.
- [91] W. Li, G. Joós, and J. Belanger, "Real-Time Simulation of a Wind Turbine Generator Coupled With a Battery Supercapacitor Energy Storage System," *IEEE Trans. Ind. Electron.*, vol. 57, no. 4, pp. 1137–1145, 2010.
- [92] M. Bouscayrol, "Energetic Macroscopic Representation (EMR)," L2EP Lab, University Lille1, May, 2011.
- [93] D. Chrenko, "Energetic Macroscopic Representation Modeling and Control of a Low Temperature Fuel Cell System Fed by Hydrocarbons," Ph.D. dissertation, Dept. Electric power., Franche-Comté Univ., Belfort, France, 2008.

- [94] A. Tabanjat et al., “Fuzzy logic-based water heating control methodology for the efficiency enhancement of hybrid PV-PEM electrolyzer systems,” *Int. J. Hydrogen Energy*, vol. 40, no. 5, pp. 2149–2161, 2015.
- [95] J. Martinez, D. Hissel, M. Pera, and M. Amiet, “Practical Control Structure and Energy Management of a Testbed Hybrid Electric Vehicle,” *Veh. Technol. IEEE Trans.*, vol. 60, no. 9, pp. 4139–4152, 2011.
- [96] K. Agbli, D. Hissel, M. Péra, and I. Doumbia, “EMR modeling of a hydrogen-based electrical energy storage,” *Eur. Phys. J. Appl. Phys.*, vol. 54, 2011.
- [97] W. Lhomme, P. Delarue, F. Giraud, B. Lemaire-Semail, and A. Bouscayrol, “Simulation of a Photovoltaic Conversion System using Energetic Macroscopic Representation,” *Proceedings of the 15<sup>th</sup> international power electronics and motion control conference*, 2012, pp. 1–6.
- [98] K. Reddy, M. Kumar, T. Mallick, H. Sharon, and S. Lokeswaran, “A review of Integration, Control, Communication and Metering (ICCM) of renewable energy based smart grid,” *Renew. Sustain. Energy Rev.*, vol. 38, pp. 180–192, 2014.
- [99] H. Sharif, “A Survey on Smart Grid Communication Infrastructures : Motivations, Requirements, and Challenges A Survey on Smart Grid Communication Infrastructures : Motivations, Requirements, and Challenges,” *IEEE Commun. Sur. & Tuts.*, pp. 1–16, 2013.
- [100] E. Ancillotti, R. Bruno, and M. Conti, “The role of communication systems in smart grids: Architectures, technical solutions, and research challenges,” *Comput. Commun.*, vol. 36, pp. 1665–1697, 2013.
- [101] E. Wolf, “Large-Scale Hydrogen Energy Storage,” in *Electrochemical Energy Storage for Renewable Sources and Grid Balancing*, 1<sup>st</sup> ed., P. Moseley and J. Garche, Ed. Waltham: Elsevier, 2014, pp. 129–142.
- [102] N. Briguglio and V. Antonucci, “Overview of PEM Electrolysis for Hydrogen Production,” in *PEM Electrolysis for Hydrogen Production Principles and Applications*, 1<sup>st</sup> ed., D. Bessarabov et al., Ed. New York: CRC Press, 2016, pp. 1–9.
- [103] D. Das et al., “Introduction,” in *Biohydrogen Production Fundamentals and Technology Advances*, 1<sup>st</sup> ed., D. Das et al., Ed. New York: CRC Press, 2014, pp. 1–21.
- [104] T. Zhou and B. Francois, “Energy management and power control of a hybrid active wind generator for distributed power generation and grid integration,” *IEEE Trans. Ind. Electron.*, vol. 58, no. 1, pp. 95–104, 2011.

- [105] L. Horrein, A. Bouscayrol, Y. Cheng, and, M. El. Fassi, "Multiphysical modeling and description of a permanent magnet synchronous machine using energetic macroscopic representation for EV/HEV applications," Proceedings of the 15<sup>th</sup> European conference on power electronics and applications, 2013, pp. 1–10.
- [106] A. Bouscayrol, X. Guillaud, R. Teodorescu, P. Delarue, and W. Lhomme, "Hardware-in-the-loop simulation of different wind turbines using Energetic Macroscopic Representation," Proceedings of the IECON, 32<sup>nd</sup> annual conference on IEEE industrial electronics, 2006, pp. 5338–5343.
- [107] Ph. Delarue, A. Bouscayrol, A. Tounzi, X. Guillaud, and G. Lancigu, "Modelling, control, and simulation of an overall wind energy conversion system," Renew. Energy, vol. 28, pp. 1169–1185, 2003.
- [108] A. Bouscayrol, Ph. Delarue, and X. Guillaud, "Power strategies for maximum control structure of a wind energy conversion system with a synchronous machine," Renew. Energy, vol. 30, pp. 2273–2288, 2005.
- [109] A. Bouscayrol, X. Guillaud, Ph. Delarue, and B. Semail, "Energetic macroscopic representation and inversion-based control illustrated on a wind-energy-conversion system using hardware-in-the-loop simulation," IEEE Trans. Ind. Electron., vol. 56, no. 12, pp. 4826–4835, 2009.
- [110] L. Drouen, J. Charpentier, E. Semail, and J. Clenet "Study of an innovative electrical machine fitted to marine current turbines," Proceedings of the Ocean. 2007 - Europe conference., pp. 1–6.
- [111] R. Balme et al., "A Simulation Model for the Evaluation of the Electrical Power Potential Harnessed by a Marine Current Turbine in the Raz de Sein," IEEE J. Oceanic.Ener, vol. 32, no. 4, pp. 786-797, 2007.
- [112] S. Ben Elghali, M. Benbouzid, and M. Charpentier, "Marine Tidal Current Electric Power Generation Technology: State of the Art and Current Status," Proceedings of the IEEE international electric machines & drives conference, 2007, pp. 1407–1412.
- [113] H. Li, Z. Chen, and H. Polinder, "Optimization of multi bird permanent-magnet wind generator systems," IEEE Trans. Energy Convers., vol. 24, no. 1, pp. 82–92, 2009.
- [114] J. Liang and B. Whitby, "Field Oriented Control of a Permanent Magnet Synchronous Generator for use in a Variable Speed Tidal Stream Turbine," Proceedings of the international universities' power engineering conference, 2011.

- [115] Z. Zhou, F. Scuiller, J. Charpentier, M. Benbouzid, and T. Tang, "Grid-connected marine current generation system power smoothing control using supercapacitors," Proceedings of the IECON-38<sup>th</sup> annual conference on the IEEE industrial electronics society, pp. 4035–4040, 2012.
- [116] Z. Zhou, F. Scuiller, J. Charpentier, M. Benbouzid, and T. Tang, "Power limitation control for a PMSG-based marine current turbine at high tidal speed and strong sea state," Proceedings of the IEEE international electric machines and drives conference, 2013, pp. 75–80.
- [117] Z. Zhou, F. Scuiller, J. Charpentier, M. Benbouzid, and T. Tang, "Power smoothing control in a grid-connected marine current turbine system for compensating swell effect," IEEE Trans. Sustain. Energy, vol. 4, no. 3, pp. 816–826, 2013.
- [118] S. Djbarri, J. Charpentier, F. Scuiller, M. Benbozid, "Influence of Fixed - Pitch Tidal Hydrodynamic Characteristic on the Generator Design," Proceedings of the 11<sup>th</sup> European wave and tidal energy conference, 2015.
- [119] Z. Zhou et al., "Power Control of a Nonpitchable PMSG-Based Marine Current Turbine at Overrated Current Speed With Flux-Weakening Strategy," IEEE J. Ocean. Eng., vol. 40, no. 3, pp. 536–545, 2015.
- [120] G. El Saady, E. Ibrahim, H. Ziedan, and M. Soliman, "Analysis of Wind Turbine Driven Permanent Magnet Synchronous Generator under Different Loading Conditions," Proceedings of the international middle-east power systems conference-MEPCON'2014, pp. 97–112.
- [121] T. Smolinka and E. Ojong, "Hydrogen Production from Renewable Energies d Electrolyzer Technologies," in Electrochemical Energy Storage for Renewable Sources and Grid Balancing, P. T. Moseley and J. Garche, Ed. Waltham: Elsevier, 2015, pp. 103–128.
- [122] T. Smolinka et al., "Fundamentals of PEM Water Electrolysis," in Fundamentals of PEM Water Electrolysis, 1<sup>st</sup> ed., D. Bessarabov et al., Ed. New York: CRC Press, 2016, pp. 11–33.
- [123] F. Menzl and M. Wenske, "Investigation of the Steady State and Transient Operating Behaviour of a 20 kW Pressure Electrolyser," in Hydrogen Power: theoretical and engineering solutions, T. Saetre, Grimstad, Norway: Proceedings of the Hypothesis II Symposium, 1997, pp. 185–190.
- [124] Ø. Ulleberg, "Modeling of advanced alkaline electrolyzers: A system simulation approach," Int. J. Hydrogen Energy, vol. 28, no. 1, pp. 21–33, 2003.



- [125] M. Santarelli and D. Pellegrino, "Mathematical optimization of a RES-H<sub>2</sub> plant using a black box algorithm," *Renew. Energy*, vol. 30, no. 4, pp. 493–510, 2005.
- [126] S. Kélouwani, K. Agbossou, and R. Chahine, "Model for energy conversion in renewable energy system with hydrogen storage," *J. Power Sources*, vol. 140, no. 2, pp. 392–399, 2005.
- [127] A. Bilodeau and K. Agbossou, "Control analysis of renewable energy system with hydrogen storage for residential applications," *J. Power Sources*, vol. 162, no. 2 SPEC. ISS., pp. 757–764, 2006.
- [128] T. Zhou, B. Francois, M. Lebbal, and S. Lecoeuche, "Real-time emulation of a hydrogen-production process for assessment of an active wind-energy conversion system," *IEEE Trans. Ind. Electron.*, vol. 56, no. 3, pp. 737–746, 2009.
- [129] T. Zhou and B. Francois, "Modeling and control design of hydrogen production process for an active hydrogen/wind hybrid power system," *Int. J. Hydrogen Energy*, vol. 34, no. 1, pp. 21–30, 2009.
- [130] A. Badi et al., "Performance of a Stand-Alone Renewable Energy System Based on Hydrogen Energy Storage," *Proceedings of the 6<sup>th</sup> international symposium on communications, control, and signal processing*, 2014, pp. 2321–2324.
- [131] R. Datta, D. Martino, Y. Dong, and P. Choi, "Modeling of PEM Water Electrolyzer," in *PEM Electrolysis for Hydrogen Production: Principles and Applications*, 1<sup>st</sup> ed., D. Bessarabov, H. Wang, H. Li, and N. Zhao, Eds. New York, 2016, pp. 243–267.
- [132] H. Görgün, "Dynamic modelling of a proton exchange membrane (PEM) electrolyzer," *Int. J. Hydrogen Energy*, vol. 31, pp. 29–38, 2006.
- [133] K. Agbli et al., "Multiphysics simulation of a PEM electrolyzer: Energetic Macroscopic Representation approach," *Int. J. Hydrogen Energy*, vol. 36, pp. 1382–1398, 2011.
- [134] K. Agbli, D. Hissel, M. Péra, and I. Doumbia, "Energetic Macroscopic Representation (EMR): New approach for multiphysics energetic flows modelling," *IFAC Proc.* Vol.45, no. 21, pp. 723–728, 2012.
- [135] F. Barbir, "Introduction," in *PEM Fuel Cells Theory and Practice*, 2nd ed., F. Barbir, Ed. Waltham: Elsevier, 2012, pp. 1–16.
- [136] D. Feroldi, R. Outbib and M. Basualdo, "Introduction," in *PEM Fuel Cells with Bio-Ethanol Processor Systems, Part I PEM Fuel Cells: Modeling, Simulation, Advanced Control and Diagnosis*, 1<sup>st</sup> ed., D. Feroldi, R. Outbib and M. Basualdo, Elsevier. Ed. Verlag London: Springer, 2012, pp. 3–48.

- [137] IEA Energy Technology Essentials, “Fuel Cells,” pp. 1–4, 2007, Available online (<https://webstore.iea.org/iea-energy-technology-essentials-fuel-cells>), Last access 30<sup>th</sup> April, 2018.
- [138] M. Wohr et al , “Dynamic modelling and simulation of a polymer membrane fuel cell including mass transport limitation,” *Int. J. Hydrogen Energy*, vol. 23, no. 3, pp. 213–218, 1998.
- [139] J. Hamelin, K. Agbossou, A. Laperrière, F. Laurencelle, and T. Bose, “Dynamic behavior of a PEM fuel cell stack for stationary applications,” *Int. J. Hydrogen Energy*, vol. 26, no. 6, pp. 625–629, 2001.
- [140] J. Corrêa, F. Farret, L. Canha, and M. Simoes, “An electrochemical-based fuel-cell model suitable for electrical engineering automation approach,” *IEEE Trans. Ind. Electron.*, vol. 51, no. 5, pp. 1103–1112, 2004.
- [141] W. Caisheng, M. Nehrir, and S. Shaw, “Dynamic models and model validation for PEM fuel cells using electrical circuits,” *Energy Conversion, IEEE Trans.*, vol. 20, no. 2, pp. 442–451, 2005.
- [142] R. Seyezhai and B. Mathur, “Mathematical modeling of proton exchange membrane fuel cells,” *Int. J. Comput. Appl.*, vol. 20, no. 5, pp. 1–6, 2011.
- [143] N. Benchouia and A. Hadjadj, “Modeling and validation of fuel cell PEMFC,” *Revue des Energies Renouvelables*, vol. 16, no. 2, pp. 365–377, 2013.
- [144] I. Martín, A. Ursúa, and P. Sanchis, “Modelling of PEM fuel cell performance: Steady-state and dynamic experimental validation,” *Energies*, vol. 7, pp. 670–700, 2014.
- [145] D. Candusso et al., “Characterisation and modelling of a 5 kW PEMFC for transportation applications,” *Int. J. Hydrogen Energy*, vol. 31, pp. 1019–1030, 2006.
- [146] B. Mahmah, A. M'raoui, M. Belhamel, and H. Benmoussa, “Experimental Study and Modelling of a Fuel Cell PEMFC Fed Directly in Hydrogen / Oxygen,” *Proceedings of the 16<sup>th</sup> world hydrogen energy conference*, 2006, pp. 1–11.
- [147] M. Outeiro, R. Chibante, A. Carvalho, and A. Almeida, “A new parameter extraction method for accurate modeling of PEM fuel cells,” *Int. J. Energy Res.*, vol. 33, pp. 978–988, 2009.
- [148] M. Outeiro and A. Carvalho, “MatLab/Simulink as design tool of PEM Fuel Cells as electrical generation systems,” *Proceedings of the European fuel cell forum*, 2011, pp. 1–9.

- [149] J. Amphlett et al, "Simulation of a 250 kW diesel fuel processor/PEM fuel cell system," J. Power Sources, vol. 71, pp. 179–184, 1998.
- [150] M. El-Sharkh, N. Sisworahardjo, M. Uzunoglu, O. Onar, and M. Alam, "Dynamic behavior of PEM fuel cell and microturbine power plants," J. Power Sources, vol. 164, pp. 315–321, 2007.
- [151] R. Wilckens, "Hydrogen as a Means of Transporting and Balancing Wind Power Production," in *Wind Power in Power Systems*, 1<sup>st</sup> ed., T. Ackermann, John Wiley & Sons, Ltd., West Sussex, England, 2005, pp. 505-521.
- [152] M. Péra and D. Chrenko, D. Hissel, and A. Bouscayrol, "Représentation énergétique macroscopique d'une pile à combustible," *Eur. J. Electr. Eng.*, vol. 11, no. 4–5, pp. 603–623, 2008.
- [153] N. Zafer and G. Luecke, "Stability of gas pressure regulators," *Appl. Math. Model.*, vol. 32, pp. 61–82, 2008.
- [154] A. Alaboudy, A. Daoud, S. Desouky, and A. Salem, "Converter controls and flicker study of PMSG-based grid connected wind turbines," *Ain Shams Eng. J.*, vol. 4, pp. 75–91, 2013.
- [155] W. Friedl, E. Schmutz, M. Sakulin, and R. Braunstein, "Electrical Energy and Power Saving Potentials in the Area of Agriculture," *Proceedings of the DUE (Domestic Use of Electrical Energy)*, 2007, pp. 53–58.
- [156] C. Reese and L. Hofmann, "Determination of load and generation composition in distribution grids," *Proceedings of the IEEE/PES power systems conference and exposition*, 2009, pp. 1–7.
- [157] Department for Business Energy & Industrial Strategy, "Energy Consumption in the UK (2016)," Available online ([https://assets.publishing.service.gov.uk/government/uploads/system/uploads/attachment\\_data/file/633503/ECUK\\_2016.pdf](https://assets.publishing.service.gov.uk/government/uploads/system/uploads/attachment_data/file/633503/ECUK_2016.pdf)), Last access 30<sup>th</sup> April 2018.
- [158] K. Agbli, M. Barakat, H. Gualous, and D. Hissel, "Large Scale Tidal Hydrogen Production for Fuel Cell based EVs," *Proceedings of the ELECTRIMACS 2017*, Toulouse, France.
- [159] K. Bae, S. Choi, and J. Kim, and Y. Jung, "LiFePO<sub>4</sub> Dynamic Battery Modeling for Battery Simulator," *Proceedings of the IEEE international conference on industrial technology*, 2014, pp. 354–358.

- [160] G. Shi, M. Zhu, X. Cai, Z. Wang, and L. Yao, "Generalized average model of DC wind turbine with consideration of electromechanical transients," Proceedings of the IECON (Industrial Electronics Conference), 2013, pp. 1638–1643.
- [161] L. Xu, G. Wang, L. Fu, Q. Shi, and Y. Wu, "General Average Model of D-PMSG and Its Application with Virtual Inertia Control," Proceedings of the IEEE international conference on mechatronics and automation, 2015, pp. 802–807.
- [162] J. Baert, J. Pouget, D. Hissel, and M. Péra, "Modeling and Design of Control Structure for Railway Hybrid Systems," Proceedings of the 9<sup>th</sup> world congress of railway research, 2011, pp. 1–8.
- [163] D. Mehrzad, J. Luque, and M. Cuenca, "Vector Control of PMSG for Grid-Connected Wind Turbine Applications," M.S. thesis, Institute of Energy Technology, AALBORG Univ., 2009.
- [164] S. Li, T. Haskew, E. Muljadi, and C. Serrentino, "Characteristic Study of Vector-controlled Direct-driven Permanent Magnet Synchronous Generator in Wind Power Generation," *Electr. Power Components Syst.*, vol. 37, no. 10, pp. 1162–1179, 2009.
- [165] Ø. Ulleberg, "The importance of control strategies in PV – hydrogen systems," *Sol. Ener.*, vol. 76, pp. 323–329, 2004.
- [166] R. López, J. Bernal-Agustín, and J. Contreras, "Optimization of control strategies for stand-alone renewable energy systems with hydrogen storage," *Renew. Ener.*, vol. 32, pp. 1102–1126, 2007.
- [167] H. Dinushi et al., "Defining Multi Agent System for a Reliable Micro-Grid," Proceedings of the Moratuwa engineering research conference, 2015, pp. 4–9.
- [168] J. Oyarzabal, J. Jimeno, J. Ruela, A. Engler, and C. Hardt, "Agent based Micro Grid Management System," Proceedings of the international conference on future power systems, 2002, pp. 1–6.
- [169] J. Pinto, "Analysis of Extended Constant Power Speed Range of the Permanent Magnet Synchronous Machine Driven By Dual Mode," Ph.D. dissertation, The University of Tennessee, Knoxville, 2001.
- [170] S. Morimoto, Y. Tong, Y. Takeda, and T. Hirasu, "Loss minimization control of permanent magnet synchronous motor drives," *IEEE Trans. Ind. Electron.*, vol. 41, no. 5, pp. 511–517, 1994.
- [171] M. Rahman, L. Zhong, and K. Lim, "A Direct Torque-Controlled Interior Permanent Magnet Synchronous Motor Drive," *IEEE Trans. Ind. Appl.*, vol. 34, no. 6, pp. 1246–1253, 1998.

- [172] S. Morimoto, H. Nakayama, M. Sanada, and Y. Takeda, "Sensorless Output Maximization Control for Variable-Speed Wind Generation System using IPMSG," *Ind. Appl. IEEE Trans.*, vol. 41, no. 1, pp. 60–67, 2005.
- [173] M. Barakat et al., "Energetic Macroscopic Representation of a Marine Current Turbine System with Loss Minimization Control," *IEEE Trans. Sustain. Energy*, vol. 9, no. 1, pp. 106–117, 2018.
- [174] M. Hussein, T. Senjyu, M. Orabi, M. Wahab, and M. Hamada, "Control of a Stand-Alone Variable Speed Wind Energy Supply System," *Appl. Sci.*, vol., pp. 437–456, 2013.
- [175] E. Anderson, "Megawatt-Scale PEM Electrolysis: The Pathway to Enabling Renewable Hydrogen Based Energy Storage and Infrastructure," in the 11<sup>th</sup> international hydrogen & fuel cells conference, Birmingham, UK, March. 17, 2015.
- [176] R. Harvey et al., "Large-scale water electrolysis for power-to-gas," in *PEM electrolysis for hydrogen production: principles and applications*, 1<sup>st</sup> ed., D. Bessarabov et al, Eds. New York: CRC Press, 2016, pp. 303–313.
- [177] B. Pitschak and J. Mergel, "Electrolytic Processes," in *Hydrogen and fuel cell: technologies and market prospective*, 1<sup>st</sup> ed, J. Töpler and J. Lehmann, Ed Verlag Berlin Heidelberg: Springer, 2016, pp. 187–207.
- [178] E. Anderson et al., "Long Life PEM Water Electrolysis Stack Experience and Future Directions Proton's Markets, Products & Capabilities," in the technical forum Hannover Messe, Germany, April. 9, 2013.
- [179] Proton on Site, "C Series - Hydrogen Generation Systems." Factsheet, 2013.
- [180] M. Schiller and E. Anderson, "Five Considerations for Large-Scale Hydrogen Electrolyzer Development," *Gas for Energy conference*, 2014, pp. 45–46, Available online ([www.gas-for-energy.com](http://www.gas-for-energy.com)), Last access 30<sup>th</sup> April 2018.
- [181] Proton on Site, "Proton M Series PEM Electrolyzers for MW Scale Energy Storage." Factsheet, 2014.
- [182] E. Wahlmüller, "H2 Technologies for Industrial Applications," in the ACStyria hotspot FCH H2: Building Synergies in Mobility –The European perspective airport Graz, 22-23 October 2015.
- [183] D. Thomas, "Alkaline vs PEM electrolyzers: lessons learnt from Falkenhagen and WindGas Hamburg," in the *Hydrogen Days*, Prague, Czech Republic, 2016.
- [184] M. Waidhas, "Electrolyzer Technology- the Siemens View," in the *HFC Nordic*, Sandviken, Sweden, Oct 26, 2016.

- [185] Association Franciase for Hydrogen and Fuel Cell, “Production d'Hydrogene par Electrolyse de l'Eau,” Mémento de l'Hydrogène, Fiche 3.2.1, Révision 2017, Available online (<http://www.afhypac.org/document>), Last access 30<sup>th</sup> April, 2018.
- [186] J. Pennanen and L. Kannari, “PEM electrolyzer model for Apros,” NEO-CARBON ENERGY, February, 2016, Available online ([http://www.neocarbonenergy.fi/wp-content/uploads/2016/02/13\\_Pennanen.pdf](http://www.neocarbonenergy.fi/wp-content/uploads/2016/02/13_Pennanen.pdf)), Last access 30<sup>th</sup> April, 2018.
- [187] P. Kubiak, Z. Cen, C. López, and I. Belharouak, “Calendar aging of a 250 kW/500 kWh Li-ion battery deployed for the grid storage application,” *J. Power Sources*, vol. 372, pp. 16–23, 2017.
- [188] Z. Cen, P. Kubiak, C. López, and I. Belharouak, “Demonstration study of hybrid solar power generation/storage micro-grid system under Qatar climate conditions,” *Sol. Energy Mater. Sol. Cells*, vol. 180, pp. 280–288, 2017.
- [189] J. Thiébot, P. Bailly du Bois, and S. Guillou, “Numerical modeling of the effect of tidal stream turbines on the hydrodynamics and the sediment transport - Application to the Alderney Race (Raz Blanchard), France,” *Renew. Energy*, vol. 75, pp. 356–365, 2015.
- [190] P. Pei, X. Yuan, J. Gou, and P. Li, “Dynamic Response during PEM Fuel Cell Loading-up,” *Materials.*, vol. 2, pp. 734–748, 2009.
- [191] M. Casagni and M. Lyell, “Comparison of two-component frameworks: the FIPA-compliant multi-agent system and the web-centric J2EE platform,” *Proceedings of the 25<sup>th</sup> international conference on software engineering*, 2003, pp. 341–351.
- [192] Z. Shi et al., “MAGE: Multi-agent environment,” *Proceedings of the international conference on computer networks and mobile computing*, 2003, pp. 181–188.
- [193] Z. Shi et al, “MAGE : An Agent-Oriented Software Engineering Environment,” *Proceedings of the third IEEE international conference on cognitive informatics*, 2004.
- [194] R. Bordini et al., “A survey of programming languages and platforms for multi-agent systems,” *Inform.*, vol. 30, pp. 33–44, 2006.
- [195] S. Theiss, V. Vasyutynskyy, and K. Kabitzsch, “AMES - A Resource-Efficient Platform for Industrial Agents,” *Proceedings of the IEEE international workshop on factory communication systems*, 2008.
- [196] C. Nunes et al, “Comparing stability of implementation techniques for multi-agent system product lines,” *Proceedings of the European conference on software maintenance and reengineering*, 2009, pp. 229–232.

- [197] C. Bădică, Z. Budimac, H. Burkhard, and M. Ivanović, “Software agents: Languages, tools, platforms,” *Comput. Sci. Inf. Syst.*, vol. 8, pp. 255–296, 2011.
- [198] S. Yang, “Developing a cloud energy-saving and case-based reasoning information agent with web service techniques,” *Proceedings of the fifth international symposium on parallel architectures, algorithms and programming*, 2012, pp. 178–185.
- [199] A. Sujil, J. Verma, and R. Kumar, “Multi agent system: concepts, platforms and applications in power systems,” *Artif. Intell. Rev.*, vol. 49, pp. 153–182, 2018.
- [200] K. Kravari and N. Bassiliades, “A Survey of Agent Platforms,” *J. Arti. Soci. Soc. Sim.*, vol. 18, no. 1, pp. 1–19, 2015.
- [201] F. Bellifemine, G. Caire, and D. Greenwood, “Agent Technology Overview,” in *Developing Multi-Agent Systems with JADE*, 1<sup>st</sup> ed., F. Bellifemine, G. Caire, and D. Greenwood, Ed. John Wiley & Sons, Ltd, 2007, pp. 3-28.
- [202] F. Bellifemine, G. Caire, and D. Greenwood, “The JADE Platform,” in *Developing Multi-Agent Systems with JADE*, 1<sup>st</sup> ed., F. Bellifemine, G. Caire, and D. Greenwood, Ed. John Wiley & Sons, Ltd, 2007, pp. 29-50.
- [203] F. Bellifemine, G. Caire, and D. Greenwood, “Programming with JADE –Basic Features,” in *Developing Multi-Agent Systems with JADE*, 1<sup>st</sup> ed., F. Bellifemine, G. Caire, and D. Greenwood, Ed. John Wiley & Sons, Ltd, 2007, pp. 51-76.
- [204] P. Mendham and T. Clarke, “MACSim: A simulink enabled environment for multi-agent system simulation,” *IFAC Proc.* vol. 38, no. 1, pp. 325–329, 2005.
- [205] C. Robinson, “Decentralised Data Fusion Using Agents,” Ph.D dissertation, The University of York, Department of Electronics, 2008.
- [206] L. Chen, “Multi Agent Ssystem-Based Simulation of a Laboratory-Scale Microgrid,” M.S. thesis, The Pennsylvania State University, The School of Science, Engineering and Technology, 2014.
- [207] L. Raju, R. Milton, and S. Mahadevan, “Multi Agent Systems based Distributed Control and Automation of Micro-grid using MACSimJX,” *Proceedings of the 10<sup>th</sup> international conference on intelligent systems and control*, 2016, Coimbatore, India, pp. 1–6.
- [208] J. Gómez-Gualdrón, M. Vélez-Reyes, and L. Collazo, “Self-Reconfigurable Electric Power Distribution System using Multi-Agent Systems,” *Proceedings of the IEEE electric ship technologies symposium*, 2007, pp. 180–187.

- [209] L. Raju, R. Milton, and S. Mahadevan, “Multiagent Systems Based Modeling and Implementation of Dynamic Energy Management of Smart Microgrid Using MACSimJX,” *Sci. World J.*, vol. 2016, pp. 1–14, 2016.
- [210] C. R. Robinson, P. Mendham, and T. Clarke, “MACSimJX: A tool for enabling agent modeling with simulink using JADE,” *J. Phys. Agents*, vol. 4, no. 3, pp. 1–7, 2010.
- [211] C. Robinson, “MACSimJX - MACSim with JADE extension, Pack A,” document version 1.8, 2012, Available online (<http://www.agentcontrol.co.uk/>), Last access 30<sup>th</sup> April 2018.
- [212] CEN-CENELEC-ETSI Smart Grid Coordination Group, “Smart Grid Reference Architecture,” November 2012, Available online ([https://ec.europa.eu/energy/sites/ener/files/documents/xpert\\_group1\\_reference\\_architecture.pdf](https://ec.europa.eu/energy/sites/ener/files/documents/xpert_group1_reference_architecture.pdf)), Last access 30<sup>th</sup> April 2018.
- [213] KTH Royal Institute of Technology, “Systems Architecture-The Smart-grid Architecture Model,” Lecture 8, October 2015, Available online (<https://www.kth.se/social/files/561f7ba4f2765422170264e7/Lecture%208%20Smartgrid%20Architecture%20Model.pdf>), Last access 30<sup>th</sup> April 2018.







## Summary

This thesis presents a unique model of the SGAM (Smart Grid Architecture Model) with considering the state of the art of the different research directions of the smart grid. The hybrid marine-hydrogen active power generation system has been modeled to represent the component layer of the SGAM. The system integrates MW scale PEM electrolyzer and fuel cell as the main energy balance components. A LiFePO<sub>4</sub> battery is used to cover the fast dynamics of the electrical energy. Moreover, the thesis analyzes the centralized and the decentralized energy management system. The MAS (Multi-Agent Systems) represents the paradigm of the decentralized system. The JADE platform is used to develop the MAS. The JADE based energy management system balances the energy between the generation (marine-current energy conversion system) and the demand side (residential load profile) during the stand-alone and the grid-connected modes of operation. The proposed model of the SGAM can be considered as a pilot case study that enables the detailed analysis and the applications of the different smart grid research directions.

**Key words :** Marine current energy, MW PEM electrolyzer and fuel cell, Energy management system, JADE based Multi Agent System.

## Résumé

Cette thèse présente un modèle unique du SGAM (Smart Grid Architecture Model) en considérant l'état de l'art des différentes directions de recherche du smart grid. Le système actif hybride de génération d'énergie marine-hydrogène a été modélisé pour représenter la couche des composants du SGAM. Le système intègre un électrolyseur et une pile à combustible PEM à l'échelle du MW en tant que composants principaux du bilan énergétique. Une batterie LiFePO<sub>4</sub> est utilisée pour couvrir la dynamique rapide de l'énergie électrique. En outre, la thèse analyse les systèmes de gestion d'énergie centralisé et décentralisé. Le MAS (Multi Agent System) représente le paradigme du système décentralisé. La plate-forme JADE est utilisée pour développer le MAS. Le système de gestion d'énergie basé sur JADE équilibre l'énergie entre la génération (système de conversion d'énergie des courants marins) et la demande (profil de charge résidentielle) pendant les modes de fonctionnement autonome et connecté au réseau. Le modèle proposé de la SGAM peut être considéré comme une étude de cas pilote qui permet l'analyse détaillée et les applications des différentes directions de recherche du smart grid.

**Mots clés :** Energie Hydrolienne, Electroiseur et pile à combustible PEM à l'échelle du MW, System de gestion d'énergie, Système multi-agents de gestion d'énergie basé sur JADE.